Development of a Synthetic uPAR Targeted Gene Delivery System

Thomas Kean

A thesis submitted to Cardiff University in accordance with the requirements for the degree of Doctor of Philosophy

Centre for Polymer Therapeutics
Welsh School of Pharmacy
Cardiff University

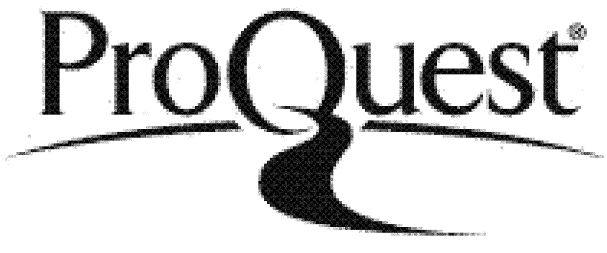

ProQuest LLC
789 East Eisenhower Parkway
P.O. Box 1346
Ann Arbor, MI 48106-1346

Declaration

This work has not previously been accepted in substance for any degree and is not being concurrently submitted in candidature for any degree.

Signed ..... (candidate)

Date ...1/3/06.....

STATEMENT 1

This thesis is the result of my own investigations, except where otherwise stated.

Other sources are acknowledged by footnotes giving explicit references. A bibliography is appended.

Signed ..... (candidate)

Date ...1/3/06.....

STATEMENT 2

I hereby give consent for my thesis, if accepted, to be available for photocopying and for inter-library loan, and for the title and summary to be made available to outside organisations.

Signed ..... (candidate)

Date ...1/3/06.....

Acknowledgments

This thesis would not have been possible without the love and support of my friends and family, thank you to all, this is dedicated to you. A special thanks goes to mum for taking the time to proof read this thesis. The dissertation would have been much poorer if it were not for the guidance and knowledge of Prof. Ruth Duncan and Dr. Maya Thanou. Without your vision Maya, this project would not have started.

I would like to thank all of CPT, each of you has contributed to the pleasant atmosphere making it a wonderful working environment. Thanks also to the visiting Professors Ringsdorf and Veronese. I would especially like to acknowledge Fran, Karen and Zeena.

To those of you who have not been named individually, it is not because you were not thought of but that I did not want this to be akin to an Oscar acceptance speech.

My students all deserve a mention, perhaps the best way of learning something thoroughly is to teach it. Thanks must therefore go to Susanne Roth, Lee Jones, Maria Harvey and Helen Pritchett. Susanne, you were exceptional, I wish you the best of luck for the future.

Praise is due to all of my teachers, those in academia and those in 'the real world', I hope I have learned some of what you taught. I would not be where I am now if it were not for your efforts.

I echo the words of Sir Isaac Newton "If I have seen further it is by standing on the shoulders of giants..." and I appreciate all of their hard work.

Finally, I would like to acknowledge Cardiff University for funding my PhD.

Abstract

Development of a Synthetic uPAR Targeted Gene Delivery System

Receptor targeted gene therapy as an improved cancer treatment is an attractive concept as it has the potential to avoid the side-effects associated with current chemotherapy. The urokinase plasminogen activator (uPA) receptor (uPAR) is a particularly attractive target as it is over-expressed in a variety of cancers (including breast and prostate) and it is thought to be involved in the invasion, migration and metastasis of tumour cells. Furthermore, the receptor binding region of uPA has been identified. The natural polymer chitosan (derived from chitin), was chosen as a vector. Chitosans are very promising non-viral gene delivery systems due to their relatively low toxicity, and in addition, trimethylated chitosans show increased solubility at physiological pH and increased gene delivery efficiency. The overall aim of this project was to develop a novel uPAR targeted non-viral gene delivery system based on chitosan which could eventually be used in cancer therapy.

In this study chitosan oligomers (3-6 kDa) and polymers (100 kDa) were trimethylated to different degrees and characterised by ^{1}H NMR spectroscopy. Toxicity (using the tetrazolium dye 3-(4,5-dimethylthiazol-2-yl)-2,5-diphenyl tetrazolium bromide cytotoxicity assay) and transfection efficiency (using the luciferase plasmid pGL3 luc) were assessed in COS-7 (monkey kidney fibroblast) and MCF-7 (human breast cancer epithelial) cell lines. Preliminary flow cytometry experiments studied the ability of the peptides, CLNGGTC (u7) and GVSNKYFSNIHWG (Gu11G), derived from the binding region of uPA to inhibit uPA-FITC binding to U937 cells. The optimised trimethylated chitosan oligomer (TMO) was functionalised with chloroacetic acid to give 6-O-carboxymethyl *N,N,N*-trimethyl chitosan (CMTMO). Two peptides derived from the binding region of uPA, u7 and Gu11G were conjugated to the 6-O-carboxymethyl functionality using 1-[3-(dimethylamino)propyl]-3-ethylcarbodiimide methiodide and hydroxy-2,5-dioxopyrrolidine-3-sulfonicacid. Fluorescent derivatives of u7-CMTMO and Gu11G-CMTMO were then produced by reaction with the succinimidyl ester of 5-(and-6)-carboxyfluorescein and Oregon Green® 488-X, succinimidyl ester. The cell-association of the fluorescent u7-CMTMO and Gu11G-CMTMO was assessed in U937 cells (a histocytic lymphoma known to over-express uPAR) and DU145 cells (a human prostate carcinoma) over time at 37 °C and 4 °C. The development of an improved gene delivery system using Gu11G-CMTMO was then investigated in COS-7, DU145 and MCF-7 cells.

It was shown that chitosan could be trimethylated in a controllable and repeatable manner by increasing reaction time. Increasing degree of trimethylation decreased cell viability, an effect more pronounced in polymeric (TMC) over oligomeric (TMO) derivatives. The calculated IC_{50} value for TMO with 44 % trimethylation was > 10 mg/ml which is 100-fold higher than the transfection concentration. The transfection efficiency of TMO increased with the degree of trimethylation up to maximum with TMO which was 44 % trimethylated. Binding assays using fluorescent ligands showed that, whereas free Gu11G decreased the binding of uPA-FITC to U937 cells, u7 had no effect. Peptide-PEG conjugates were also investigated and none (including Gu11G-PEG) decreased the binding of uPA-FITC. The Gu11G peptide was conjugated on CMTMO which was previously fluorescently labelled. The Gu11G-CMTMO-FAM showed an increase in cell-associated fluorescence (>5 fold) compared to CMTMO-FAM on U937 cells. u7-CMTMO-FAM showed decreased cell association compared to CMTMO. When Gu11G-CMTMO was mixed with TMO/pDNA or PEI/pDNA in the transfection mixture the transfection efficiency, as measured by the luciferase expression, was equal to that of the transfection achieved with uncoated polyplexes. Although Gu11G was shown to bind uPAR selectively, it was not possible to translate into an improved conjugate.

Index

Tables

Figures

Glossary of Terms

Abbreviation	Meaning
a2MG/LRP	α2-macroglobulin receptor/lipoprotein related receptor
aa	Amino acid
Ab	Antibody
ABC	Antibody binding capacity
ADEPT	Antibody directed enzyme prodrug therapy
AML	Acute myeloid leukaemia
AMP	Adenosine monophosphate
ANOVA	Analysis of variance
APS	Ammonium persulphate
ASGR	Asialoglycoprotein receptor
ATCC	American Tissue and Cell Culture
ATF	Amino-terminal fragment of uPA
ATP	Adenosine triphosphate
BCA	Bicinchoninic acid
β-gal	β-galactosidase
BHT	2,6-di-tert-butyl-4-methyl phenol
BSA	Bovine serum albumin
CAR	Coxsackievirus and adenovirus receptor
CAT	Chloramphenicol transferase
CD##	Cluster of differentiation ##
CEA	Carcinoembryonic antigen
Chitosan-9-anthraldehyde	9-anthraldehyde labelled chitosan polymer
cHSA	Cationic human serum albumin
CIMPR	Cation independent mannose-6-phosphate receptor
CMTMO	6-O-carboxymethyl trimethyl chitosan
CMTMO-FAM	Fluorescein labelled CMTMO
CMTMO-OG	Oregon Green labelled CMTMO
D_2O	Deuterium oxide
DADMAC	Poly(diallyl-dimethyl-ammonium chloride)
DAEA-Dextran	Diethylaminoethyl-dextran
DEAE	Diethylaminoethyl
DMAP	4(dimethylamino)pyridine
DMEM	Dulbecco's modified Eagle's medium
DMF	Dimethylformamide
DMSO	Dimethylsulphoxide
DOPC	Di-oleoyl phosphatidylcholine
DOPE	Di-oleoyl phosphatidylethanolamine
DOSPA	Di-oleoyl phosphatidylethanolamine : cholesterol (3:1:3.36)
DOTAP	Di-oleoyl trimethylammonium propane

Abbreviation	Meaning
Dox	Doxorubicin
DSC	disuccinimidyl carbonate
DTAT	Amino terminal fragment of uPA to diphtheria toxin
DTM	Degree of trimethylation
ECL	Enzyme linked chemiluminescence
ECM	Extracellular matrix
EDC	1-ethyl-3-(3-dimethylaminopropyl)-carbodiimide hydrochloride
EDTA	Ethylene diamine tetraacetic acid
EGF	Epidermal growth factor
EGFR	Epidermal growth factor receptor
EPR	Enhanced permeability and retention
EtBr	Ethidium Bromide
EtOH	Ethanol
fAb	Antibody fragment
FAM	Fluorescein
FBS	Foetal bovine serum
FGF2	Fibroblast growth factor 2
FITC	Fluorescein isothiocyanate
FLPR	Formyl like peptide receptor protein
FTIR	Fourier transform infra-red
GDEPT	Gene directed enzyme prodrug therapy
GP330	Glycoprotein 330
GPC	Gel permeation chromatography
GPI	Glycosylphosphatidyl inositol
HEPES	*N*-2-hydroxyethylpiperazine-*N*'-ethanesulphonic acid
HMWK	High molecular weight kallikrine
HPMA	*N*-(2-hydroxypropyl) methacrylamide
HRP	Horse raddish peroxidase
LDLRP	Low density lipoprotein related protein
LEAPT	Lectin directed enzyme activated prodrug therapy
LTT	Ligand targeted therapeutics
mAb	Monoclonal antibody
MeOH	Methanol
MMP	Matrix metalloproteinase
MOPS	4-Morpholinepropanesulfonic acid
mPEG	Monomethoxy poly(ethylene)glycol
MTT	3-(4,5-dimethylthiazol-2-yl)-2,5-diphenyl-2H-terazoliumbromide
N/P	Nitrogen/phosphorus ratio
nHSA	Native human serum albumin
NMP	N-methyl pyrolidinone
NMR	Nuclear magnetic resonance
OG	Oregon Green

Abbreviation	Meaning
Oligo-9-anthraldehyde	9-anthraldehyde labelled chitosan oligomer
p(DMEAMA)	poly(2-(dimethylamino)ethyl methacrylate)
PAA	linear poly(amidoamine)
PAI-1	Plasminogen activator inhibitor
PAMAM	Poly(amido amine) dendrimer
PBS	Phosphate buffered saline
PCS	Photon correlation spectrophotometer
PDEPT	Polymer directed enzyme prodrug therapy
pDMAEMA	Poly(2-dimethylamino) ethyl methacrylate
pDNA	plasmid DNA
PECAM	Platelet endothelial cellular adhesion molecule
PEG	Poly(ethylene glycol)
PEI	Poly(ethylenimine)
pGL3 luc	Plasmid encoding for luciferase
PK1	HPMA-Dox copolymer
PK2	Galactose targeted HPMA-Dox copolymer
PLGA	Poly(lactide-co-glycolide)
PLL	Poly-(L-lysine)
PMA	Phorbol 12-myristate 13-acetate
PMSF	Phenylmethylsulfonyl fluoride
PNP	*p*-nitrophenol chloroformate
PNP-mPEG	*p*-nitrophenol chloroformate activated mPEG
PSMA	Prostate specific membrane antigen
PVDF	Polyvinylidene fluoride
PVPBr	Poly(vinyl pyridinium bromide)
r.t.	Room temperature
RCF	Relative centrifugal force (gravitational force)
RE	Recticulo endothelial system
rf	retention factor
RGD	Arginine-Glycine-Aspartic acid
RI	Refractive index
RLU	Relative light units
RME	Receptor mediated endocytosis
SC-mPEG	Succinimidyl activated mPEG
sc-uPA	Single chain urokinase plasminogen activator
SD	Standard deviation
SDS	Sodium dodecyl sulphate
SDS-PAGE	Sodium dodecyl sulphate polyacrylamide gel electrophoresis
SEM	Standard error of the mean
serpin	Serine protease inhibitor
SMANCS	Styrene-maleic acid neocarzinostatin
SPPS	Solid phase peptide synthesis

Abbreviation	Meaning
Sulpho-NHS	N-hydroxysulphosuccinimide
TBE	Tris borate EDTA buffer
TEA	Triethylamine
TEM	Transmission electron microscopy
TEMED	N,N,N,N'-tetra-methyl-ethylenediamine
THF	Tetrahydrofuran
TLC	Thin layer chromatography
TMC	Trimethylated chitosan (polymer)
TMC-Block	Citraconic anhydride protected TMC
TMO	Trimethylated chitosan (oligomer)
TMO-9-anthradehyde	9-anthraldehyde labelled TMO
TMO-Block	Citraconic anhydride protected TMO
TMO-FAM	Fluorescein labelled TMO
Tris-Base	Tris(hydrocymethyl)aminomethane
Tris-HCl	Tris(hydrocymethyl)aminomethane hydrochloride
Tween 20	Polyoxyethylene sorbitan monolaurate
u11	Valine-Serine-Asparagine-Lysine-Tyrosine-Phenylalanine-Serine-Asparagine-Isoleucine-Histidine-Tryptophan
u11-CMTMO	u11-targeted CMTMO
u11-CMTMO-FAM	u11-targeted, fluorescein labelled CMTMO
u11-CMTMO-OG	u11-targeted, Oregon Green labelled CMTMO
u7	Cystein-Leucine-Asparagine-Glycine-Glycine-Threonine-Cystein
u7-CMTMO	u7-targeted CMTMO
u7-CMTMO-FAM	u7-targeted, fluorescein labelled CMTMO
uPA	Urokinase type plasminogen activator
uPA-FITC	FITC labelled uPA
uPAR	Urokinase type plasminogen activator receptor
UV	Ultraviolet-visible
VDEPT	Virus directed enzyme prodrug therapy
VEGF	Vascular endothelial growth factor
VEGFR	Vascular endothelial growth factor receptor
VLDL	Very low-density lipoprotein receptor
Vn	Vitronectin
WHO	World Health Organisation
X-Gal	5-bromo-4-chloro-3-indolyl β-D-galactoside
X-SCID	X-linked severe combined immunodeficiency
XTT	sodium 39-[1-(phenylaminocarbonyl)-3, 4-tetrazolium] - bis(4-methoxy-6-nitro)benzenesulfonic acid

Chapter 1

General Introduction

1.1 General Introduction and Overall Aim

Delivery of a drug to a specific site within the body is a necessity in improving disease treatment and is an ongoing aim of the pharmaceutical scientist. Through selective accumulation in the pathological site and lower accumulation elsewhere, the drug's therapeutic value is increased. Although this idea was first conceived by Ehrlich for the treatment of syphilis by targeting bacteria in the late 1800's, targeted drug delivery remains a challenge today. Nevertheless, antibody-based targeting systems have been successful. The first antibody drug conjugate, gemtuzumab ozogamicin (Mylotarg®), targeting CD33 for the treatment of leukaemia was brought to market in 2000 (Wyeth, 2003).

Since Ringsdorf (1975) proposed a polymer carrier with a targeting ligand as a selective therapy, much work has been concentrated in this field (Fig.1.1). This has seen the first targeted polymer-drug conjugate (PK2, galactose targeted *N*-(2-hydroxypropyl) methacrylamide copolymer (HPMA-Dox)) enter phase I/II clinical trials as anticancer agents (Seymour et al., 2002). Currently a number of targeted drug delivery systems based on antibodies, polymers and liposomes are in clinical trials and a higher number developed pre-clinically (Table 1.1). This study is based upon Ringsdorf's visionary model and the pioneering work of Wu & Wu (1988) who were the first to design a targeted non-viral vector for gene therapy. This employed the covalent linkage of a galactose-terminated protein (asialoorosomucoid) to poly-(L-lysine) (PLL) which was then used to non-covalently condense DNA (Fig.1.1).

With the advent of the human genome project and its completion much hope has been pinned on gene therapy as a means to treat life threatening or debilitating diseases. The use of gene therapy has been embraced by the scientific community, particularly as a means for the treatment of cancer (Edelstein, 2005). Currently, clinical gene therapy trials are using several therapeutic genes for the treatment of cancer. Examples include: the introduction of wild type cell cycle regulatory gene e.g. p53 (Lane, 2004) (now approved by regulatory authorities in China (Gendicine™) (Surendran, 2004)); introduction of a foreign enzyme gene e.g. thymidine kinase to activate a drug treatment delivered later, in this case ganciclovir (Mesnil & Yamasaki, 2000); introduction of a cytokine gene e.g. interleukin 2 (Schreiber et al., 1999).

Table 1.1 – Actively targeted drugs

Phase	Carrier (Name)	Target	Ligand	Drug/ treatment	Reference
A	Antibody (Mylotarg®)	CD33	Recombinant humanised antibody	Calicheamicin/ Acute Myeloid Leukaemia	(Allen & Cullis, 2004, Sievers et al., 2001, Wyeth, 2003)
A	Antibody (Zevalin®)	CD20	Mouse anti CD20	^{90}Y/ non-Hodgkin Lymphoma	(Ross et al., 2004, Wiseman et al., 2001)
A	Antibody (Bexxar®)	CD20	Mouse/human chimera anti CD20	^{131}I/ non-Hodgkin Lymphoma	(Allen, 2002)
I/II	HPMA Copolymer (PK2)	Asialoglycoprotein receptor	Galactose	Doxorubicin/ Hepatocarcinoma	(Seymour et al., 2002, Duncan, 2002)
I	Antibody	Prostate specific membrane antigen	mAb J591	Radionuclides ^{90}Y, ^{111}In, ^{177}Lu/ diagnosis and treatment	(Bander et al., 2003)
I/Pc	Chelating agents, peptides	Folate receptor	Folic acid	Radionuclides, ^{67}Ga, ^{111}In, ^{99m}Tc, ^{66}Ga, ^{64}Cu/ Diagnosis	(Reviewed in Ke et al., 2004)
Pc	PEG-coated liposomes	$\alpha_v\beta_3$ integrin	RGD (cyclic Arg-Gly-Asp)	Doxorubicin/ colon carcinoma	(Schiffelers et al., 2003)
Pc	Poly [lactid acid]	$\alpha_v\beta_3$ integrin	RGD (Gly-Arg-Gly-Asp-Ser)	Poly-lactic microbubble ultrasound contrast agent/ diagnosis	(Lathia et al., 2004)

Table 1.1 continued – Actively targeted drugs

Phase	Carrier (Name)	Target	Ligand	Drug/ Treatment	Reference
Pc	Liposomes	HER2	mAb	Doxorubicin/ Breast cancer	(Park et al., 2002)
Pc	Poly-L-Glutamic acid	EGFR	mAb	Doxorubicin/ vulvar squamous carcinoma (A431 tumour)	(Vega et al., 2003)
Pc	Palmitoylated glycol chitosan vesicles	Transferrin receptor	Transferrin	Doxorubicin/ vulvar squamous carcinoma (A431), ovarian carcinoma (A2780), prostate carcinoma (PC3)	(Dufes et al., 2004)
Pc	Transferrin	Transferrin receptor	Transferrin	Paclitaxel/ prostate carcinoma (PC3)	(Sahoo et al., 2004)
Pc	Transferrin	Transferrin receptor	Transferrin	Mitomycin C/ Ehrlich ascites carcinoma (EAC), sarcoma 180 (S180)	(Reviewed in Tanaka et al., 2004)
Pc	PEG or HPMA	Bone	Alendronate and aspartic acid peptide	FITC/ model drug	(Wang et al., 2003)

Pc = pre-clinical; A = Approved; mAb = monoclonal antibody; fAb = fragments of monoclonal antibody; EGFR = epidermal growth factor receptor; FITC = fluorescein isothiocyanate

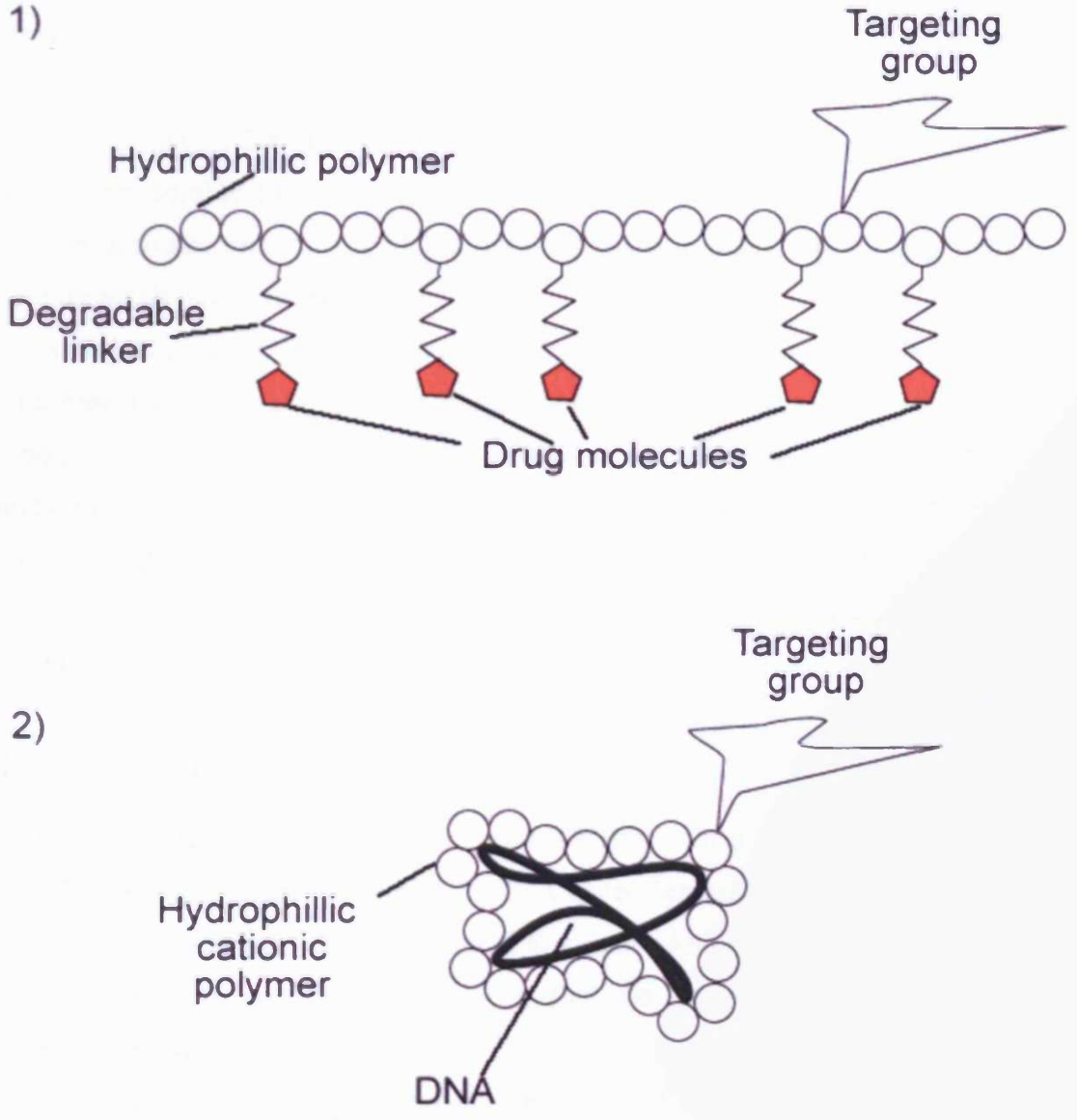

Figure 1.1 – Targeted delivery models

1) Ringsdorf's targeted polymer model (Ringsdorf, 1975), 2) Proposed targeted non-viral gene delivery model.

Current clinical trials are mainly using viral vectors for gene delivery, however it is largely believed that non-viral gene therapy will be safer. The first clinical trial using PEI-mediated gene therapy was published in 2004: poly(ethylenimine) (PEI) complexed diphtheria toxin A-chain plasmid to treat bladder cancer (Ohana et al., 2004).

Targeting specific proteins on the surface of cells for drug delivery requires the engineering of a suitable carrier bearing the appropriate ligand. In targeted drug therapies, carriers such as liposomes (Zhang et al., 2002), antibodies (Ross et al., 2004) and polymers (Duncan, 2003) have been suggested. In this study the focus was on the design of water soluble cationic polymers for targeted gene delivery. The urokinase plasminogen activator receptor (uPAR) is over-expressed in many cancers and it has a high affinity for its ligand (Blasi, 1997).

In this project the development of a peptide targeted non-viral gene delivery system based on biocompatible polymers was investigated and the chosen target was uPAR. From potential polymers, chitosan was chosen as the delivery vector due to its biocompatibility (Corsi et al., 2003, Lee et al., 2001), good transfection efficiency (Thanou & Junginger, 2004), and potential for chemical modification. The following sections of the introduction outline the background to this research starting with the need for targeted cancer therapy.

1.2 The Need for Targeted Therapy of Cancer

According to the world health organisation (WHO) cancer is responsible for six million (12 %) deaths worldwide (WHO, 2005). Cancer Research UK report that cancer has recently overtaken heart disease as the UK's major killer (Cancer Research UK, 2005). With an aging population it is likely that the treatment of cancer will be increasingly important.

In 2001 breast and prostate cancers contributed 26 % to the UK incidence of cancer and 14 % of the mortality (Cancer Research UK, 2005). This large incidence and mortality shows the necessity for improvement in the treatment of these diseases. Both breast and prostate cancers have been reported to over-express uPAR (Blasi, 1997). This is one of the factors leading to the choice of this receptor as a target for non-viral gene delivery. The receptor and its function are described more fully in Section 1.4.

Great advances have been made in the treatment of cancer, but there remains much to accomplish. Current clinical anticancer drugs fall into two general categories:

cytotoxics and hormone based. Cytotoxins assault DNA at some level, either in its synthesis, replication or processing (Denny, 2001). Cytotoxins can be further split into: alkylating agents e.g. cyclophosphamide; antimetabolites e.g. methotrexate; cytotoxic antibiotics e.g. doxorubicin and vinca alkaloids e.g. taxol (Rang et al., 1996). When tumours are formed from hormone sensitive tissue they may be hormone-dependent and hormone antagonism (e.g. tamoxifen) can be used to delay the tumour growth. The main problems associated with the above mentioned therapies are their lack of specificity for tumour cells leading to non-specific toxicity and the development of resistance. Most small molecules are rapidly distributed throughout the body without selective accumulation in the tumour. They achieve their action due to the increased proliferation of cancer cells but have debilitating side effects and low efficiency. The use of a targeting method to deliver the therapy to cancer cells reduces non-specific action by localising cytotoxic drugs to the tumour.

Genetic therapies offer a new approach to the treatment of cancer. The main focus of gene therapy investigations is for the treatment of cancer (Fig. 1.2). It is considered that toxicity may even be abolished through the use of gene therapy. Indeed, adenovirus carrying p53 (Gendicine®) has been approved in China; 64 % of patients treated with radiotherapy and Gendicine® showed complete tumour regression compared with three times lower tumour regression in radiotherapy only patients (Surendran, 2004).

1.3 Targeting Therapeutics

Through targeting, scientists have tried to achieve greater success in the treatment of cancer. The word "Targeting" is used in this project to describe methods employed to achieve preferential localisation of a therapeutic in the region of disease and subsequently an increase of the local concentration. It was realised back in the 16th century "Poison is in everything, and no thing is without poison. The dosage makes it either a poison or a remedy" (Paracelsus, 1490-1541). Through targeting the delivery of a drug, and therefore increasing its concentration in the region of pathology, it is suggested that a lower total dose may be administered compared with a non-targeted drug. The lower concentrations at non-pathological sites would decrease the non-specific dose related toxicity of the therapeutic.

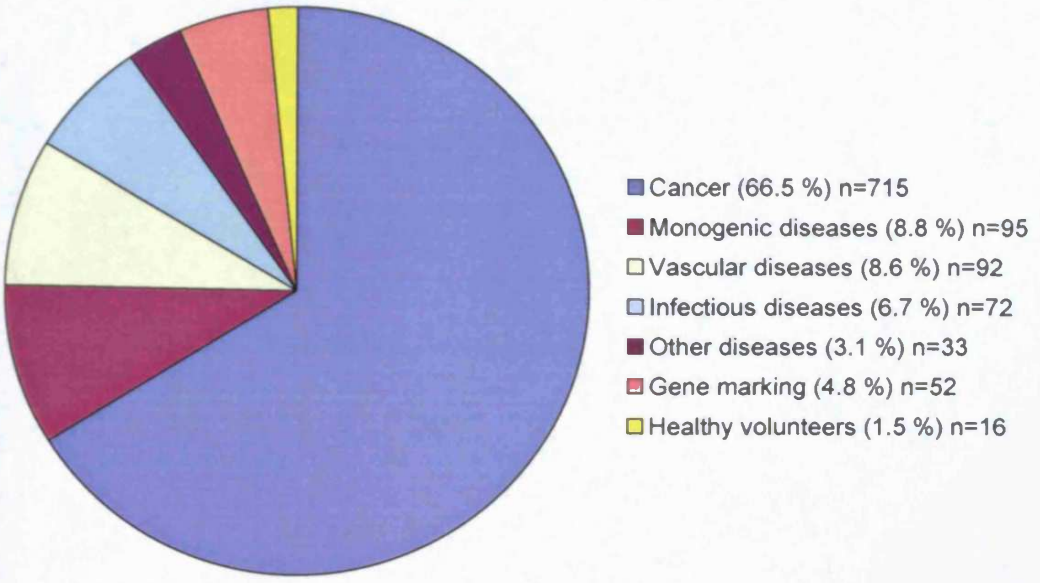

Figure 1.2 - Gene therapy treatment by disease

A chart showing the diseases investigated in gene therapy clinical trials worldwide (adapted from Edelstein, 2005).

It is envisioned that through the use of drug targeting strategies unwanted side-effects, i.e. those seen with many chemotherapies, will be drastically diminished. The targeting of a pathway or enzyme such as selective tyrosine kinase inhibition shows promise, however, it is outside the scope of this project and not considered further (for a review see Ross & Hughes, 2004).

Therapeutic delivery can be considered at different levels within the body: system, organ, cell and subcellular compartment (Duncan, 2005) (Fig. 1.3). The areas that are particularly relevant to this project are those of the organ and the cell. However, the intracellular trafficking of non-viral vectors is another important issue. The enhanced permeability and retention effect (EPR) can be considered to exist at the organ level (discussed in Section 1.3.1) and would surely be applicable to the nano-sized particles used in gene therapy, whilst ligand targeted therapy occurs at a cellular level (discussed in Section 1.3.2).

Many researchers have attempted to categorise drug targeting mechanisms. The peptide-targeted delivery developed in this thesis is termed ligand-targeted therapy (LTT) after that described by Allen (2002). According to Schatzlein (2003) targeting strategies fall into two categories; intrinsic and extrinsic (Schatzlein, 2003). Intrinsic targeting refers to the use of pharmacokinetic and/or biodistribution characteristics of a drug or carrier system and extrinsic to the use of a ligand to provide a specific interaction with cell receptors and therefore selective accumulation in the pathology (Schatzlein, 2003). This categorisation is synonymous with passive and active targeting systems respectively (Duncan, 2002, Moghimi et al., 2005, Schatzlein, 2003). LTT would fall into the categories of active or extrinsic targeting. The uptake found due to the EPR effect is considered as passive targeting.

Many intricate and ingenious methods utilising both passive and active targeting have been developed to achieve greater control over site-specific drug release, these are summarised in Table 1.2 but further discussion of their concepts is outside the scope of this thesis. I expect these multi-stage methods, especially those with external control, to find applications in several diseases.

As gene therapy, especially non-viral gene therapy, is such a novel area, the targeting of chemotherapy for the treatment of cancer is first considered. Seymour et al. (2002) found liver targeting and lower toxicity using PK2 (LTT: galactose targeted HPMA-Dox copolymer) compared with free doxorubicin.

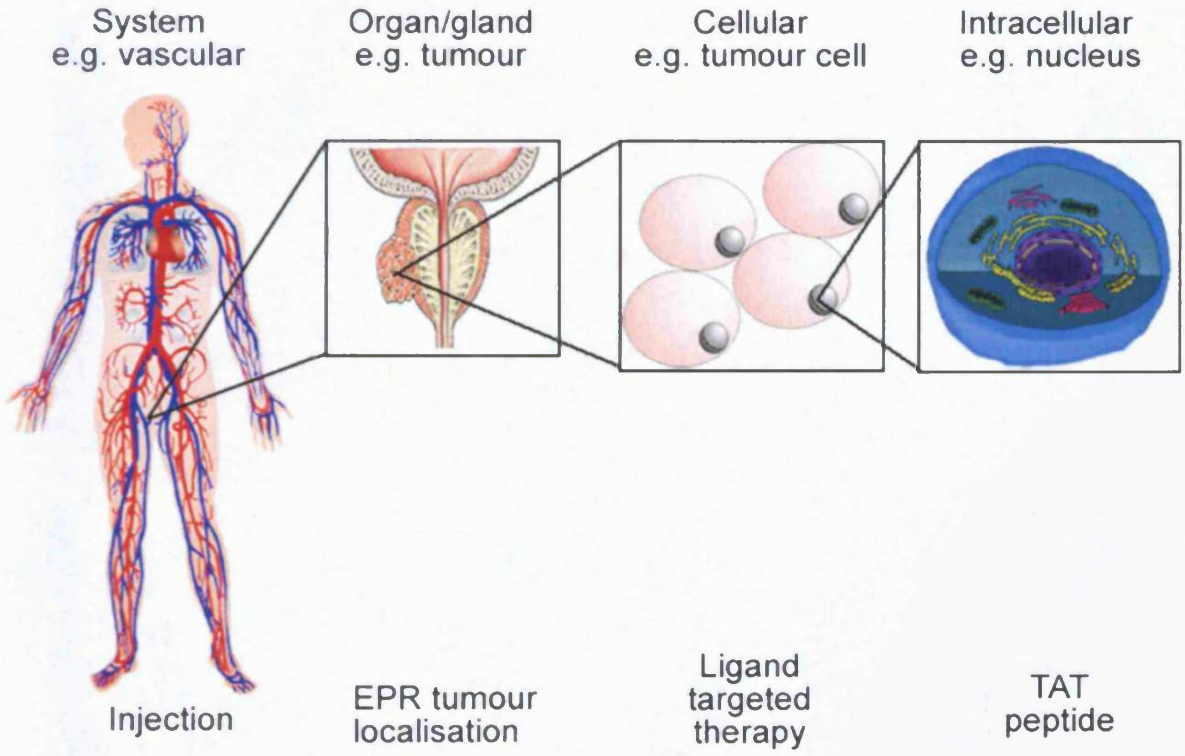

Figure 1.3 - Levels of targeting within the body

Targeting is considered to occur at the levels outlined above the diagrams. Below the diagrams are examples of targeting mechanisms used at each level (Diagrams adapted from Familydoctor, 2005, Harcourtschool, 2005, Talktransplant, 2005).

Table 1.2 – Multi-stage targeting methods

Mechanism of Targeting	Example	Reference
Temperature (increased in tumour and inflammation or applied locally)	Poly(N-isopropylacrylamide-coacrylamide), elastin like polypeptide	(Reviewed in Chilkoti et al., 2002) (Meyer et al., 2001)
Ultrasound (applied externally)	High intensity focused ultrasound increased β-galactosidase delivery	(Huber et al., 2003)
Magnetism (applied externally)	Superparamagnetic particles formed with PEI/DNA	(Reviewed in Plank et al., 2003)
*Antibody directed enzyme prodrug therapy (ADEPT)	fAb against CEA targets carboxypeptidase G2 which catalyses cleavage of a carbamate bond to activate a di-iodophenol mustard drug	(Francis et al., 2002, Monks et al., 2000)
Lectin-directed enzyme-activated prodrug therapy (LEAPT)	Galactose targeted α-L-rhamnopyranosidase followed by rhamnose-doxorubicin activation	(Robinson et al., 2004)
Gene directed enzyme prodrug therapy (GDEPT)	Gene encoding for a non-native enzyme is delivered and expressed in the tumour, a prodrug is administered and activated in the tumour	(Reviewed in Denny, 2001)
Virus directed enzyme prodrug therapy (VDEPT)	A more specific case of GDEPT: nitroimidazole reductase gene delivered to tumour cells by adenoviral vector activates CB1954	(Chung-Faye et al., 2001)
Polymer directed enzyme prodrug therapy (PDEPT)	EPR accumulation of HPMA-β-lactamase followed by EPR accumulation of HPMA-copolymer-methacyloyl-glycine-glycine-cephalosporin-doxorubicin	(Satchi-Fainaro et al., 2003)
Protein targeted enzyme prodrug	VEGF fused to carboxypeptidase G2 to activate prodrug	(Spooner et al., 2003)

* - in phase I clinical trials, fAb – antibody fragment, CEA – carcinoembryonic antigen, CB1954 - 5-(aziridin-1-yl)-2,4-dinitrobenzamide

Nevertheless, the maximum tolerated dose was lower than that of the passively targeted HPMA-Dox (PK1). There was an accumulation of 15-20 % of the total dose in the liver as opposed to a general body distribution with PK1 (Seymour et al., 2002). The source of toxicity observed in PK2 over PK1 was not clear. Table 1.1 gave an overview of the current research on receptor targeting for drug delivery.

The antibody (anti-CD33)-calicheamicin (Mylotarg®) showed no cardiac or cerebellar toxicity, but grade 4 neutropenia and thrombocytopenia was observed (Sievers et al., 2001). It was however predicted that this type of toxicity may occur due to the targeting of CD33 which is also present on normal maturing haematopoietic progenitor cells (Sievers et al., 2001). Calicheamicin, the active component of Mylotarg®, does not appear to be used as a single drug entity. Therefore it is not possible to make a comparison to the single drug efficacy. From these studies it can be seen that targeting has a role to play in the arsenal against cancer but more specific targets should be sought to improve therapy.

A reduction of the side-effects of a gene therapy cannot be truly considered as this is a new field. The therapeutic gene could be engineered in such a way that no toxicity is expected and it may be the vector rather than the gene/protein which is toxic. In non-viral gene therapy targeting is used to overcome the cell membrane barrier and increase uptake, through receptor mediated endocytosis (RME), of the polyplex. This is addressed in Section 1.5.3.

1.3.1 Passive Targeting of Drugs and/or Carriers

It was reported in 1984 (Maeda et al., 1984) that macromolecules can accumulate selectively in tumour tissues. Later it was observed that the polymer-protein conjugate styrene-maleic acid neocarzinostatin (SMANCS) selectively accumulated in mouse solid tumours (Matsumura et al., 1987). To explain this phenomenon Maeda and Matsumura introduced the term "enhanced permeability and retention (EPR) effect" (Matsumura et al., 1987). Neovascular tissue angiogenically formed by the tumour is disorganised, meaning macromolecules can extravasate into the interstitial space in a tumour (Dvorak et al., 1988). Neovascular tissue is formed by the tumour due to its increased nutrient requirements (Folkman & Shing, 1992, Satchi-Fainaro et al., 2004). The epithelium of these new blood vessels is disordered and therefore more permeable than normal vasculature (Maeda et al., 2000). Although now accepted, the EPR effect

was originally opposed as there is high intratumoural pressure which, it was thought, would prevent the extravasation of macromolecules. Passive targeting using the EPR effect has already been utilised in the clinical treatment and imaging of solid tumours and has wide applicability (Maeda et al., 2000). Liposomes, polymer-drug conjugates and nanoparticles all target tumours via the EPR effect and all polymer-drug conjugates in clinical development use the EPR effect for tumour specific targeting (Duncan, 2003). Nanoparticles consisting of polymeric materials and therapeutic(s) can be small enough to extravasate due to the enhanced permeability of neovascular tissue yet large enough to both be retained in the tumour due to the reduced lymphatic drainage, and not to extravasate in normal tissue (Brigger et al., 2002, Maeda et al., 2001, Satchi-Fainaro et al., 2004) (Fig. 1.4).

Polymeric colloids were found to accumulate in tumour xenografts in mice (Nakanishi et al., 2001). They studied a polymeric doxorubicin containing micelle formulation (NK911) consisting of poly(ethylene glycol) (PEG)-coated polyaspartic acid conjugated to doxorubicin which has an average size of 41.9 nm and was found to accumulate in tumours in mice 3.4-fold over free doxorubicin (Nakanishi et al., 2001).

Glycol-chitosan doxorubicin nanoparticles of up to 300 nm have been found to accumulate in tumour tissue in rats (Son et al., 2003). Although the actual cut off size value for extravasation in tumours due to EPR may be as large as 500 nm, it could vary in different tumours (Torchilin, 2000).

Polyplexes are formed through the interaction of negatively charged nucleic acids with positively charged polymers (Leclercq et al., 2003). Polyplex size is controlled by the concentration and type of polyelectrolyte used (Ogris & Wagner, 2002b) they generally have < 200 nm sizes (Koping-Hoggard et al., 2001, Reineke & Davis, 2003b, Reineke & Davis, 2003a). It is envisaged that polyplexes will accumulate in tumours due to the EPR effect (Ogris & Wagner, 2002b). This accumulation was reported in tumour bearing mice treated with poly-lysine dendrimer complexes when compared to accumulation with a liposome formulation (Kawano et al., 2004). It has also been found that at the site of the tumour, LTT enhances cell binding and uptake. LTT is the next idea considered.

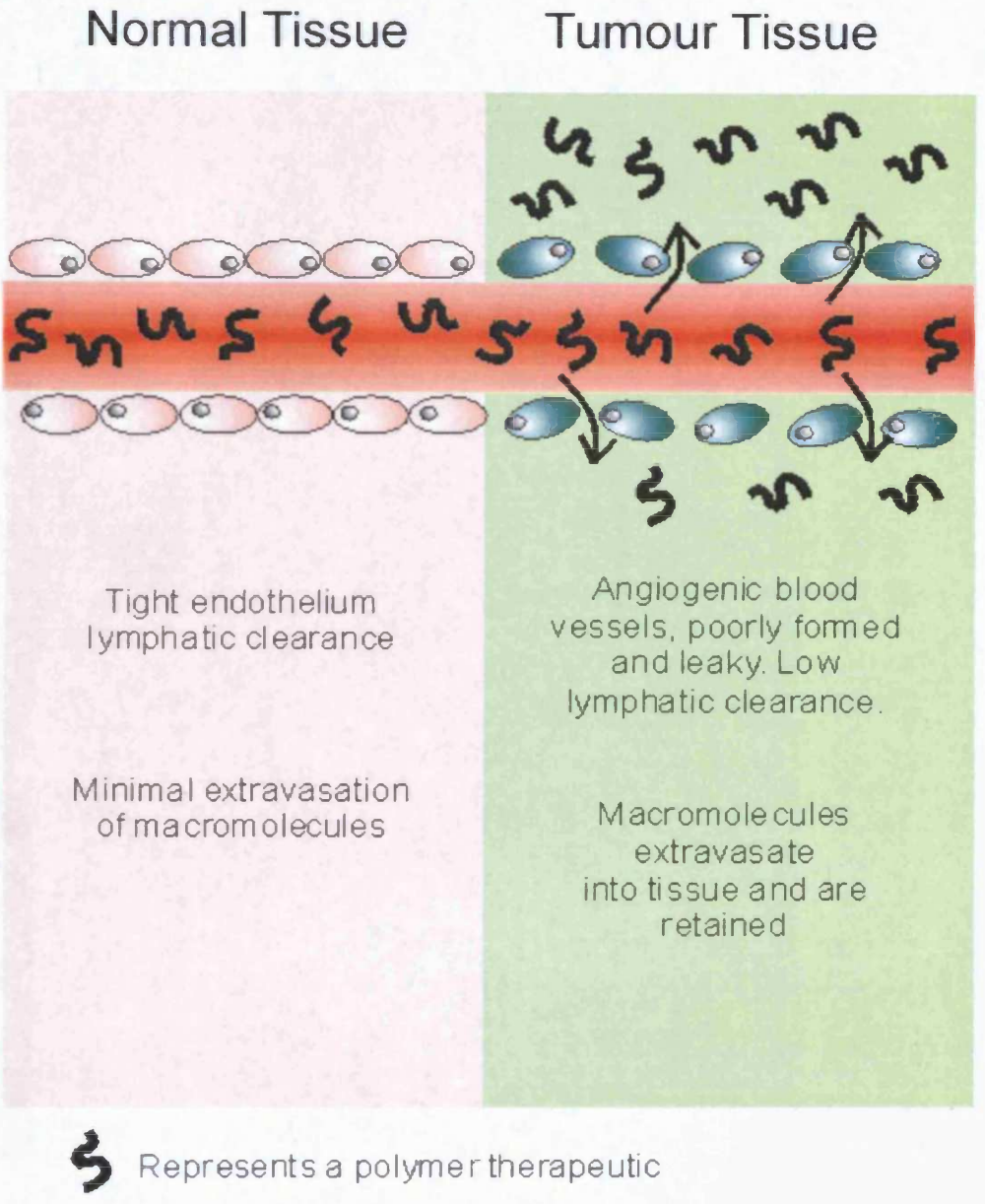

Figure 1.4 - Schematic showing the EPR effect

In normal tissue the macromolecules/nanoparticles cannot escape the vascular endothelium. In contrast cancer tissue angiogenic neovasculature is more permeable allowing them to extravasate into the interstitial space. Lympatic drainage of tumour tissues is impaired and macromolecules/nanoparticles are retained (Adapted from Duncan, 2003).

1.3.2 Ligand-Targeted Therapeutics: Types of Ligand; Advantages and Limitations

Researchers have widely embraced the concept of targeted delivery and a scientific database search on 'receptor targeted delivery' showed 862 studies (to 05/02/06), with 149 studies reported in 2005.

Ligand-targeted therapeutics refers to therapies directed against a receptor or epitope that is over-expressed in the diseased cell/tissue. It was the aim of this project to design a polyplex able to use RME to increase the internalisation of the polyplex and thereby increase the expression of a reporter gene. The targeting of cancer cells is complex as these cells are derived from normal cells but they are no longer growth regulated and can also evade attack by the immune system (Vander et al., 1994). Receptors that are being targeted in cancer therapy come from a diverse range having many different functions. Table 1.3 gives an overview of the receptors being targeted in non-viral gene therapy. Ideally a receptor or antigen is sought that is expressed only on tumour cells i.e. it is not present on cells elsewhere in the body. This is rarely, if ever, the case but cancer cells frequently over-express plasma membrane localised receptors due to their increased nutrient requirements for growth, invasion and metastasis (Prodi et al., 1998). Receptor over-expression can be used to differentiate tumour cells from normal cells and thus they provide a target for delivery systems. Although non-cancerous cells expressing the same receptors will take up targeted vector by receptor-mediated endocytosis, this uptake is expected to be less compared with uptake in cancerous cells over-expressing the receptor. The characteristics of each class of ligand are discussed below (Sections 1.3.2.1-1.3.2.4). The mechanisms involved with these receptors are often not truly characterised i.e. their endocytic pathway, rate of endocytosis. The mechanisms may also differ when the therapeutic is coupled to the ligand.

Ligands have been conjugated with the therapeutic e.g. fusion protein of urokinase and diphtheria toxin (Ramage et al., 2003), the carrier of the drug/imaging agent e.g. PK2 or form the therapeutic themselves e.g. Trastuzumab (Table 1.1). More discussion of uPAR as a target is developed in Section 1.4. The following parts of this section discuss the different targeting ligands being utilised and their advantages/disadvantages.

Table 1.3 – Receptors being targeted in cancer therapy

Target	Function	Reference
$\alpha_v\beta_3$ integrin	Cellular adhesion, over-expressed in angiogenic blood vessels	(Anwer et al., 2004)
Aminopeptidase N (CD13)	Membrane bound metalloprotease, over-expressed in angiogenic blood vessels	(Arap et al., 1998)
Folate receptor	Folate uptake, over-expressed in several cancer cells due to requirement for DNA replication	(Russell-Jones et al., 2004)
Transferrin receptor	Iron (transferrin) uptake, expressed in blood brain barrier, used in brain cancer targeted therapies	(Wagner et al., 1990)
Asialoglycoprotein receptor	Removes partially deglycosylated proteins from circulation, expressed in hepatocytes.	(Nishikawa et al., 2000)
Vasculature endothelial growth factor receptor (VEGFR)	Growth factor receptor over-expressed in angiogenic blood vessels	(Spooner et al., 2003)
Epidermal growth factor receptor (EGFR)	Growth factor receptor over-expressed in angiogenic blood vessels	(El-Rayes & LoRusso, 2004)

1.3.2.1 Antibody-Based Targeted Delivery

Much research has been focused on antibody-based targeting as this was seen to be the "magic bullet" described by Ehrlich. Recently, antibody-directed targeting has progressed to the market: gemtuzumab ozogamicin (Mylotarg®) is an antibody against CD33 conjugated to calicheamicin for the treatment of leukaemia (Wyeth, 2003). This is the first antibody-drug conjugate to enter routine clinical use. Each antibody has 2-3 molecules of calicheamicin covalently bound to it. Once the conjugate is internalised calicheamicin is released in the endosome/lysosome via the degradation of a pH-sensitive linker and binds DNA in the minor groove causing double strand breaks which kills the cell. Trastuzumab (Herceptin®) is an antibody against the epidermal growth factor receptor 2 protein (HER2) (Genetech, 2000) for treating breast cancers that is available clinically. In this case the antibody itself is the therapy. This toxicity is described as antibody-dependent cellular cytotoxicity.

Although antibody-based targeting has been the most successful strategy so far and offers very selective targeting, with tumour specific antigens such as prostate-specific membrane antigen (PSMA) (Bander et al., 2003). However, the use of antibodies has several disadvantages:

- Identification of an appropriate antigen
- Difficulties in large scale production
- Cost
- Possible immune reactions – inducing the human anti-mouse antibody response
- Large size – limits number of antibodies which can be attached to a carrier
- Size limits tumour penetration (Bagshawe, 1995, Shadidi & Sioud, 2003)
- Blood clearance can be quick
- Internalisation of antigen/antibody complex does not always occur
- Cross-reactivity with normal tissue (Ross et al., 2004)

Methods to help overcome some of these disadvantages have been developed. For example: immune reactions are reduced by the production of humanised monoclonal antibodies, clearance can be decreased by pegylation (Leong et al., 2001), antibody fragments are being used to reduce their size. Internalisation is not required in all cases, e.g. radionuclide imaging (Ke et al., 2004).

Antibody-based targeting employed in non-viral gene delivery is discussed in Section 1.5.3.

1.3.2.2 Proteins as Ligands in Targeted Delivery

For the purposes of this thesis a protein is defined as a chain of more than 20 amino acids (aa). The smallest protein described being a 20 aa Trp cage motif (Neidigh et al., 2002). Molecules with less aa are considered to be peptides, discussed in Section 1.3.2.4. Compared to antibodies proteins are easier to produce, store, are less likely to be immunogenic and are easier to specifically modify. However, many protein receptors investigated have a widespread expression in the body, e.g. the transferrin receptor (Qian et al., 2002). Protein-targeted therapy has similar problems to antibody-based targeting with their endogenous activity presenting an additional challenge.

Using transferrin-targeted poly(lactide-co-glycolide) (PLGA) paclitaxel containing nanoparticles Sahoo et al. (2004) found a greater reduction in tumour size (PC3 in mice) and increased survival compared with un-targeted nanoparticles or a paclitaxel formulation Cremophore® (Sahoo et al., 2004). In contrast, although greater tumour uptake was found using transferrin-targeted palmitoylated glycol chitosan vesicles containing doxorubicin compared with that seen using un-targeted vesicles, the targeted system was less effective in terms of antitumour activity than the free drug *in vivo* (Dufes et al., 2004). This suggests that, as tumour targeting was successful, the release of drug from the carrier must have been poor.

uPAR has been successfully targeted using a diphtheria toxin-urokinase fusion protein which showed selective toxicity in leukaemic cell lines expressing > 5000 receptors/cell (Ramage et al., 2003). This fusion protein was tested in mice against glioblastoma tumours and found to significantly regress tumours (Vallera et al., 2002). These successful studies targeting uPAR are promising indicators for this study. Protein-based targeting employed in non-viral gene delivery is discussed in Section 1.5.3.

1.3.2.3 Saccharide-Targeted Delivery

The term saccharide encompasses a wide range of molecules from simple sugars to complex polymers. Two saccharides widely employed as targeting ligands are mannose (to target the mannose receptor on macrophages (Ferkol et al., 1996)) and galactose (to target the asialoglycoprotein receptor (ASGR) on hepatocytes (Plank et al., 1992)). This targeting method has seen some success with the only actively targeted polymer-drug conjugate to reach clinical trial: PK2, an HPMA-doxorubicin-galactosamine copolymer,

which has progressed to phase I/II (Seymour et al., 2002). Both mannose and ASGR expression is, however, found on both cancerous and normal cells (Hashida et al., 2001). E-selectin, a receptor exclusively expressed in endothelial cells, has been targeted using Sialyl Lewis-X-coated PLGA microparticles containing fluorescent dyes (Eniola et al., 2002). Saccharide-based targeting employed in non-viral gene delivery is discussed in Section 1.5.3.

1.3.2.4 Peptide-Targeted Delivery

Peptide-targeted delivery has a basis in nature as many peptides are used as attachment ligands by bacteria and viruses. The use of peptides as ligands for receptor-targeting has been investigated by several groups (reviewed in Shadidi & Sioud, 2003). The approach chosen for this study uses peptides identified from the binding region of uPA. Peptide ligands have a number of advantages. These include their lower antigenic potential, making them less likely to cause an immune reaction. They are also easier to synthesise and characterise. Their smaller size means multiple peptides could be attached to a single nanoparticle conferring multivalent attachment.

The use of phage display libraries to determine binding peptides for tumour targets is a powerful method that has shown much success (Nilsson et al., 2000). This method is akin to combinatorial chemistry producing large numbers of potential molecules and selecting for them by their activity, in this case binding to the cell of interest. Essentially the technique involves the recombinant insertion of a peptide motif into the coat of the phage, application to cells and harvesting of attached phage, and the process repeated to purify the most effective phage (Nilsson et al., 2000).

Arap et al. (2002) targeted prostate cancer with a short peptide sequence (SMSIARL) derived from a prostate homing phage. This phage peptide was found to be in 15 times greater amounts in mouse prostate than a control peptide, signifying that targeting had been successful (Arap et al., 2002). In a fusion between this peptide and a proapoptotic peptide they found tissue destruction in the prostate and delayed development of cancer in prostate cancer prone transgenic mice (Arap et al., 2002). Phage display experiments are usually carried out using cell culture and the results are therefore less physiologically relevant. *In vivo* selection of phage has also been developed with great success (Reviewed in Trepel et al., 2002). However, the *in vivo* panning is made in animal models and therefore may have less specificity for human

targets. This limitation of murine models may have been overcome using *ex vivo* panning on human umbilical veins. The latter model has identified a heptapeptide that bound 5 times more efficiently to HUVEC (human umbilical vascular endothelial cells) than to B16F10 (murine melanoma) and other cell lines (Maruta et al., 2003).

The most widely investigated receptor family for targeting with peptide ligands is the integrin family. These receptors are expressed on the neo-vasculature of various tumours and are involved in adhesion and cell signalling (Vander et al., 1994). Their peptide ligands are defined as arginine-glycine-aspartic acid (RGD) peptides, and comprise a range of linear and cyclic peptides containing the RGD motif (Arap et al., 1998). Arap et al. (1998) found that mice treated with RGD-targeted doxorubicin had greater survival than mice treated with doxorubicin alone in a murine tumour model. Many other targets are being investigated with peptide ligands targeting the tumour vasculature, cancer cell surface and surface immunoglobulins (reviewed in Shadidi & Sioud, 2003).

Such peptide ligands can be easily prepared in bulk quantities using peptide synthesis. Peptide synthesis is a procedure that involves the activation of carboxylic acids and their reaction with amines to produce a peptide bond. However, as aa contain both a carboxylic acid group and an amino group the amine is first protected to prevent unwanted reactions. This protected aa can then be activated and reacted with an unprotected aa to give the dipeptide. The protecting group is then removed resulting in the dipeptide product desired. The synthesis of peptides and proteins was simplified by Merrifield who won the Nobel Prize in chemistry in 1984 for developing an automated solid phase peptide synthesis (Solomons, 1996). In this advance the C-terminal aa is attached to a resin and the subsequent aa added in deprotection, washing, addition with activator, washing, deprotection etc. until all aa have been added and the peptide is cleaved from the resin (as described in Section 2.3.10).

The peptides studied in this thesis, CLNGGTC (u7) and VSNKYFSNIHW (u11) (Fig. 1.5), were identified and selected from the binding region of uPA (Appella et al., 1987). Their smaller size compared with uPA means that one would expect less disruption in the formation of polyplexes. The use of such peptides also removes the catalytic activity of uPA, preventing degradation of the extracellular matrix during use. u7 has been seen to increase the uptake of adenovirus in human airway epithelia (Drapkin et al., 2000).

A)

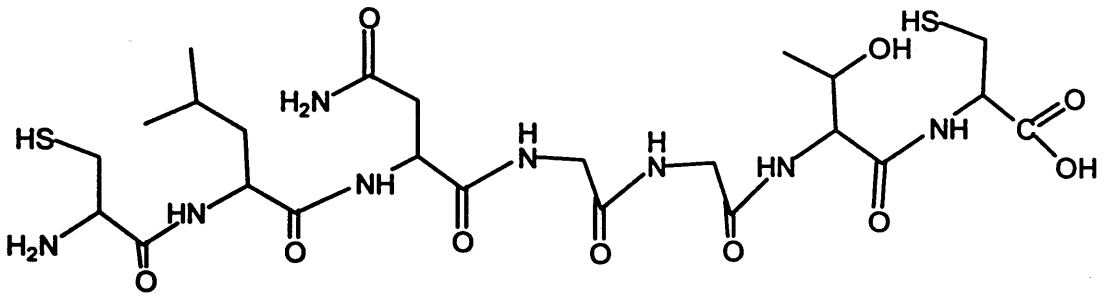

Cysteine-----Leucine---Asparagine---Glycine---Glycine---Threonine---Cysteine

B)

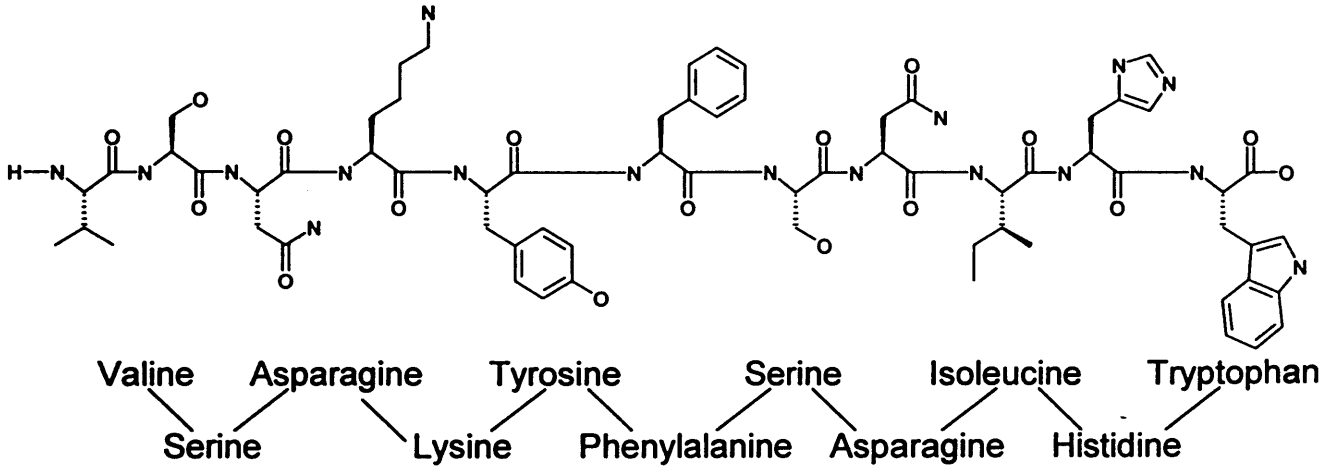

Figure 1.5 – Chemical structure of peptide ligands for uPAR

Panel A) u7, single letter amino acid sequence = CLNGGTC B) u11, single letter amino acid sequence = VSNKYFSNIHW

The peptide increased adenoviral uptake when applied in solution and when conjugated to PEG attached to the viral capsid (Drapkin et al., 2000). Peptide-based targeting employed in non-viral gene delivery is discussed in more detail in Section 1.5.3.

Having discussed the need for improved therapy and the methods employed to target therapies, the uPA receptor and its use as a novel target are now examined.

1.4 Rationale for the Choice of uPAR as a Target

A cancer cell receptor of increasing interest for targeting is uPAR. Though currently less well understood than many of the other targets being investigated, this receptor may show advantages for targeting either for novel therapeutics or delivery systems. In this section the role, presence and targeting potential of uPAR are described.

1.4.1 Physiological Role and Functions of uPAR

uPAR, also designated CD87, it is a glycosylphosphatidyl inositol (GPI)-linked receptor of approximately 55 kDa. This GPI linkage means that the protein is attached to the cell membrane at the C-terminal aa only (Fig. 1.6). It is composed of three similar disulphide bonded domains (Fig. 1.7; (Blasi & Carmeliet, 2002)). The crystal structure of the soluble (cleaved at the GPI link) receptor was recently solved with a non-natural peptide ligand antagonist bound (AE147) (Llinas et al., 2005). There is a central cavity 19 Å deep formed between the three domains where the antagonist peptide binds (Llinas et al., 2005). It has been proposed that uPA also binds in this cavity (Llinas et al., 2005). The primary function of uPAR is to bind uPA, which catalyses plasminogen activation to plasmin (Ramage et al., 2003). Plasmin is a serine protease that hydrolyses peptide bonds in fibrin clots and thus prevents thrombosis (Fig. 1.8; (Stryer, 1995)).

By binding uPA at the surface of the cell, uPAR focalises the activity of uPA. It is suggested that this enables cell migration through the digestion of extracellular molecules (Blasi & Carmeliet, 2002). The binding of uPA to uPAR is a high affinity interaction with a K_d in the low nM range 0.1 - 17 nM (Picone et al., 1989). This makes it particularly attractive in the concept of receptor targeting. The affinity of uPA for uPAR expressed in a (uPAR) transfected cell line (LB6, murine fibroblast) was reported as 1-10 nM (Roldan et al., 1990).

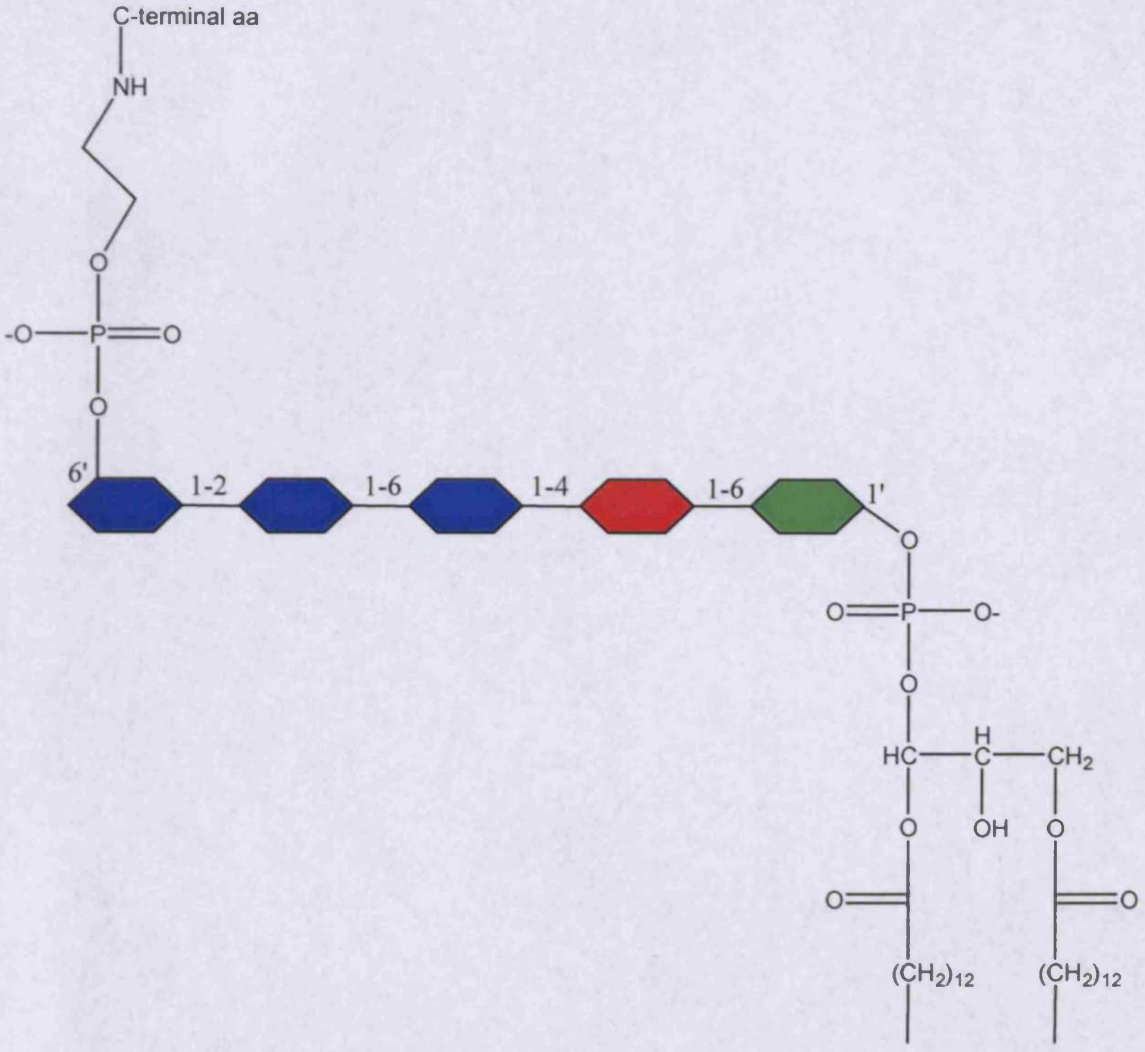

Figure 1.6 - GPI anchor structure

Diagrammatic representation of the general structure of a GPI linkage. Blue hexagons represent mannose, red hexagon represents glucosamine and green hexagon represents inositol. The saccharide linkage is shown between the sugars. The oligosaccharide unit is variable between GPI linked proteins, the glycerol phosphate and phosphoethanolamine units are conserved (adapted from Doering et al., 1990).

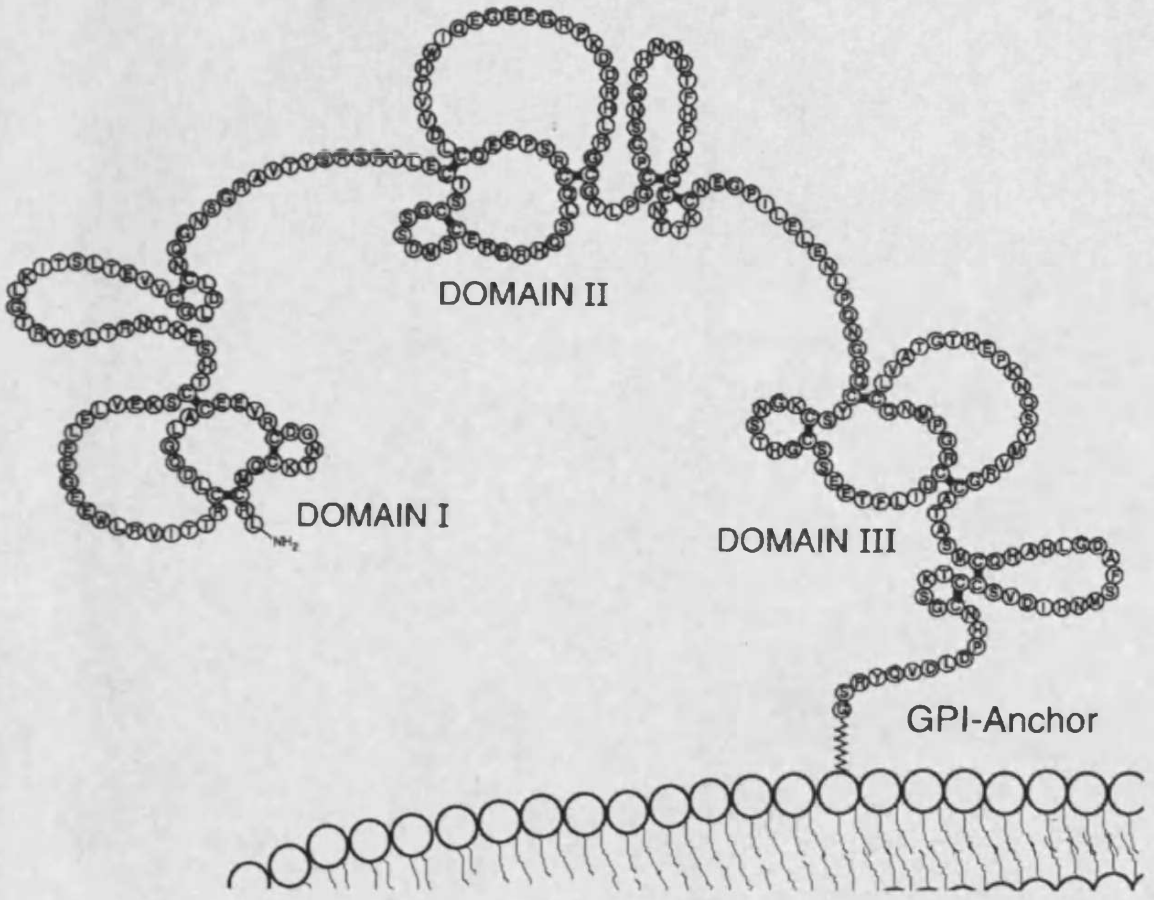

Figure 1.7 - Amino acid sequence and predicted structure of uPAR

uPA binds to domain I and may form a composite binding with domain II. Black bars between cysteine residues indicate disulphide connections (adapted from Ploug et al., 2002).

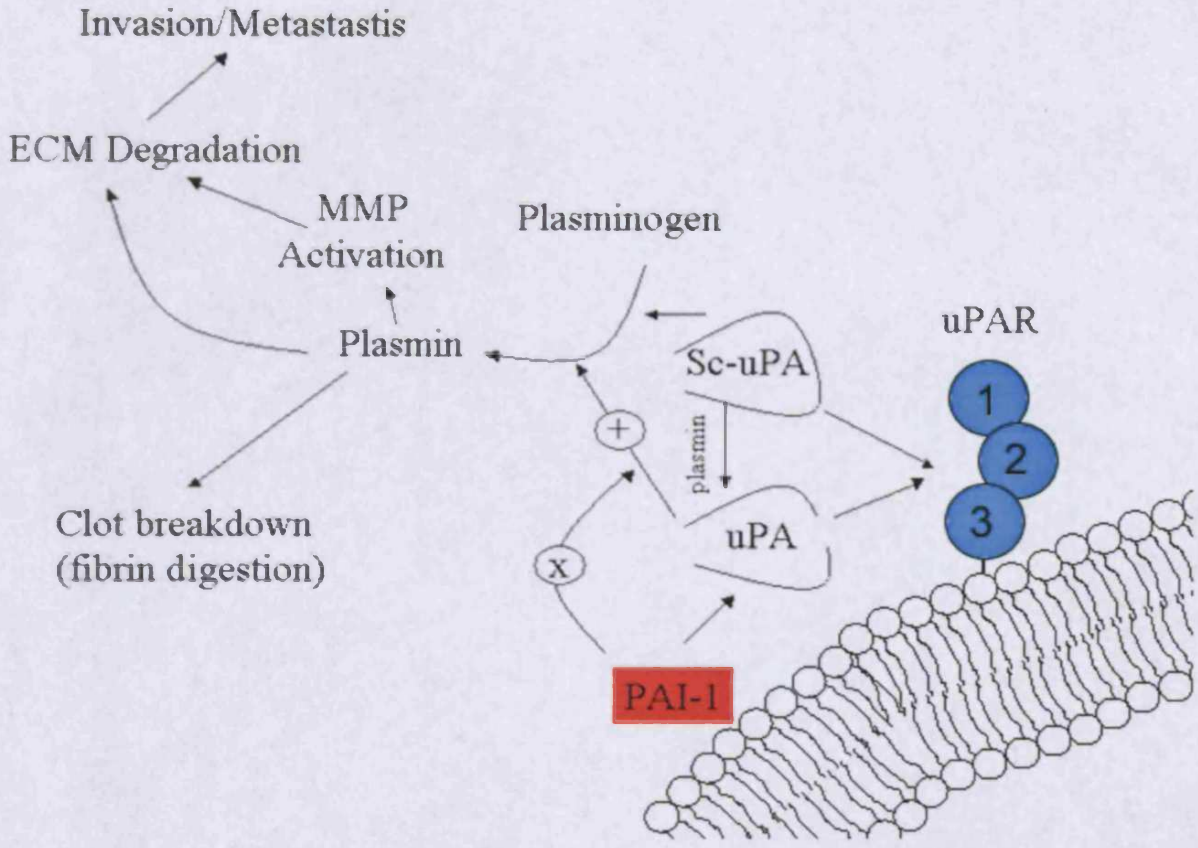

Figure 1.8 - Physiological role of the uPA system

Key; Sc-uPA = Single chain (pro) urokinase plasminogen activator, uPA = urokinase plasminogen activator, uPAR = urokinase plasminogen activator receptor (having domains 1,2 & 3), PAI-1 = plasminogen activator inhibor 1, ECM = Extra cellular matrix, MMP = Matrix metalloproteinases (Compiled from: Blasi & Carmeliet, 2002, Ploug et al., 2002, Vander et al., 1994)

uPAR is endogenously expressed on the surface of many normal cell types including: blood neutrophils, eosinophils, monocytes, bone marrow, CD34 negative myelomonocytic precursors, mast cells, fibroblasts, fetal thyroid cells, and endothelial cells (Lanza et al., 1998, Nykjaer et al., 1994b, Plesner et al., 1997, Sillaber et al., 1997). This expression is a disadvantage for targeting as these cells would also take up the targeted therapeutic. However, receptor expression on these cells is lower than in cancerous cells.

uPA is secreted as pro-uPA or sc-uPA which are the single chain form with a molecular weight of 55 kDa (Ghosh et al., 2000b). This secretion is performed by many cell types including neutrophils, endothelial and epithelial cells (Abraham et al., 2003, Ghosh et al., 2000a). The single chain protein is cleaved by plasmin at the Lys^{158}-Ile^{159} site to give an activated two chain form linked by cystine bonds (Mazar et al., 1999). In addition to activation by plasmin, activation of sc-uPA by kallikrein, mast cell tryptase, T cell-associated serine proteinase and cathepsin B are also reported (Ghosh et al., 2000b, Kobayashi et al., 1991).

uPA binds to domain I in the amino terminal portion of uPAR (Fig. 1.7). It was later suggested that domains I and III form a composite binding site for uPA (Blasi & Carmeliet, 2002), and, as suggested by Llinas et al. (2005), all three domains may make a cavity which binds uPA. Soluble uPAR is formed through the cleavage of the GPI anchor (Blasi & Carmeliet, 2002). Cleavage of uPAR can be made by several different enzymes including trypsin, chymotrypsin, human neutrophil elastase, phospholipase C (Ploug et al., 2002) and plasmin itself producing the fragments domain 1, domain 2/domain 3 (Montuori et al., 2002). As uPAR is a GPI linked receptor it does not have an intracellular signalling domain, which is the case for many other receptors (Wise et al., 2002).

Plasminogen activator inhibitor (PAI-1) is the primary physiological inhibitor of uPA and tissue-type plasminogen activator. It is a multi-functional serine protease inhibitor (serpin) protein that is also involved in many other physiological and pathophysiological processes (Wind et al., 2002). PAI-1 binds to uPA (but not sc-uPA) stopping its catalytic activity both in circulation and when attached to the receptor (Goretzki & Mueller, 1997). It can both inhibit invasion (through inactivation of proteolytic activity) and promote it (through disruption of cell adhesion) (Bajou et al., 2004, Degryse et al., 2001, Deng et al., 1996).

In addition to the many specific components of the uPA system shown in Fig. 1.8, internalisation of uPAR is complex. It proceeds after the recruitment of other cell membrane components (Blasi, 1997, Blasi & Carmeliet, 2002, Nykjaer et al., 1998, Nykjaer et al., 1997, Nykjaer et al., 1994a). There appears to be many mechanisms by which uPAR internalisation can occur. An understanding of the endocytic fate is important to the proposed use of uPAR as a target and it is discussed in detail in Section 1.4.3.

1.4.2 Evidence for Over-Expression of uPAR in Cancer

It has been shown that uPAR is over-expressed in a variety of cancers including: monocytic, myelogenous and megakaryocytic leukemias (Lanza et al., 1998, Plesner et al., 1994), bladder transitional carcinomas (Carriero et al., 1997), thyroid (Hudson & McReynolds, 1997), stomach (Plebani et al., 1997), liver (De Petro et al., 1998), pleura (Shetty & Idell, 1998), lung (Morita et al., 1998), pancreatic (Taniguchi et al., 1998), ovarian (Sier et al., 1998) cancers and glioblastomas (Mori et al., 2000). The upregulation of uPAR has also been shown in prostate cancer cell lines by microarray analysis (Han et al., 2002). This group found an increase (2.2x to 10.3x) in several cell lines in comparison with normal pancreas cells (Han et al., 2002). Lanza et al. (1998) found that those patients with acute myeloid leukaemia (M5 French-British-American subtype) having the worst survival rates showed a significant increase in uPAR levels ($>12x10^3$ antibody binding capacity (ABC)/cell compared to $<12x10^3$ ABC/cell) in their tumour (Lanza et al., 1998). It was also shown that high uPAR expression was associated with chromosome abnormalities and disease relapse (Lanza et al., 1998). Similarly, Suzuki et al. (1998) reported that expression of uPAR in colorectal carcinomas correlated with increasing disease severity, whereas there was no detectable expression in matched normal cells.

The number of uPAR receptors expressed per cell has been determined using radioligand binding assays for several cell lines. U937 (human histocytic lymphoma monocyte) cells have ~31000 receptors/cell and MCF-7 (human breast cancer epithelial) cells have ~4600 receptors/cell (Rajagopal & Kreitman, 2000). All prostate cancer cells (Gleason score 4-9) tested by Garilov et al. (2001) were positive for uPAR protein expression. The Gleason score, or grade, is an indicator of how differentiated the tumour cells are. Well differentiated cells (i.e. normal cells) have a score of 1 and poorly differentiated cells have higher scores. Overall it is apparent that in many cancers

uPAR is over-expressed with good correlation between the expression of uPAR and the invasiveness/metastatic potential of the cancer. One important factor is that uPA/uPAR focalises the conversion of plasminogen to plasmin. Plasmin then digests fibrin extracellular matrix (ECM) and this subsequently facilitates metastasis and invasion. Plasmin has also been shown to activate precursors of matrix metalloproteinases which are also involved in ECM degradation which would be expected to potentiate the effect (Murphy & Gavrilovic, 1999).

The expression of uPA and PAI-1 also seems to be increased in several cancers (De Petro et al., 1998, Gavrilov et al., 2001, Mori et al., 2000, Morita et al., 1998). uPA has also been shown to release fibroblast growth factor 2 (FGF2) from the ECM (Ribatti et al., 1999), and this can be cleaved by matrix metalloproteinase 9 to form angiostatin (Patterson & Sang, 1997). The formation of angiostatin from uPA shows adroit control over the angiogenic/angiostatic mechanism and the complex interplay between molecules in the body. The non-catalytic amino terminal fragment was not found to be angiogenic as it does not release FGF2 from the ECM (Ribatti et al., 1999). Binding of uPA to uPAR provokes a mitogenic response as does the amino terminal fragment and cyclic uPA_{19-31} (disulphide bridge between cysteins, CVSNKYFSNIHWC) in human ovarian cancer cells (Fischer et al., 1998). The cell model used was treated with antisense against uPA to reduce the auto/paracrine effect on cells and the cyclic peptide was added at a 12x higher molar concentration than uPA, these factors may have contributed to the observed increase in cell proliferation. The amino terminal fragment was not found to induce proliferation of breast cancer cells (8701-BC cells) (Luparello & Del Rosso, 1996).

1.4.3 Interactions of Membrane Components with uPAR

GPI-linked receptor internalisation is poorly understood in comparison with transmembrane receptors. However, internalisation of uPAR proceeds after recruitment of various cell membrane components. The endocytosis of uPAR has been observed through several different mechanisms which are summarised in Fig. 1.9. Both clathrin-mediated and non-clathrin mediated endocytosis of uPAR have been reported (Vilhardt et al., 1999). Clathrin-mediated endocytosis has been more widely studied and characterised (Slepnev & Camilli, 1998).

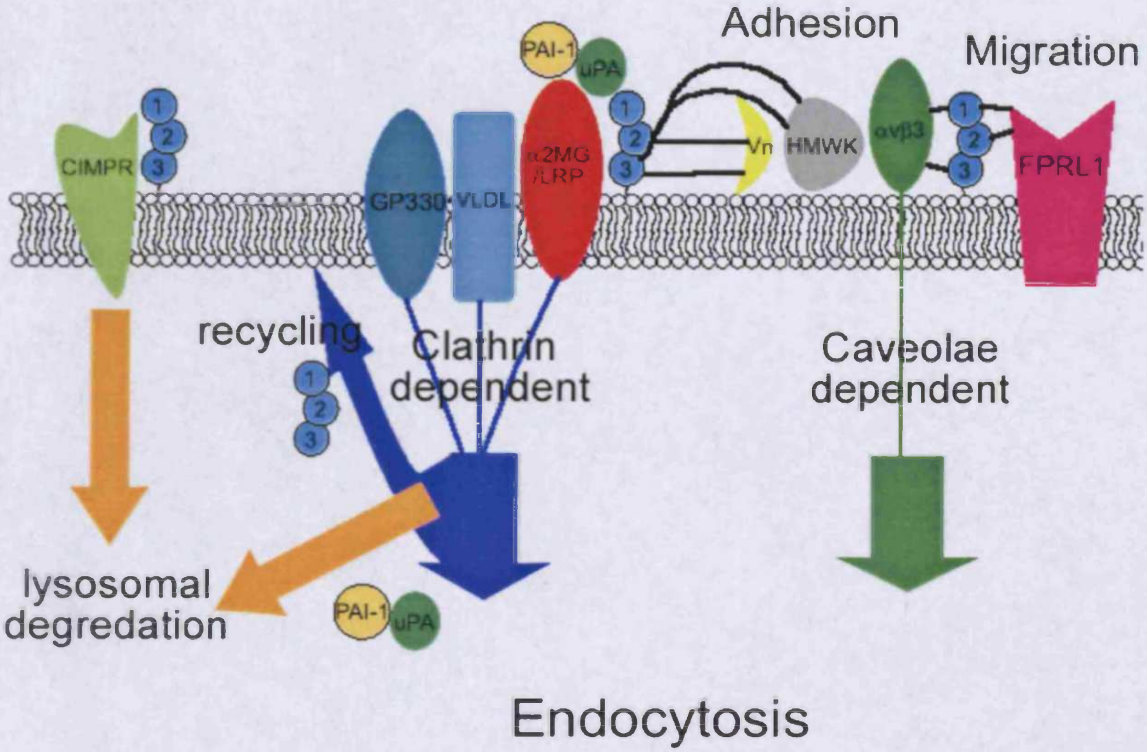

Figure 1.9 - Co-receptors that interact with uPAR

Key: CIMPR – cation independent mannose-6-phosphate receptor; GP330 – glycoprotein 330; VLDL – very low density lipoprotein receptor; α2MG/LRP – α2-macroglobulin receptor/lipoprotein related receptor; Vn – vitronectin, HMWK – high molecular weight kallikrine; αvβ3 – $\alpha_v\beta_3$ integrin; FPRL1 – formyl like peptide receptor (Compiled from: Andreasen et al., 2000, Blasi & Carmeliet, 2002, Brown & London, 1998, Czekay et al., 2001, Moestrup et al., 1993, Nykjaer et al., 1998, Nykjaer et al., 1997, Nykjaer et al., 1994a)

Clathrin is a protein found on the cytosolic side of the cell. It consists of three heavy chains (180 kDa) and three light chains (~35 kDa) (Stryer, 1995). These chains come together to form a three legged structure, a triskelion, which forms into a lattice and creates a coating around endocytic vesicles as they form (Stryer, 1995). The release of this polyhedral lattice constructed from pentagons and hexagons formed from triskelions of clathrin is facilitated by an adenosine triphosphate (ATP)-driven uncoating enzyme (Stryer, 1995).

The low density lipoprotein receptor family are most heavily implicated in the endocytosis of uPAR. These receptors are commonly found in lipid rafts (Brown & London, 1998) and are endocytosed in clathrin coated pits. This family includes low density lipoprotein related protein (LDLRP) (Czekay et al., 2001), α-2-macroglobulin/lipoprotein receptor protein (Nykjaer et al., 1994a), very low density lipoprotein receptor (VLDL) (Nykjaer et al., 1997) and glycoprotein 330 (megalin) receptor (Moestrup et al., 1993). These receptors are involved in the internalisation of hydrophobic metabolites.

Integrins and the formyl like peptide receptor protein (FLPR) have both been reported to be recruited in uPAR endocytosis, with integrins being associated with uPAR in caveolae (Blasi & Carmeliet, 2002) (Fig. 1.9). However, on the surface of the cells the interaction with integrins, vitronectin, high molecular weight kallikrein and fibronectin is thought to be an adhesive role or one that mediates intracellular signalling events (Andreasen et al., 2000, Liu et al., 2002, Wei et al., 1996, Wei et al., 1999).

It has been suggested that particles up to 200 nm can be endocytosed by a clathrin-dependent pathway, whereas particles between 200 nm and 500 nm rely on caveolae for internalisation in B16-F10 cells (murine melanoma) (Rejman et al., 2004). This fact, in conjunction with the knowledge that uPAR is endocytosed in conjunction with LDLRP in clathrin-coated vesicles and it is transported to the early endosome (Czekay et al., 2001), means that some degree of control over the endocytic pathway may be gained from adjusting ligand-polyplex size to < 200 nm.

Endocytosis, endocytic mechanisms and intracellular trafficking are often studied using fluorescent probes and they can be utilised in live cell imaging experiments. In addition to labelling with fluorescent dyes the use of fluorescent protein as genetically engineered fusion proteins (e.g. green fluorescent protein tagging) has also enabled a greater understanding of intracellular pathways (for a review see Watson et al., 2005).

After endocytosis uPAR has been shown to be recycled to the membrane without degradation in human monocyte-like U937 cells and in murine LB6 clone 19 cells, a mouse cell line transfected to overexpress the human uPAR (Nykjaer et al., 1997). The endocytosis in U937 cells is an interesting case both because this is the most widely studied cell line with regards to uPAR and because there is a fusion between the mixed-lineage leukaemia translocated to 10 gene and the gene coding for phosphatidylinositol-binding clathrin assembly protein (Cottier et al., 2004). This may mean that this pathway is aberrant in this cell line (Cottier et al., 2004). Through a different endocytic mechanism uPAR has been shown to associate with the cation-independent mannose 6-phosphate insulin-like growth factor-II receptor independent of uPA for endocytosis and lysosomal degradation in human fibroblasts (Nykjaer et al., 1998).

1.4.4 Targeting uPAR

Clearly, uPAR presents a new and interesting target that has the potential to promote tumour-specific drug delivery. Indeed, a German company, Wilex, has several small molecule and antibody products aimed at the urokinase system in clinical trials (Wilex, 2005). These include a small molecule serine protease inhibitor (WX-UK1) in two Phase 1b clinical trials (Wilex, 2005). Wilex are also testing an orally available small molecule serine protease inhibitor (WX-671) to block metastasis and tumour growth in Phase I clinical trials (Wilex, 2005). Small molecule uPA inhibitors are being developed, as are ligands for soluble uPAR (Wilex, 2005).

An alternative approach has been to target uPAR using a diphtheria toxin/urokinase fusion protein (Ramage et al., 2003, Vallera et al., 2002). A recombinant fusion protein of the amino terminal fragment of uPA to diphtheria toxin (DTAT) was made (Vallera et al., 2002). An *in vitro* assay using human glioblastoma cells (U118MG) showed that DTAT toxicity had an IC_{50} <1 nM. *In vivo* DTAT regressed U118MG tumours in mice (Vallera et al., 2002). DTAT toxicity, tested against acute myeloid leukaemia (AML) cells expressing uPAR *in vitro*, correlated with uPAR expression (Ramage et al., 2003). Fusion proteins of ATF with pseudomonas exotoxin have also been made, these were shown to be endocytosed without the α_2-macroglobulin receptor with cytotoxicity being retained; IC_{50} = 2.8 pM in MCF7 cells (Rajagopal & Kreitman, 2000). So far, few studies have used uPAR as a target to improve gene therapy. Some of the advantages/disadvantages of targeting uPAR that have been identified are in Table 1.4.

Table 1.4 Summary of avantages and disadvantages of uPAR as a target

Potential Advantages	Potential Disadvantages
Over-expressed in many solid tumours	uPA is also over-expressed – increasing receptor competition
Endocytosed in conjunction with many membrane receptors – downregulation of one endocytic partner may not prevent endocytosis	Different pathways of receptor endocytosis – less control over fate of therapeutic
High affinity ligand – uPA has a 0.1-20 nM affinity for uPAR	uPAR can be cleaved from the membrane – therapeutic may bind cleaved uPAR in the circulation
Novel target – may succeed where other therapies have failed	uPAR expression on normal cells – would lead to uptake of therapeutic in non-cancerous cells

In a similar approach we hypothesise that peptides derived from the uPA ATF binding region may have ligand properties to uPAR. Therefore, the aim of this project was to use the u7 peptide, shown by Drapkin et al. (2000) to increase adenoviral uptake, and the u11 peptide, identified from the binding region determined by Apella et al. (1987), to target the over-expressed uPAR on cancer cells and hijack its entry into the cell as a means to internalise a non-viral gene therapy.

In the study by Drapkin et al. (2000) adenovirus was modified with bifunctional PEG and the u7 peptide conjugated. These surface modified adenoviruses were applied to the surface of excised human airway epithelia and β-galactosidase expression was found to be 10-fold higher than adenovirus coated with PEG or adenovirus coated with PEG and a mutated u7 peptide (Drapkin et al., 2000). The u11 sequence was proposed by Appella et al. (1987) as essential to the binding specificity of uPA whereas the u7 sequence has homology with the EGF growth factor domain (Appella et al., 1987).

1.5 Cancer Gene Therapy

Introducing a gene to correct a defect in the genetic makeup of a cell is an attractive strategy for the treatment of many diseases including cancer. The completion of the human genome project gives us a plethora of information from which we can source targets and design therapies against them (Venter et al., 2001). With increasing knowledge, the methods employed in gene therapy are almost as varied as the diseases under attack. These include: DNA immunisation (Toda et al., 1998), GDEPT/VDEPT (Chung-Faye et al., 2001, Martiniello-Wilks et al., 2004), restoration of a cell checkpoint protein (Dolivet et al., 2002), cytokine introduction, inhibition of tumour angiogenesis, gene silencing/antisense (Brooks, 2002, Lattime & Gerson, 1999). Through the last decade the main challenge in the above mentioned therapies has been difficulties in achieving successful delivery of the genetic material through the circulation to the target tissue and then to the correct compartment of the target cell.

1.5.1 Viral Vectors in Gene Therapy

The majority of gene therapy that has progressed to clinical trials is viral (69.2 %; Fig. 1.10; (Edelstein, 2005)) with polymeric delivery agents having just arrived at the clinical setting (Ohana et al., 2004).

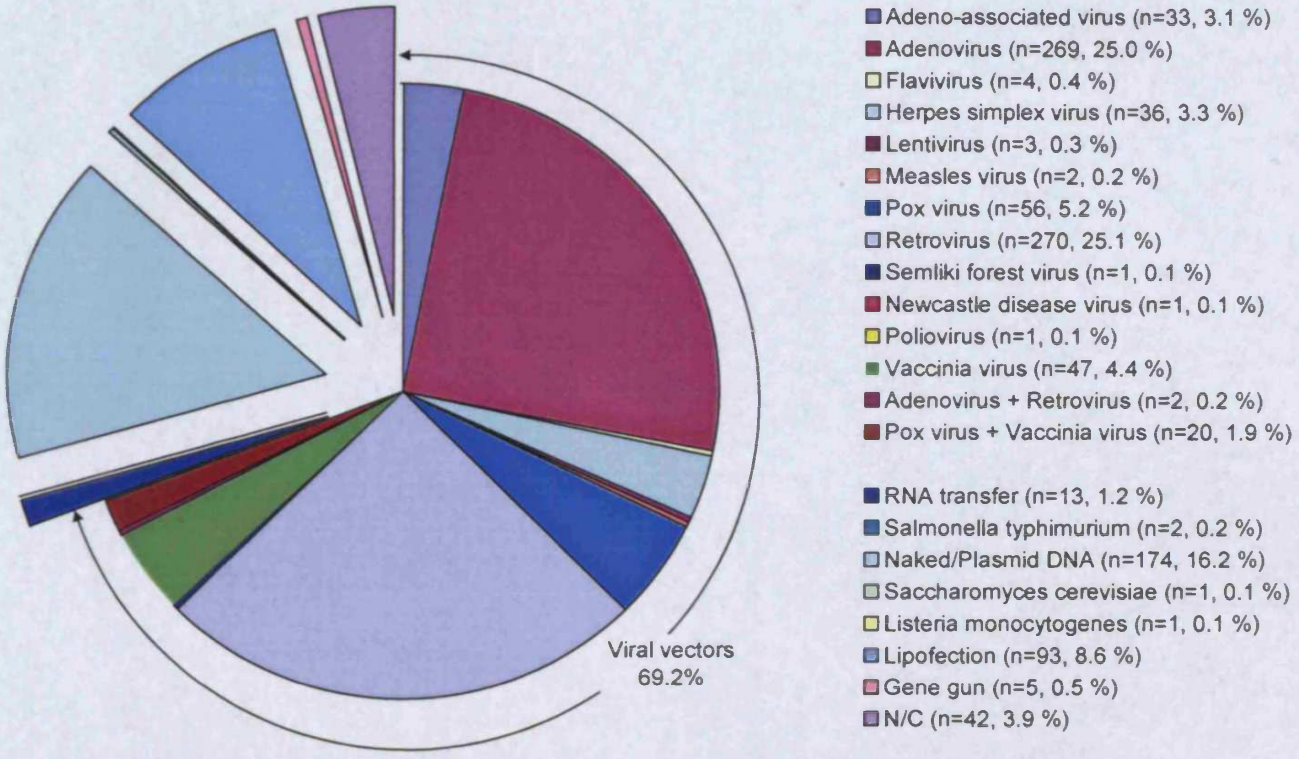

Figure 1.10 - Gene therapy clinical trial vectors

Analysis of gene delivery vectors in clinical trials worldwide (adapted from Edelstein, 2005)

Viral vectors include: adenovirus (St George, 2003), adeno-associated virus (Porteus et al., 2003), lentivirus (Rubinson et al., 2003) and retrovirus (Kafienah et al., 2003). However, with the development of leukaemia in two of the ten children treated in the Cavazzana-Calvo (Cavazzana-Calvo et al., 2000) trial treating children with X-linked severe combined immunodeficiency (X-SCID) there is a great deal of concern (Check, 2003, Kohn et al., 2003, Lemoine, 2002). This has not stopped the Chinese approval of Gendicine®, a replication-deficient adenoviral vector carrying the p53 gene (Surendran, 2004). A similar viral carrier is in late stage clinical trials in the USA (Lane, 2004).

Viral gene therapy is characterised by high efficiency of gene transfer and possible long-term gene incorporation, although it is thought that this incorporation into actively replicating genes is responsible for unwanted gene expression i.e. insertional mutagenesis such as the leukaemia found in X-SCID children (Check, 2003).

Targeting, or re-targeting, has not been ignored by those pursuing viral gene delivery and re-targeting of viral vectors has been attempted with some success (Buning et al., 2003, Drapkin et al., 2000, Wickham, 2003). However, Reddy et al. (2001) attempted to re-target retrovirus and adenovirus particles to the folate receptor, they found uptake, but no gene expression (Reddy et al., 2001). This may have been due to the virus being unable to escape the cell compartment into which it was internalised. Parker et al. (2005) successfully re-targeted HPMA-coated adenovirus with a peptide (SIGYPLP) to achieve efficient and specific uptake in HUVEC.

Many problems exist in the re-targeting of viral vectors as they have endogenous ligands in their viral coat. Adenoviral attachment is governed by coxsackievirus and adenovirus receptor (CAR), this and other attachment ligands must be removed and the 'new' targeting ligand expressed (Wickham, 2003). In this recombinant approach the targeting molecule has successfully been expressed but often results in low viral titer (Wickham, 2003).

The main problems with viral vectors are their immunogenicity, limited gene carrying capacity, manufacturing difficulties and the possibility of integration into an active gene. These factors have prompted a wider exploration of non-viral gene delivery systems (Fig. 1.11).

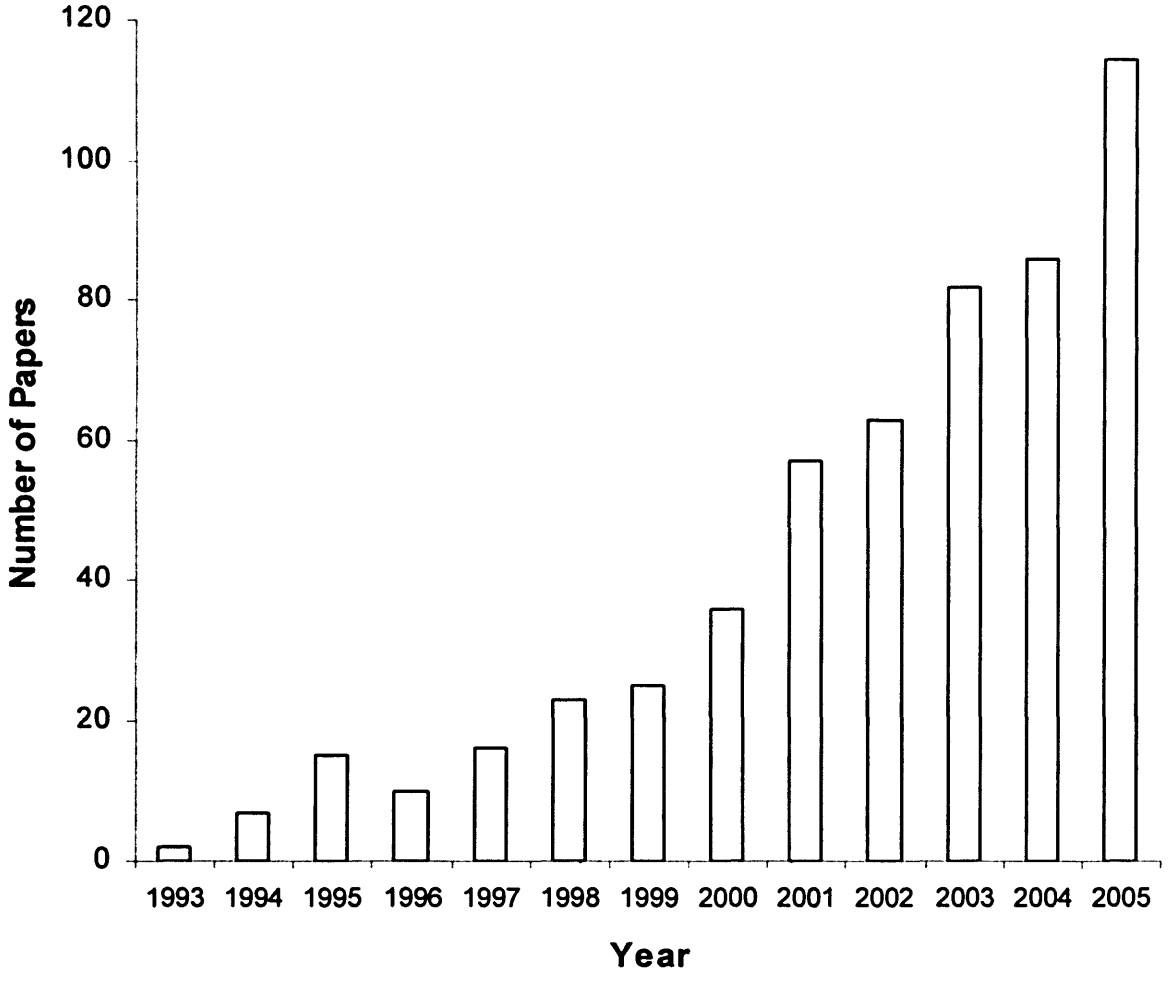

Figure 1.11 - Non-viral gene therapy studies published over the past decade

The number of articles published each year returned by pubmed (www.ncbi.nlm.nih.gov) when queried with "non-viral gene therapy". The total number of articles listed was 567.

1.5.2 Non-Viral Gene Delivery

Non-viral gene delivery encompasses the many different methods which do not use a virus as a vector, however, in this dissertation it refers to lipid-based (lipoplex) or polymer-based (polyplex) transfection agents. Electroporation, gene gun, naked DNA and other non-viral gene delivery methods will not be further considered.

Lipoplexes are formed through the interaction of cationic lipids with the negative charge on DNA. Lipofectamine (2,3-dioleyloxy-N-(2(spermine carbocamido)ethyl)-N,N-dimethyl-1-propanaminium trifluoroacetate (DOSPA) : di-oleoyl phosphatidylethanolamine (DOPE) : cholesterol (3:1:3.36)) (Mahato et al., 2003) and di-oleoyl phosphatidylcholine (DOPC)/DOPE/di-oleoyl trimethylammonium propane (DOTAP) liposomes (Safinya, 2001) are commonly used vectors. Lipoplexes have gained interest in gene therapy and 87 (8.5 %) clinical trials using lipid-based gene therapy have been reported (Edelstein, 2005). Targeted-lipoplexes are discussed further in Section 1.5.3.1.

Polyplexes (Gebhart, 2001) are particles formed through interaction of the positive charge on the polymer with the negative charge on DNA (Gebhart & Kabanov, 2001). When low polymer (+ve) : nucleic acid (-ve) ratios are used polyplexes form aggregates (dependent on the type of polymer). At higher ratios of polymer : nucleic acid the polyplexes are soluble, small and positively charged (Ogris & Wagner, 2002a). Protection of the nucleic acids against DNAses is conferred by the electrostatic interaction with cationic molecules which increases DNA stability in solution and increases the half-life in the circulation (Kircheis et al., 2001b). The electrostatic interaction also condenses the DNA to produce a smaller molecule (Lee et al., 2001). These properties make cationic polymers an interesting delivery vehicle in non-viral gene therapy. The negative charge on DNA, which would hinder entry to the cell due to the negative charges found on the plasma membrane, is balanced or made positive by the polymer and DNA condensation enables easier entry into the cell. A large number of studies have tried to develop non-viral vectors and many cationic polymers have been used; Table 1.5 lists some of the polymeric vectors being investigated. Discussion of the most widely studied cationic polymeric vector, PEI, is made below (Section 1.5.2.1.1) followed by discussion of the more biocompatible vector, chitosan, chosen for this study (Section 1.5.2.1.2).

Table 1.5 – Polymeric non-viral gene delivery vectors

Polymer	Cell lines / *in vivo*	Molecular weight (kDa)	Reference
PEI (linear)	Primary duckling hepatocytes, Caco2, KB, KBv, COS7, C2C12, MCF7, MCF7 ADR, LLC-PK1, LLC-MDR1, CT26 / ducklings, tree shrews, Wistar rats, human bladder carcinoma (clinical trial)	0.8, 22, 50	(Chemin et al., 1998, Gebhart & Kabanov, 2001, Ohana et al., 2004)
PEI (branched)	Caco2, KB, KBv, COS7, C2C12, MCF7, MCF7 ADR, LLC-PK1, LLC-MDR1, CT26	25	(Gebhart & Kabanov, 2001)
Chitosan	A549, B16, MG63, HEK293, HeLa / Balb/c mice, AKR/J mice	1.2-4.7, 40, 84, 150, 390, 400, 600	(Corsi et al., 2003, Erbacher et al., 1998, Ishii et al., 2001, Koping-Hoggard et al., 2003, Roy et al., 1999)
Poly(β-amino) esters	COS-7, NIH 3T3	1-50 (library of polymers)	(Akinc et al., 2003)
Poly(amidoamine)	HepG2	ISA1 = 12.3 ISA4 = 15 ISA22 = 16.5 ISA23 = 14.9	(Richardson et al., 2001)
Poly(amidoamine) dendrimers	CV1 / BALB/c mice	467, 10.4 – 233.3	(Kukowska-Latallo et al., 2000, Tang et al., 1996)
Poly-L-lysine	HuH7 / C57-BL6 mice	9.7, 53.7	(Ziady et al., 1999)
Diethylaminoethyl (DEAE)-Dextran	Primary human macrophages	Not stated	(Mack et al., 1998)
Poly(2-dimethylamino) ethyl methacrylate (pDMAEMA)	COS7	45, 360	(Cherng et al., 1996)
Polyphosphazines	COS7	100, 300	(Luten et al., 2003)
Polybrene/DMSO	J774, HL60	Not stated	(Chisholm & Symonds, 1988)

Non-viral gene delivery systems have several advantages over viral vectors. These include (i) the size of DNA incorporated is largely unlimited, (ii) they can display low toxicity and repeated administration can be made without provoking an immune reaction and (iii) there is greater control over production and characterisation of the vector and the vector/DNA complexes.

1.5.2.1 Cationic Polymers in Non-viral Gene Delivery

1.5.2.1.1 Poly(ethylenimine) as a Non-viral Vector

The most widely studied cationic polymeric vector is PEI (von Harpe et al., 2000). This vector has a high cationic charge density producing efficient transfection (Boussif et al., 1995). The mechanism of endosomal escape has been widely debated. Studies suggest that the PEI polyplex is taken up into endosomes where the pH is buffered causing osmotic swelling and endosomal membrane rupture. This has been termed the 'proton sponge effect' (Boussif et al., 1995, Cho et al., 2003, Zuber et al., 2001). The buffering of ATP driven H^+ ion influx causes concomitant influx of Cl^-. This increases the osmotic potential of the endosome and, in turn causes an increase in volume until such point as the membrane bursts (Akinc et al., 2005).

Another hypothesis proposed that the efficient transfection properties of PEI are due to the protonation of the amines causes ionic repulsion leading to extension of the PEI molecule and endosomal membrane disruption. This theory is supported by the lack of difference in the lysosomal pH found between that measured in PEI transfected cells and that measured in non-transfected cells (Godbey et al., 2000). The transfection efficiency of pDNA polyplexes with PEI is 10-fold higher when PEI is added dropwise to the pDNA (Boussif et al., 1995). Polyplexes have been found to form toroid structures of 40-80 nm when condensed with PEI (Kircheis et al., 2001b).

The main problem with PEI is its toxicity (Florea et al., 2002a). Low molecular weight PEI has a lower toxicity and 25 kDa linear PEI is perceived as the best compromise between toxicity and high transfection efficiency (Ahn et al., 2002). Linear PEI (22 kDa) is available commercially, JetPEI®, as a reagent for *in vitro* transfection (Fermentas, 2005).

Several PEI derivatives have been made that were found less cytotoxic *in vitro* compared to PEI. These include transferrin-PEG-PEI, galactose-PEG-PEI and N-acylated with alanine of PEI. All these derivatives showed high transfection efficiency (Kursa et al., 2003, Sagara & Kim, 2002, Thomas & Klibanov, 2002). Ahn et al. (2002)

produced a PEG-PEI with the aim of reducing toxicity whilst retaining transfection efficiency of higher molecular weight PEI (Ahn et al., 2002). Toxicity was reduced (80 % viability of control) compared to 25 kDa PEI (40 % viability of control) and transfection efficiency higher than that of the starting Mw PEI (1.8 kDa) (Ahn et al., 2002). However, no direct comparison to 25 kDa transfection efficiency was made but PEG-PEI co-polymers were acknowledged to be less efficient (Ahn et al., 2002).

The first clinical trial using a polymeric vector, PEI, was published in 2005 (Ohana et al., 2004). Bladder cancer (two human subjects) was treated through bladder installation of a transuretal catheter and a > 75 % reduction in tumour size with no adverse side effects was reported (Ohana et al., 2004).

In the studies reported in this thesis PEI has been used as a positive control. Its cytotoxicity and transfection are efficiency compared with that of the chitosan derivatives prepared. PEI was also used in some studies as an additional component in the development of an improved non-viral gene delivery system.

1.5.2.1.2 Chitosans: Natural Origin Cationic Polymers as Non-viral Vectors

Chitosan is a naturally occurring polysaccharide of β1-4 linked *N*-acetyl-D(+)glucosamine and D(+)glucosamine It is produced through the deacetylation of chitin, the extent of which is usually 40-100 % (reviewed in Thanou & Junginger, 2004). Chitin is found in the cell walls of fungi; this was where it was first discovered in 1811 by H. Braconnot who named it fungine (Domard & Domard, 2002). It is also found in the exoskeleton of insects, and crustacea (crab, shrimps) and was termed chitin, after the Greek word for coat, chitos, by C. Odier in 1823 after the discovery in the elytrum of the cock chafer beetle (Domard & Domard, 2002).

The main commercial source of chitin is shell waste from the food industry. Chitin is processed by treatment with 3-5 % (w/v) aqueous alkali (NaOH) at 80-90 °C to remove protein, this is followed by treatment with 3-5 % (w/v) aqueous acid (HCl) to remove inorganic materials (i.e. calcium carbonate). The purified chitin is deacetylated, producing primary amines, using 40 % sodium hydroxide at 120 °C for 1-3 h (Kumar, 2000).

Chitosan is widely regarded as being a non-toxic biologically compatible polymer (Corsi et al., 2003). It is approved for dietary applications in Japan, Italy and Finland (Illum, 1998) and it has been approved by the FDA for use in wound dressings (McCue, 2003). Chitosans (<5 kDa, 5-10 kDa and >10 kDa) were found to display little

cytotoxicity against CCRF-CEM (human lymphoblastic leukaemia) and L132 (human embryonic lung cells) (IC_{50} >1 mg/ml) (Richardson et al., 1999). In contrast to most reports Carreno-Gomez et al. (1997) found chitosan (hydrochloride salt) to be relatively toxic (IC_{50} 0.21 ± 0.04 mg/ml) against B16F10 (murine melanoma) cells. However, this study appears to have used solutions of the chitosan salts at the pH when dissolved, for chitosan.HCl in PBS (10 mg/ml) pH = 5.8 (Carreno-Gomez & Duncan, 1997). At this pH the MTT assay is not appropriate (Sgouras, 1990) and cell viability is sure to be compromised. However, an appreciation that the salt form of the polymer will have an effect on its interaction with cells and macromolecules should be acknowledged (Wan et al., 2004). The reported safety makes chitosan attractive for gene delivery as other cationic molecules have relatively high toxicities, e.g. PLL (Merdan et al., 2002), PEI (Florea et al., 2002a). Chitosan is soluble at acidic pH, and precipitates in neutral/alkaline solutions; it is therefore problematic in this unmodified form in the preparation of complexes and in their administration.

Chitosan has membrane perturbant properties making it an interesting polymer for gene delivery (Chan et al., 2001). Polyplexes of pDNA with chitosan were investigated by Erbacher et al. (1998) who found that pDNA was condensed to 50-100 nm sized particles having donut or rod-like structures (Erbacher et al., 1998).

Chitosan-mediated transfection has been studied by many groups (Corsi et al., 2003, Hejazi & Amiji, 2002, Ishii et al., 2001, Kiang et al., 2002, Koping-Hoggard et al., 2003, Koping-Hoggard et al., 2001, Mao et al., 2001, Roy et al., 1999). In summary, it has been suggested that transfection efficiency of chitosan polyplexes is related to the nitrogen/phosphorus (N/P) ratio, polymer chain length, salt concentration (and type) at complex formation, cell type, time prior to harvesting and complex size/shape. The fact that many parameters influence the final gene expression may be indicative of the multi-step process being studied. Several barriers exist that must be crossed and a number of processes performed in order to achieve protein expression (Fig. 1.12). The N/P ratio is based on the number of nitrogen residues in the polymer and the number of phosphate residues in the DNA, it is approximately the same as a monomer molar ratio. Investigation of N/P ratios has found 3:1 (N/P) to be the most efficient for 40 kDa chitosan (>85 % deacetylated) in SOJ cells (Ishii et al., 2001). Similar results were found in 293 cells with 190 kDa chitosan (85 % deacetylated), where a polymer : DNA ration of 3:1 was the most efficient ratio tested (Koping-Hoggard et al., 2001). This was also true in Hela cells with 70 kDa chitosan (Erbacher et al., 1998). As seen for other polymers, chitosan molecular weight influences transfection efficiency.

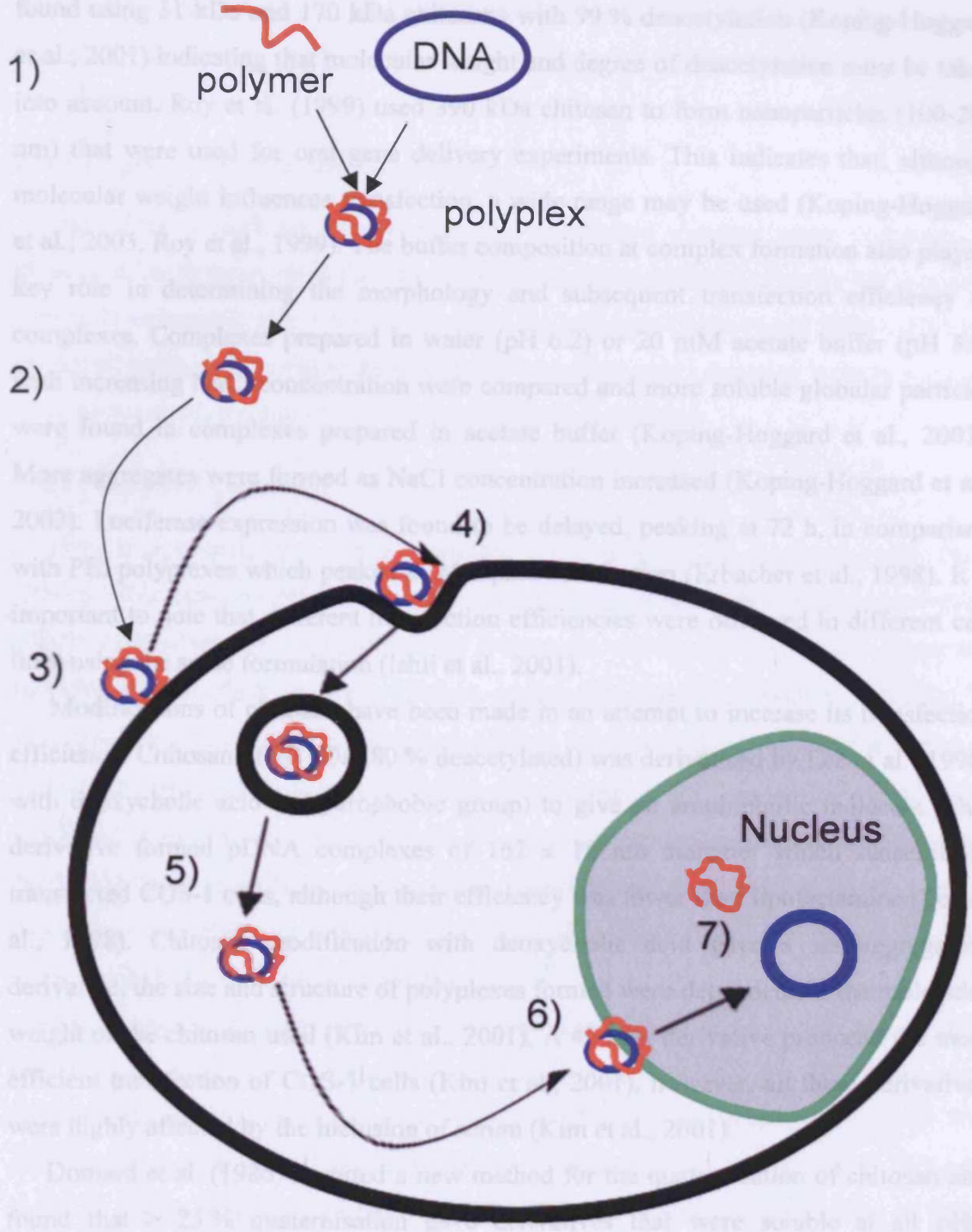

Figure 1.12 – Barriers to non-viral gene delivery

Key: 1) Achieving efficient plasmid condensation, 2) Protection of DNA from nucleases, 3) binding to cell, 4) endocytosis, 5) endosome escape, 6) nuclear entry, 7) release from vector (After Brown et al., 2001)

A molecular weight of 40 kDa was more efficient compared with 1 kDa and 84 kDa chitosans (Ishii et al., 2001). However, in other studies similar gene expression was found using 31 kDa and 170 kDa chitosans with 99 % deacetylation (Koping-Hoggard et al., 2001) indicating that molecular weight and degree of deacetylation must be taken into account. Roy et al. (1999) used 390 kDa chitosan to form nanoparticles (100-200 nm) that were used for oral gene delivery experiments. This indicates that, although molecular weight influences transfection, a wide range may be used (Koping-Hoggard et al., 2003, Roy et al., 1999). The buffer composition at complex formation also plays a key role in determining the morphology and subsequent transfection efficiency of complexes. Complexes prepared in water (pH 6.2) or 20 mM acetate buffer (pH 5.0) with increasing NaCl concentration were compared and more soluble globular particles were found in complexes prepared in acetate buffer (Koping-Hoggard et al., 2003). More aggregates were formed as NaCl concentration increased (Koping-Hoggard et al., 2003). Luciferase expression was found to be delayed, peaking at 72 h, in comparison with PEI polyplexes which peaked at 24 h post-transfection (Erbacher et al., 1998). It is important to note that different transfection efficiencies were observed in different cell lines using the same formulation (Ishii et al., 2001).

Modifications of chitosan have been made in an attempt to increase its transfection efficiency. Chitosan of 70 kDa (80 % deacetylated) was derivatised by Lee et al. (1998) with deoxycholic acid (a hydrophobic group) to give an amphiphillic molecule. This derivative formed pDNA complexes of 162 ± 18 nm diameter which successfully transfected COS-1 cells, although their efficiency was lower than lipofectamine (Lee et al., 1998). Chitosan modification with deoxycholic acid gave a self-aggregating derivative, the size and structure of polyplexes formed were dependent on the molecular weight of the chitosan used (Kim et al., 2001). A 40 kDa derivative produced the most efficient transfection of COS-1 cells (Kim et al., 2001), however, all these derivatives were highly affected by the inclusion of serum (Kim et al., 2001).

Domard et al. (1986) reported a new method for the quaternisation of chitosan and found that > 25 % quaternisation gave derivatives that were soluble at all pHs. Trimethylation of the amine groups to give quaternised amines gives a permanent positive charge and these derivatives have great potential for gene delivery applications (Murata et al., 1996). The application of trimethylation to oligomeric chitosan was first reported by Florea et al. (2002b) and Thanou et al. (2002). Trimethylated chitosan oligomer (TMO) was found to protect plasmid DNA from DNAse 1 (Florea et al.,

2002b). It was also found that transfection efficiency was increased by an order of magnitude using TMO compared to chitosan in COS-1 (African green monkey kidney fibroblast) cells (Thanou et al., 2002). This favourable profile led to the study of trimethylated chitosans as the gene delivery vector in this thesis.

1.5.3 Targeted Non-viral Gene Delivery

Non-viral vectors are poorly efficient transfection systems when compared to viruses. It has been reported that at best, PEI polyplexes were taken up by 90 % of cells (30 mM) compared with 1 virus per cell being effective (Zaric et al., 2004). This has prompted many to investigate the possibility of incorporating targeting ligands into non-viral vectors with the aim of improving transfection efficiency.

1.5.3.1 Targeted Lipoplexes

Stealth liposomes are formed through the coating of the liposome with PEG, although this increases residence time in the body, cell uptake and therefore transfection efficiency is often lost. In an attempt to restore the activity of these stealth liposomes ligands are attached to them. When pegylated immunoliposomes carrying β-galactosidase (β-gal) were prepared containing a humanised anti-transferrin antibody and administered intravenously in Sprague Dawley rats, β-gal expression was found in the blood brain barrier, liver and spleen with little expression elsewhere (Shi et al., 2001). Although specific β-gal expression was claimed, the multiple sites at which expression was observed highlights the broad expression of transferrin receptor and raises questions over its value as a target.

Asialofetuin (a glycoprotein having tri-antennary galactose terminated sugar chains that targets ASGR) was included in a lipoplex containing the chloramphenicol acetyltransferase (CAT) gene and an increase (almost double) in CAT activity was observed in HepG2 cells (Hara et al., 1995). Similarly an anti-transferrin single chain antibody fragment bound to liposomes led to a 2-6 fold increase in transfection in H358, DU145, Hep3B and HT29 cells (Xu et al., 2002). Subsequent *in vivo* studies with p53 gene lipoplexes delivered via tail vein injection into tumour bearing mice and transfection assessed by Western blotting showed markedly enhanced p53 expression in DU145 tumours and low p53 expression found elsewhere (Xu et al., 2002). Integrin receptors were efficiently targeted using a 1,2-disteraoyl-sn-glycero-3-

phosphoethanolamine-N-PEG (5 kDa) ACDC**RGD**CFCG-COOH DOTAP liposome with a 100-fold increase over the pegylated liposome without the RGD containing peptide. Lipoplexes were also targeted by Anwer et al. (2004) using RGD peptides and a 10-fold increase was observed in human umbilical vein endothelial cells (HUVEC) compared to non-targeted lipoplexes (Anwer et al., 2004).

1.5.3.2 Targeted Polyplexes

The idea of targeting polyplexes is not new and in 1988 Wu and Wu prepared asialoglycoprotein-PLL/DNA polyplexes to target ASGR (Wu & Wu, 1988). They found highly selective expression of a foreign reporter gene protein (CAT) in the liver demonstrating targeted gene delivery for the first time (Wu & Wu, 1988). Many efforts have been made to target PEI/DNA complexes (Benns et al., 2002, Blessing et al., 2001, Guo & Lee, 1999, Kircheis et al., 1997, Kircheis et al., 2001a, Kunath et al., 2003b, Kursa et al., 2003, Lee et al., 2002, Ogris & Wagner, 2002a, Sagara & Kim, 2002, Zanta et al., 1997) with varying degrees of success (Table 1.6). The PEI conjugates jetPEI-Man™ (linear PEI conjugated to mannose) and jetPEI-Gal™ (linear PEI conjugated to galactose) are available commercially for the increased efficiency of transfection of mannose receptor or ASGR expressing cells respectively (Qbiogene, 2003).

With the aim of targeting chitosan-derived polyplexes, trimethylated chitosan polymer derivatives were further modified at the 6-O-position with chloroacetic acid and then galactose (Murata et al., 1996) and antennary galactose conjugates were prepared (Murata et al., 1997). Transfection was studied using HepG2 (human hepatoma) cells. The galactose-containing trimethyl chitosan produced a small (although statistically insignificant) increase in transfection over trimethyl chitosan, with a larger increase (although probably statistically insignificant) being seen in cells transfected with tetra-antennary galactose trimethyl chitosan (Murata et al., 1996, Murata et al., 1997). Galactosylated chitosan (25 kDa, 85 % deacetylated) was prepared by Gao et al. (2003) and tested on human hepatocellular carcinoma cell lines. Again, a small (although probably statistically insignificant) increase in transfection efficiency over the un-targeted polymer was seen (Gao et al., 2003). Competitive inhibition of transfection with 50 mM lactose showed a statistically significant decrease indicating that targeting had been achieved (Murata et al., 1997).

Table 1.6 – Actively targeted gene delivery systems

Carrier	Receptor	Ligand	Fold increase over un-targeted vector	Reference
PEG-PEI	Ovarian antigen 3 (OA3)	fAb against OA3	80	(Merdan et al., 2003)
PEI	CD3	Antibody against CD3	30	(Kircheis et al., 1997)
PEI	HER2	Antibody against HER2 (trastuzumab)	10-20	(Chiu et al., 2004)
PEI	PECAM	Antibody against PECAM	100	(Li et al., 2000)
Chitosan	Transferrin receptor	Transferrin	4	(Mao et al., 2001)
PEI	Transferrin receptor	Transferrin	30-1000	(Kircheis et al., 1997)
PEI	Transferrin receptor	Transferrin	100 (*in vivo*)	(Kircheis et al., 2001)
PEI	Transferrin receptor	Transferrin	100	(Ogris & Wagner, 2002)
PEG-PEI	Transferrin Receptor	Transferrin	10-100	(Kursa et al., 2003)
Poly(L-Lysine)	Transferrin receptor	Transferrin	10	(Taxman et al., 1993)
PEI	EGF receptor	EGF	10	(Lee et al., 2002)
PEG-PEI	EGF receptor	EGF	10-100	(Blessing et al., 2001)

Table 1.6 - Continued

Carrier	Receptor	Ligand	Fold increase over un-targeted vector	Reference
Trimethyl chitosan	Asialoglycoprotein receptor	Galactose	Small probably statistically insignificant increase	(Murata et al., 1996)
Trimethyl chitosan	Asialoglycoprotein receptor	Tetra-galactose	Doubled (although probably still statistically insignificant	(Murata et al., 1997)
Chitosan	Asialoglycoprotein receptor	Galactose	Small, probably statistically insignificant increase	(Gao et al., 2003)
PEI	Asialoglycoprotein receptor	Galactose	decreased	(Kunath et al., 2003b)
PEG-Poly(L-Lysine)	Asialoglycoprotein receptor	Lactose	10	(Choi et al., 1998)
PEG-PEI	Asialoglycoprotein receptor	Galactose	2.1-2.7	(Sagara & Kim, 2002)
PEI	Asialoglycoprotein receptor	Galactose	10 000-100 000	(Zanta et al., 1997)

Table 1.6 – Continued

Carrier	Receptor	Ligand	Fold increase over un-targeted vector	Reference
PEI	integrin receptors	RGD peptide - CYGGRGDTP	10-100	(Erbacher et al., 1999)
PEI	$\alpha_v\beta_3$ integrin	RGD peptide - RGDC	50	(Kunath et al., 2003a)
PEG-PEI	Folate receptor	Folate	10-100	(Benns et al., 2002)
Poly(L-Lysine) in DOPE liposome	Folate receptor	Folate	20-30 times over DOPE liposome, no comparison to poly(L-lysine) alone made	(Lee & Huang, 1996)
PEI	Folate receptor	Folate	~500 at low N/P ratio, no increase at higher ratios	(Guo & Lee, 1999)
poly(dimethylamino methyl) methacrylate	Folate receptor	Folate	~1.5 but probably insignificant, explanation that this was due to low growth of cells without folate in medium	(van Steenis et al., 2003)
Poly(L-Lysine)	Mannose receptor	Mannose	Not determined, *in vivo* experiments showed transfection of macrophages	(Ferkol et al., 1996)

EGF = Epidermal growth factor; PECAM = Platelet endothelial cellular adhesion molecule

Chapter 2

Materials and General Methods

Transferrin and epidermal growth factor (EGF)-containing PEI/DNA complexes demonstrated up to 100-fold enhancement of luciferase gene expression in murine tumour models (Ogris et al., 2003). When transferrin was covalently attached to PEI, and complexes of transferrin-PEI/PEI/pDNA made, a 20-fold increase in gene expression was found in the tumour over other organs after administration to mice bearing neuroblastoma tumours (Kircheis et al., 2001a). Interestingly, in this study a large uptake of the polyplex was observed in the liver but with low expression of the luciferase protein; the explanation made was that uptake was performed by Kupffer cells and RES which degraded the polyplex (Kircheis et al., 2001a). It is interesting to note from Table 1.6 that Kunath et al. (2003b) found decreased transfection using galactose-PEI polyplexes whilst Zanta et al. (1997) found a massive increase in transfection using galactose-PEI polyplexes. The reason for this difference is unclear as similar PEIs were used at similar degrees of galactose substitution and the cell lines transfected were the same.

In a more complicated approach: PEI/DNA polyplexes were first prepared and then coated with streptavidin, EGF-PEG-biotin was then immobilised on the polyplex surface through the high affinity biotin-streptavidin interaction (Lee et al., 2002). The resultant polyplex lead to a 10-fold increase in the transfection efficiency for the most effective polyplex over PEI alone on A431 cells, a human epidermoid carcinoma cell line (Lee et al., 2002). From these studies it can be seen that receptor-mediated targeting of polyplexes to increase the efficiency of gene delivery is feasible but that effective solutions must still be sought.

1.6 Aims of this Research

The overall aim of this research was to develop a peptide-directed, uPAR targeted, non-viral gene delivery system based on chitosan as a non-viral vector. The hypothesis being that a peptide derived from the binding region of uPA when conjugated to 6-O-carboxymethyl trimethyl chitosan would increase the uptake of the derivative by tumour cells. Thus it was envisaged that polyplexes formed from such chitosans containing this targeted derivative would be useful for tumour-targeted cancer gene therapy.

First it was essential to optimise chitosan trimethylation and show that the reaction was reproducible. To enable later studies on the effect of trimethylated chitosan molecular weight, two chitosan molecular weight fractions were used for these studies:

chitosan oligomer (3-6 kDa) and chitosan polymer (~ 100 kDa) (Chapter 3). The chitosan-based products synthesised were then investigated for their toxicity and transfection efficiency (Chapter 4). To design the trimethylated chitosan derivatives as targeted vectors it was necessary to conjugate them to the uPA derived peptides u7 and u11. In addition, fluorescent probes were added (Oregon Green and fluorescein) (Chapter 3) to allow monitoring of uptake and intracellular localisation (Chapter 5).

Before studying the ability of the conjugates to form polyplexes for gene delivery, it was necessary to establish cell models expressing uPAR (Chapter 5). Using MCF-7, COS-7 and DU145 as uPAR-expressing cell lines, the binding and uptake of the two peptide ligands (u7 and u11) and their conjugates was investigated (Chapter 5). Finally, having selected the optimum peptide-ligand construct, the ability of this targeted polyplex to mediate transfection was investigated (Chapter 6).

2.1 Materials

2.1.1 Polymer/oligomers

Chitosan oligomers (3-6 kDa, 97 % deacetylated) and chitosan polymer (~100 kDa, 97 % deacetylated) were a gift from Primex (Norway). PEI (~25 kDa, product code: 40,872-7) was obtained from Aldrich (USA). Monomethoxy poly(ethylene)glycol (mPEG; 5 kDa, product code: 81323) was obtained from Fluka (UK). mPEG amine (5 kDa, product code: 1P4M0H02) and fluorescein-PEG-succinimidyl ester (4 kDa, product code: 1K4MOFO2) were obtained from Nektar (USA).

2.1.2 Cell Culture

Cell lines: COS-1, COS-7 (both monkey kidney fibroblast) and Caco-2 (colon carcinoma) cells were supplied by American Tissue and Cell Culture (ATCC; UK). DU145, PC3, (both prostate cancer cell lines) and MCF-7 (breast cancer cells) were a gift from Tenovus Cancer Research, Cardiff, UK. U937 (leukaemia) cells were a gift from Stuart Jones (Cardiff University College of Medicine, UK).

Cell culture reagents: RPMI 1640 (L-glutamine) and Dulbecco's modified Eagle's medium (DMEM) with or without the pH indicator phenol red were obtained from Invitrogen Life Technologies (UK). Virkon was purchased from Antec Int. (UK). Disodium hydrogen orthophosphate, sodium dihydrogen orthophosphate, sodium chloride and sodium hypochlorite were bought from Fisher (UK). Foetal bovine serum (FBS), penicillin/streptomycin (pen/strep; 5000 Units/ml, 5000 μg/ml) and trypsin/ethylene diamine tetraacetic acid (EDTA) (0.05 % (w/v) 0.53 mM) without magnesium and calcium chloride were obtained from Invitrogen Life Technologies (UK). Medical grade CO_2, N_2 (all 95 % v/v) and liquid nitrogen were supplied by BOC (UK). Trypan blue solution (0.4 % w/v), phorbol 12-myristate 13-acetate (PMA), 3-(4,5-dimethylthiazol-2-yl)-2,5-diphenyl-2H-terazoliumbromide (MTT) and sterile dimethyl sulphoxide (DMSO) were from Sigma-Aldrich (UK), copper II sulphate from BDH (UK). Pipettes (5, 10, 25 ml), bijous (~7 ml) and universal containers (~25 ml) were obtained from Elkay (Ireland). Cells were incubated in a Galaxy S incubator (Wolf laboratories; UK) or a Procell incubator (Jencons PLS; UK). Sterile cell manipulations were performed in a class II laminar flow hood from Bioair (Italy) or Servicare (UK).

2.1.3 Laboratory Reagents

The suppliers of all general chemicals used in these studies are listed in Table 2.1.

2.2 Equipment

2.2.1 Analytical Equipment

Ultraviolet-visible (UV) absorbance was measured with a Cary 1G UV-visible spectrophotometer from Varian (UK) and a Sunrise UV absorbance plate reader from Tecan (Austria). Where indicated a Cary Win UV software package was used for data acquisition and analysis.

Fluorescence was measured with an Aminco-Bowman Series 2 luminescence spectrophotometer from Spectronic Instruments and a Fluostar Optima fluorescence plate reader from BMG Labtechnologies (Germany). A Typhoon 9410 Variable Mode Imager from Amersham Biosciences (UK) was used to image agarose gels and TLC plates and data processing was performed using ImageQuant TL 2003 software from Amersham Biosciences (UK).

Nuclear magnetic resonance (NMR) spectra, ^{1}H and ^{13}C were recorded either with a Brucker DPX 300 NMR spectrometer (Brucker AG Germany) and data subsequently analysed with 3.6 XWin NMR software, or a Brucker Advanced 500 NMR and data subsequently analysed with Topspin 1.3b software (Brucker AG Germany).

Fourier transform infra-red (FTIR) spectra were recorded using an Avatar 360 FTIR (Nicolet Instrument Corp., USA) fitted with a Nicolet Smart Arc diffuse reflectance accessory. The data was collected and analysed using Nicolet E-Z Omnic E.S.P. 5.2 software (Nicolet, USA).

Direct injection electrospray ionisation mass spectrometry was performed. Mass spectra were collected using a Platform II mass spectrometer (Micromass, UK) or using a Bruker Daltonics microTOF mass spectrometer collected with Bruker Daltonics microTOF control Version 1.0 (Bruker, Germany).

Particle size measurement was performed using a N4 Plus photon correlation spectrophotometer (PCS; Coulter, USA). Measurement was made at 20.0 °C at an angle of 90 ° over 180 s.

Table 2.1 – General chemicals

Chemical	Supplier
1 kb DNA ladder	Promega (UK)
1-ethyl-3-(3-dimethylaminopropyl)-carbodiimide hydrochloride (EDC)	Pierce (USA)
2,6-di-tert-butyl-4-methyl phenol (BHT)	Sigma-Aldrich (UK)
3-(4,5-dimethylthiazol-2-yl)-2,5-diphenyl tetrazolium bromide (MTT)	Sigma-Aldrich (UK)
3-amino-1-propanol	Sigma-Aldrich (UK)
4 % w/v copper (II) sulphate pentahydrate	Sigma-Aldrich (UK)
4 (dimethylamino) pyridine (DMAP)	Sigma-Aldrich (UK)
5,6-carboxyfluorescein succinimidyl ester	Molecular Probes Inc. (USA)
9-anthraldehyde	Sigma-Aldrich (UK)
Acetone	Fisher Scientific (UK)
Acetonitrile	Fisher Scientific (UK)
Agarose; electrophoresis grade	Bioline (UK)
Ammonium persulphate (APS)	Sigma-Aldrich (UK)
Anhydrous dimethyl sulphoxide (DMSO)	Sigma-Aldrich (UK)
Aprotinin	Sigma-Aldrich (UK)
BamH1	Promega (UK)
Bicinchoninic acid (BCA)	Sigma-Aldrich (UK)
Boric acid	Fisher Scientific (UK)
Bovine serum albumin (BSA)	Sigma-Aldrich (UK)
Bovine serum albumin protein standard soln (1mg/ml)	Sigma-Aldrich (UK)
Broad range protein standards	Bio-Rad (UK)
Calcium chloride	Fisher Scientific (UK)
Citric acid monohydrate	Sigma-Aldrich (UK)
Deuterium oxide (D_2O)	Sigma-Aldrich (UK)
Diethyl ether	Fisher Scientific (UK)
Dimethylformamide (DMF)	Sigma-Aldrich (UK)
Dimethylsulphoxide lab reagent grade	Sigma-Aldrich (UK)
ECL Detection Reagents	Amersham Biosciences (UK)
EcoR1	Promega (UK)
Ethanol	Fisher Scientific (UK)
Ethidium bromide (10 mg/ml) solution	Sigma-Aldrich (UK)
Ethyl acetate	Fisher Scientific (UK)
Ethylenediaminetetraacetic acid (EDTA)	Sigma-Aldrich (UK)
FACS clean	Becton Dickinson (UK)
FACS flow	Becton Dickinson (UK)
FACS safe	Becton Dickinson (UK)
Falcon tubes	Becton Dickinson (UK)
FITC-uPA	American Diagnostica (USA)
Fluorescein	Sigma-Aldrich (UK)

Table 2.1 – General chemicals

Chemical	Supplier
Fluorescein isothiocyanate (FITC)	Sigma-Aldrich (UK)
FMOC-Asparagine-Trt	Novobiochem (UK)
FMOC-Cysteine-tbutyl	Novobiochem (UK)
FMOC-Glycine	Novobiochem (UK)
FMOC-Histidine-Trt	Novobiochem (UK)
FMOC-Isoleucine	Novobiochem (UK)
FMOC-Leucine	Novobiochem (UK)
FMOC-Lysine-Boc	Novobiochem (UK)
FMOC-Phenylalanine	Novobiochem (UK)
FMOC-Serine-tbutyl	Novobiochem (UK)
FMOC-Threonine-tbutyl	Novobiochem (UK)
FMOC-Tryptophan-Boc	Novobiochem (UK)
FMOC-Tyrosine-tbutyl	Novobiochem (UK)
FMOC-Valine	Novobiochem (UK)
Glacial acetic acid	Fisher Scientific (UK)
Hydrochloric acid	Fisher Scientific (UK)
K6 Silica Gel Plate 60 Å 250 μm thickness	Whatman (UK)
K6 (254) Silica Gel Plate 60 Å 250 μm thickness (fluorescent indicator)	Whatman (UK)
Latex beads (100 nm)	Sigma-Aldrich (UK)
Latex beads (300 nm)	Sigma-Aldrich (UK)
LB Agar tablets	Sigma-Aldrich (UK)
LB media tablets	Anachem (UK)
Leupeptin	Sigma-Aldrich (UK)
Lithium acetate	Sigma-Aldrich (UK)
Luciferase substrate	Promega (UK)
Magnesium chloride	Fisher Scientific (UK)
Megaprep plasmid purification kit	Qiagen (UK)
Methanol	Fisher Scientific (UK)
Methyl Iodide	Fisher Scientific (UK)
Monoclonal mouse α-uPAR antibody (Product #3937)	American Diagnostica (USA)
N,N disuccinimidyl carbonate	Fisher Scientific (UK)
N,N,N,N'-tetra-methyl-ethylenediamine (TEMED)	Bio-Rad (UK)
N-2-hydroxyethylpiperazine-*N'*-ethanesulphonic acid (HEPES)	Sigma-Aldrich (UK)
N-hydroxysulphosuccinimide (Sulpho-NHS)	Pierce (USA)
N-methyl pyrolidinone (NMP)	Sigma-Aldrich (UK)
Oregon Green® 488-X, succinimidyl ester *6-isomer*	Molecular Probes Inc. (USA)
Passive cell lysate (5x) buffer	Promega (UK)
Pepstatin	Sigma-Aldrich (UK)
Phenylmethylsulfonyl fluoride (PMSF)	Sigma-Aldrich (UK)
Polyclonal goat α-uPAR antibody (Product # 399R)	American Diagnostica (USA)

Table 2.1 – General chemicals

Chemical	Supplier
Polyoxyethylene sorbitan monolaurate (Tween 20)	Sigma-Aldrich (UK)
Polyvinylidene fluoride (PVDF) 0.45 μm pore size - Immobilon-P™	Millipore (UK)
Propidium iodide	Sigma-Aldrich (UK)
Rainbow broad range protein standards	Invitrogen (UK)
Sodium chloride	Fisher Scientific (UK)
Sodium dodecyl sulphate	Fisher Scientific (UK)
Sodium hydroxide pellets	Sigma-Aldrich (UK)
Sodium nitrate	Sigma-Aldrich (UK)
Succinic acid	Sigma-Aldrich (UK)
Tetrahydrofuran (THF)	Fisher Scientific (UK)
Triethylamine (TEA)	Fisher Scientific (UK)
Tris borate EDTA (10x) buffer (TBE)	Sigma-Aldrich (UK)
Tris(hydrocymethyl)aminomethane (Tris-Base)	Sigma-Aldrich (UK)
Tris(hydrocymethyl)aminomethane hydrochloride (Tris-HCl)	Sigma-Aldrich (UK)
Triton X-100	Sigma-Aldrich (UK)
Tyrosinamide	Sigma-Aldrich (UK)
Urokinase, high molecular weight. Product code: 672081	Calbiochem (UK)

Gel permeation chromatography (GPC) was performed using a Jasco PU-980 high-performance liquid chromatography pump (Jasco UK Ltd, UK) on Waters Ultrahydrogel 1000 and 250 columns (7.8 x 300 mm) in series with detection made using a Gilson 133 refractive index (RI) detector (Gilson Inc, USA) and an SA6504 programmable absorbance detector (Severn analytical, UK). The flow rate used was 1 ml/min and the mobile phase is described where appropriate. PEG standards: 18.3, 32.5, 58.4, 965 kDa were supplied by Polymer Laboratories, UK, 5 kDa PEG and glucose were supplied by Fluka. Data were recorded and processed using Caliber software (version 7.0.4) provided by Polymer Laboratories, UK. Gravitational separation was performed on PD10 columns (Amersham Biosciences, UK) containing Sephadex G25. Sephadex LH20 (Amersham Biosciences, UK) was used to pack a 45 x 2.5 cm chromatography column (Pharmacia) and mobile phase was pumped at ~2 ml/min by a P-1 pump (Pharmacia) and 2 ml fractions collected using a Frac 100 fraction collector (Pharmacia). Organic GPC was performed on a PL-GPC20 system (Polymer Laboratories, UK) equipped with a Resipore® guard column (50 x 4.6 mm) followed by two Resipore® columns (300 x 7.5 mm) in series. A 100 µl injection loop with a rheodyne injection system was used to introduce samples with a THF (stabilised with 250 ppm BHT) eluent with detection being made by RI. Control, processing and recording of chromatograms was made using Cirrus GPC software (V 2.0). Calibration of this equipment was made using EasiCal® PS-2 polystyrene standards (Mw 0.58 – 377.4 kDa).

A FACSCalibur flow cytometer (Becton Dickinson, UK) equipped with a single argon laser (excitation wavelength 486 nm) was used for all flow cytometry studies. Logarithmic-transformed data were acquired in 1024 channels with band pass filters FL-1 (530 nm ± 30 nm), FL-2 (585 nm ± 42 nm) and FL-3 (670 nm long pass filter) and subsequently processed with Cell Quest software (version 3.3).

Epifluorescent images of cells were viewed with an inverted Leica DM IRB fluorescence microscope (Germany) with an incident light 450 nm – 490 nm and a dichroic mirror at 510 nm (i.e. for fluorescein associated fluorescence) and captured with a 12-bit cooled monochrome Retiga 1300 camera from Qimaging (Canada). Images were collected and handled using Openlab software (version 3.0.9) from Improvision (UK). Live cell imaging was performed using glass bottom culture dishes (diameter 35 mm;

Matteck Corporation, USA). This microscope was also used to acquire bright-field images of cells.

2.2.2 General Equipment

A Toledo 320 pH meter from Mettler (Toledo, Switzerland), 3150 pH meter (Jenway) or Hydrion pH indicator paper (Sigma-Aldrich; UK) were used for pH measurements.

Samples were freeze-dried with a Flexi Dry FD-1.540 freeze-dryer from FTS Systems (USA) connected to a DD75 double stage, high vacuum pump from Javac (Australia).

SDS-Page gels were cast in a Bio-Rad vertical gel cast and the electrophoresis current supplied by Bio-Rad Power Pac 300 (Bio-Rad, UK). Agarose gels were prepared in a 11x14 cm gel cast and the subsequent electrophoresis was performed in a Horizon 11.14 electrophoresis tank from Life Technologies, Gibco (UK) with current supplied by EC135 Transformer (EC Apparatus Corp., USA).

Centrifugation was performed with a Varifuge 3.0 RS centrifuge supplied by Heraeus Instruments (Germany). When speeds greater than 4000 relative centrifugal force (RCF) were needed an Optima LE-80K centrifuge from Beckman Coulter (USA) was used. Eppendorfs were centrifuged in an Eppendorf 5417 R bench-top centrifuge with standard fixed angle rotor (model 5417 C/R; Eppendorf, Germany).

2.3 General Methods

Here, those general methods are described which were used throughout the studies repeated in more than one of the following Chapters. Specific methods integral to the substance of the specific studies e.g. synthetic methods are repeated in the relevant Chapter.

2.3.1 Cell Culture

Cell culture was carried out according to the guidelines provided by ATCC (ATCC, 2003). All manipulations with the exception of the centrifugation step, were performed in a class II laminar flow hood using sterilised consumables that had first been decontaminated with 70 % (v/v) ethanol. Cells were incubated and maintained in incubators at 37 °C in a 5 % CO_2 atmosphere that had a water humidifying tray containing copper II sulphate unless otherwise stated. All cells were mycoplasma free

(test performed using the polymerase chain reaction technique by Kerri Winship, Welsh School of Pharmacy, Cardiff University, UK).

2.3.1.1 Thawing of Cryopreserved Cells

Cells were obtained from the supplier as a cryopreserved cell suspension. They were rapidly thawed in a 37 °C water bath and then placed in a universal container containing 5 ml of complete medium (Table 2.2) and centrifuged at 200 RCF for 5 min to remove the cryopreservative (DMSO). After centrifugation, the supernatant was decanted and replaced with fresh medium containing 10 % v/v FBS (5 ml). The cell pellet was gently re-suspended using a pipette. The resulting cell suspension was placed in a flask (25 cm^2) and allowed to grow for 24 h. Cells were then washed once with PBS and supplemented with complete medium (Table 2.2) and maintained as described below.

2.3.1.2 Maintenance of Adherent Cell Lines (COS-1, COS-7, MCF-7, Caco-2, DU145 and PC3)

Cells were maintained in 75 cm^2 vented tissue culture flasks in the appropriate media (Table 2.2). Cells were subcultured weekly i.e. when they were 70-90 % confluent. First the cell culture medium was removed from the flask using a sterile quill then cells were washed with phosphate buffered saline (10 ml, PBS 0.1 M; pH 7.4) before the cells were trypsinised (1 ml trypsin/EDTA <3 min incubation at 37 °C). The flask was then tapped to free adhered cells, and 10 ml of culture medium used to wash the cells off the side of the flask, the resultant cell suspension was transferred to a universal container and centrifuged at 200 RCF for 5 min. The supernatant was removed and the cells re-suspended in 5 ml of culture medium with a 23 gauge needle and syringe. The resulting cell suspension was then used to subculture the cells at their appropriate split ratio (Table 2.2). All cell lines were used for a maximum of 30 passages before culturing a new batch of cells. This ensured that the cells were always within the same passage range for all studies.

2.3.1.3 Maintenance of Cells in Suspension

U937 cells were subcultured 2-3 times weekly i.e. when they were at 70-90 % of their maximum cell density. Cells were harvested by centrifugation at 200 RCF for 5 min. Supernatant was removed and the pellet was re-suspended in culture medium with a 10 ml pipette and used to subculture the cells at the appropriate ratio (Table 2.2). Again, U937 cells were kept for a maximum of 30 passages before culturing a new batch.

Table 2.2 – Cell culture conditions

Cell line	Culture Medium	Subculture ratio
COS-1	DMEM, 10 % FBS, pen/strep (100 Units/ml, 100 µg/ml)	1/25
COS-7	DMEM, 10 % FBS, pen/strep (100 Units/ml, 100 µg/ml)	1/25
DU145	DMEM, 10 % FBS, pen/strep (100 Units/ml, 100 µg/ml)	1/50
CACO-2	DMEM, 10 % FBS, pen/strep (100 Units/ml, 100 µg/ml)	1/15
MCF-7	DMEM, 10 % FBS, pen/strep (100 Units/ml, 100 µg/ml)	1/15
PC3	DMEM, 10 % FBS, pen/strep (100 Units/ml, 100 µg/ml)	1/50
U937	RPMI, 10 % FBS, pen/strep (100 Units/ml, 100 µg/ml)	1/10
U937 PMA	RPMI, 10 % FBS, pen/strep (100 Units/ml, 100 µg/ml), PMA 150 nM	-

2.3.1.4 Differentiation of U937 Cells

Before western blot and flow cytometry experiments U937 cells were differentiated. Cells were re-suspended in culture medium containing PMA (150 nM) then left to differentiate for 24 h to give an adherent macrophage-like phenotype (Picone et al., 1989).

2.3.1.5 Cell Counting

For the adherent cell lines the cells were washed, trypsinised, and re-suspended in a known volume of medium to form a cell suspension as described above. From this cell suspension, an aliquot (100 µl) was removed and diluted by half with a trypan blue solution in PBS (100 µl; 0.2 % w/v), mixed and allowed to stand for 1 min to stain dead cells. A coverslip was placed onto the haemocytometer slide, and following the appearance of Newton's rings, the counting chamber was filled with the cell suspension. A total of eight (0.1 mm^3) squares were counted. To count viable cells, any non-viable cells stained with trypan blue were excluded. An average of the counts was made and this equates to the number of cells $x10^4$ per ml, this is doubled to account for the trypan blue dilution to give the number of cells/ml in the suspension i.e. average of 8 squares x 2 = cells/ml $x10^4$.

In the case of the suspension cells (U937) cell counting was undertaken as described above with the exception that cells were removed from the flask, centrifuged at 200 RCF, and re-suspended in a known volume before placing on the haemocytometer slide.

2.3.1.6 Cell Freezing

Cells were regularly frozen to maintain stocks. At any time at least two frozen vials were stored in liquid N_2. To freeze cells, a cell suspension was first counted to give numbers of viable cells, re-centrifuged, and the resulting pellet was then re-suspended in cold FBS containing 10 % DMSO with a pipette to give $1x10^6$ cells/ml. Then 1 ml of this cell suspension was added to a cryogenic vial, wrapped in tissue paper and placed in a polystyrene box which was maintained at -20 °C for 1 h, then at -80 °C overnight. Finally the vial was placed in liquid N_2. Slow freezing is essential as it helps to preserve the cells because ice crystals (that can be produced by rapid freezing) are less likely to form, and rupture the cells.

2.3.2 Evaluation of Cell Growth Using the MTT Assay

Growth curves were determined to ensure that cells used in experiments were within the exponential growth phase. Cell proliferation was assessed by monitoring the conversion of MTT to formazan. The reduction of MTT is catalysed by mitochondrial dehydrogenase enzymes and is therefore a measure for cell viability (Fig 2.1) (Mosmann, 1983).

Briefly, cells (100 µl/well) were seeded at seeding densities of $1x10^5$, $1x10^4$ or $1x10^3$ cells/ml into 96 well microtitre plates and allowed to adhere for 24 h. Cell viability was assessed on a daily basis by adding 20 µl of filter sterilised MTT (5 mg/ml in PBS) to a single row of six wells. Following a 5 h incubation period with MTT, media was removed with a needle and syringe and the blue formazan crystals trapped in cells dissolved in sterile DMSO (100 µl) by incubating at 37 °C for 30 min. The absorbance at 550 nm was measured with a plate reader. Only the inner rows of the microtitre plate were used for these studies to minimise cell growth variations due to different medium evaporation rates at the periphery. The growth curve was constructed by plotting absorbance (blanked with DMSO) against time. The growth curves for DU145 cells are shown in Fig. 2.2.

2.3.3 Evaluation of Cytotoxicity Using the MTT Assay

The MTT assay (as described above) was also used to assess the *in vitro* cytotoxicity of polymers and polyplexes used in this study (see Chapter 4) (Sgouras & Duncan, 1990). In brief, COS7 and MCF7 cells (100 µl; $1x10^5$ cells/ml) were seeded into 96 well microtitre plates as before and left to adhere for 24 h. The next day, the medium was removed from the wells and replaced with filter sterilised complete medium containing polymer or polyplex. The plates were then incubated with polymer solutions for either 6 h or 24 h. In the case of the 6 h incubation; medium was removed after 6 h and replaced with culture medium only and further incubated to the total time of 24 h. Chitosan derivatives and PEI were applied onto the cells in DMEM at concentrations ranging from 20 to 10^4 µg/ml (100 µl/well) and cell viability compared to cells treated with DMEM only. In the case of the 24 h incubation media containing polymer was removed at 24 h and replaced with complete media. MTT (20 µl of 5 mg/ml in PBS) was added to each well of the plates for both incubation times. Plates were incubated for a further 5 h. Then the medium was removed and DMSO (100 µl) added before a further incubation of 30 min at 37 °C.

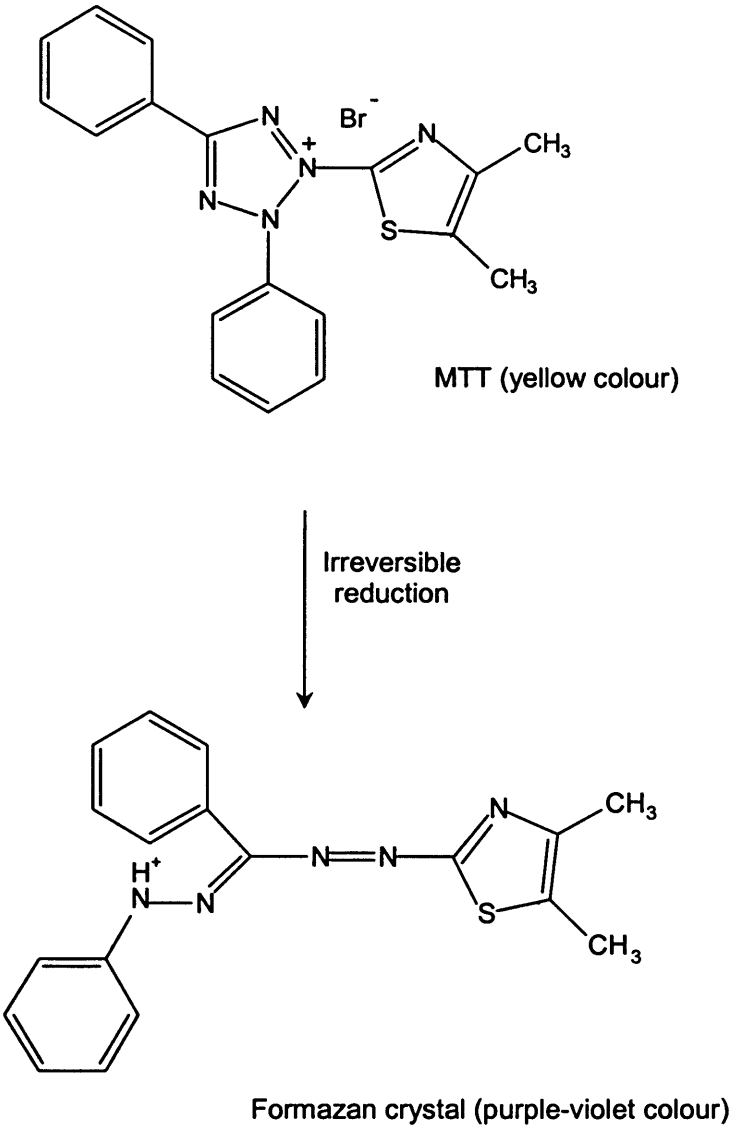

Figure 2.1 - Reduction of MTT

The reduction of MTT is produced by mitochondrial respiratory chain reductases, is irreversible, and is therefore an indication of cell viability.

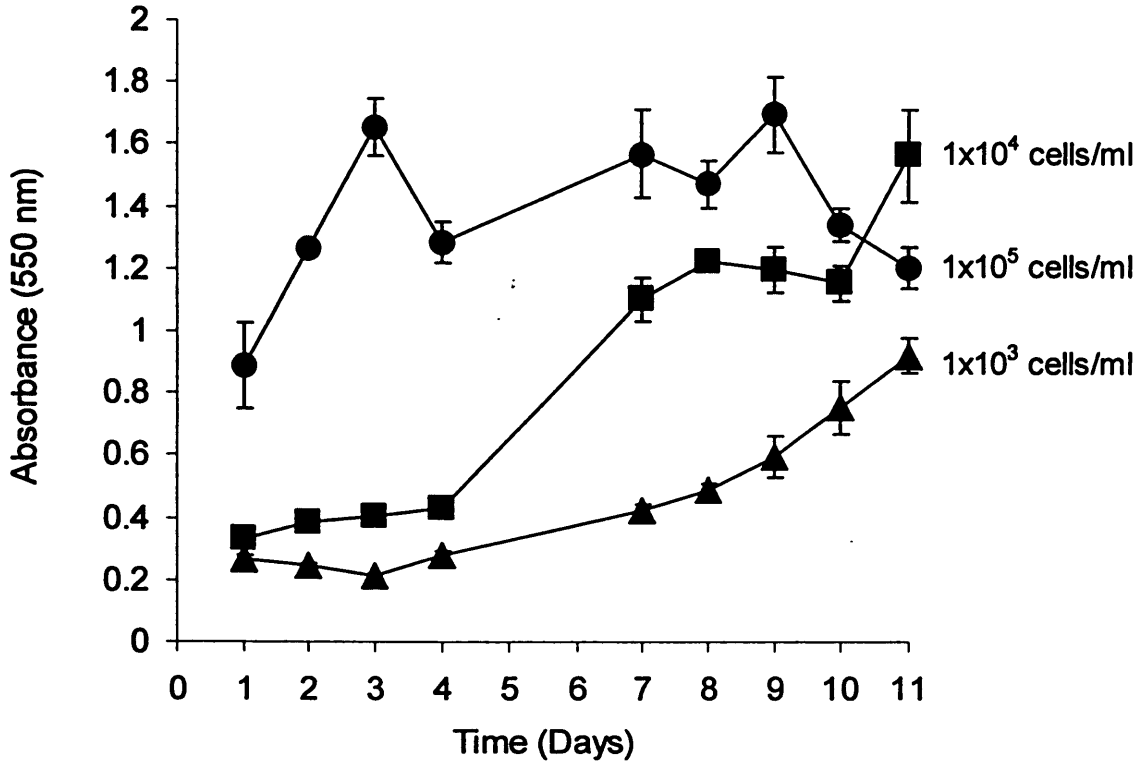

Figure 2.2 - Cell growth curves of DU145 cells

The DU145 cells were seeded at a density of $1x10^5$ cells/ml (●), $1x10^4$ cells/ml (■) or $1x10^3$ cells/ml (▲). Data represent mean ± SEM, n=6; error bars are within symbols when not visible.

Finally the absorbance at 550 nm of the plates was read with the Tecan plate reader. Absorbance values were blanked against DMSO and the absorbance of cells exposed to medium only (i.e. no polymer or polyplex added) were taken as 100 % cell viability (i.e. the control).

2.3.4 Flow Cytometry: General Procedure for the Analysis of Cells

To exclude non-viable cells and debris from the analysis by flow cytometry, the viable cell population was determined. Viable cells have different scatter characteristics to non-viable cells due to their morphology; the scatter plot was therefore used to select the viable cell population. Flow cytometry was used in Chapter 5 to assess cell association and relative binding affinity of ligands for uPAR. Following incubation with fluorophores all subsequent steps were conducted at 4 °C. After treatment with fluorophores and rinsing with PBS adherent cells were scraped in PBS and centrifuged (2000 RCF, 2 min, 4 °C), the supernatant removed and the cell pellet re-suspended in 300 µl of PBS (4 °C). U937 cells were centrifuged after treatment with fluorophores and rinsed by re-suspension in PBS/BSA (0.1 %, 4 °C) twice. The method was derived from that described by Ormerod et al. (2000). In the side/forward scatter plot viable cells were selected as a region and this region used to collect events, 10000 events were collected for each sample. Forward and side scatter settings for the different cell lines are shown in Table 2.3, as is the gain for FL-1 (530 nm).

2.3.5 Evaluation of Protein Content Using the Bicinchoninic Acid (BCA) Assay

The BCA assay is widely used to quantify protein (Smith et al., 1985). The method reported previously was used and scaled accordingly. The protein content of cell homogenates was determined to standardise the amount loaded in western blots (Chapter 5), and to establish the specific activity of luciferase in transfection experiments (Chapters 4 and 6). Briefly, in both cases BCA was added to a $CuSO_4$ pentahydride solution (4 % w/v) at a ratio of 1:50 and 200 µl of this reagent was added to 20 µl of cell lysate (Sections 2.3.7 and 2.3.8.1) and incubated at 37 °C for 25 min. The absorbance of the copper-I-BCA complex was measured at 550 nm using the Tecan plate reader. Calibration standards of bovine serum albumin (BSA) in homogenisation buffer were treated identically to samples and used to quantify the amount of protein in the fractions (Fig. 2.3).

Table 2.3 – Flow cytometer settings for the detection of cell fluorescence

Detector	Voltage	Amplification Gain	Mode	Cell Line
FSC	E – 1	4.00	Linear	DU145
SSC	290	1.00	Linear	DU145
FL1	398	1.00	Log	DU145
FSC	E – 1	4.00	Linear	U937
SSC	360	1.00	Linear	U937
FL1	450	1.00	Log	U937

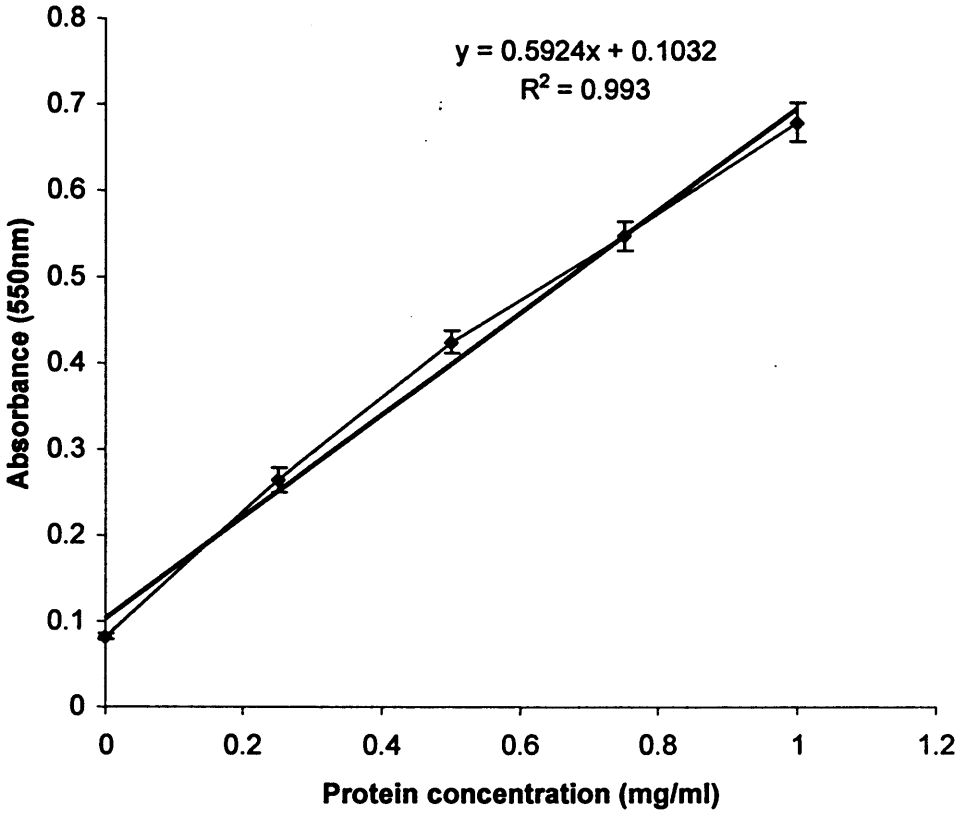

Figure 2.3 – BCA standard protein curve

A typical BCA protein assay calibration curve using BSA as a standard (n=3, ± S.D.)

2.3.6 Luciferase Assay – Preparation of Cell Lysate

Luciferase enzyme catalyses the conversion of luciferin to an oxidated form in a chemiluminescent reaction (Fig 2.4). The manufacturer's method was followed as described (Promega, 2003). Passive cell lysate solution was prepared from passive cell lysate solution (5x) by a 5 fold dilution with ddH_2O. Following transfection, cells were lysed through addition of 200 µl of passive cell lysate solution to each well. They were then incubated on ice for 5 min whilst rocking. Following this, they were frozen -80 °C to ensure complete cell rupture. Wells were then scraped with a rubber policeman, solutions transferred to eppendorfs and vortexed briefly (2 s), centrifuged at 12000 RCF at 4°C for 5 min. Supernatants were transferred using a pipette into fresh eppendorfs and stored at -80 °C until analysis.

2.3.6.1 Luciferase Assay – Analysis of Cell Lysate

This assay was performed with 50 µl of luciferase substrate, added to a luminometer tube and 10 µl of cell lysate mixed in using the pipette. Readings were taken at room temperature with a 3 s delay and 10 s acquisition time in duplicate and results are expressed as relative light units per mg protein.

2.3.7 Plasmid (pGL3 luc) Amplification, Isolation and Characterisation
2.3.7.1 Preparation of Competent E.coli (DH5α)

pGL3 luc (Fig. 2.5) was brought to the group by Dr M. Thanou. A glycerol stock of DH5α was taken out of the -80 °C freezer and defrosted on ice. It was loop inoculated into a sterile bijou containing 2.5 ml of LB medium and grown overnight at 37 °C with shaking at 225 rpm. This culture was inoculated into 250 ml of LB medium containing 20 mM $MgSO_4$ in a 1 L aerated flask and grown for 6 h (A_{600} = 0.4-0.6). The cells were then pelleted by centrifugation at 4500 RCF for 5 min at 4 °C. The cell pellets were then re-suspended in a total volume of 50 ml ice cold 0.1 M $CaCl_2$ and all subsequent procedures were made on ice. Cells were incubated for 5 min at 4 °C then centrifuged (4500 RCF) for 5 min at 4 °C. The pellet was re-suspended in 10 ml of ice cold $CaCl_2$ (0.1 M) and incubated on ice for 40 min then 40 % glycerol (10 ml) was added (v/v in 0.1 M $CaCl_2$). Aliquots (0.2 ml) of this stock solution were then quick frozen in isopropanol/dry ice and stored at -80 °C until use.

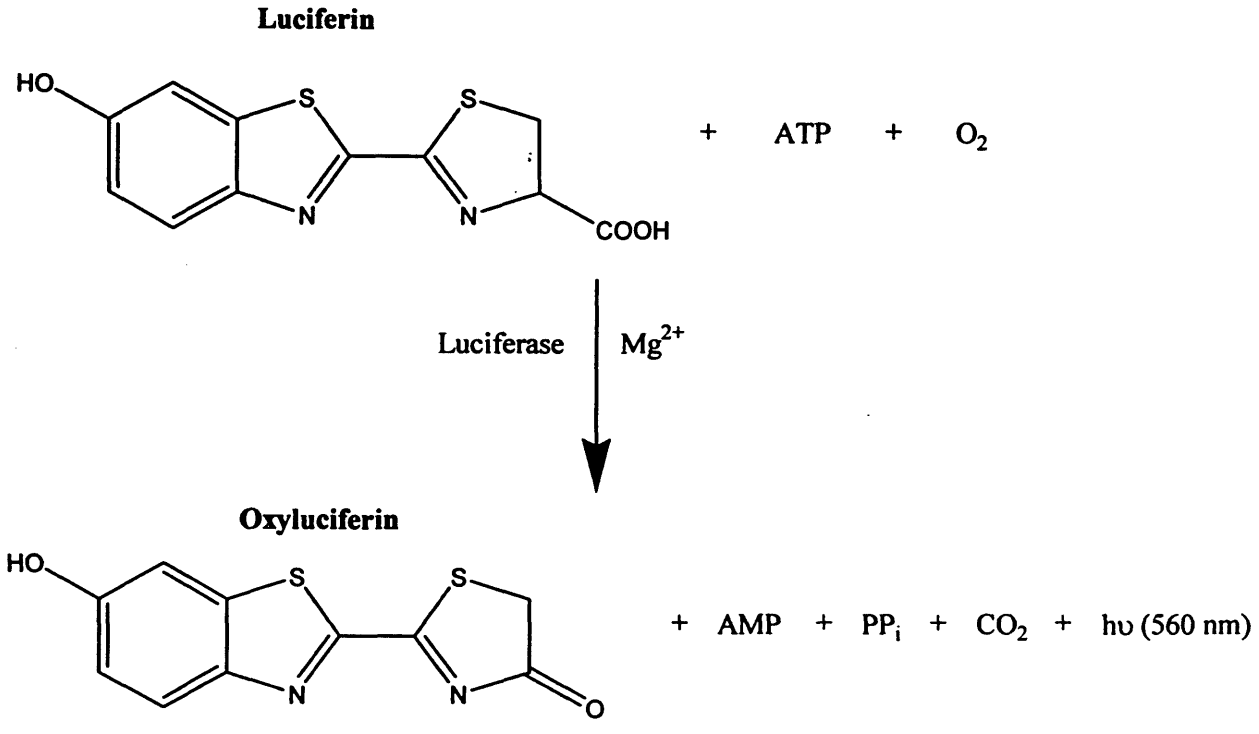

Figure 2.4 – Oxidation of luciferin

Diagram of the enzymatic oxidation of luciferin by luciferase (Adapted from Promega, 2003a).

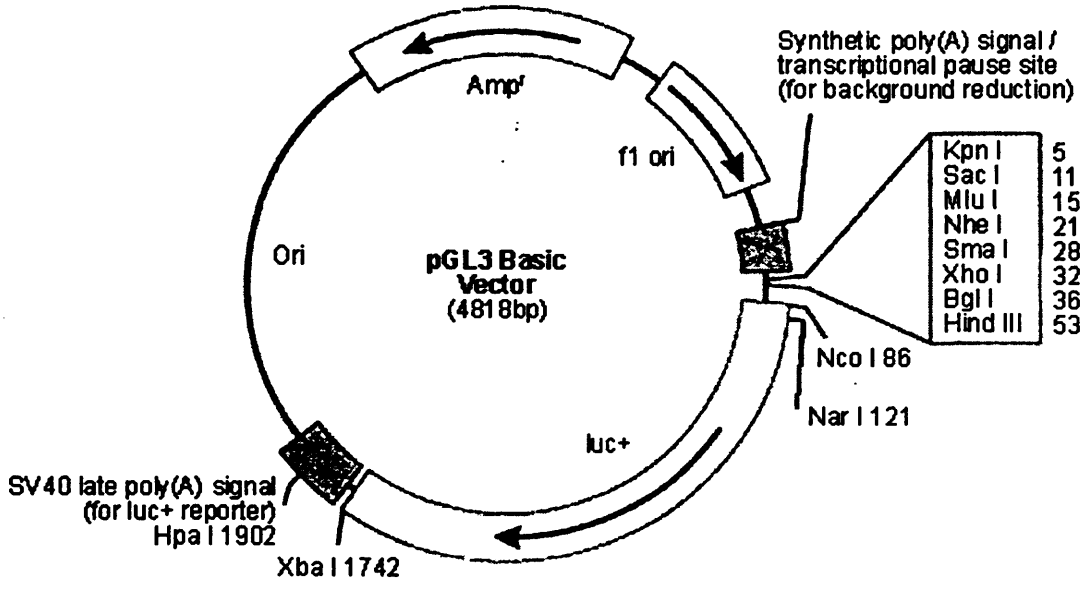

Figure 2.5 - Restriction map of pGL3 luc

Restriction enzyme plasmid map of pGL3 luciferase (from Promega, 2003b). As can be seen the basic pGL3 luciferase vector contains both the luciferase gene and the ampicillin resistance gene.

2.3.7.2 Transformation of Competent DH5α

An aliquot of competent DH5α in glycerol was removed from storage at -80 °C and thawed on ice. pGL3 luc plasmid (~10 ng) was added to the eppendorf (in less than 10 µl) and mixed gently with the pipette tip to avoid shearing the pDNA. This aliquot was incubated on ice for 30 min, then at 42 °C for 1 min before returning to ice for 2 min (heat shock). LB medium (800 µl) was added and the eppendorf incubated for 45 min at 37 °C with shaking at 150 rpm. This culture was then pour plated onto an LB agar plate containing ampicillin (100 µg/ml).

2.3.7.3 Amplification of Transformed DH5α

Amplification of DH5α was performed according to the QIAGEN® plasmid purification method (Qiagen, 2000) and all buffers used are included in the Megaprep plasmid purification kit. A single colony from the ampicillin selection plate was picked with an inoculation loop and inoculated into 10 ml of LB medium containing ampicillin (100 µg/ml) and incubated for 8 h at 37 °C under shaking at 220 rpm. All of this starter culture was inoculated into 500 ml of LB medium in a 1L aerated flask and grown overnight (16 h) at 37 °C under shaking at 220 rpm.

2.3.7.4 Isolation and Purification of the pGL3 luc Plasmid

Transformed DH5α (prepared as described above) were pelleted by centrifugation at 6000 RCF for 15 min at 4 °C. A QIAfilter Mega-Giga cartridge was attached to a 1 L Pyrex bottle. The bacterial pellet was re-suspended thoroughly using a pipette in a total volume of 50 ml of the buffer P1 (50 mM Tris.Cl pH 8.0, 10 mM EDTA, 100 µg/ml RNase A) and transferred to a 500 ml bottle. To this, 50 ml of the buffer P2 (200 mM NaOH, 1 % SDS (w/v)) was added and mixed thoroughly by inversion of the bottle 4-6 times. This solution was incubated at room temp for 5 min. Neutralisation of pH was achieved by addition of 50 ml of chilled buffer P3 (3.0 M potassium acetate pH 5.5) and the solution was mixed by inversion 4-6 times. A white precipitate formed.

The lysate was transferred to the QIAfilter Mega-Giga cartridge prepared at the start and incubated at room temperature for 10 min to allow the protein precipitate to float on top of the rest of the solution. The precipitate was removed by vacuum filtration and the solution collected. The vacuum was stopped and 50 ml of buffer FWB (750 mM NaCl, 50 mM 4-Morpholinepropanesulfonic acid (MOPS) pH 7.0, 15 % isopropanol (v/v))

was added with gentle stirring of the white precipitate. Then the vacuum was reapplied and the flow-through solution was combined with the previous filtrate. A sample (120 µl) of the cleared lysate was removed and stored for analysis.

The buffer ER (12.5 ml) was then added to the filtered lysate and mixed by inversion 10 times before a 30 min incubation on ice. A QIAGEN-tip 2500 was equilibrated with 35 ml of buffer QBT (750 mM NaCl, 50 mM MOPS pH 7.0, 15 % isopropanol (v/v), 0.15 % triton X-100) with flow being gravity driven and flow stopping when the meniscus reached the top of the column. The filtered lysate was then added to the column. The QIAGEN-tip was washed with 200 ml of buffer QC (1.0 M NaCl, 50 mM MOPS pH 7.0, 15 % isopropanol (v/v)) and a 160 µl sample of the eluent was taken for analysis.

DNA was then eluted from the column with 35 ml of buffer QN (1.6 M NaCl, 50 mM MOPS pH 7.0, 15 % isopropanol). A sample of the eluent (22 µl) was taken for analysis. The DNA was precipitated from the eluent solution by addition of isopropanol (26 ml). The centrifuge tube was marked on the back to indicate the expected position of the pellet and the solution centrifuged at 15000 RCF for 30 min at 4 °C. The supernatant was carefully decanted to avoid loss of the DNA pellet. Ethanol (70 % v/v) was used to wash the pellet and then re-centrifuged at 15000 RCF for 10 min at 4 °C. The ethanol was decanted and the pellet air dried for 10 min. The dried pellet was re-dissolved in 2 ml of buffer TE (10 mM Tris.Cl pH 8.0, 1 mM EDTA).

2.3.7.5 Quantification of pGL3 luc

Quantification of plasmid concentration was made using both UV absorbance and quantification of band intensity in agarose gel. The UV absorbance (280 nm) of a 50 µg/ml solution of pDNA has an absorbance of 1. Therefore, by measuring the UV absorbance (280 nm) of the isolated pGL3 luc (as described above) it was possible to calculate the concentration in a sample of plasmid.

For the agarose gel characterisation a known concentration of pDNA was loaded onto a lane and the band intensity of the sample compared, intensity was measured with ImageQuant (Amersham, UK). Agarose gel electrophoresis also confirms the identity of the plasmid through the comparison of restriction digests of the stock and plasmid preparation. As can be seen in Fig. 2.6 the retention factor (rf) of the complete plasmid and EcoR1/BamH1 restriction digest fragments are the same in the stock (lanes 3 and 4) and plasmid preparation (lanes 5 and 6) confirming the plasmid production.

2.3.8 DNA Agarose Gel Electrophoresis

Agarose (350 mg) was dissolved in Tris/Borate EDTA buffer (50 ml; TBE) by heating in a microwave until boiling, this solution was allowed to cool and ethidium bromide was added (0.05 μg/ml). Gels (0.7 %) were then cast in a 10 x 20 cm gel tank, any bubbles were removed with a pipette tip and then gel comb was added and the gel allowed to set. Gel electrophoresis was carried out in a horizontal tank containing TBE buffer and was run at 100 V for 1.5 h. Gels were imaged using the Typhoon 9410 Variable Mode Imager. This technique was used for the analysis of polyplexes (Chapters 4 and 6) and in the confirmation of plasmid preparation and purification (Fig. 2.6).

2.3.9 Western blotting

2.3.9.1 Preparation of a Cell Lysate

First a cell lysis buffer was prepared: 1 % (v/v) triton-X-100, 0.5 mM EDTA, 15 mM NaCl, 2 mM Tris base. This solution was aliquoted and stored at -20 °C. Before use the following protease inhibitors were added: leupeptin (2 μg/ml), pepstatin A (1 μg/ml), aprotinin (2 μg/ml) and phenylmethylsulphonyl fluoride (100 μg/ml).

In the case of the adherent cell lines: Caco-2; COS-1; COS-7; DU145; MCF-7 and PC3 cells, the cells were grown to 70-90 % confluence in a 75 cm^2 flask, washed with ice cold PBS on ice and 1 ml of the lysis buffer was added to cells. They were incubated on ice with rocking for 5 min before transfer to a -80 °C freezer. The flasks were removed from -80 °C and defrosted on ice, cells were scraped from the flask and the contents transferred to 1.5 ml eppendorfs. These were vortexed for 30 s then centrifuged at 13000 RCF at 4 °C for 10 min. The supernatant was removed and analysed for protein content using the BCA assay as described in Section 2.3.5. This solution was aliquoted and the samples stored at -80 °C until use in western blot experiments. In the case of the suspension cell line: U937, 20 ml of culture (at 70-90 % maximum cell density) was centrifuged at 200 RCF and resuspended in 1 ml of lysis buffer. This was incubated on ice for 5 min then frozen at -80 °C. This was removed from the freezer and defrosted on ice before a 30 s vortex. The lysate was then cleared by centrifugation at 13000 RCF for 10 min at 4 °C then the supernatant was removed. This solution was analysed for protein content using the BCA assay as described in Section 2.3.5. The remaining solution was aliquoted and stored at -80 °C until use in western blot experiments.

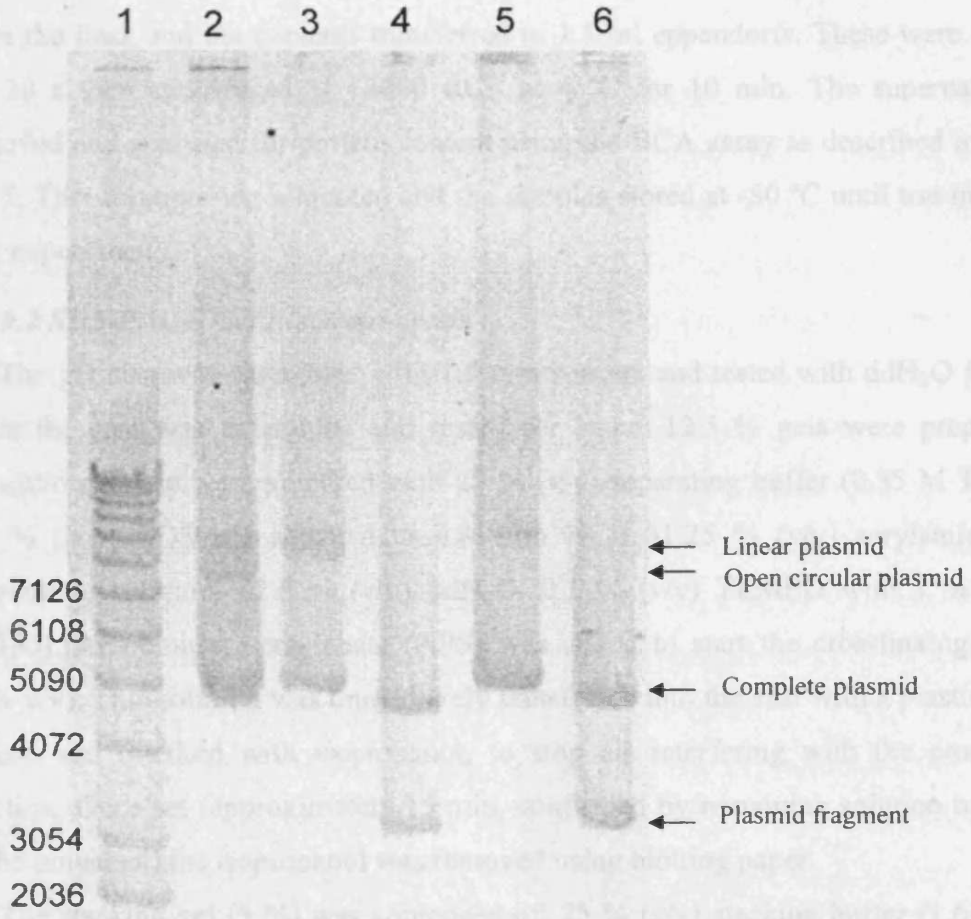

Figure 2.6 - Agarose gel electrophoresis of pGL3 plasmid preparation

Image of the electrophoretic separation of pGL3 luciferase plasmids. Lanes: 1) 1 kb ladder (bp sizes indicated on left); 2) Cleared DH5α lysate; 3) Stock pGL3 luc plasmid; 4) Stock pGL3 luc digested with the restriction enzymes EcoR1 and BamH1; 5) Purified plasmid preparation; 6) Purified plasmid preparation digested with EcoR1 and BamH1. The gel was imaged using Typhoon 9410 Variable Mode Imager.

In the case of the differentiated U937 cells, 1 x 10^6 cells were re-suspended in cell culture medium (10 ml) containing PMA (150 nM) and transferred to a 75 cm^2 flask. After 24 h the cells were washed with ice cold PBS on ice and 1 ml of the lysis buffer added. They were incubated on ice with rocking for 5 min before transfer to a -80 °C freezer. The flasks were removed from -80 °C and defrosted on ice, cells were scraped from the flask and the contents transferred to 1.5 ml eppendorfs. These were vortexed for 30 s then centrifuged at 13000 RCF at 4 °C for 10 min. The supernatant was removed and analysed for protein content using the BCA assay as described in Section 2.3.5. This solution was aliquoted and the samples stored at -80 °C until use in western blot experiments.

2.3.9.2 SDS-PAGE Gel Electrophoresis

The gel cast was assembled with 1.5 mm spacers and tested with ddH_2O for leaks. Once the cast was assembled and tested for leaks, 12.5 % gels were prepared for separation. These were prepared with 25 % (v/v) separating buffer (0.55 M Tris base, 0.4 % (w/v) SDS pH adjusted to 6.8 with HCl) 31.25 % (v/v) acrylamide / bis-acrylamide solution, 42.6 % (v/v) ddH_2O, 0.1 % (v/v) TEMED with 1 % (w/v in ddH_2O). Ammonium persulphate (APS) was added to start the crosslinking reaction (1 % v/v). This solution was immediately transferred into the cast with a plastic Pasteur pipette and overlaid with isopropanol, to stop air interfering with the crosslinking reaction. Once set (approximately 15 min, confirmed by remaining solution having set in the universal) the isopropanol was removed using blotting paper.

The stacking gel (5 %) was composed of: 25 % (v/v) stacking buffer (1.64 M Tris base, 0.4 % (w/v) SDS pH adjusted to 8.8 with HCl), 12.5 % (v/v) acrylamide / *bis*-acrylamide, 61.5 % (v/v) ddH_2O, 0.1 % (v/v) TEMED and 1 % APS (w/v in ddH_2O). After addition of APS this was immediately overlaid on the separating gel and the gel comb inserted making sure no bubbles were in the wells. This was allowed to set for 15 min (confirmed by the remaining gel setting in the universal tube) then the comb was removed.

The gel assembly was taken out of the casting apparatus and put into the gel tank, running buffer (0.025 M Tris base, 0.192 M Glycine, 0.1 % SDS) was then poured into the tank so that the buffer level was above the top of the gel (~800 ml). Cell lysate aliquots were removed from -80 °C, appropriate volumes transferred to eppendorfs and non-reducing solubilising buffer (0.12 M Tris base, 4 % (w/v) SDS, 20 % (w/v) sucrose,

0.004 % (w/v) bromophenol blue pH adjusted to 6.8 with HCl) added at $1/6^{th}$ of the volume of lysate and then boiled (100 °C) for 5 min. Lysates were loaded into wells using gel loading tips and ran against protein standards. Gels were electrophoresed at 150 V for 45 min.

Transfer of protein from SDS-PAGE gel onto PVDF membrane was made. PVDF membrane was cut to the correct size for the gel and prepared for transfer by soaking in methanol. Sponges and blotting paper were soaked in cold transfer buffer (0.025 M Tris base, 0.192 M Glycine, 20 % methanol (v/v)). Gels were removed from the electrophoresis tank and carefully removed from the glass plates. They were sandwiched in a transfer cassette as shown in Fig. 2.7. The transfer cassette was loaded into the gel tank and an ice pack added before cold transfer buffer addition; electrophoresis was performed at 150 mA overnight in the cold room (4 °C).

Western blotting (Fig. 2.8) of the PVDF membrane was performed after protein transfer. The MW marker lane was cut off the PVDF membrane and stored at 4 °C. First, the membrane was blocked with blocking buffer (40 ml; 0.01 M Tris base, 0.2 M NaCl pH adjusted to 7.4 with HCl 0.05 % Tween 20, 5 % (w/v) milk protein) for 30 min on a rocker followed by three washes of 5 min with blotting buffer (10 ml; 0.01 M Tris base, 0.2 M NaCl pH adjusted to 7.4 with HCl 0.05 % Tween 20).

Following this, the primary antibody was incubated on the membrane (polyclonal = 1 h, monoclonal = 2 h). Three washes of 10 min were then made with blotting buffer before addition of the secondary antibody for 45 min. Finally 3 washes of 10 min were made before chemiluminescent detection was made. The secondary antibodies used were horse radish peroxidase conjugates. Detection was made in a dark room using enzyme linked chemiluminescence (ECL) detection reagents (A and B) from Amersham (UK) (Fig. 2.8). This works on the basis of the horse radish peroxidase antibody conjugate catalysis of luminol in alkaline conditions. The luminol is then in an excited state which decays in a chemiluminescent reaction. ECL reagent A was mixed with ECL reagent B in a 1:1 ratio to give sufficient solution to cover the membrane at 0.125 ml/cm^2. The ECL reagent was then incubated on the membrane for 1 min before transfer of the membrane to be sandwiched between clingfilm then placement in an x-ray cassette containing film. Films were scanned using a Canoscan8000F scanner.

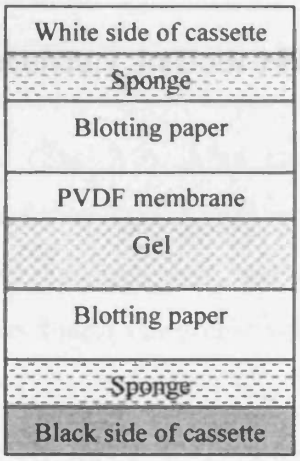

Figure 2.7 - Assembly of SDS-PAGE transfer cassette.

After electrophoresis of cell lysates they were transferred electrophoretically in a transfer cassette. The gel was placed in the cassette as shown and protein was transferred and retained by the PVDF membrane.

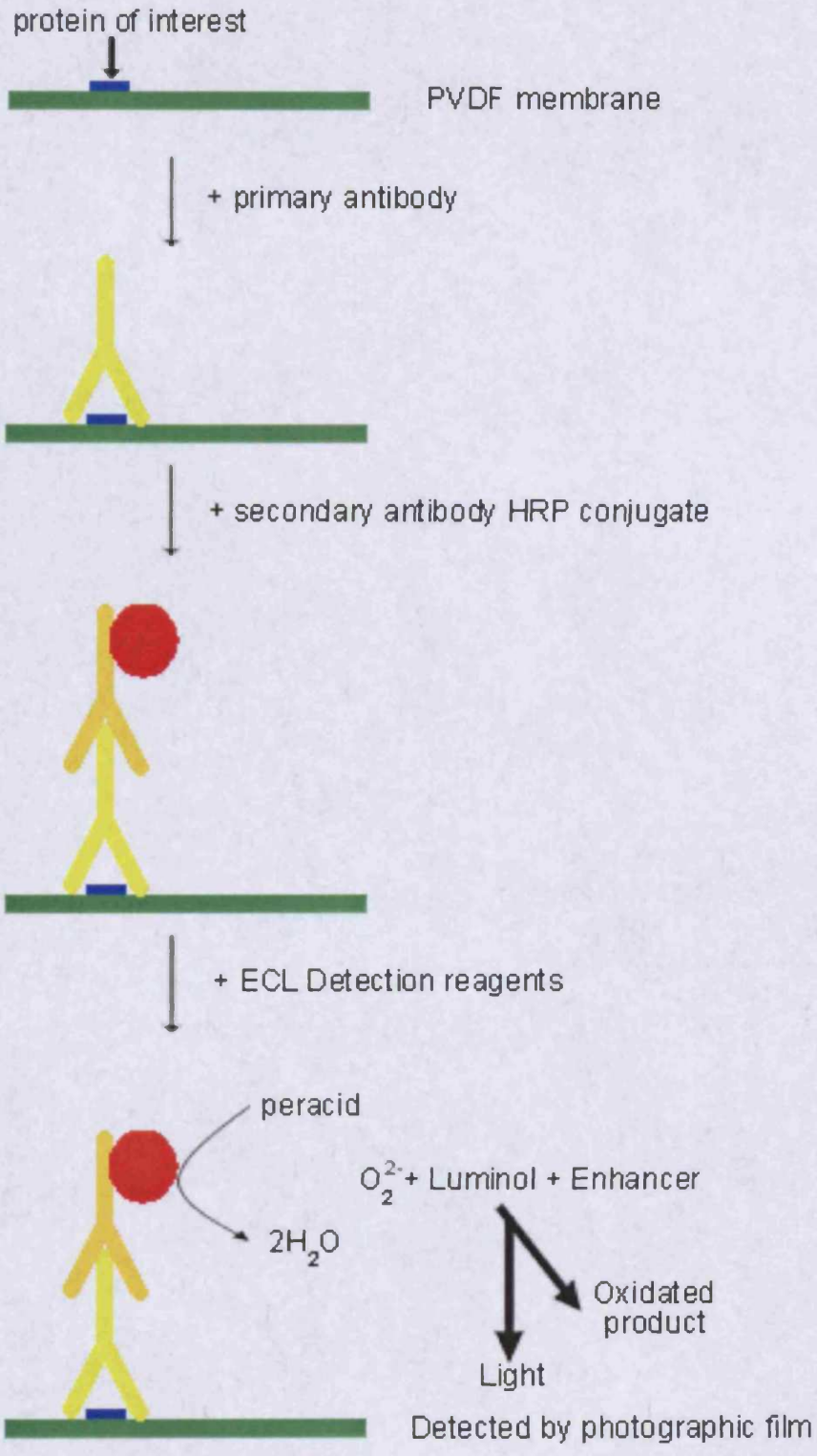

Figure 2.8 - Western blotting and detection

Figure showing the western blot process after transfer of protein to PVDF membrane has been performed.

2.3.10 Solid Phase Peptide Synthesis (SPPS)

Solid phase peptide synthesis was performed using standard FMOC-based chemistry. The peptides u7 and Gu11G were prepared in the Univ Nijmegen by Dr M. Thanou. Scrambled u7 and scrambled u11 peptides were synthesised in collaboration with Sian Owens (Welsh School of Pharmacy, Cardiff University, UK) on an automated Symphony Quartet Peptide Synthesiser (Zinsser analytic, UK). First the amino groups of the rink amide resin were deprotected with a solution of 20 % w/v piperidine in DMF, this was done three times. The resin was then washed twice with NMP and the Kaiser test performed which should be positive indicating free NH_2. Sequential coupling of the amino acids and cleavage of N-protecting group was then performed in the C-N direction as outlined (Fig. 2.9). After the final coupling, deprotection and cleavage from the resin was performed using trifluoroacetic acid. The peptides prepared are shown in Fig. 2.10. Mass spectroscopy was used to characterise the products (Fig. 2.11). The molecular mass found correlated with the predicted molecular masses, the predominant ion in the analysis of Gu11G was the ½ mass peak due to ionisation producing 2 +ve charges, probably on the terminal amine and the amine of lysine.

2.3.11 Gel Permeation Chromatography (GPC)

For the GPC characterisation of PEG conjugates, PBS (0.1 M, pH 7.4) was used as mobile phase and it was first filtered (0.22 μm nylon Micropore filter) then sonicated for 30 min to remove dissolved gases. The flow rate was set to 1 ml/min, the system was purged and the baseline allowed to stabilise before injecting any samples. Samples were introduced to the system through a 20 μl sample loop. A calibration curve was made with PEG standards and samples characterised against it (Fig. 2.12) using Caliber software.

An organic GPC system was also used. The flow rate was also set to 1 ml/min with the system being purged and stabilised before injection of samples. Toluene was used as a flow rate marker. The calibration curve (Fig. 2.13) was made with polystyrene standards using Cirrus GPC software.

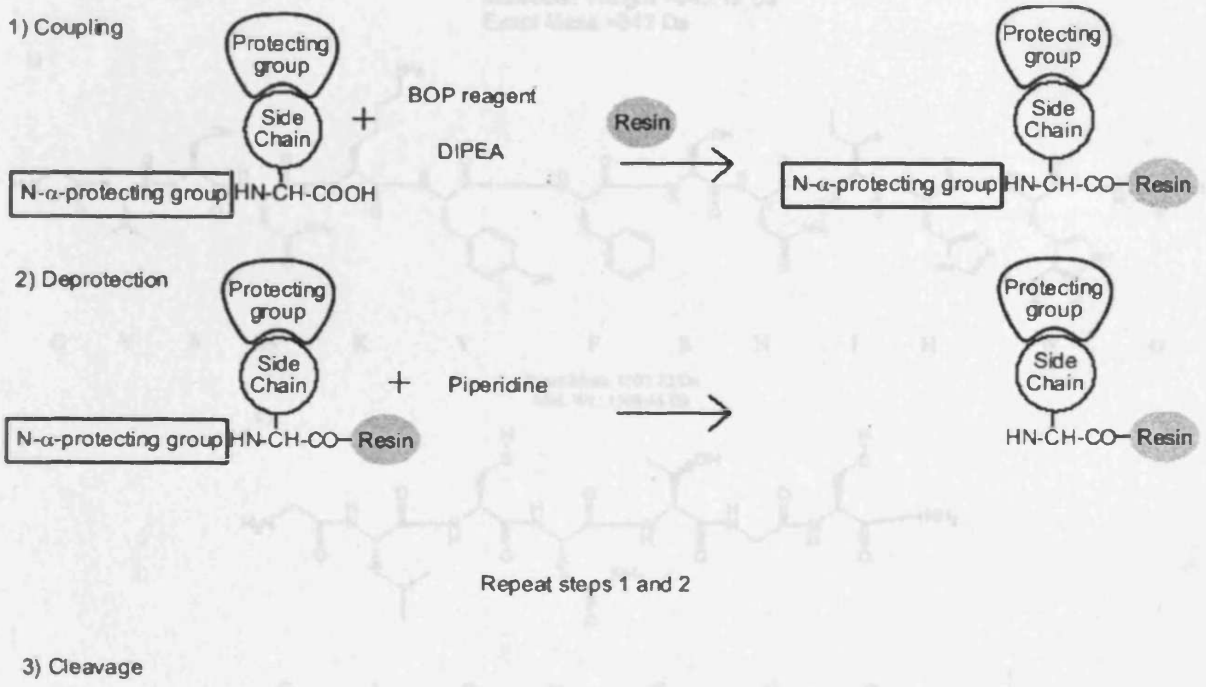

Figure 2.9 - Solid phase peptide synthesis

Peptides were synthesised by the above scheme in a sequential addition in the C-N direction.

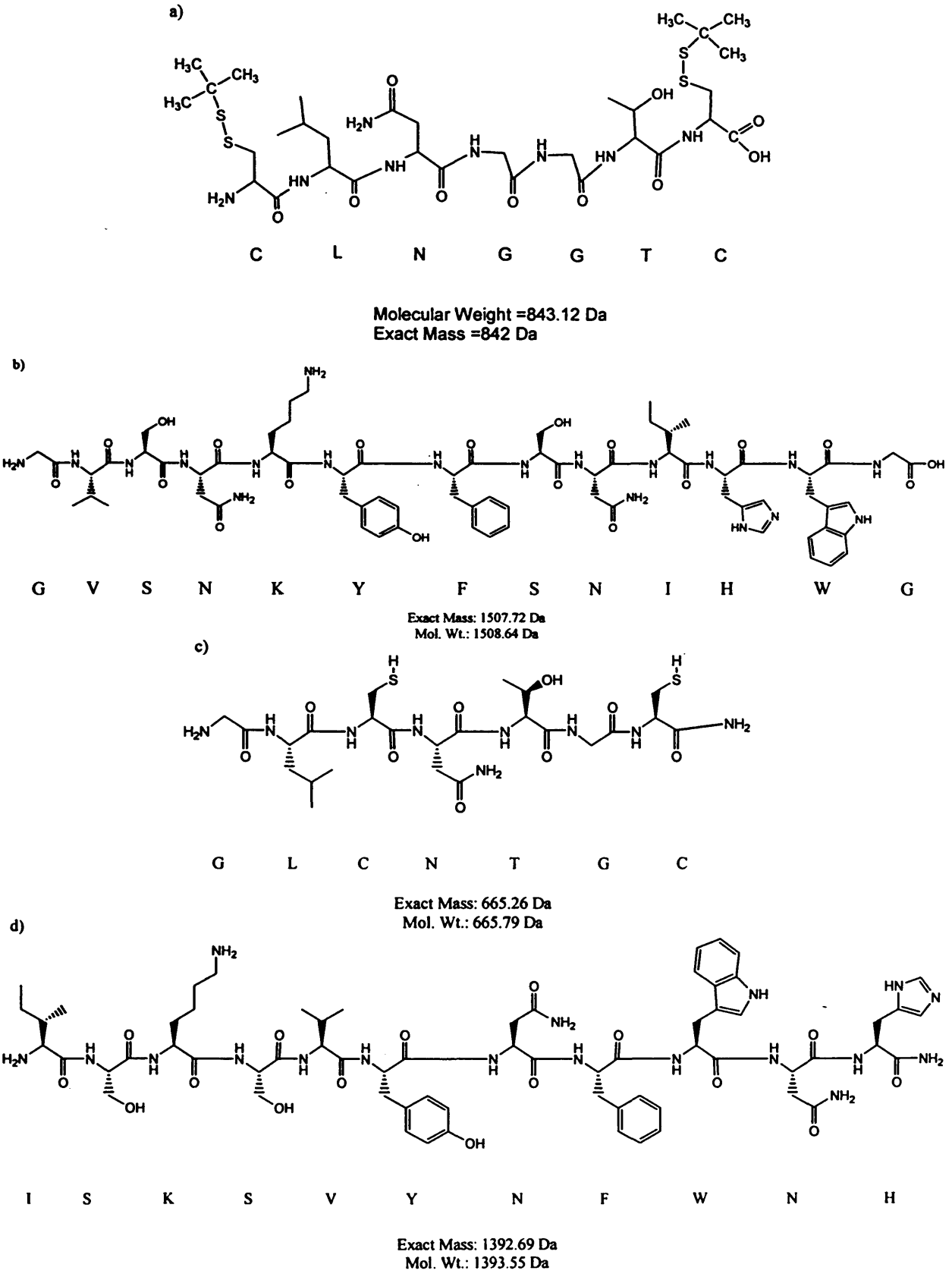

Figure 2.10 - Peptide structures

Structures of peptides synthesised by SPPS, a) u7 with t-butyl protecting groups, b) Gu11G, c) scrambled u7, d) scrambled u11.

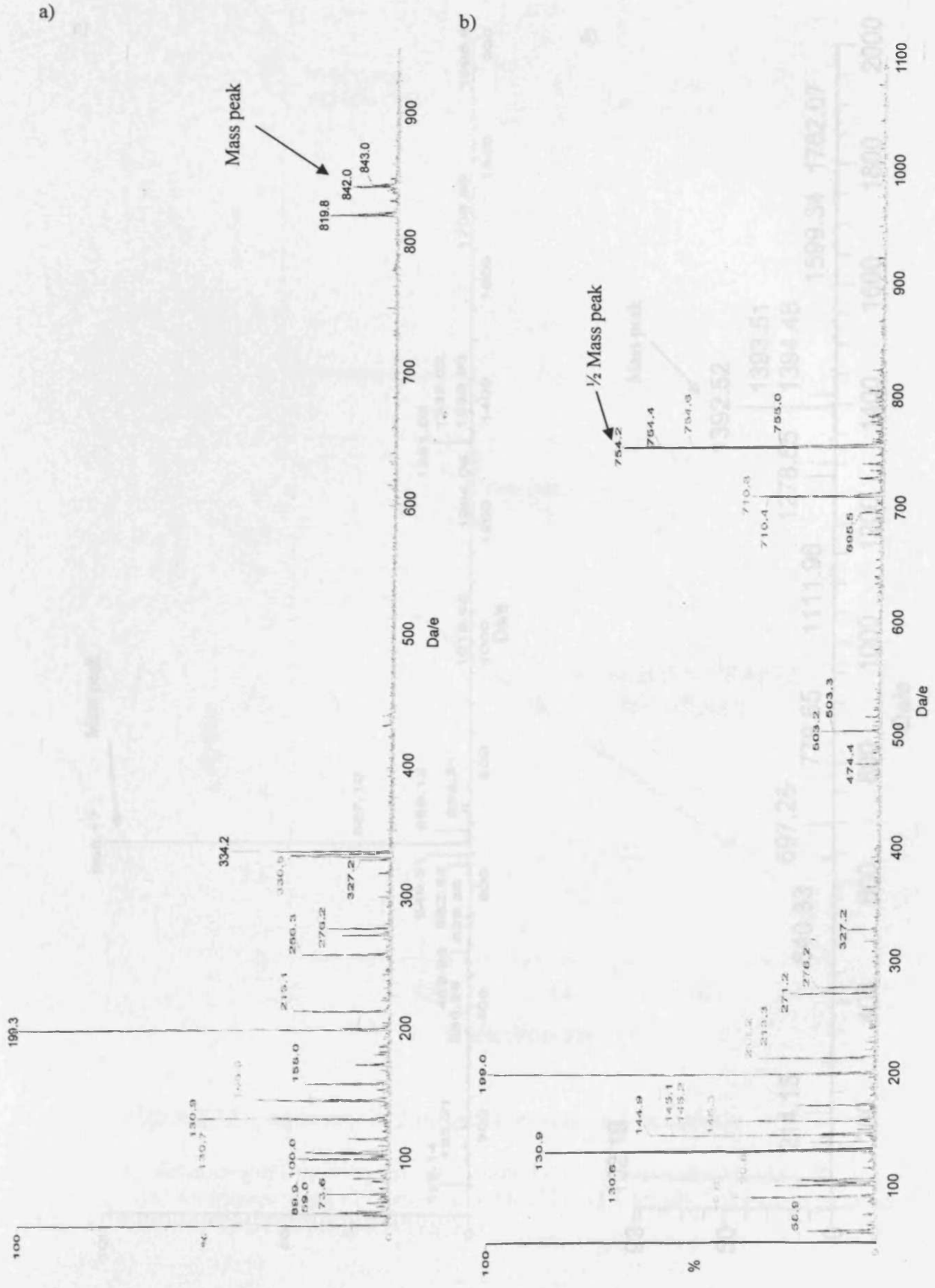

Figure 2.11 – Mass spectra of peptides

Mass spectra confirming the synthesis of peptides a) u7 with t-butyl protecting groups, b) Gu11G

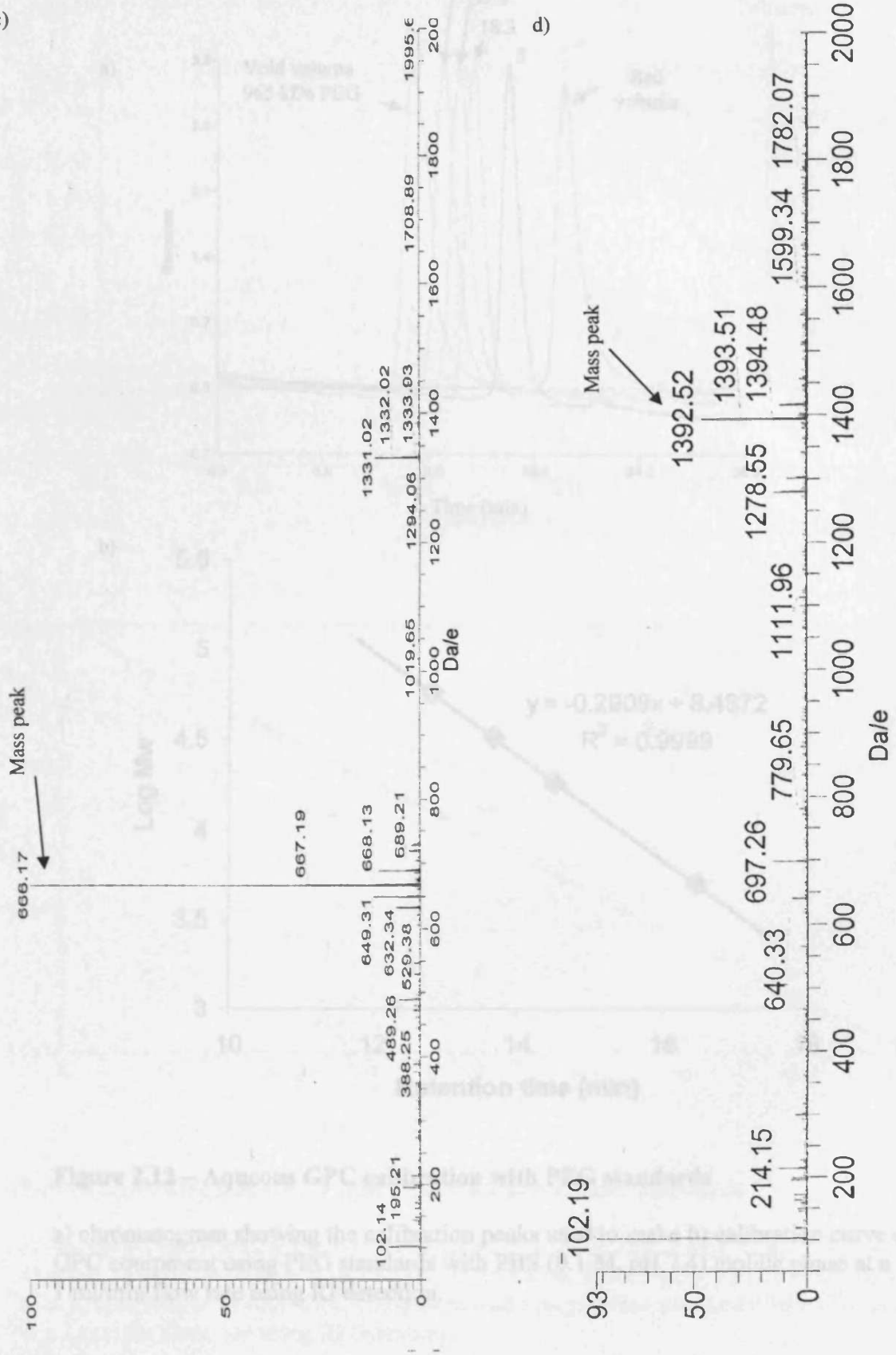

Figure 2.11 continued – Mass spectra of peptides

Mass spectra confirming the synthesis of peptides c) Scrambled u7, d) Scrambled u11

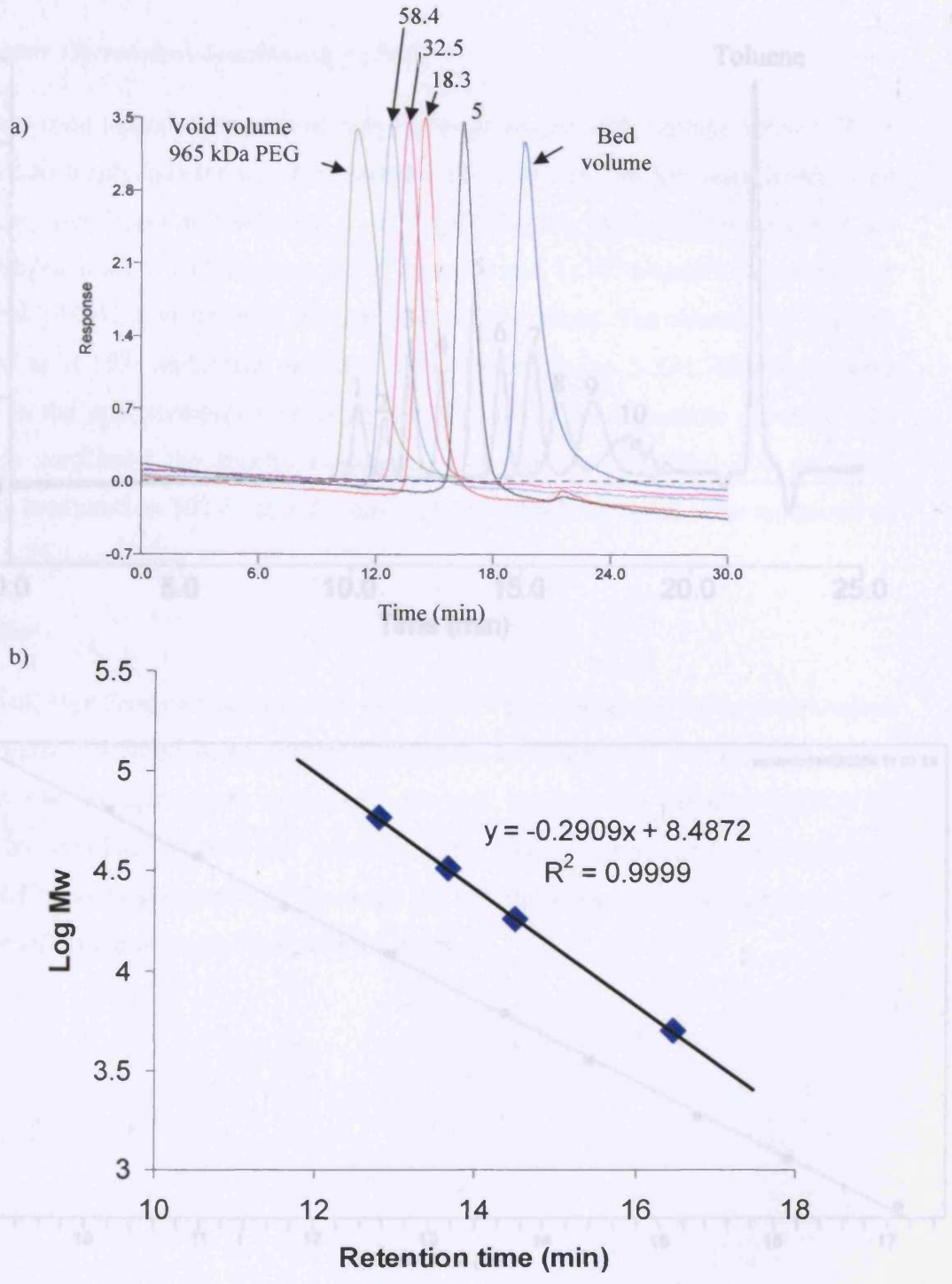

Figure 2.12 – Aqueous GPC calibration with PEG standards

a) chromatogram showing the calibration peaks used to make b) calibration curve of GPC equipment using PEG standards with PBS (0.1 M, pH 7.4) mobile phase at a 1 ml/min flow rate using RI detection.

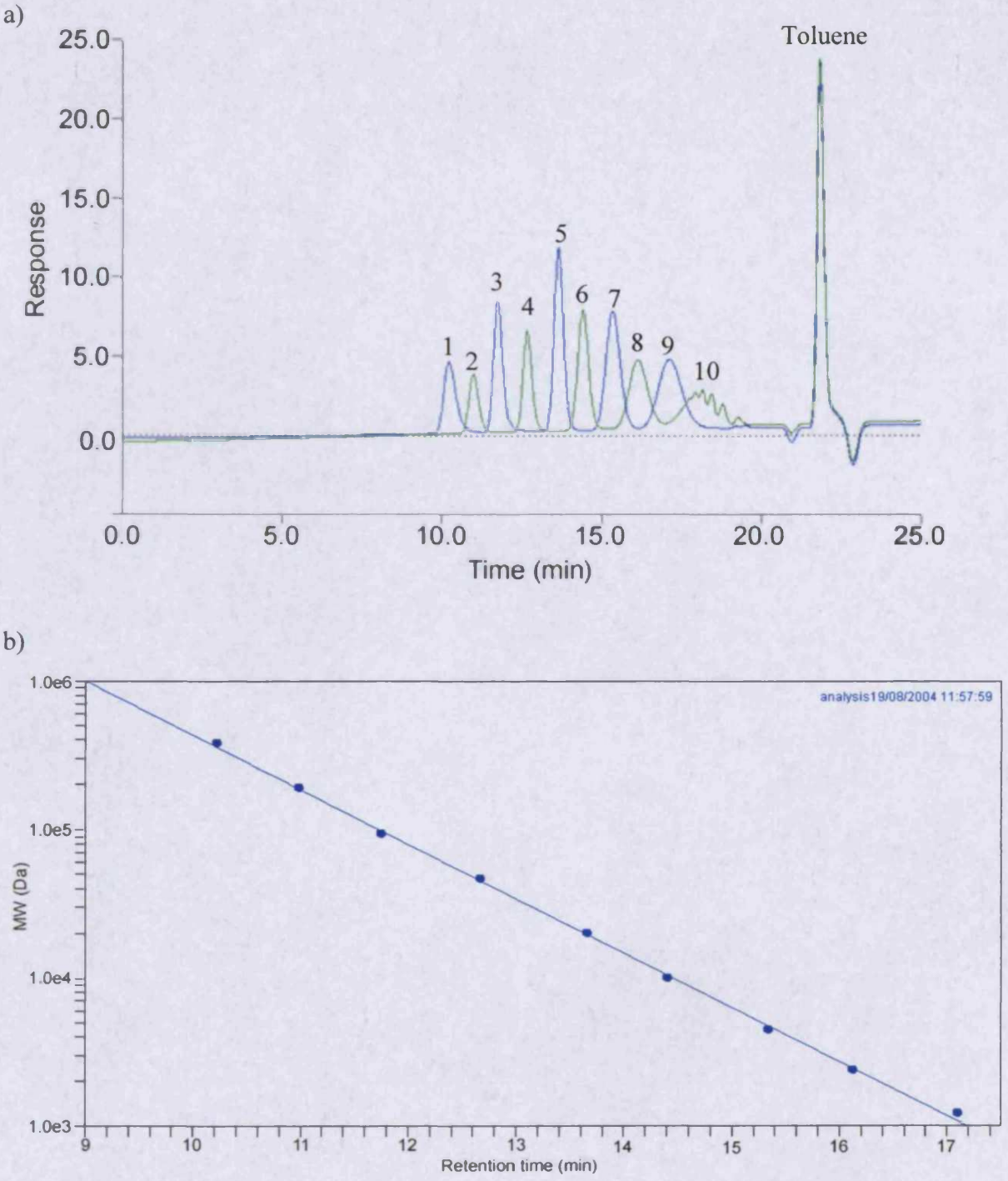

Figure 2.13 – Organic GPC calibration with polystyrene standards

a) chromatogram showing the calibration peaks: 1) 380 kDa, 2) 187.6 kDa, 3) 92.4 kDa, 4) 46.03 kDa, 5) 19.76 kDa, 6) 9.91 kDa, 7) 4.46 kDa, 8) 2.35 kDa, 9) 1.20 kDa, 10) 0.58 kDa b) calibration curve of GPC equipment using polystyrene standards with THF eluent at a 1 ml/min flow rate using RI detection.

2.3.12 Photon Correlation Spectroscopy (PCS)

PCS was used to assess the size of polyplexes produced with cationic vectors. Prior to use the spectrophotometer was first tested using 100 and 300 nm latex beads. One microlitre of latex beads was added to 3 ml of DMEM, the intensity measured and the solution diluted until it was between $1x10^4$ counts/s and $1x10^6$ counts/s. Measurement was made at 20.0 °C at an angle of 90 ° over 180 s three times. The viscosity of DMEM was stated as 1.657 centipoise and the refractive index as 1.334. Solutions were measured in the spectrophotometer using at least 600 µl in disposable cuvettes. The latex beads confirmed the spectrophotometer was working correctly; 100 nm latex beads were measured as 102.8 nm ± 8.6 nm (SD), 300 nm latex beads were measured as 317.4 nm ± 74.5 nm (SD).

2.4 Statistics

Statistical significance was assigned to $p < 0.05$ and calculated using a two-tailed Student's t-test (paired/unpaired as indicated) for the comparison of two samples. When more than two samples were compared one-way analysis of variance (ANOVA) followed by Bonferroni post-hoc analysis was used. Where indicated, standard deviation (SD) or standard error of the mean (SEM) for data points was calculated and the number (n) of experiments/replicates are given.

Chapter 3

Synthesis and Characterisation of Modified Chitosans

3.1 Introduction

Development of a targeted non-viral gene delivery system requires a biocompatible and versatile transfection reagent. Having chosen trimethylated chitosan as the vector for study, it was necessary to prepare a library of modified chitosans that could be used to optimise the targeted non-viral gene delivery system. As mentioned in Section 1.5.2.1.2 chitosan is derived from chitin, the second most abundant biopolymer after cellulose (Jeuniaux & Voss-Foucart, 1991), by a process of de-acetylation. This gives a random copolymer containing α1-4 linked N-acetyl glucosamine and glucosamine monomers. The term 'chitosan' therefore encompasses a wide range of polymers that have various degrees of de-acetylation and molecular weight. In this study chitosan oligomers (3-6 kDa) and polymers (~100 kDa) have been modified to investigate the effect of molecular weight on the properties of the derivatives.

Although chitosan is readily available as an abundant natural resource it is poorly soluble at neutral pH creating problems for its use in formulation. As mentioned (Section 1.5.2.1.2) trimethylation of chitosan increases the pH range over which the derivative is soluble and gives a permanent cationic charge. Based upon previous chitosan trimethylation work (Domard et al., 1986, Thanou et al., 2000) it was important to study the trimethylation reaction in polymers and oligomers.

From the work of Murata et al. (1996, 1997) it was clear that a 6-O-carboxymethyl functionality could be introduced using chloroacetic acid. This functionality could be used to conjugate the peptide ligands using EDC coupling (Hermanson, 1996). Although EDC activation of carboxylic acids for their coupling to amines is a widely used reaction, the molar ratios of EDC : COOH used vary from 1:1 (Lathia et al., 2004) to 10:1 (Kim et al., 2003) or are not specified in reaction schemes. This method of conjugation of peptides to the carboxymethyl functionality was therefore studied.

In order to visualise the derivatives and their uptake in the cell, fluorescent labelling was investigated. Radiolabelling was considered but regulatory and safety issues encouraged the application of fluorescent labelling. Fluorescence is exhibited by structurally restricted molecules having aromatic bonds. The process of fluorescence occurs over three stages: excitation, excited state lifetime and emission. Excitation is made by light which is absorbed by the aromatic system; this energy absorption raises the molecule to an excited state. The rigid structure of the molecule means that this energy is lost by emission of light (at a longer wavelength called stokes shift).

Increasing the temperature means more energy is lost through bond rotation, quenching the fluorescence. An increase in concentration has a similar effect, this time energy being lost through collision. Although the fluorescent label alters the chemical structure of the compound being investigated, and therefore may affect the physicochemical properties of the compound, it has the benefit of its application in microscopy and flow cytometry. Fluorescent labelling at a low ratio was sought to give as little disruption to the normal structure and function as possible. Labelling of chitosan has been performed by Tommeraas (2001) using 9-anthraldehyde and this fluorescent derivatisation was investigated. To produce trimethylated fluorescent chitosans, amine protection with citraconic anhydride was examined. Further investigation of the fluorescent probes fluorescein and Oregon Green was made to give improved imaging capacity.

It was with these points in mind that it was decided to create a library of chitosans (Fig. 3.1) with different degrees of trimethylation for study in cytotoxicity and transfection experiments (Chapter 4). The fluorescent labelling and conjugation of peptides enabled the study of the binding and uptake in cell models (Chapter 5). The construct formed from these experiments was then studied in optimisation of polyplexes made with pDNA (Chapter 6).

3.2 Methods

3.2.1 Preparation of N,N,N-Trimethyl Chitosan Oligomer (TMO)

Trimethylation of chitosan oligomer (3-6 kDa, Primex) was performed according to a modification of the method of Sieval et al. (1998) and that described by Domard et al. (1986) (Fig. 3.2). Chitosan oligomer (1.0 g) was dissolved in NMP (40 ml) with sodium iodide (2.4 g) at 60 °C under stirring in a round bottom flask. Addition of sufficient NaOH (10 ml of 15 % w/v; aq.) was made in order to maintain an alkaline environment throughout the reaction. Methylation was achieved through nucleophillic substitution by addition of methyl iodide (12 ml) to the solution and reaction under reflux conditions. Products were precipitated by addition of 5 volumes diethyl ether : ethanol (1:1 v/v) to 1 volume of solution at 20, 40, 60 and 120 min in order to achieve different degrees of trimethylation (DTM) in each case. The precipitates were centrifuged at 3000 RCF for 15 min at 4 °C and the supernatants discarded. Products were then dried under nitrogen to avoid oxidation of iodide and re-dissolved in 0.5 M NaCl to exchange the iodide for chloride ions.

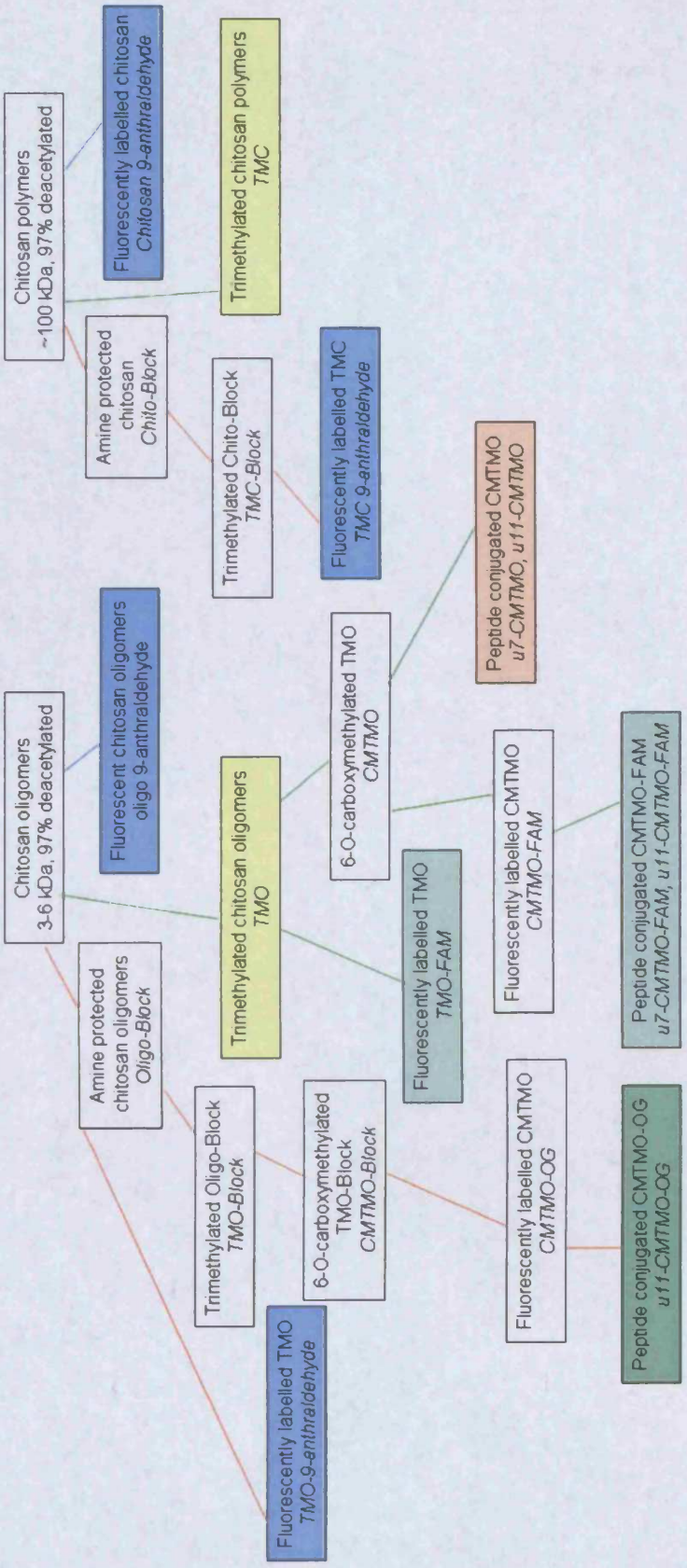

Figure 3.1 – Chitosan modification product map

Labels of products are in italics and shaded boxes indicate final products

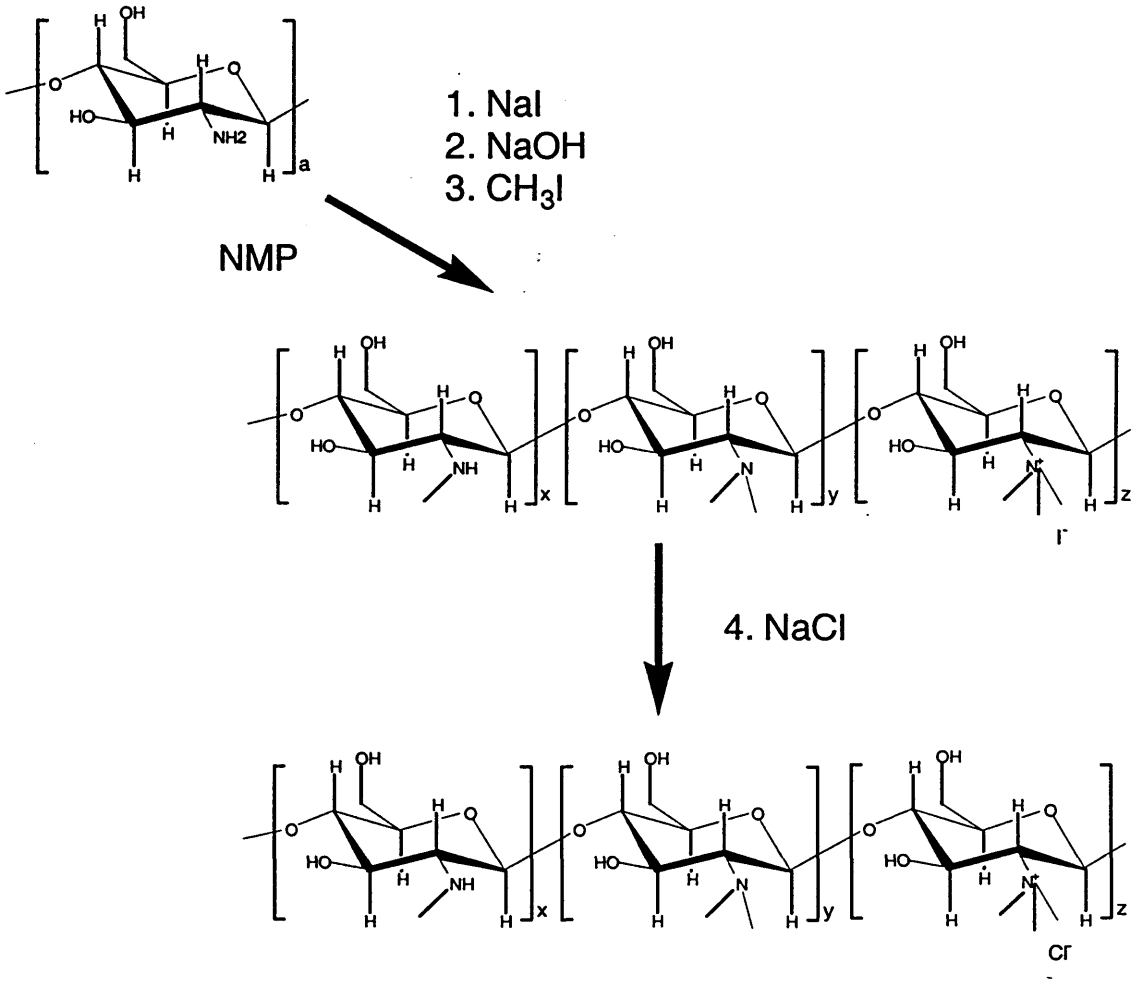

Figure 3.2 – Synthesis of trimethyl chitosan

Reaction scheme of chitosan trimethylation followed by counter ion replacement. The reaction was performed at 60 °C and stirred under reflux conditions. A possible side reaction in the methylation step is methylation at 3-O and 6-O positions.

Counter ion replacement was performed to prevent iodine oxidation and give a smaller counter ion for better complex formation with pDNA. TMO was precipitated again with diethyl ether : ethanol. The precipitates were then centrifuged at 3000 RCF for 15 min (4 °C) and supernatant discarded. The pellet was then thoroughly washed with the diethyl ether : ethanol solution. Finally, after drying the pellet in a vacuum at room temperature, the product was dissolved in H_2O and freeze dried.

Several batches of trimethylated chitosan were made, with the degree of trimethylation being controlled by the length of reaction and the purification as above. Some of this work was performed in collaboration with a visiting student whom I supervised, Susanna Roth. DTM was characterised by ^1H NMR in D_2O.

3.2.2 Preparation of N,N,N-Trimethyl Chitosan Polymer (TMC)

The chitosan polymer (~100 kDa, Primex) used in these studies was trimethylated as above with the exception that precipitation was performed after 30 and 60 min. After the 60 min precipitation the product was dried and re-dissolved in NMP. Trimethylation was repeated as described above with precipitation after a further 30 and 60 min. This gave the products of 30, 60, 90 and 120 min. This work was also performed in collaboration with Susanna Roth. Products were dissolved in D_2O and the DTM characterised by ^1H NMR.

3.2.3 Preparation of 6-O-carboxymethyl N,N,N-Trimethyl Chitosan Oligomers (CMTMO)

A modification of the method described by Murata et al. (1996) was used (Fig. 3.3) to functionalise TMO by reaction with chloroacetic acid to give 6-O-carboxymethylation. TMO (100 mg) was dissolved in NMP (10 ml) and the pH adjusted to 10 with NaOH (2 ml; 15 % w/v, aq.). Initially a range (5, 10, 15 or 20) of chloroacetic acid : TMO monomer molar ratio was used to optimise the synthesis. The pH was re-adjusted to 10 with NaOH (15 % w/v, aq.).

Subsequently a 7.5:1 and 15:1 ratio was used for further study and the 7.5:1 ratio taken forward into future experiments. The reaction was performed under stirring at room temperature for 3 h.

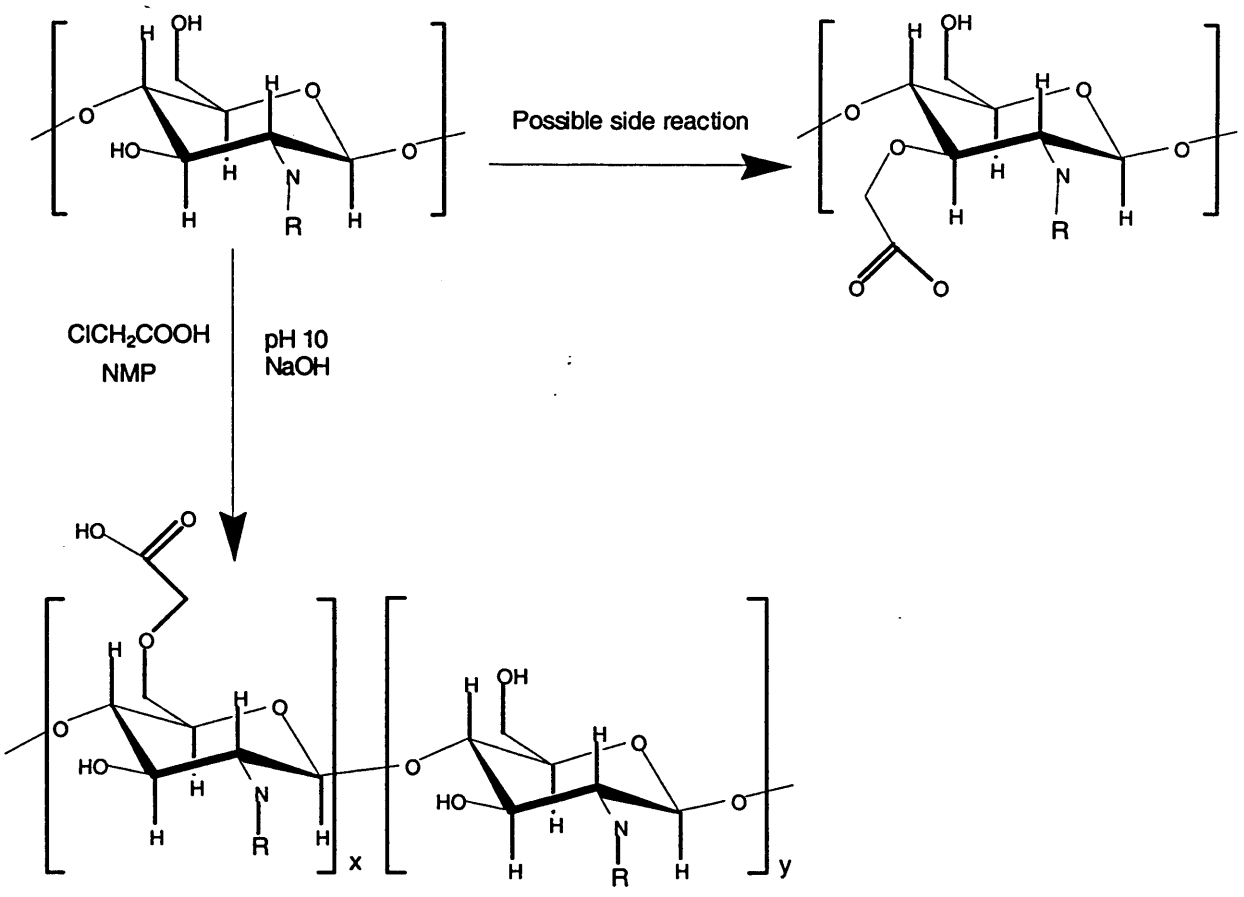

Figure 3.3 - 6-O-carboxymethylation of TMO

Reaction scheme of 6-O-carboxymethylation, R group represents monomethyl, dimethyl or trimethyl substituent. Different degrees of modification are achieved by changing the ratio of chloroacetic acid : modified glucosamine.

The functionalised CMTMO was then precipitated by addition of 5-10 volumes diethyl ether : ethanol (1:1 v/v). It was then centrifuged at 3000 RCF for 20 min at 4 °C. The supernatant was discarded and the pellet was re-dissolved in ddH_2O and washed twice by precipitation with 5-10 volumes diethyl ether : ethanol (1:1 v/v). Finally, the product was re-dissolved in ddH_2O and lyophilised. Products were characterised by ^{1}H and ^{13}C NMR and FTIR (Jansma et al., 2003).

3.2.4 Introducing Protecting Groups on the Amine of Chitosan

This method was developed from the amine protection reaction outlined by Hermanson (1996). In a pilot study conducted with an MPharm project student whom I supervised, Lee Jones, chitosans were protected (Fig. 3.4) for their later reaction with the fluorescent probe 9-anthraldehyde. Chitosan (1 g; oligomer or polymer) was dissolved in sodium carbonate solution (100 ml, 0.1 M, pH 9). A solution containing either a 0.1:1 or 0.4:1 ratio of citraconic anhydride : glucosamine unit was added. The pH of the reaction mixture was maintained at 9 by addition of NaOH (15 % aq.) whilst the mixture was stirred at room temperature for 2 h. Product was precipitated in a mixture of diethyl ether : ethanol (1:1 v/v) and centrifuged at 3000 RCF for 15 min at 4 °C. It was then washed once in ethanol and finally once in diethyl ether. The precipitate was dried under vacuum for 48 h at room temperature.

To develop this technique further, a second study was made with only the chitosan oligomer. Chitosan oligomer (200 mg) was dissolved in water (2 ml) and separated into 5 reaction vessels. This reduced the volume of the solution, in comparison to previous experiments, and aided subsequent steps. The pH of the solution was modified by addition of borate buffer (pH 9, 4 ml) and the 5 reactions performed simultaneously. Chitosan oligomer 3-6 kDa has 18-36 monomer units, so assuming an average of 27 monomer units; the number of moles weighed is divided by 27 to aim for one protected amine per chain. The ratios of citraconic anhydride : glucosamine used were: 0:1, 0.185:1, 0.37:1, 0.56:1 and 0.74:1 added in EtOH. The reaction was performed under stirring at r.t. for 7 h. The products were precipitated by addition of 10 volumes diethyl ether : ethanol (1:1 v/v) followed by centrifugation at 3000 RCF 10 min 4 °C. Supernatants were discarded and pellets re-dissolved in ddH_2O, these were then precipitated with diethyl ether : ethanol (1:1 v/v) followed by centrifugation at 3000 RCF 10 min 0 °C three times.

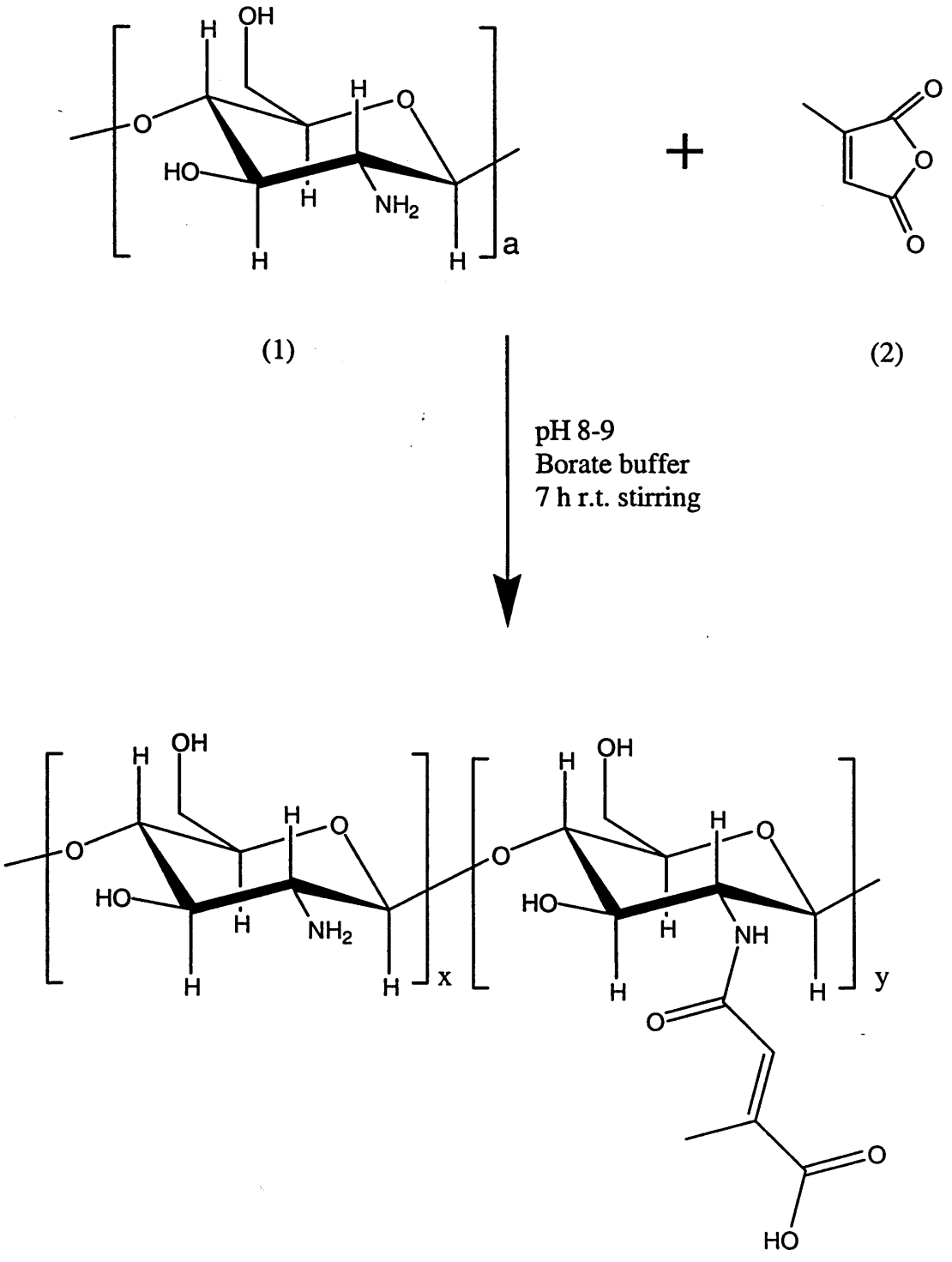

Figure 3.4 - Protection of amine groups on chitosan with citraconic anhydride

Amines on chitosan (1) were reversibly protected with citraconic anhydride (2) in the reaction outlined here. Different degrees of protection were achieved with different ratios of citraconic anhydride: glucosamine.

Products were then dried under vacuum at 30 °C overnight. Products were dissolved in D_2O and analysed by ^1H NMR.

Following this study, it was estimated that to give 10 % protection (so that at least 1 amine per oligomer chain is protected and the peak would be visible in ^1H NMR) a ratio of 0.15:1 citraconic anhydride : glucosamine should be used. The quantity of chitosan in the reaction was scaled up to ensure there was sufficient protected chitosan for any later reaction with Oregon Green to yield fluorescently labelled derivatives (Section 3.2.5.3). Chitosan oligomer (1.43 g) was dissolved in water (14 ml) and the pH modified by addition of borate buffer (28 ml). Citraconic anhydride was then added (144 mg in MeOH) and the reaction performed under stirring at r.t. for 7 h. The product was precipitated by addition of 10 volumes diethyl ether : ethanol (1:1 v/v) followed by centrifugation at 3000 RCF for 10 min 4 °C. Supernatant was discarded and the pellet re-dissolved in ddH_2O, this solution was then precipitated with diethyl ether : ethanol (1:1 v/v) followed by centrifugation at 3000 RCF 10 min 0 °C three times. The product was then dried under vacuum at 30 °C overnight. The product was dissolved in D_2O and characterised by ^1H NMR.

3.2.4.1 Trimethylation of Protected Chitosan

Protected chitosan was trimethylated in a similar reaction to that of unmodified chitosan (Section 3.2.1). In the pilot work with Lee Jones: protected chitosan (1 g) was weighed into a round bottom flask and dissolved in NMP (40 ml) with NaI (2.4 g) and NaOH (10 ml, 15 % w/v) was added to provide an alkaline environment. The reaction mixture was stirred under reflux conditions at 60 °C, methyl iodide added (6 ml) and the reaction performed for 1 h.

In further work the increase in monomer average molecular weight due to the protecting group was taken into account (Equation 3.1) and the same molar ratio of methyl iodide : monomer used as that used in the trimethylation of chitosan.

	Mw		
N-acetyl glucosamine	% x 203		
Protected glucosamine	% x 274		Equation 3.1
Glucosamine	% x 161		
	Sum	= Average monomer weight	

For protected chitosan which was determined to have a 7.7 % degree of protection the average monomer molecular weight was calculated as 171 Da (from Equation 3.1). This protected chitosan derivative was weighed (866 mg) into a round bottom flask, dissolved in NMP (40 ml) under stirring at 60 °C and NaI added (1.961 g). The solution was made alkaline by addition of NaOH (5 ml, 15 % w/v) and methyl iodide was added (9.9 ml) this was reacted for 43 min at 60 °C whilst being stirred under reflux conditions. All other steps were as Section 3.2.1. The product was dissolved in D_2O and characterised by ^1H NMR.

3.2.4.2 Trimethylated Protected Chitosan's 6-O-Carboxymethylation

Trimethylated protected chitosan was 6-O-carboxymethylated in a similar reaction to that of TMO. The increase in monomer average molecular weight was calculated according to Equation 3.2.

To a round bottom flask, 466.4 mg of trimethylated protected chitosan was weighed and dissolved in NMP (50 ml). Alkaline conditions were made by addition of NaOH (4 ml; 15 % w/v). Chloroacetic acid (675 mg) was added to this solution and the pH re-adjusted to 10 with NaOH (~ 1 ml). All other steps were as Section 3.2.3. The product was characterised by ^1H and ^{13}C NMR and FTIR.

	Mw	
N-acetyl glucosamine	% x 203	
Protected glucosamine	% x 274	
Trimethyl glucosamine	% x 206	
Dimethyl glucosamine	% x 189	Equation 3.2
Monomethyl glucosamine	% x 174	
	Sum	= Average monomer weight

3.2.5 Preparation of Fluorescent Chitosan Derivatives

3.2.5.1 Fluorescent Derivatives (9-Anthraldehyde)

3.2.5.1.1 Chitosan-Anthraldehyde

Chitosan was fluorescently labelled with 9-anthraldehyde in an adaptation of a reported method with the aid of Lee Jones (Fig. 3.5) (Tommeraas et al., 2001). A solution of chitosan (1 g polymer or oligomer) was made in 120 ml 2 % acetic acid (aq.), 9-anthraldehyde was dissolved in methanol and added to the chitosan upon stirring at a 10:1 amine : 9-anthraldehyde ratio, i.e. to give 10 % amine labelling at most. This solution was stirred at room temperature for 24 h before addition of sodium cyanoborohydride (0.07 mMoles in MeOH), the pH was increased by addition of NaOH and the solution was allowed to react for a further 12 h. After this reaction the mixture was evaporated to ~100 ml, i.e. aqueous solution only (rotary evaporator, 65 °C, 95 mbar). This solution was then extracted three times with ethyl acetate (1:1 v/v) before lyophilisation.

3.2.5.1.2 Trimethyl Chitosan-Anthraldehyde

In order to produce chitosan-9-anthraldehyde, both protected TMO (0.5 g) and protected TMC (0.5 g) were dissolved in ddH_2O (5 ml) and de-protected by decreasing the pH of the solution using HCl (1M) to give a pH of 3.5-4 and stirred overnight. Following this, the products were precipitated with diethyl ether : ethanol (1:1 v/v) and centrifuged at 3000 RCF for 10 min at 0 °C. The pellet was then re-dissolved in ddH_2O, precipitated with diethyl ether : ethanol and centrifuged at 3000 RCF for 10 min 0 °C. This washing process was repeated three times before drying under vacuum at room temperature for 48 h. These trimethylated derivatives having free amine groups were then reacted with 9-anthraldehyde using the same method as that used for chitosan (Section 3.2.5.1.1). Products were characterised by ^{1}H NMR and fluorescence spectroscopy. TLC was performed to determine free probe content.

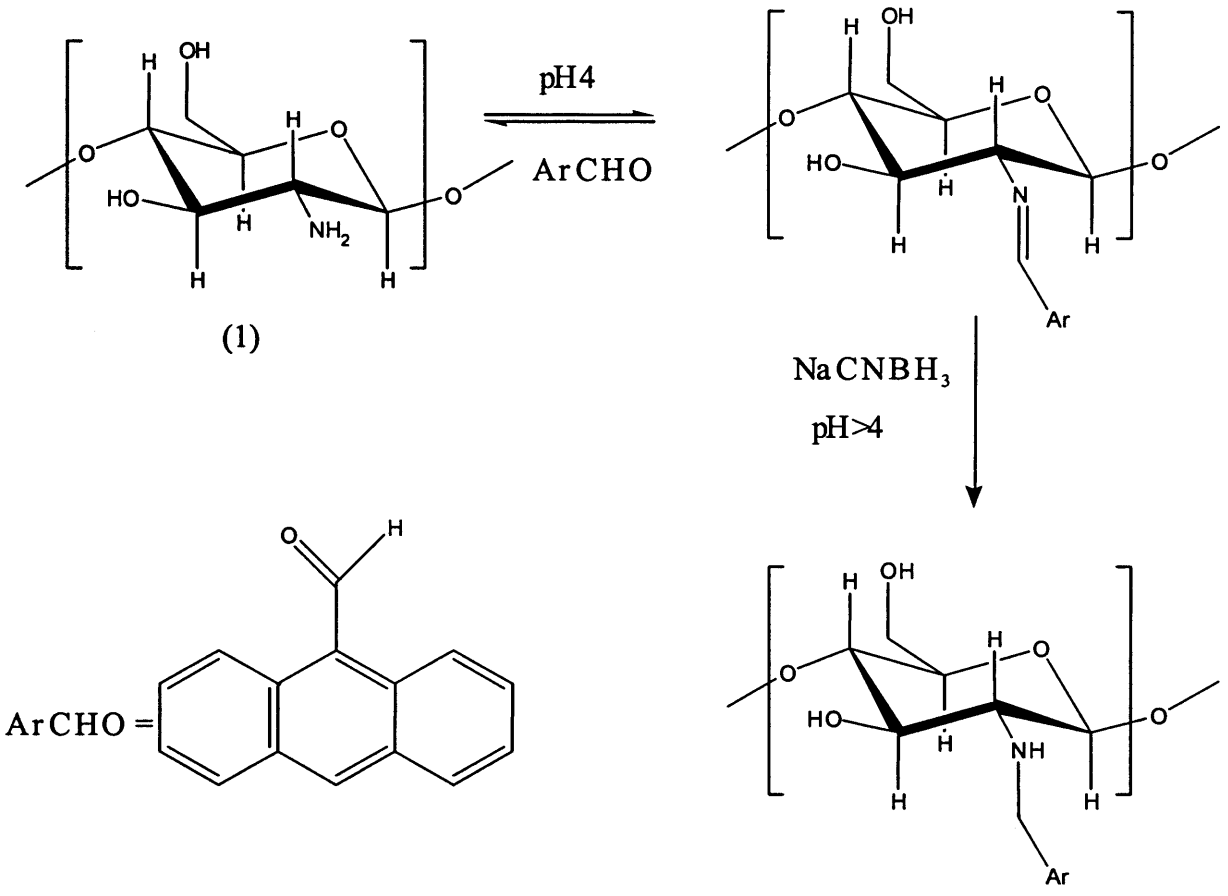

Figure 3.5 - Fluorescent modification of chitosan with 9-anthraldehyde

Reaction scheme showing the derivatisation of chitosan (1) with 9-anthraldehyde by reductive amination. ArCHO = 9-anthraldehyde.

3.2.5.2 Fluorescent Derivatives (5/6-Carboxy Fluorescein)

3.2.5.2.1 TMO-Fluorescein (TMO-FAM)

In a preliminary experiment to determine if TMO (44 % DTM) would react with fluorescein, TMO was reacted with 5/6-carboxyfluorescein succinimidyl ester by the scheme shown in Fig. 3.6. TMO (12 mg) was dissolved in NMP (5 ml) and the activated ester added to the reaction mixture in a 5x molar excess, reaction was performed for 24 h before precipitation with 10 volumes diethyl ether : ethanol (1:1 v/v) and isolation by centrifugation 3000 RCF 20 min. Product was re-dissolved in ddH_2O then precipitated in diethyl ether : ethanol (1:1 v/v) twice. The pellet was dried under vacuum for 48 h. TLC was performed to detect free fluorescein and the product characterised by ^1H NMR, UV and fluorescent spectroscopy.

3.2.5.2.2 CMTMO-Fluorescein (CMTMO-FAM)

CMTMO was derivatised using 5/6-carboxyfluorescein succinimidyl ester by the reaction shown in Fig. 3.7. CMTMO (100 mg; DTM 51.8 %) which had been produced with 7.5 equivalents of chloroacetic acid and had a 37 % calculated degree of modification of 6-O-carboxymethylation was dissolved in ddH_2O (5 ml). The activated ester was added to the reaction mixture in a 5x excess, reaction was performed for 60 h before precipitation in diethyl ether : ethanol (1:1 v/v) and centrifugation 3000 RCF 20 min. Products were re-dissolved in ddH_2O then precipitated in diethyl ether : ethanol (1:1 v/v) twice. TLC was performed to detect free fluorescein and the product characterised by ^1H NMR, UV and fluorescent spectroscopy.

3.2.5.3 CMTMO-Oregon Green (CMTMO-OG)

CMTMO (DTM 29.4; see Section 3.2.4.2) with protected NH_2 groups was de-protected by dissolving the material in sodium citrate buffer (0.1 M, pH 3) and stirring for 24 h (Fig. 3.8). The product did not precipitate upon addition of 10 volumes diethyl ether : ethanol (1:1 v/v) but following centrifugation at 3000 RCF for 10 min at 0 °C a separation of two solutions had been made and the supernatant was removed. The remaining solution precipitated upon addition of 10 volumes diethyl ether : ethanol (1:1 v/v), this was centrifuged at 3000 RCF 0 °C for 10 min. The supernatant was discarded and product dried at 30 °C under vacuum overnight. ^1H NMR was performed and there were both contaminating citric acid peaks and residual protection (5.42, 1.84 ppm).

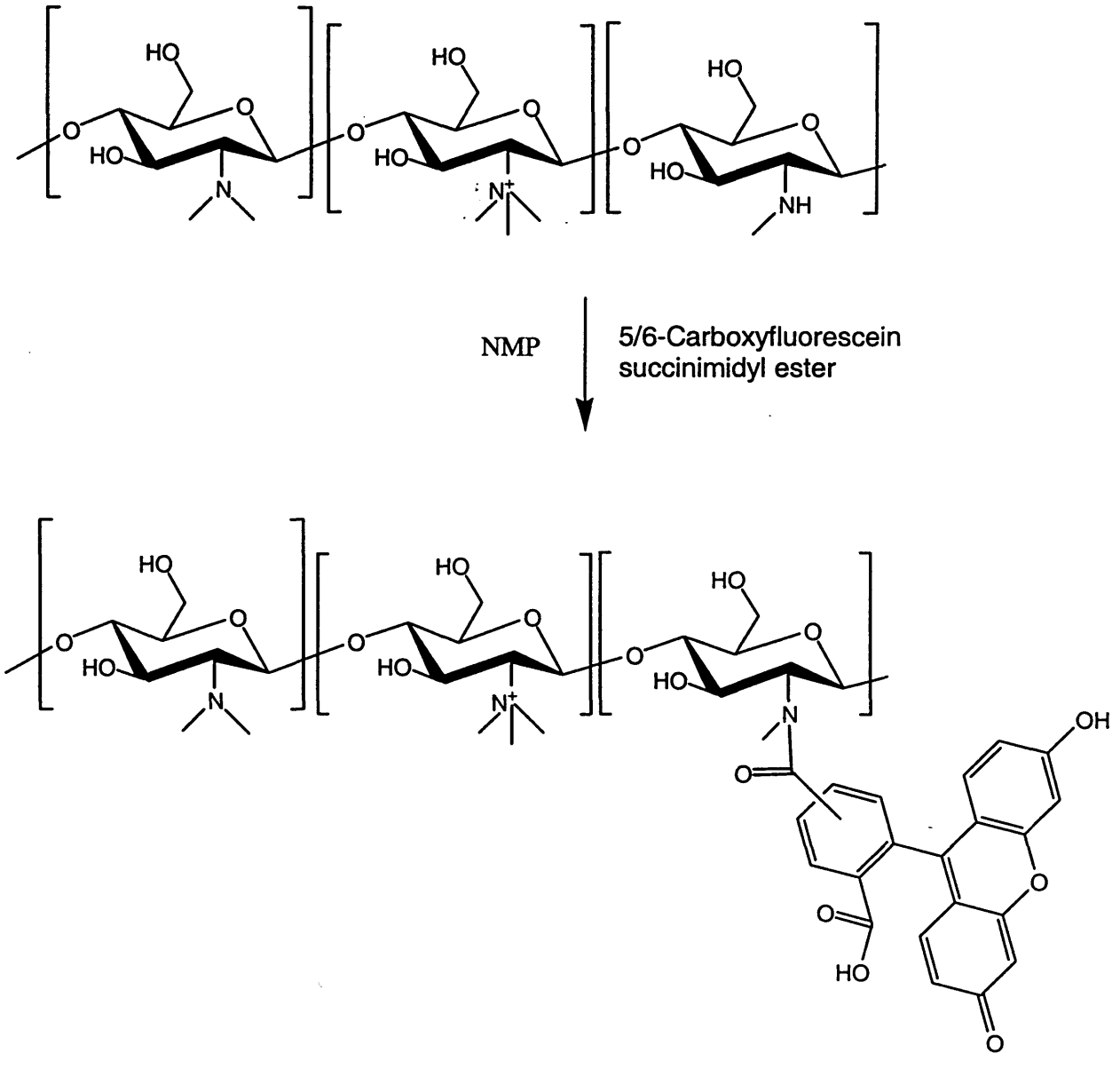

Figure 3.6 - Reaction of TMO with 5/6-carboxyfluorescein succinimidyl ester

Proposed labelling of TMO with the activated ester 5/6-carboxyfluorescein through reaction with monomethylated amine groups.

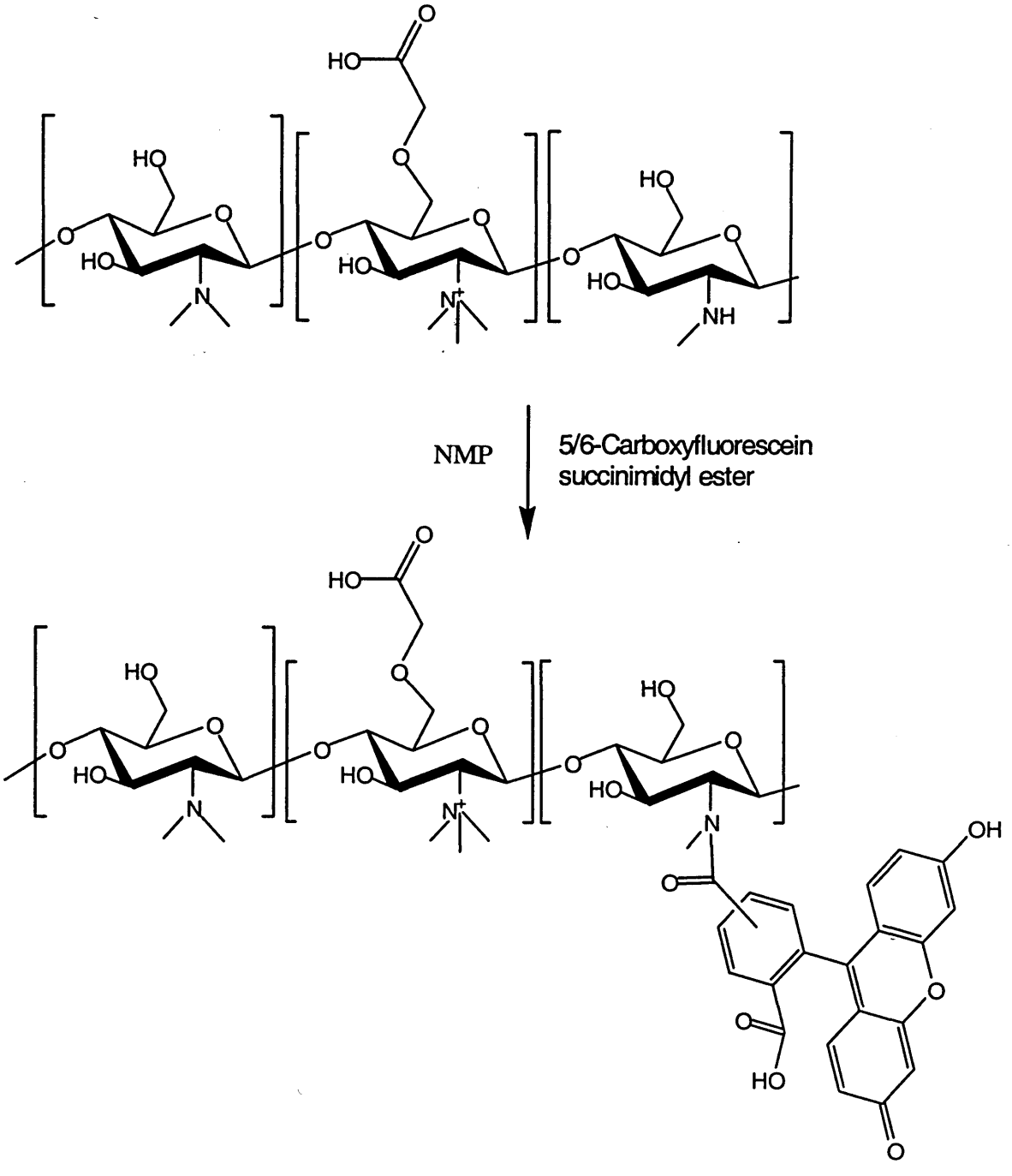

Figure 3.7 - Reaction of CMTMO with 5/6-carboxyfluorescein succinimidyl ester

Fluorescent modification of CMTMO performed by addition of an activated fluorophore, 5,6-carboxymethyl fluorescein succinimidyl ester.

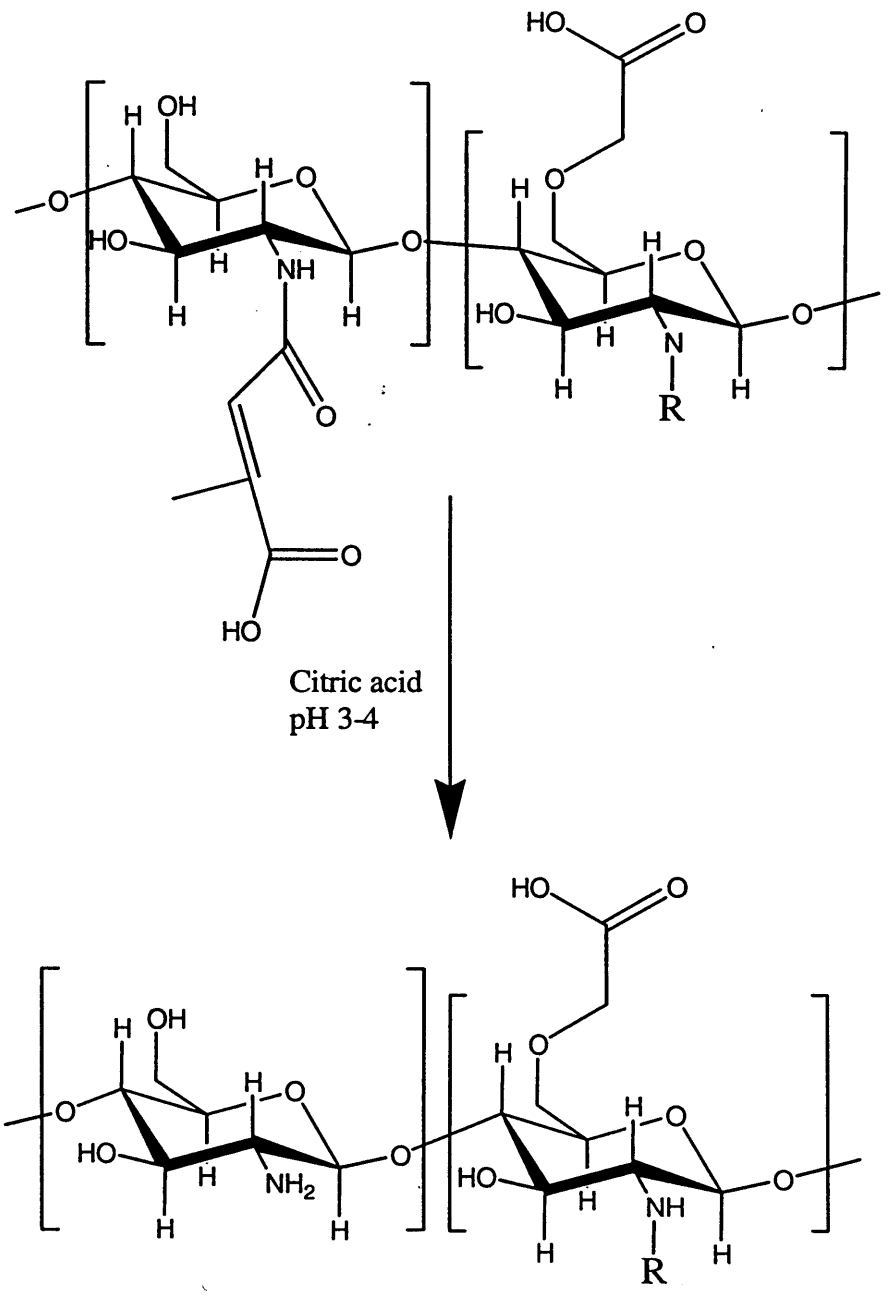

Figure 3.8 – De-protection of 6-O-carboxymethylated trimethyl chitosan

Reaction scheme of the de-protection of 6-O-Carboxymethylated trimethyl chitosan, R represents monomethyl, dimethyl or trimethyl substituents.

The product was re-dissolved in citric acid and stirred overnight at room temperature, this solution was neutralised by addition of NaOH (1 M). The product was precipitated with diethyl ether : ethanol (1:1 v/v) and centrifuged at 3000 RCF for 10 min 0 °C. The product was re-dissolved in ddH_2O, precipitated by addition of diethyl ether : ethanol (1:1 v/v) and centrifuged at 3000 RCF for 10 min 0 °C twice before drying under vacuum overnight at 30 °C.

The product of the de-protection reaction, CMTMO with 7.7 % free NH_2, was then dissolved in borate buffer (pH 9) and a methanolic solution of Oregon Green 488-X was added in a 1:1 ratio with free amine groups and reacted under stirring at room temperature for 24 h (Fig. 3.9). Precipitation of the product was made with diethyl ether : ethanol (1:1 v/v), centrifuged at 3000 RCF for 10 min 0 °C and the supernatant discarded. The product was then re-dissolved in ddH_2O, precipitated with diethyl ether : ethanol (1:1 v/v), centrifuged at 3000 RCF for 10 min 0 °C and the supernatant discarded. This washing step was performed four times before TLC was performed to test for residual free Oregon Green. Free Oregon Green was detected by TLC so chloroform extraction was performed three times; 5 ml of CMTMO-OG : 20 ml chloroform, to remove it. Following this, the product was precipitated from the aqueous layer by addition of 10 volumes diethyl ether : ethanol (1:1 v/v). The precipitate containing solution was then centrifuged at 3000 RCF for 10 min 0 °C and supernatant was visibly more fluorescent than the solution from the final precipitation prior to chloroform extraction. Product was analysed by ^1H NMR, UV and fluorescent spectrometry and TLC.

3.2.6 Conjugation of Peptides to CMTMO or Fluorescent CMTMO

The peptides u7 and Gu11G were conjugated to CMTMO using EDC and sulpho-NHS by the reaction shown in Fig. 3.10. CMTMO (50 mg) was weighed into a round bottom flask and dissolved in ddH_2O (0.5 ml) and NMP added (5 ml). EDC (4.4 mg in DMF) and sulpho-NHS (3.1 mg in ddH_2O) were added to the flask and stirred for 30 min. Gu11G (42.55 mg) was dissolved in anhydrous DMF and added to the reaction vessel. The reaction was performed under N_2 at r.t. for 24 h. The product was precipitated in diethyl ether : ethanol (1:1 v/v) and centrifuged at 3000 RCF for 20 min. Pellets were washed in diethyl ether : ethanol (1:1 v/v) and centrifuged at 3000 RCF for 20 min twice before a final wash in diethyl ether followed by drying under vacuum at 30 °C overnight and then stored in the fridge.

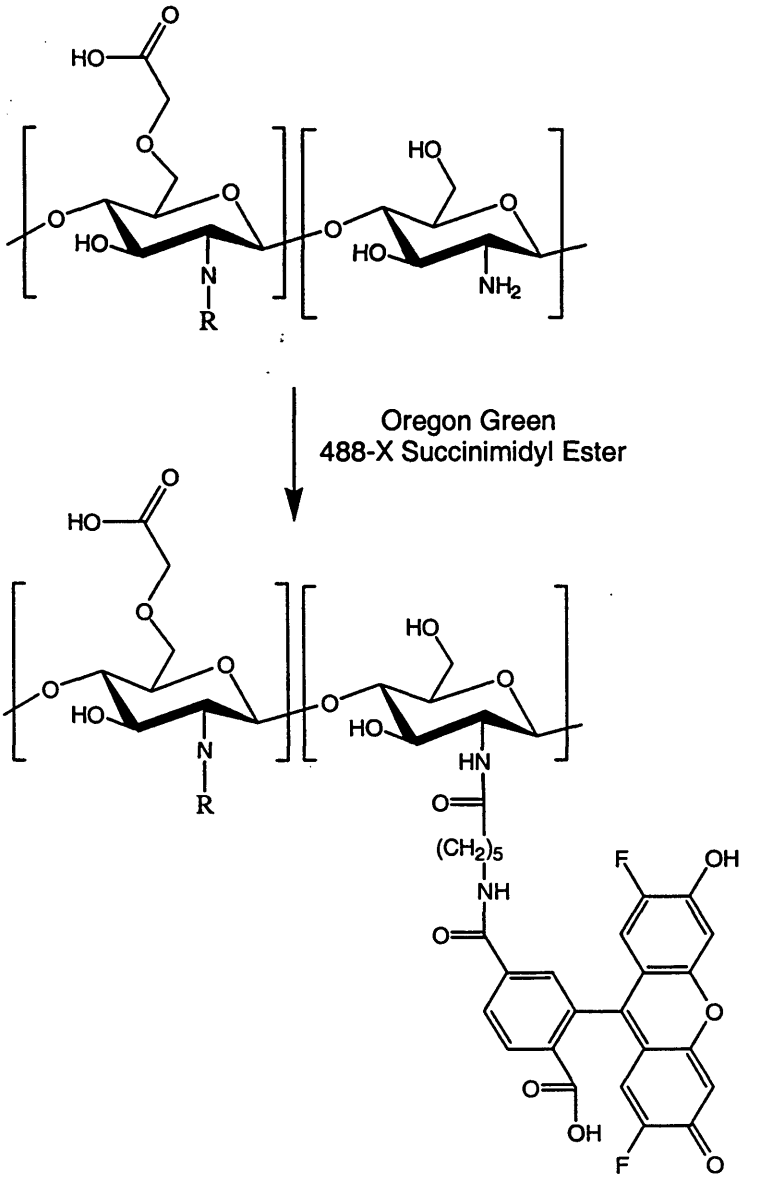

Figure 3.9 - Oregon Green modification of de-protected CMTMO

Reaction scheme of the modification of de-protected CMTMO with Oregon Green. R represents mono-, di- or tri-methyl substituent.

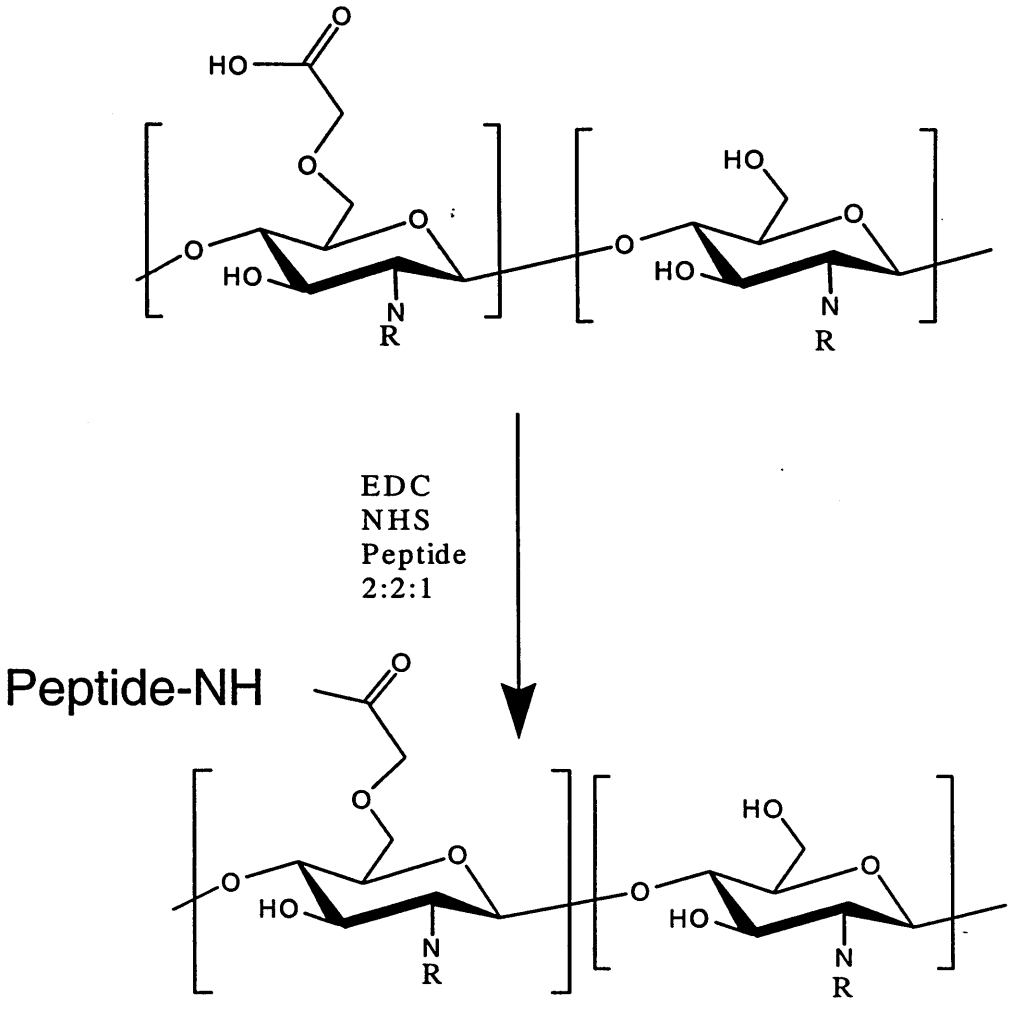

Figure 3.10 - Conjugation of peptides to CMTMO

Reaction scheme of peptide conjugation to CMTMO. R represents mono-, di- or tri-methyl substituents.

In a similar reaction u7 and Gu11G were conjugated to CMTMO-FAM (Fig. 3.11) with adjustment of the ratios of reactants due to increased average monomer molecular weight. The same is true for the reaction of CMTMO-OG with Gu11G (Fig. 3.12).

Products were characterised by ^{1}H and ^{13}C NMR and FTIR. In the case of fluorescent peptide conjugates, UV, fluorescent spectroscopy and TLC were used to characterise the amount of fluorophore both bound and free.

3.3 Results

3.3.1 Trimethylation of Chitosan

In this study chitosans, both oligomeric and polymeric (low molecular weight), have been successfully trimethylated by the reaction scheme outlined in Fig. 3.2. This reaction proceeded in a controlled manner as shown by the linear curves seen in Fig. 3.13. The degree of trimethylation (DTM) was calculated (Equation 3.3) from the integration of ^{1}H-NMR (Fig. 3.14) according to the method previously described (Thanou et al., 2000).

$$\frac{\int 3.4 \text{ ppm}}{9(\Sigma \int > 4.7 \text{ ppm})} \qquad \text{Equation 3.3}$$

The degree of trimethylation of oligomeric chitosan increased linearly with time, to almost complete trimethylation after two hours (Fig. 3.13). Trimethylation of polymeric chitosan showed a similar reaction profile (Fig. 3.13). Scaling up of the reaction with oligomeric chitosan did not give the same degree of trimethylation/time profile. This scaled up reaction was not performed with polymeric chitosan. The trimethylation reaction was repeated several times and reactions gave expected degrees of trimethylation. After freeze drying all derivatives were soluble in water up to 10 mg/ml. A yield of 80-90 % was achieved in these reactions.

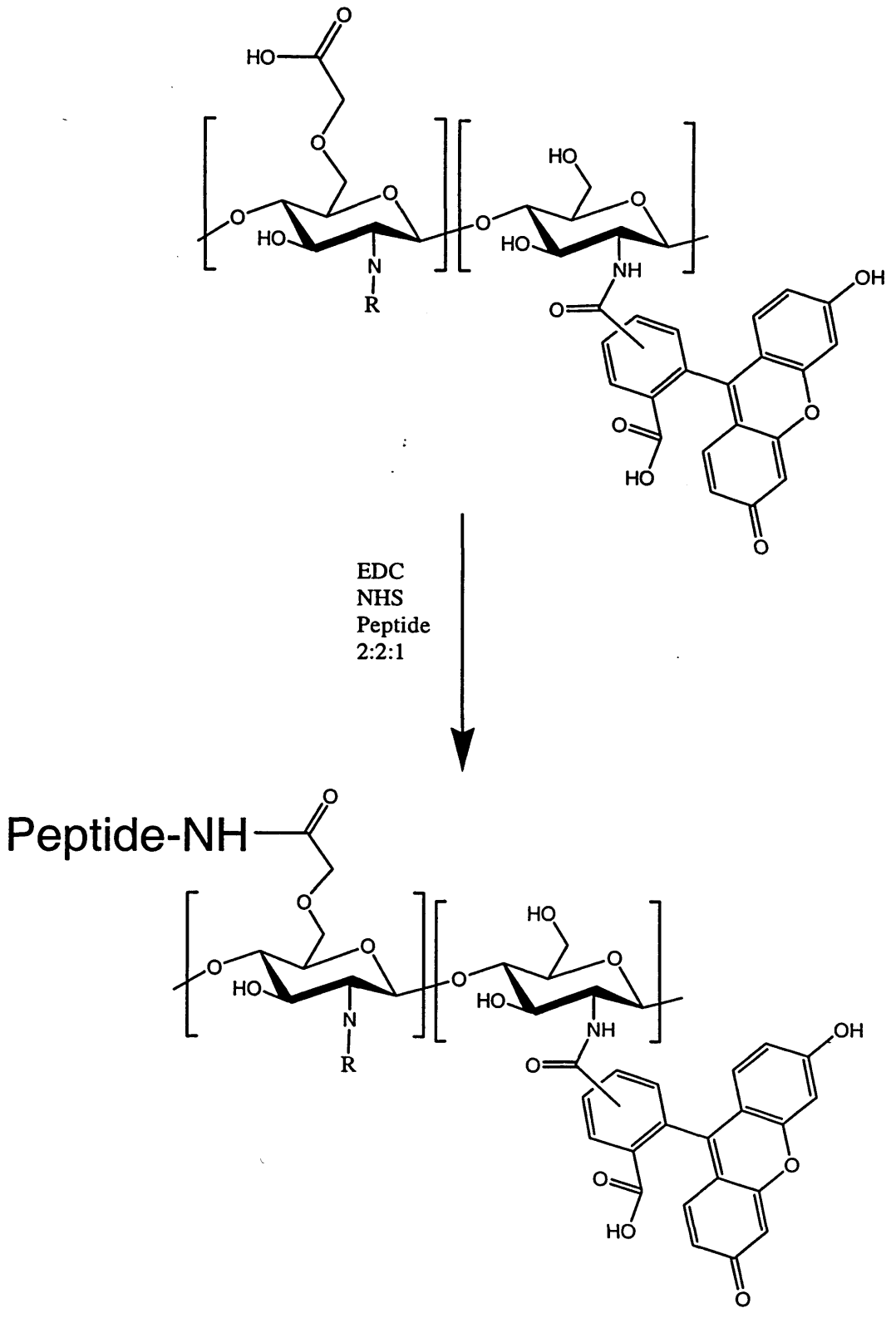

Figure 3.11 Conjugation of peptides to CMTMO-FAM

Scheme of the conjugation of peptides to fluorescein derivatised CMTMO. R represents mono-, di- or tri-methyl substitute.

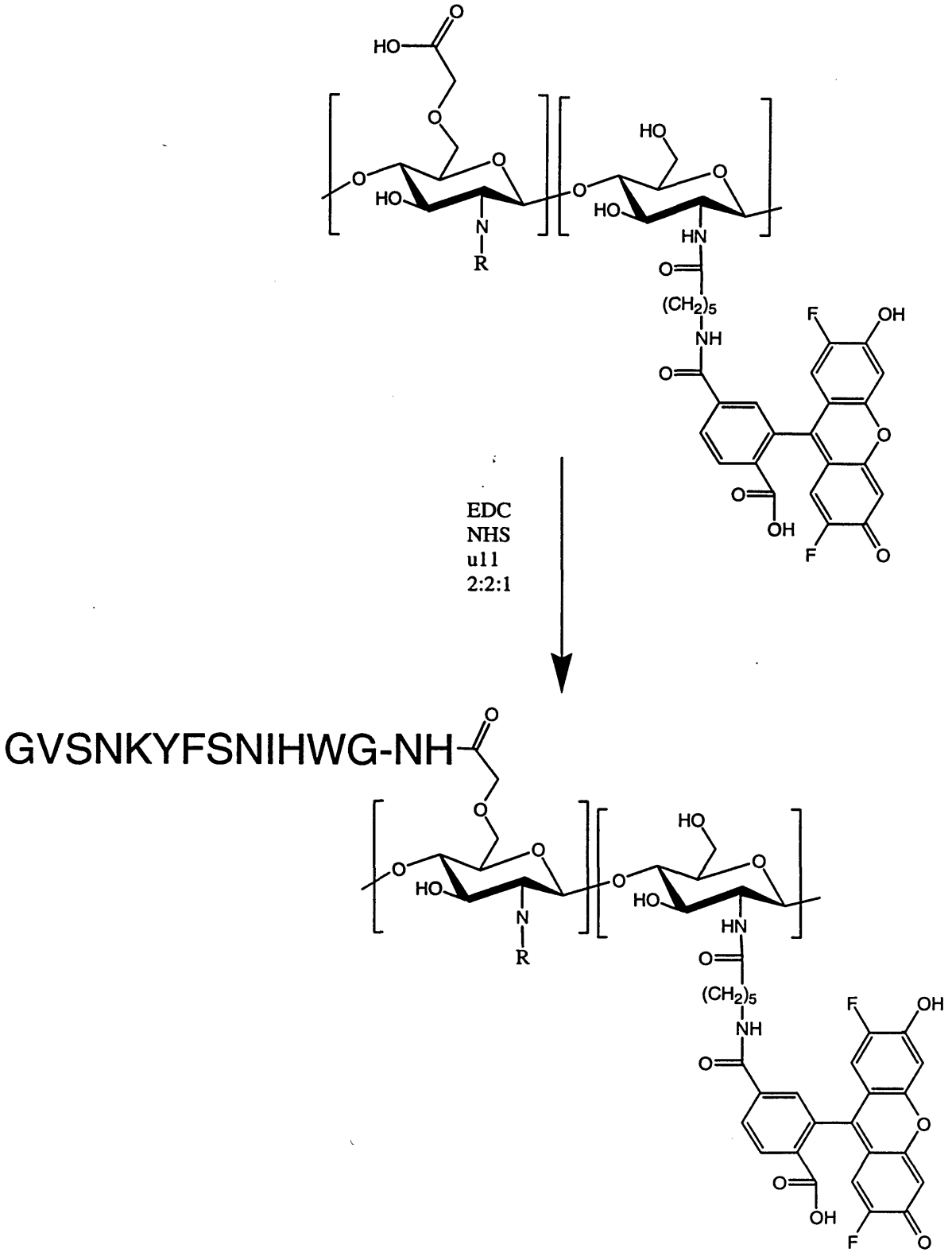

Figure 3.12 - Conjugation of Gu11G to CMTMO-OG

Scheme of the conjugation of Gu11G to Oregon Green derivatised CMTMO. R represents mono-, di- or tri-methyl substitute.

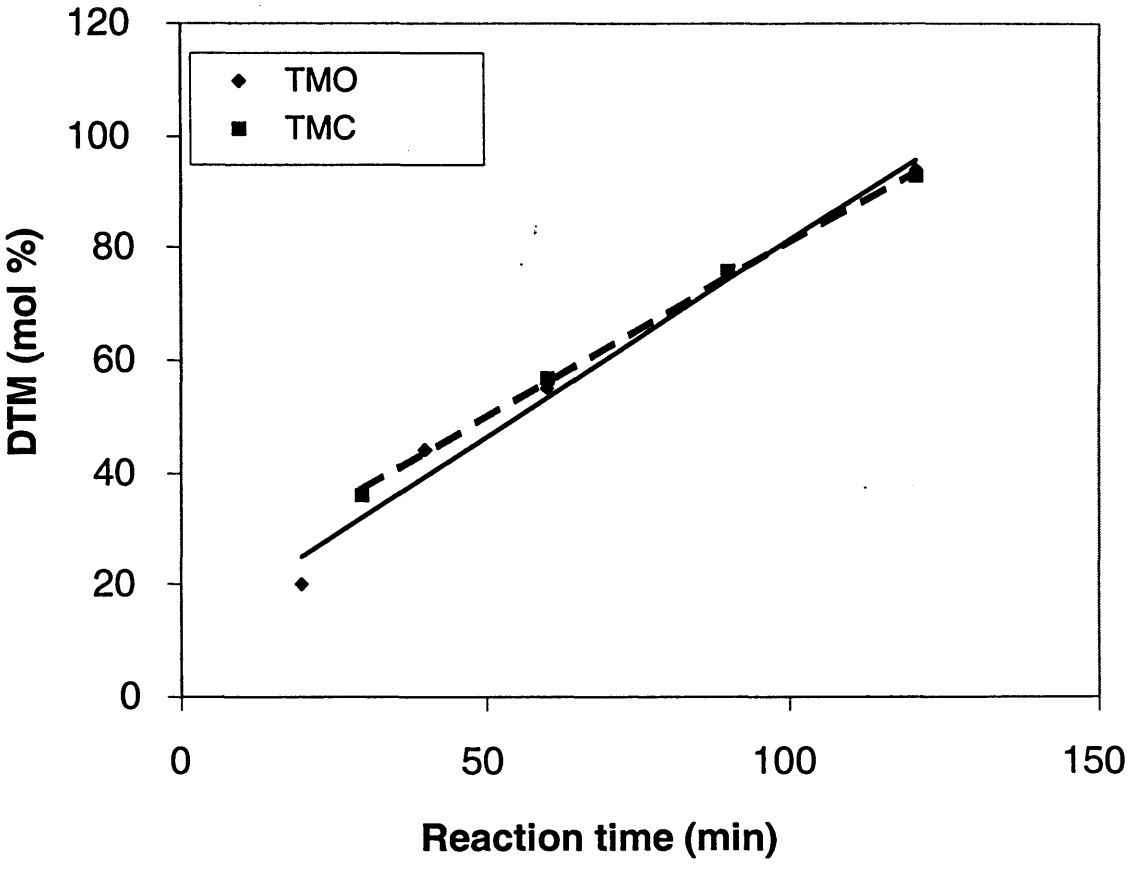

Figure 3.13 - Degree of chitosan trimethylation with increasing reaction time

Increase in degree of trimethylation (DTM) of chitosans with increasing reaction time. TMO = trimethyl oligomer, TMC = trimethyl chitosan polymer.

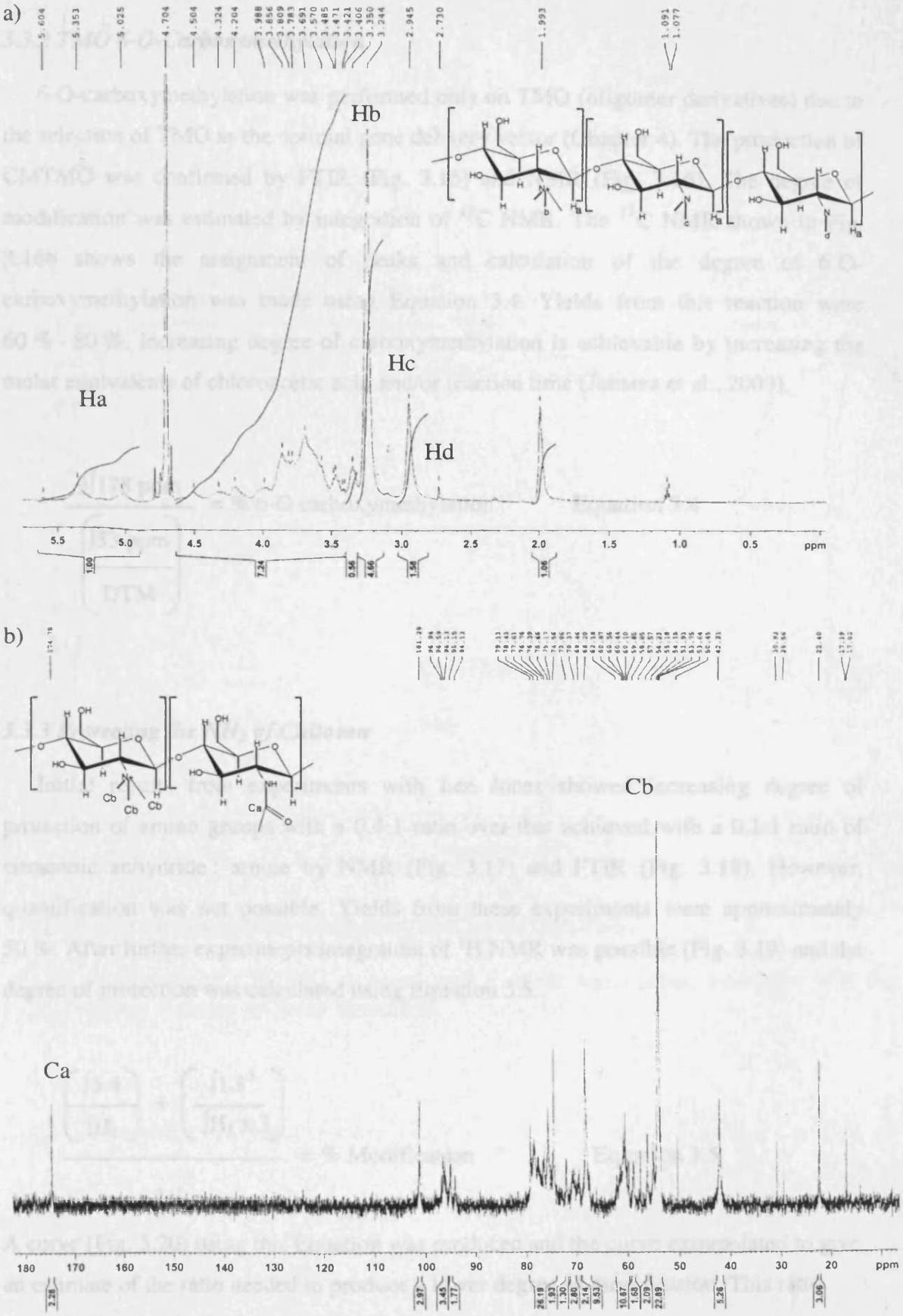

Figure 3.14 - NMR spectra of *N,N,N*-trimethyl chitosan

a) ^{1}H NMR of TMO, b) ^{13}C NMR of TMO

3.3.2 TMO 6-O-Carboxymethylation

6-O-carboxymethylation was performed only on TMO (oligomer derivatives) due to the selection of TMO as the optimal gene delivery vector (Chapter 4). The production of CMTMO was confirmed by FTIR (Fig. 3.15) and NMR (Fig. 3.16). The degree of modification was estimated by integration of ^{13}C NMR. The ^{13}C NMR shown in Fig. 3.16b shows the assignment of peaks and calculation of the degree of 6-O-carboxymethylation was made using Equation 3.4. Yields from this reaction were 60 % - 80 %. Increasing degree of carboxymethylation is achievable by increasing the molar equivalents of chloroacetic acid and/or reaction time (Jansma et al., 2003).

$$\frac{3\int 178\ ppm}{\left(\frac{\int 53\ ppm}{DTM}\right)} = \%\ 6\text{-O carboxymethylation} \qquad \text{Equation 3.4}$$

3.3.3 Protecting the NH_2 of Chitosan

Initial results from experiments with Lee Jones showed increasing degree of protection of amino groups with a 0.4:1 ratio over that achieved with a 0.1:1 ratio of citraconic anhydride : amine by NMR (Fig. 3.17) and FTIR (Fig. 3.18). However, quantification was not possible. Yields from these experiments were approximately 50 %. After further experiments integration of ^1H NMR was possible (Fig. 3.19) and the degree of protection was calculated using Equation 3.5.

$$\frac{\left(\frac{\int 5.4}{\int H_1}\right) + \left(\frac{\int 1.8}{\int H_1 \times 3}\right)}{2} = \%\ \text{Modification} \qquad \text{Equation 3.5}$$

A curve (Fig. 3.20) using this Equation was produced and the curve extrapolated to give an estimate of the ratio needed to produce a lower degree of modification. This ratio was calculated to be 0.15:1 to confer 10 % protection.

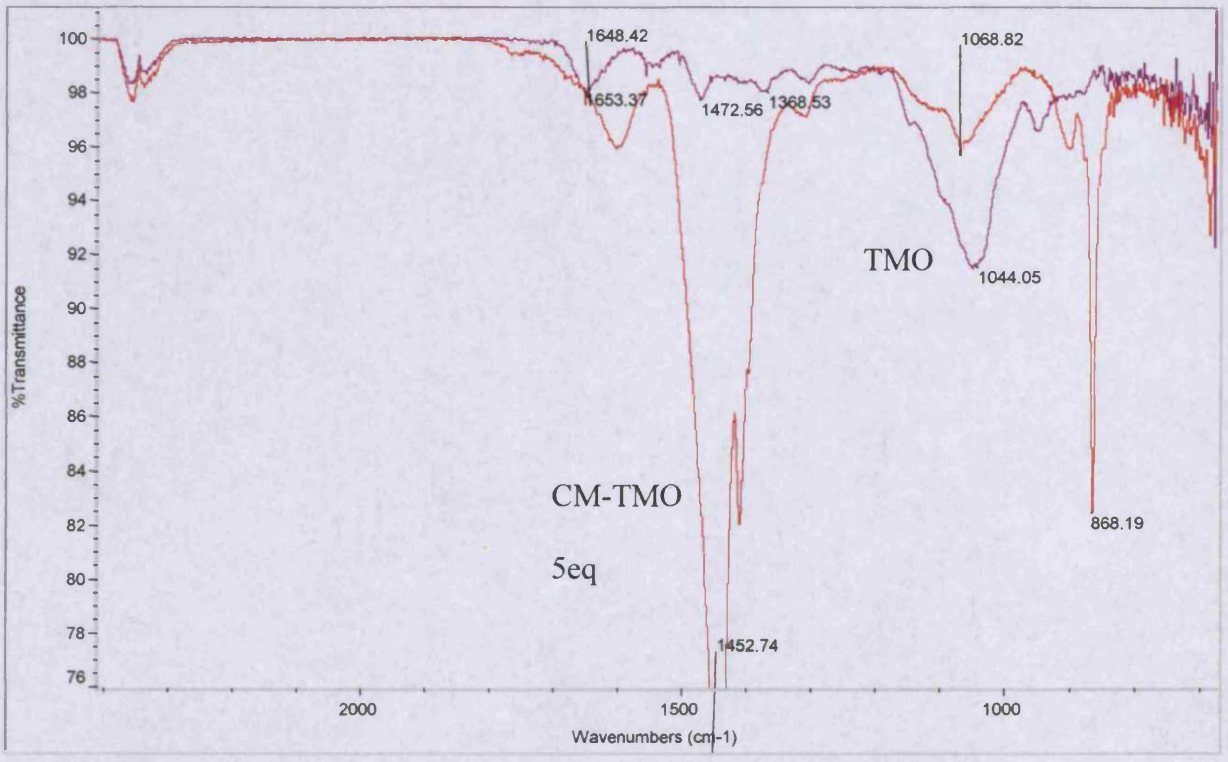

Figure 3.15 - FTIR spectra comparing TMO with CM-TMO

FTIR comparison of CMTMO prepared with 5 molar equivalents: monomer with the TMO starting material. 64 scans were made.

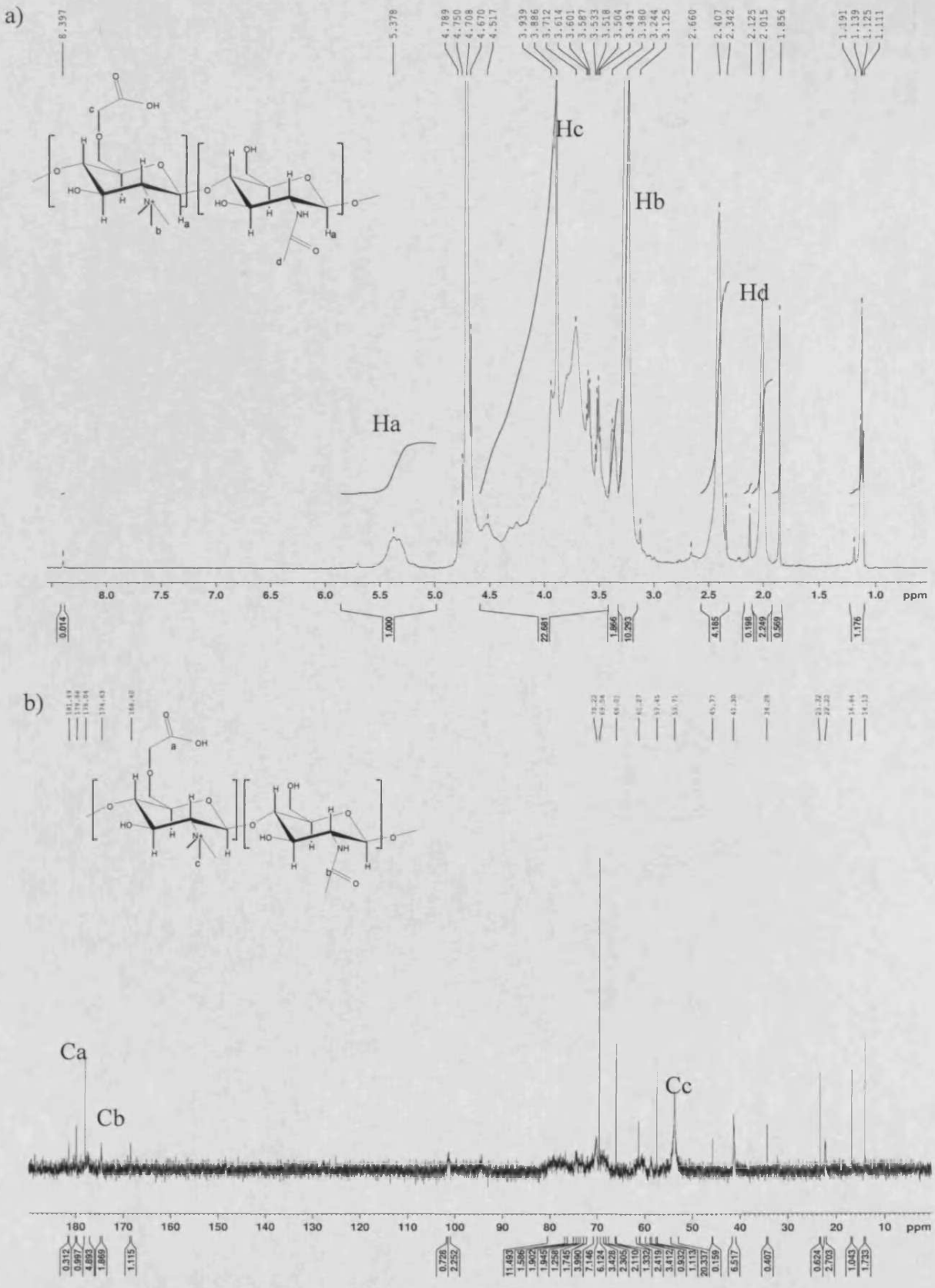

Figure 3.16 - NMR of CMTMO

a) ^{1}H NMR of CMTMO prepared with 7.5 molar equivalents of chloroacetic acid : monomer b) ^{13}C NMR of same CMTMO

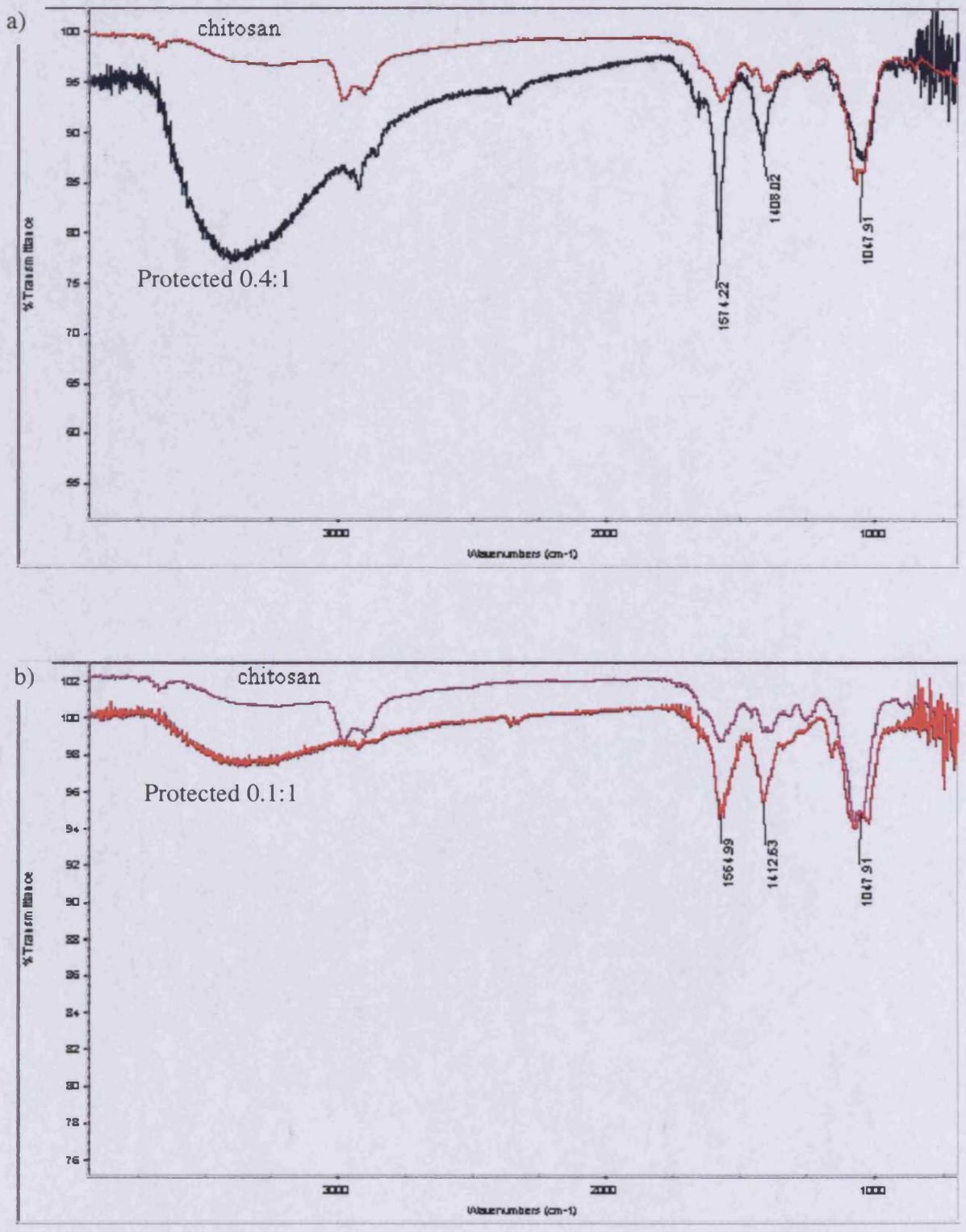

Figure 3.17 – Protection of chitosan polymer shown by FTIR

Polymeric chitosan protected with a) 0.4:1 and b) 0.1:1 ratios of citraconic anhydride: amine compared with the unreacted polymer. 128 scans made

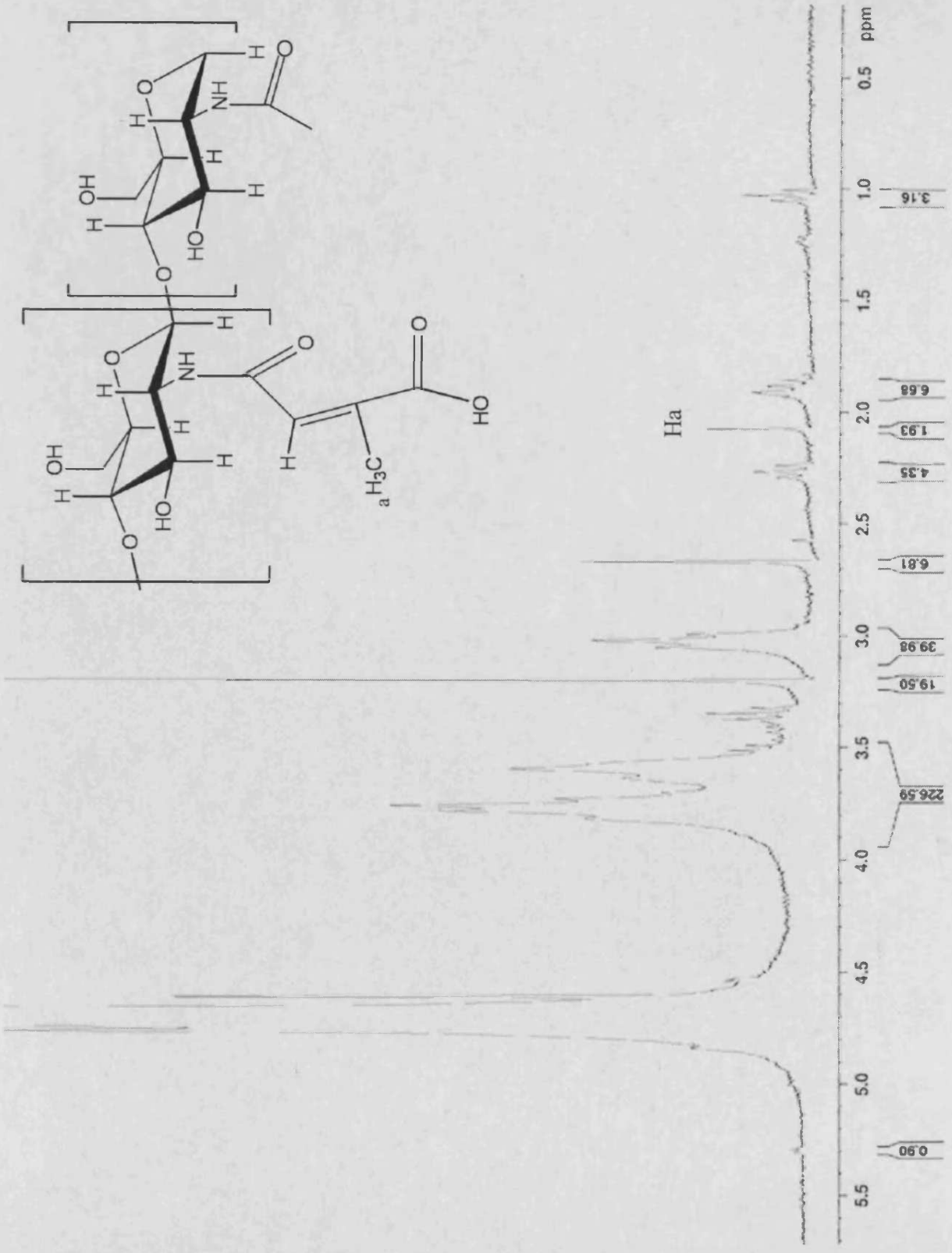

Figure 3.18 – Protection of chitosan oligomer shown by ^{1}H NMR

Introduction of protecting groups to chitosan oligomer ^{1}H NMR

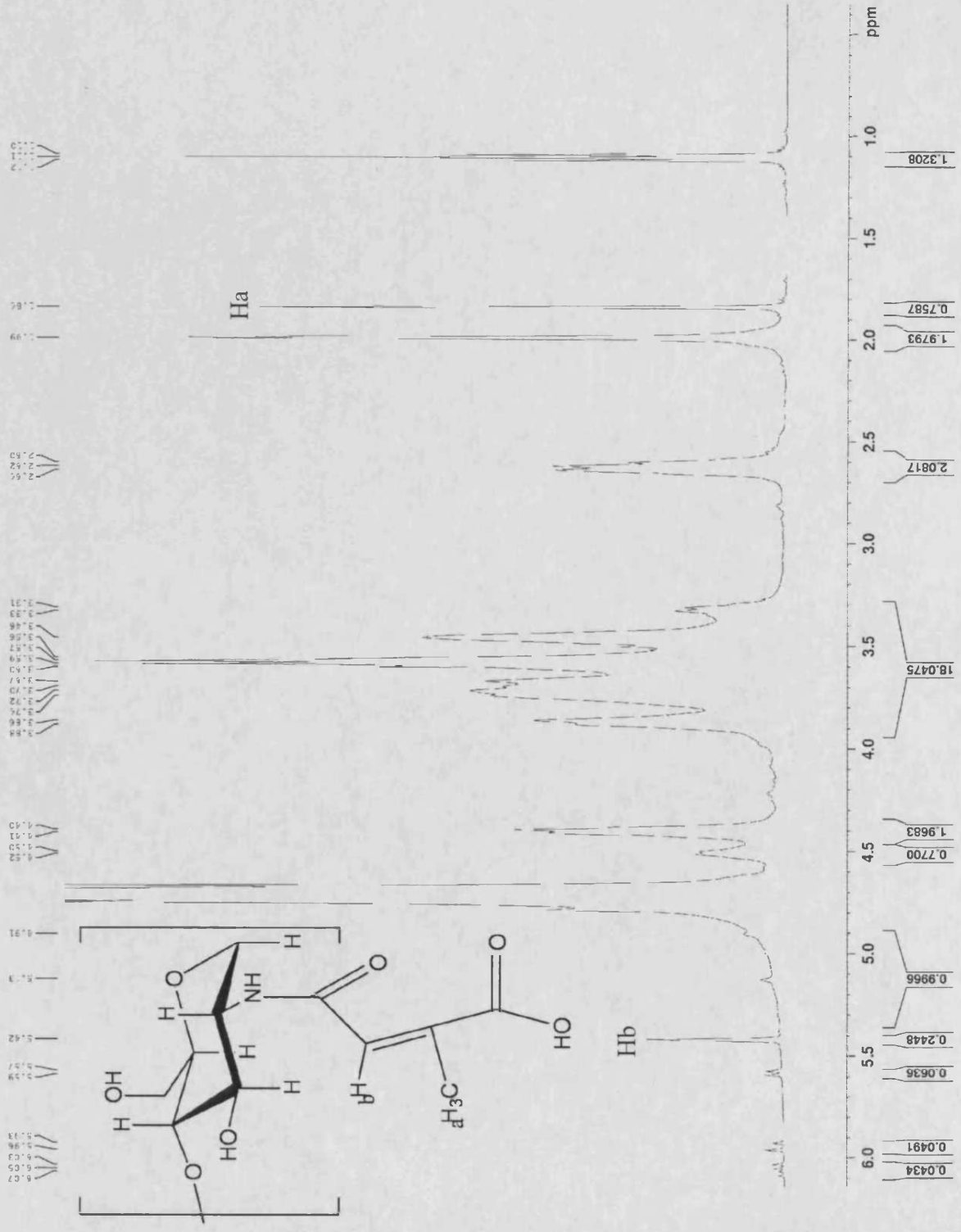

Figure 3.19 - ^{1}H NMR of protected chitosan (0.37:1 citranconic anhydride : amine)

Proton NMR showing the protection of chitosan with 0.37 equivalents of citraconic anhydride, peaks at δ 1.84 and δ 5.42 are assigned to the protecting group.

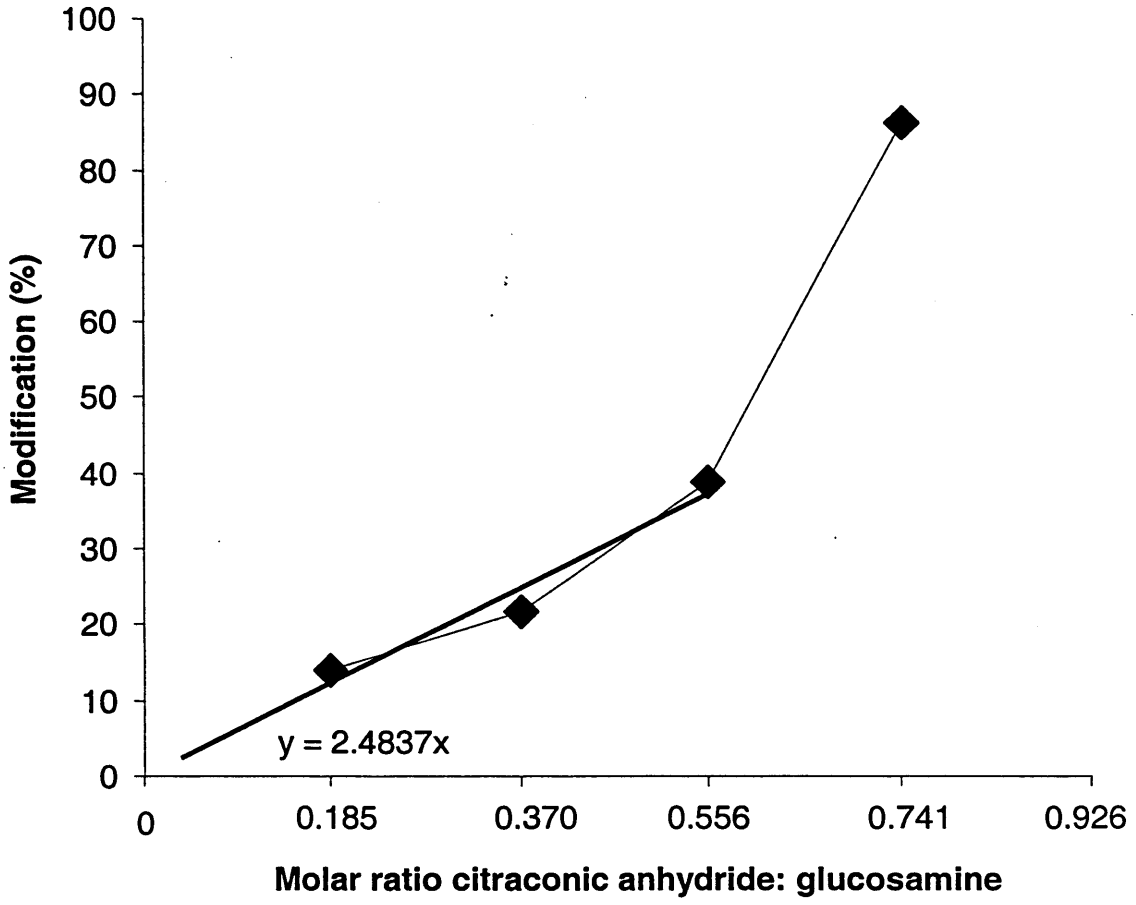

Figure 3.20 - Chart of chitosan protection achieved with citraconic anhydride

Increasing amine group protection on chitosan was achieved with increasing molar ratio of citraconic anhydride : glucosamine.

Using this determined ratio (0.15:1 citraconic anhydride : amine) the reaction was scaled up. The product of this reaction determination of protection group peaks was not straightforward (Fig. 3.21a). In order to better characterise the product, ^{1}H NMR was performed at 60 °C to give better resolution of peaks (Fig. 3.21b), the peak at δ6 ppm was assigned to the protecting group and calculation of protection was made using ∫6 ppm / ∫Σ remaining peaks > 5.9 ppm. From this reaction the amount of protection was calculated to be 7.7 % of the amine groups.

3.3.3.1 Trimethylation of Protected Chitosan

In initial experiments the peak assigned to trimethyl amine groups of protected chitosan after reaction was clearly visible in ^{1}H NMR. However in later experiments, the H_1 peaks were not clear and therefore the calculation of DTM was not possible. This product was de-protected and used for labelling experiments with 9-anthraldehyde. In later experiments these peaks were resolved and the degree of quaternisation was then calculated using Equation 3.6 after the integration of ^{1}H NMR (Fig. 3.22).

$$\left(\frac{\int 3.4 \text{ ppm}}{9(\Sigma\int > 4.7 \text{ ppm except } \int 5.4 \text{ ppm})} \right) \times 100 \qquad \text{Equation 3.6}$$

3.3.3.2 Trimethylated Protected Chitosan's 6-O-Carboxymethylation

Trimethylated protected chitosan was 6-O-carboxymethylated, as shown by NMR analysis (Fig. 3.23). In ^{1}H NMR carboxymethylation is apparent through the appearance of a peak at δ 3.89 ppm and confirmed through the peak in ^{13}C NMR visible at δ 178 ppm. This was further confirmed by FTIR (Fig. 3.24). This derivative was used in Oregon Green labelling experiments.

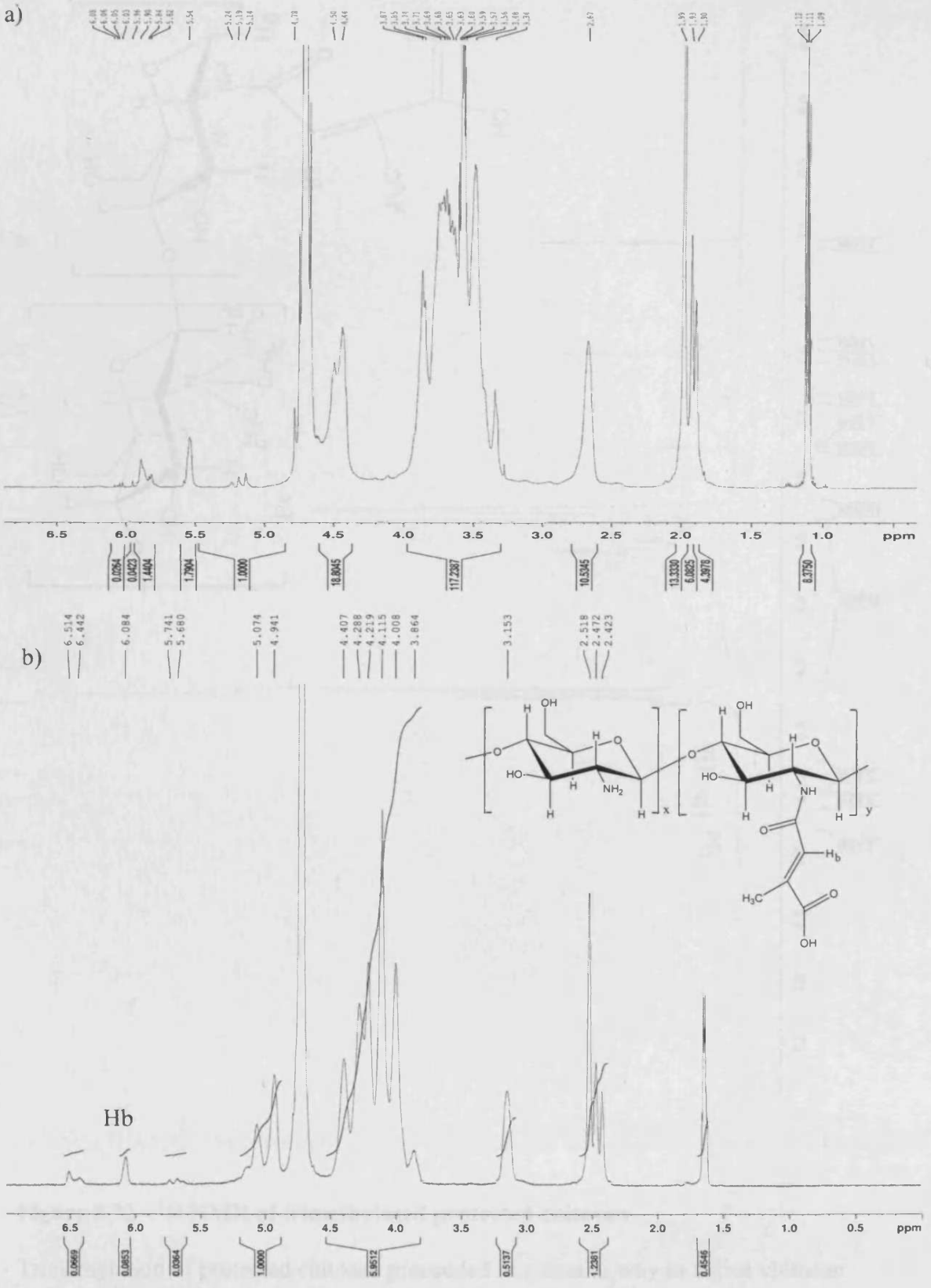

Figure 3.21 - ^{1}H NMR of protected chitosan produced in scaled reaction

a) Protected chitosan at 298 ºK b) Protected chitosan at 333 ºK, peak at δ 6 ppm assigned to protecting group.

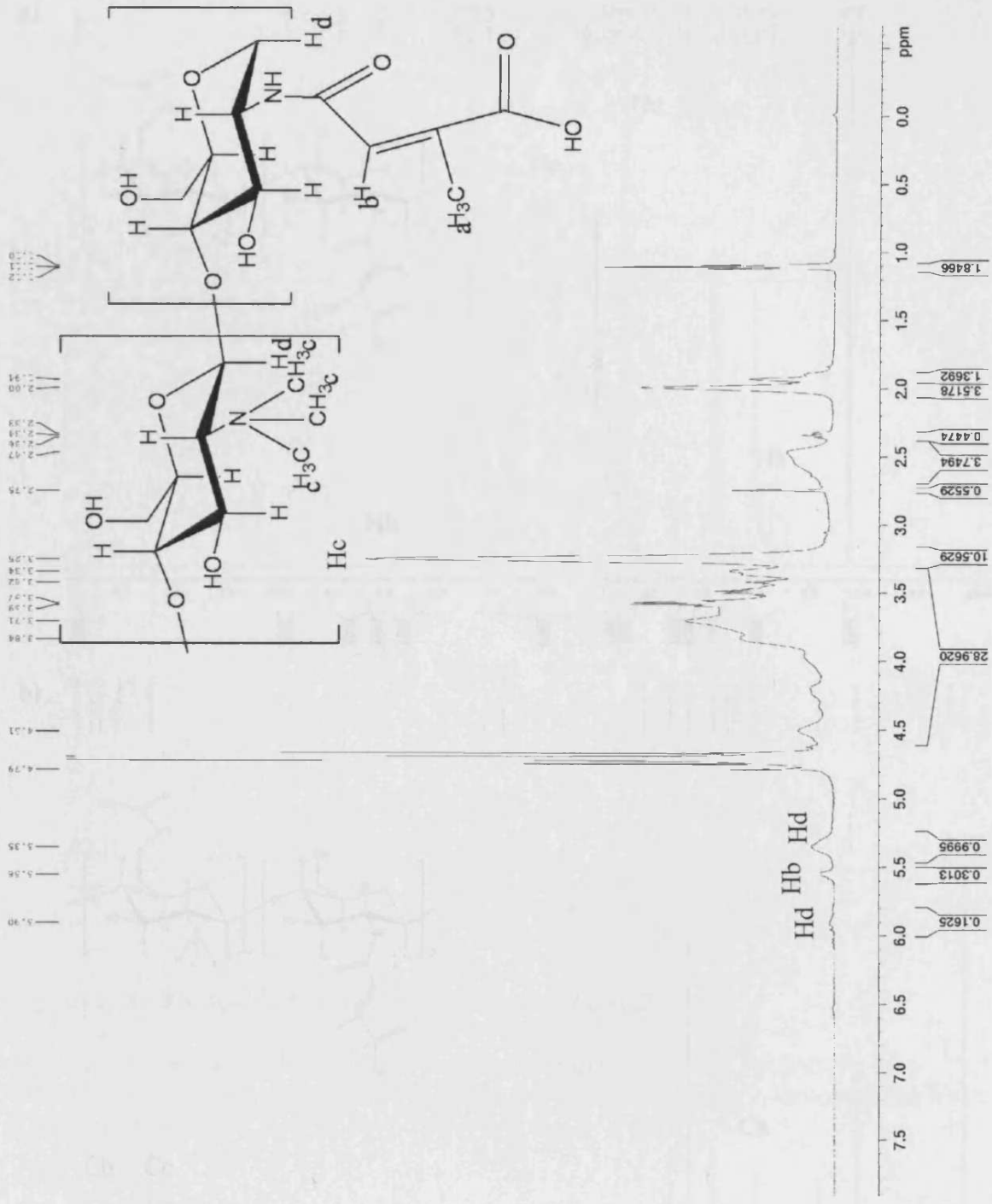

Figure 3.22 - ^{1}H NMR of trimethylated protected chitosan

Trimethylation of protected chitosan proceeded in a similar way to native chitosan with quaternisation of the amine shown at δ 3.25 ppm.

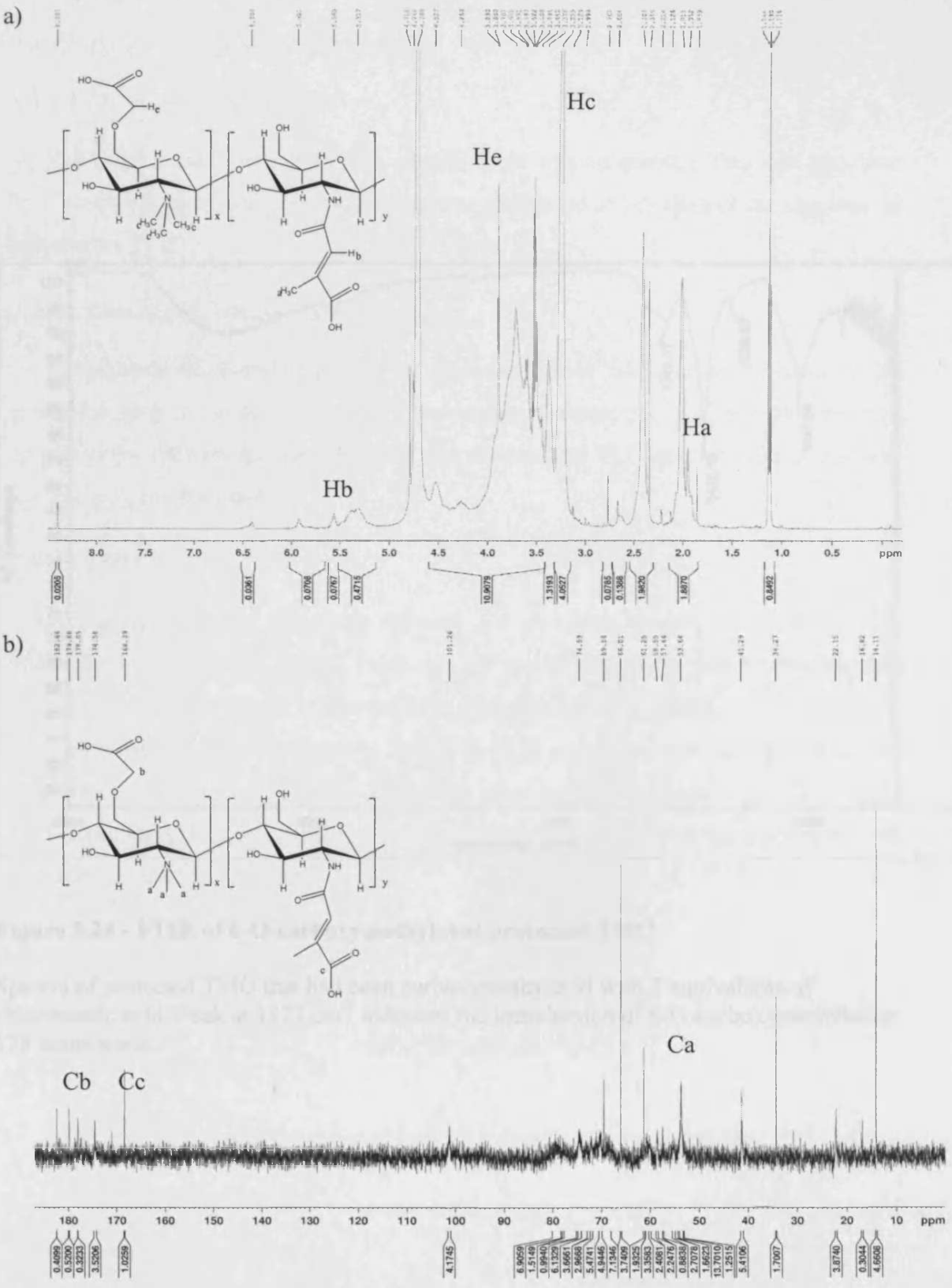

Figure 3.23 - NMR spectra of 6-O-carboxymethylated protected TMO

a) ^{1}H NMR showing the protecting group and 6-O-carboxymethyl group b) ^{13}C NMR showing the introduction of 6-O-carboxymethyl group at δ 178 ppm.

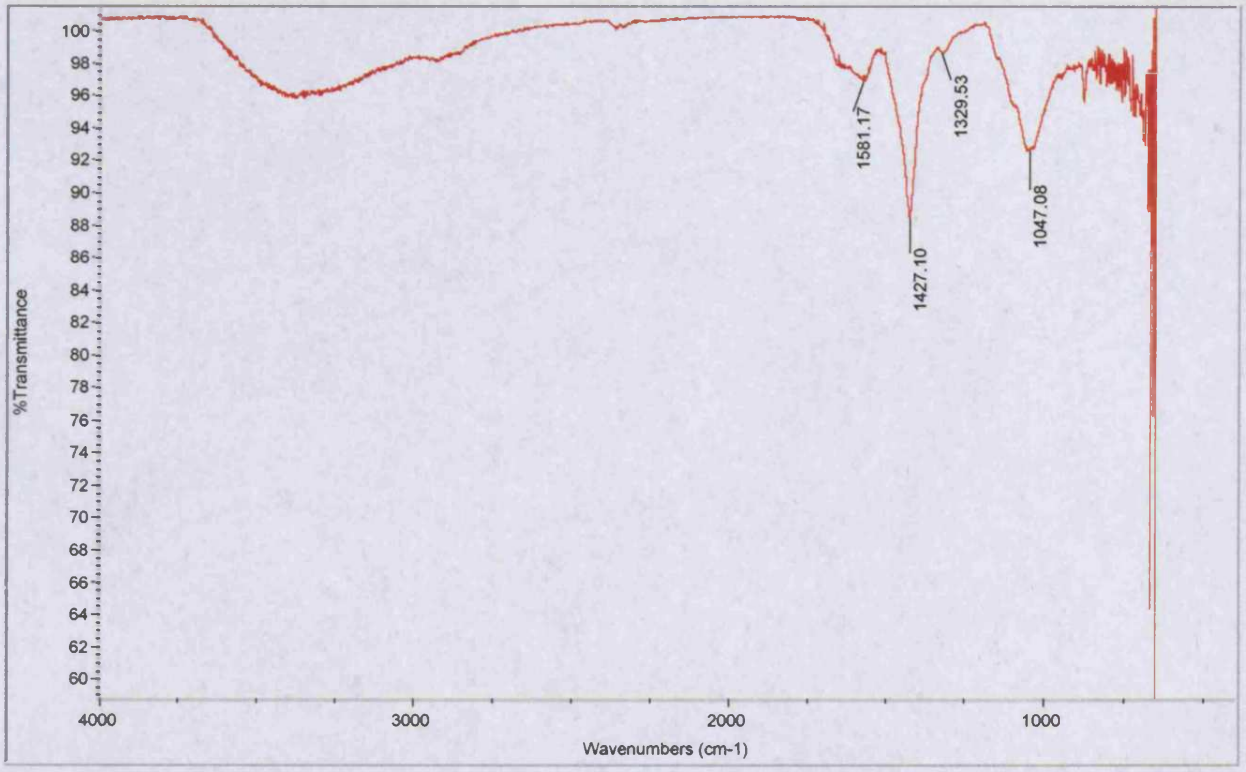

Figure 3.24 - FTIR of 6-O-carboxymethylated protected TMO

Spectra of protected TMO that had been carboxymethylated with 3 equivalents of chloroacetic acid. Peak at 1427 cm^{-1} indicates the introduction of 6-O-carboxymethylation. 128 scans made.

3.3.4 Fluorescent Derivatives of Chitosan

3.3.4.1 Chitosan-Anthraldehyde

The fluorescent labelling with 9-anthraldehyde was successful. This was observed by UV and fluorescence spectroscopy and was confirmed as labelling of the oligomer or polymer by TLC.

3.3.4.2 Trimethyl Chitosan-Anthraldehyde

Conjugation of 9-anthraldehyde to protected TMO was performed after a de-protection step in an acidic (pH 3-4) environment overnight. UV and fluorescence spectroscopy showed that fluorescence was present and TLC confirmed that this was not due to free anthraldehyde.

3.3.4.3 TMO-FAM

UV analysis of the derivative showed a clear peak around the expected UV absorbance maxima λ_{480}= 0.0030. From this UV absorbance the degree of labelling was calculated using Equation 3.7 (Derived from Molecular Probes, 2005).

The % loading was calculated to be 1.6 %. TLC confirmed that the amount of free fluorescein was less than 1 % (Fig. 3.25). This pilot experiment showed that TMO could be fluorescently labelled with the activated ester of 5/6-carboxyfluorescein by the reaction proposed in Fig. 3.6.

$$\frac{\text{Absorbance (480 nm)}}{\varepsilon \text{ of FAM (68000 at pH 8)}} = \text{FAM concentration (M)}$$

$$\text{FAM concentration (M)} \times \text{FAM Mw (360)} = \text{FAM concentration (g/L)}$$

$$\left[\frac{\text{FAM concentration (g/L)}}{\text{Concentration of solution}}\right] \times 100 = \%\ \text{loading}$$

Equation 3.7

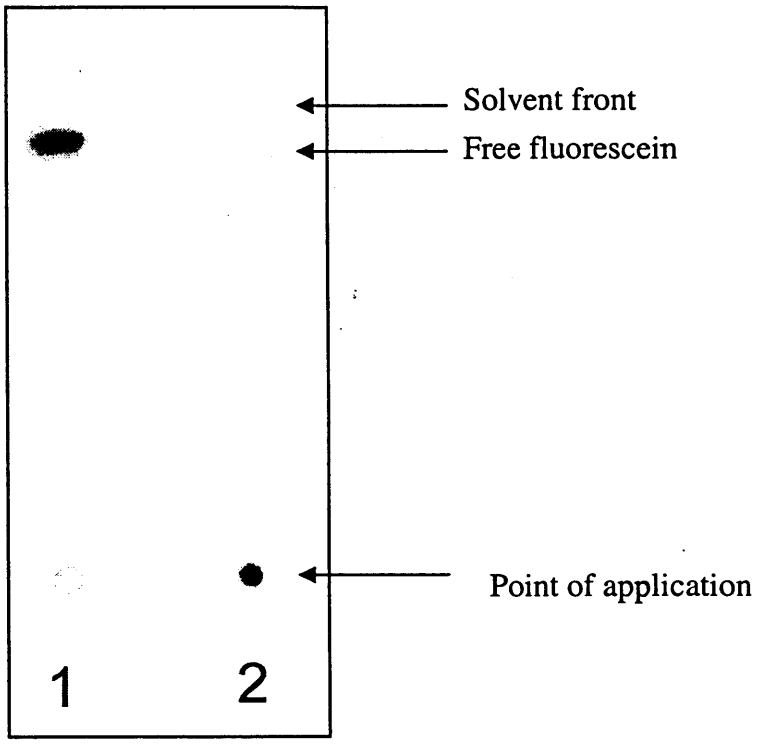

Figure 3.25 - TLC analysis of TMO-FAM

TLC of 1) fluorescein (1.60 μg/ml) 2) TMO-FAM (9.8 mg/ml). The mobile phase was acetonitrile and separation occurred over 6 cm. The plate was imaged using a Typhoon Variable Mode Imager.

3.3.4.4 CMTMO-FAM

In order for it to be possible to study the interaction of the targeted derivatives with uPAR expressing cells (Chapter 5) it was necessary to produce a fluorescently labelled derivative with a functional group available for conjugation. Therefore, following on from the successful modification of TMO the derivatisation of CMTMO was performed in a similar way. UV (Fig. 3.26) and fluorescent spectroscopy confirmed the presence of fluorescence.

Using Equation 3.7 the degree of labelling was calculated and a 1 % limit test performed by TLC, this showed that less than 1 % of fluorescence was free fluorophore (Fig. 3.27). Proton NMR confirmed the presence of fluorescein through peaks around δ 8 ppm (Fig. 3.28).

3.3.4.5 CMTMO-OG

In order to achieve efficient conjugation of Oregon Green to CMTMO a continuation of protection/de-protection experiments was made. Derivatisation with the activated ester of Oregon Green produced a fluorescent oligomer and the extent of labelling was determined by UV spectroscopy using Equation 3.8 as 0.53 % (Derived from Molecular Probes, 2005).

$$\frac{\text{Absorbance (480 nm)}}{\varepsilon \text{ of OG (70000 at pH 8)}} = \text{OG concentration (M)}$$

$$\text{OG concentration (M)} \times \text{OG Mw (508)} = \text{OG concentration (g/L)}$$

Equation 3.8

$$\left(\frac{\text{OG concentration (g/L)}}{\text{Concentration of solution}} \right) \times 100 = \%\ \text{loading}$$

3.3.4.6 Conjugation of Peptides

In the first experiments conjugation of the peptides u7 and Gu11G to CMTMO was seen by ^{1}H NMR and FTIR although the extent of derivatisation was unclear. In a later conjugation to CMTMO of Gu11G the introduction of peptide was clearly seen. The extent of conjugation was estimated by ^{1}H NMR to be 1-2 % from the integration of peaks corresponding to the peptide (Fig. 3.29).

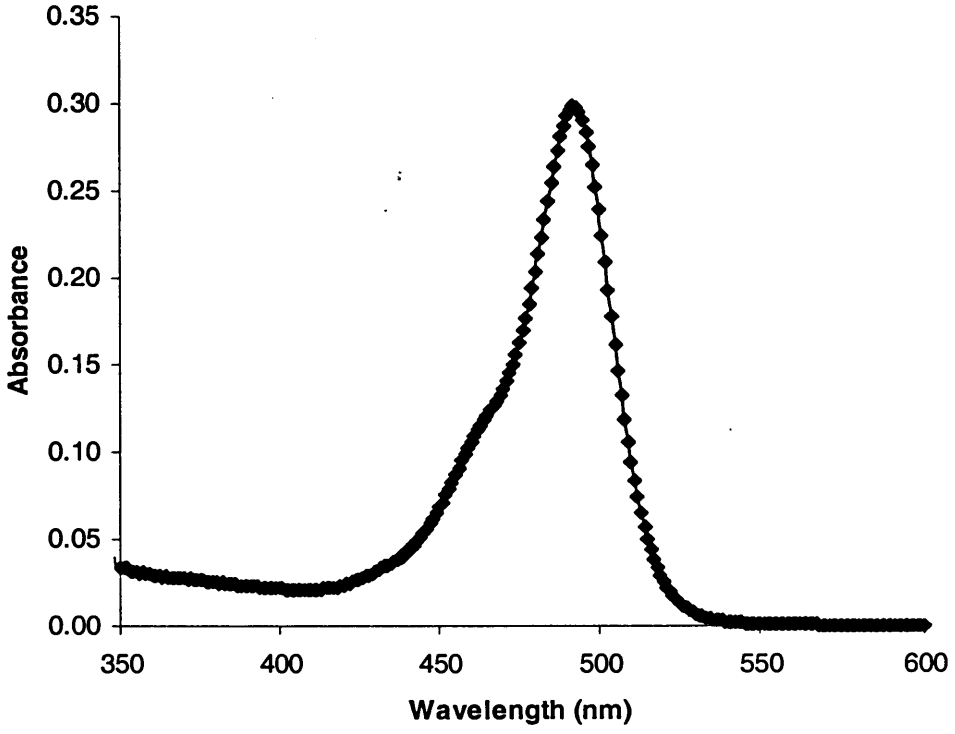

Figure 3.26 - UV spectrum of CMTMO-FAM

UV analysis of 6-O-carboxymethyl *N,N,N*-trimethyl chitosan derivatised with 5/6-carboxyfluorescein. $\lambda_{max} = 492$, A = 0.2984

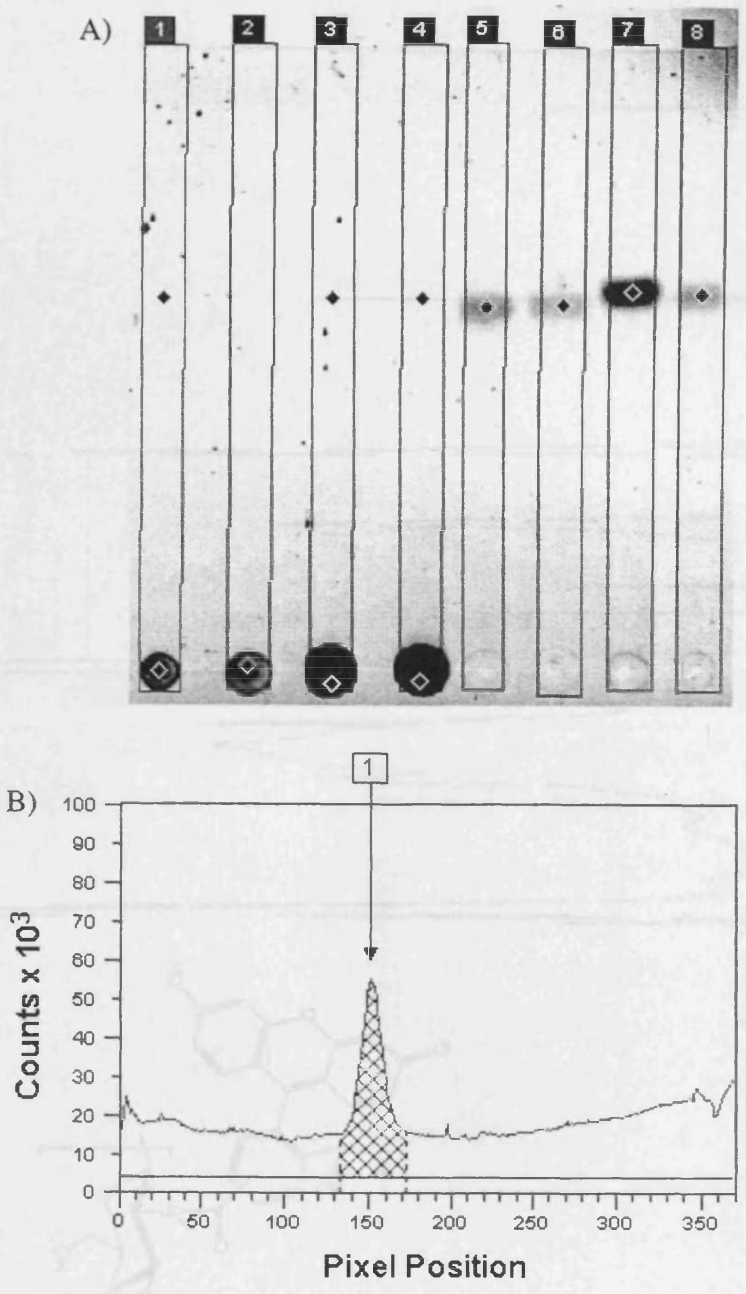

Figure 3.27 - TLC of CMTMO-FAM derivatives

A) TLC plate of conjugates, diamonds indicate the centre of the peak identified by ImageQuant software, Lane: 1) u11-CMTMO-FAM 0.1 mg/ml, 2) u7-CMTMO-FAM 0.1 mg/ml, 3) CMTMO-FAM 0.1 mg/ml, 4) CMTMO-FAM2 0.1 mg/ml, 5) FAM 0.00195 µg/ml, 6) FAM 0.00113 µg/ml, 7) FAM 0.01651 µg/ml. B) Lane 5 report of pixel intensity measured with Typhoon 9410 Variable Mode Imager, ImageQuant software.

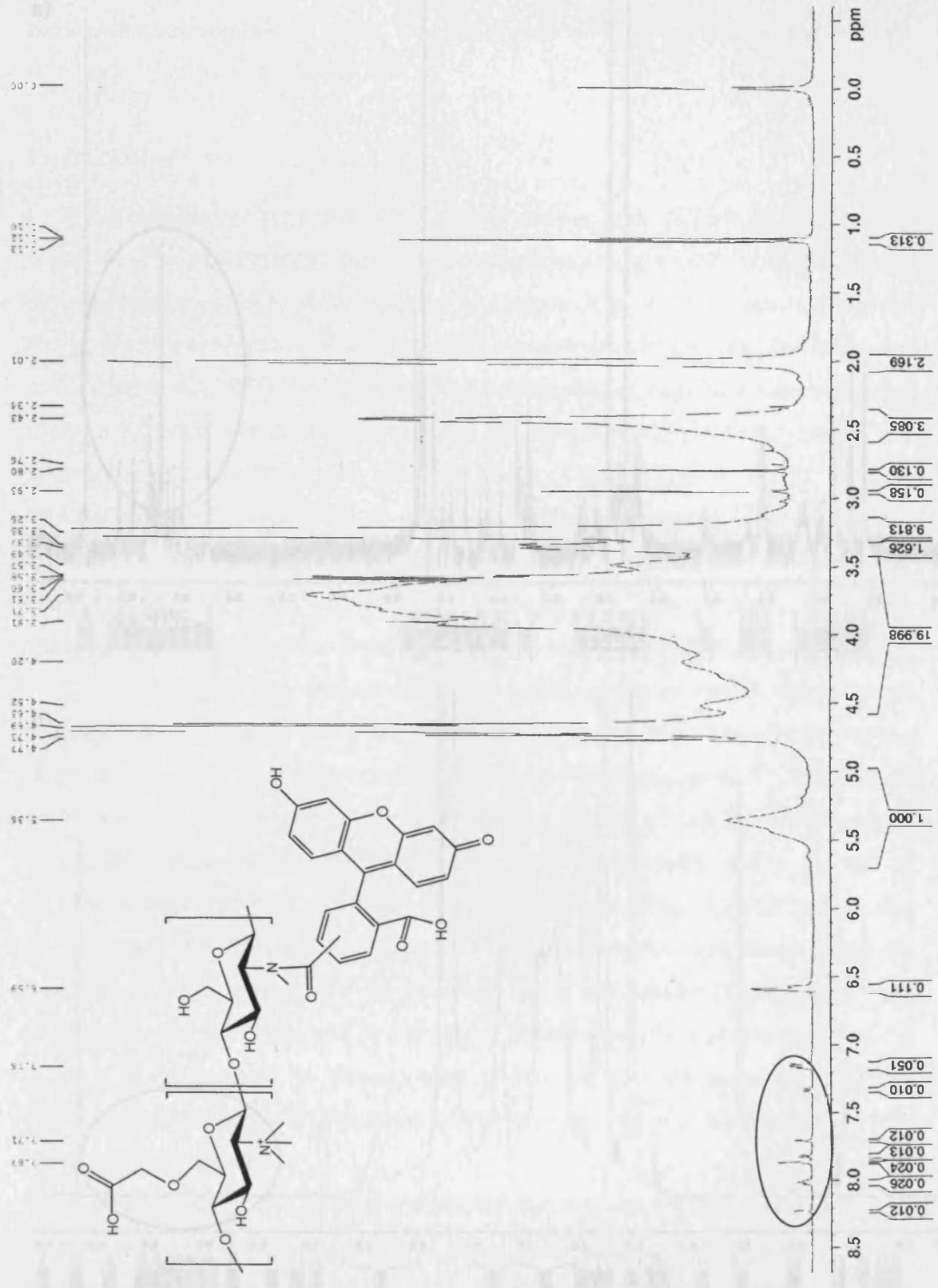

Figure 3.28 - ^{1}H NMR of CMTMO-FAM

Proton NMR showing the presence of aromatic protons at δ8 ppm

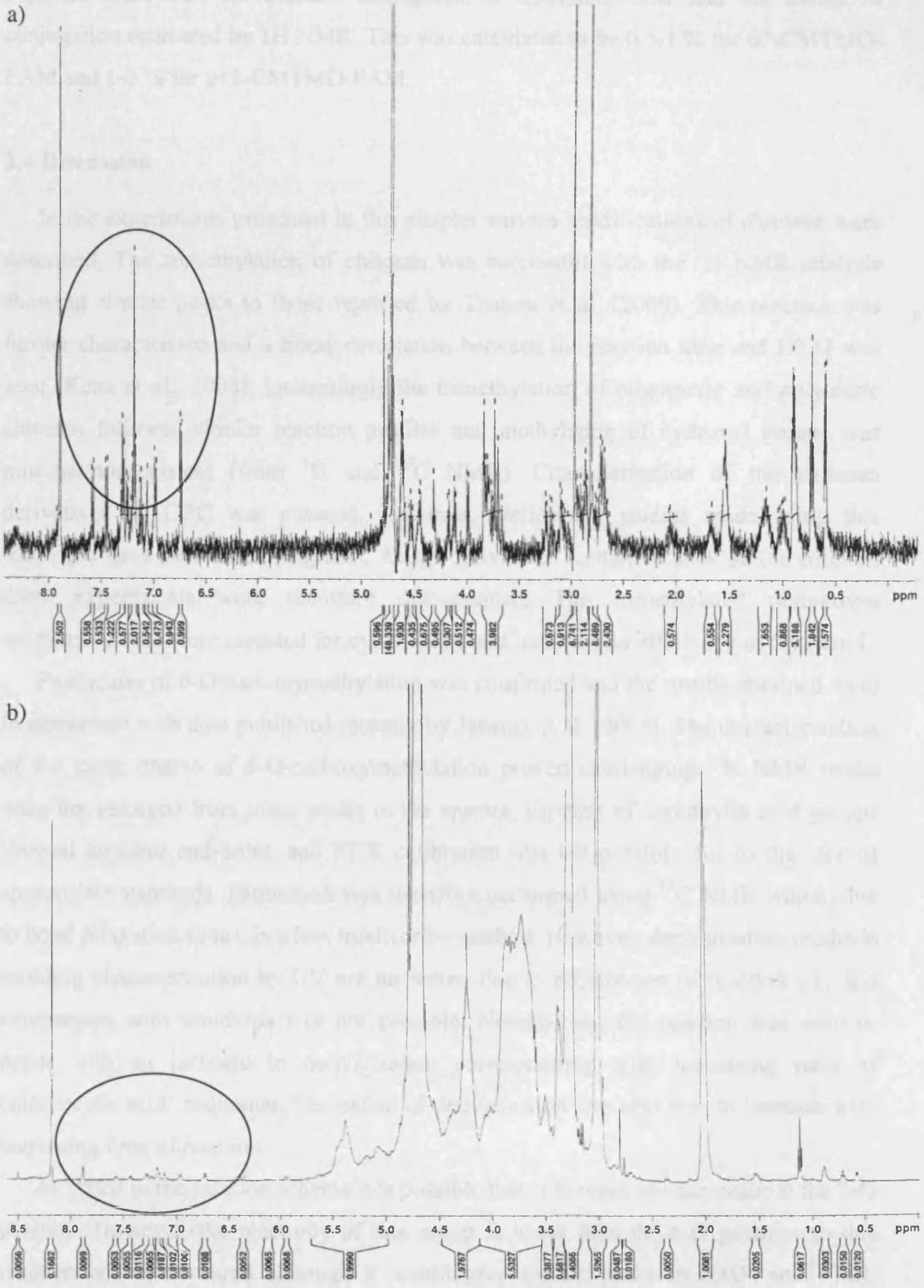

Figure 3.29 - u11-CMTMO NMR

^{1}H NMR of a) u11 and b) u11-CMTMO, u11 peaks are highlighted in the oval.

Peptides were also successfully conjugated to CMTMO-FAM and the extent of conjugation estimated by 1H NMR. This was calculated to be 0.5-1 % for u7-CMTMO-FAM and 1-3 % for u11-CMTMO-FAM.

3.4 Discussion

In the experiments presented in this chapter various modifications of chitosan were described. The trimethylation of chitosan was successful with the ^{1}H NMR analysis showing similar peaks to those reported by Thanou et al. (2000). This reaction was further characterised and a linear correlation between the reaction time and DTM was seen (Kean et al., 2005). Interestingly the trimethylation of oligomeric and polymeric chitosan followed similar reaction profiles and methylation of hydroxyl groups was minimal/non-existent (from ^{1}H and ^{13}C NMR). Characterisation of the chitosan derivatives by GPC was pursued. However, preliminary studies made using this technique gave poor chromatograms. As the derivatives seemed to stick on the column, these experiments were therefore discontinued. The trimethylated derivatives synthesised here were assessed for cytotoxicity and transfection efficiency in Chapter 4.

Production of 6-O-carboxymethylation was confirmed and the results obtained were in agreement with data published recently by Jansma et al. (2003). The characterisation of the exact degree of 6-O-carboxymethylation proved challenging: ^{1}H NMR peaks were not resolved from other peaks in the spectra, titration of carboxylic acid groups showed no clear end-point, and FTIR calibration was not possible due to the lack of appropriate standards. Estimation was therefore performed using ^{13}C NMR which, due to bond relaxation times, is a less trustworthy method. However, derivatisation methods enabling characterisation by UV are no better, due to efficiencies of reaction etc. and comparison with standards was not possible. Nonetheless, the reaction was seen to occur with an increase in derivatisation corresponding with increasing ratio of chloroacetic acid : monomer. The extent of derivatisation was also seen to increase with increasing time of reaction.

As stated in the reaction scheme it is possible that side reactions can occur at the 3-O position. However, the reactivity of this group is lower than the 6-O position so this reaction is less favoured although it would give similar peaks in NMR and FTIR. Determination of the presence of this side-product was not pursued. Carboxymethylation introduced a functional group for the later conjugation of peptides.

The method used for conjugation of peptides to CMTMO using EDC coupling was first studied using tyrosinamide as a model compound to demonstrate that conjugation was possible. Tyrosinamide was used due to the expense and time needed to synthesise the peptides and successful conjugation was found. Following this proof, the conjugation of u7 and Gu11G peptides was performed. A possible side reaction in the conjugation of peptides is the polymerisation of the peptide, through activation of its C-terminal carboxylic acid by EDC. To prevent this, the activation of CMTMO, CMTMO-FAM and CMTMO-OG with EDC was made prior to addition of peptide. In addition, the molar ratio of 2:1 EDC : COOH was chosen as this was sufficient to activate the carboxylic acid of CMTMO without activating the C-terminal of the peptide. This protein polymerisation reaction was prevented by C-amidation of the scrambled peptides.

Another possible side reaction during Gu11G conjugation is reaction of the activated carboxylic acid with the lysine of the peptide. Conducting the reaction at pH 9 should have reduced this possibility as the ε amine group of lysine has a higher pKa than the α amine of the N-terminal glycine. An alternative method to prevent this side reaction is the synthetic peptide could have been cleaved from the solid phase resin with a lysine protecting group intact, unfortunately it was not possible to pursue this reaction due to time limitations.

A further factor that was considered was the linkage of the peptide, in these experiments it has only been possible to link through the N-terminal amino acid. This may not be the most efficient point of conjugation and could restrict the peptide's access to the binding pocket of uPAR. The conjugation of peptides through the C-terminal amino acid would have involved the production of the protected TMO, de-protection followed by reaction with the activated C-terminal amino acid of the peptide. The peptide would have had to be cleaved from SPPS resin with the N-terminal protecting group intact. Regrettably this synthesis has not been performed. Peptide conjugates with CMTMO were studied for their effect on the production of complexes and transfection efficiency (Chapter 6).

The extent of peptide modification was difficult to determine. The lack of chromophore in u7 meant that UV spectroscopic quantification was not possible. As Gu11G has the amino acids tyrosine, phenylalanine and tryptophan in its structure it has a UV absorbance and an estimation of the amount bound to CMTMO was made, this

did not correlate well with NMR and UV spectra were poor. CMTMO exhibited some absorbance at the UV maxima of u11 making this method of characterisation difficult and unreliable. Also, the absorbance of the amino acid residues may be affected by the presence of the CMTMO in the solution and by being bound to the oligomer. The first experiments showed very small peaks in the NMR due to the peptides but these were not quantifiable. Later experiments, where greater quantities were produced, enabled more concentrated NMR samples to be made and an estimation of peptide content possible.

In later experiments where the peptides were bound to fluorescent derivatives UV quantification could not be made. Destructive methods (e.g. peptide analyser) of quantification were not investigated. The ^{1}H NMR shows a peak at δ 9.2 ppm which cannot be attributed to any of the reactants and the group responsible could not be determined. Although this characterisation was not as definitive as I would have liked, given the amount of sample available and the differences seen over controls (Chapter 5) I think it is clear that peptide conjugation has been successful.

Characterisation of the percentage of amines protected was challenging in preliminary experiments. Although ^{1}H NMR confirmed the presence of the protecting groups, peak quantification was not possible. This may have been due to the concentration of the NMR sample used and/or the lower power of the NMR spectrometer (300 MHz). In later experiments the peaks at δ 1.84 and δ 5.42 were resolved and could be integrated reliably to quantitate the content of protected amine. It was confirmed that these peaks were not due to free citraconic anhydride, as NMR of the protected chitosan containing citraconic anhydride showed a separate peak at δ 5.81 ppm. In the extrapolation of the curve (Fig. 3.20), to estimate the ratio which should be used in the subsequent reaction to produce 10 % protection, the highest degree of protection was excluded from the curve fit. This is because this was well beyond the degree of modification desired and the efficiency of reaction may have increased due to increased solubility of the oligomer chain with increased degree of modification. The actual degree of modification achieved was 7.7 % which is lower than expected but this could also be due to the scaling of the reaction.

FTIR confirmed the introduction of the carboxylic acid but as no standards exist to calibrate the FTIR peak ratio this is unsuitable as a method of quantification. A more

thorough investigation of the reaction profile of amine protection on chitosan was not possible due to both lack of time and limited oligomer stock. This protection/de-protection reaction of the amine groups of chitosan has not been reported by others (to the author's knowledge).

The degree of trimethylation of protected chitosan was lower than that of chitosan. This could have been due to steric hindrance of neighbouring monomer units which had been protected or, more likely, the interaction of the carboxylic acid in the protecting group with free amine on other chains. Nevertheless, protected chitosan was successfully trimethylated in both preliminary experiments and in later ones confirmed by ^{1}H NMR.

Chitosan was successfully labelled with 9-anthraldehyde and UV/fluorescence confirmation was in agreement with Tommeraas et al. (Tommeraas et al., 2001). The protection of chitosan followed by its trimethylation, de-protection then labelling with 9-anthraldehyde provided a fluorescently labelled trimethyl derivative and confirmed that the reaction scheme was viable. This method paved the way for future fluorescent labelling studies and some epifluorescent microscopy was performed (Chapter 5). However, the probe was determined as unsuitable for further microscopy or flow cytometry studies due to its excitation (254 nm) and emission (413 nm). This reaction provided validation of the protection, trimethylation and de-protection process for the subsequent set of experiments where the fluorescent label was replaced with Oregon Green. Due to the cost of OG only a small amount of labelled oligomer could be made making the full chemical characterisation difficult. The purification of the fluorescent oligomer from free OG proved problematic. Although OG was soluble in diethyl ether : ethanol, the oligomer bound or entrapped some OG during precipitation as free OG was visible when TLC was performed. Separation on a PD10 column was also poor and resulted in the loss of oligomer, presumably due to interaction with the sepharose gel. However, chloroform extraction followed by precipitation with diethyl ether : ethanol did result in good purification, providing a fluorescently labelled oligomer containing less than 1 % free OG. This derivative, u11-CMTMO-OG, was used in epifluorescent microscopy and flow cytometry experiments (Chapter 5). Although the conjugation of activated esters to secondary amines is less likely than to primary amines it was achieved in reactions with the succinimidyl ester of fluorescent with TMO and CMTMO, with u7 and Gu11G then being conjugated to CMTMO-FAM to give u7-

CMTMO-FAM and u11-CMTMO-FAM. These fluorescent derivatives were also studied by flow cytometry and fluorescent microscopy (Chapter 5).

3.5 Conclusions

A library of chitosan derivatives has been successfully prepared (summarised in Table 3.1) that could be used in the subsequent studies detailed in Chapters 4, 5 and 6.

Table 3.1 – Chitosan products

Label	Description	Characterisation
TMO20	Trimethylated oligomer with 20 % DTM	^{1}H NMR
TMO44	Trimethylated oligomer with 44 % DTM	^{1}H NMR
TMO55	Trimethylated oligomer with 55 % DTM	^{1}H NMR
TMO94	Trimethylated oligomer with 94 % DTM	^{1}H NMR
TMC36	Trimethylated polymer with 36 % DTM	^{1}H NMR
TMC57	Trimethylated polymer with 57 % DTM	^{1}H NMR
TMC76	Trimethylated polymer with 76 % DTM	^{1}H NMR
TMC93	Trimethylated polymer with 93 % DTM	^{1}H NMR
TMO51	Trimethylated oligomer with 51 % DTM	^{1}H NMR
CMTMO7.5	6-O-Carboxymethylated trimethylated chitosan oligomer (TMO51) produced with 7.5 equivalents of chloroacetic acid having 37 % 6-O-Caboxymethylation	^{1}H NMR, ^{13}C NMR, FTIR
CMTMO15	6-O-Carboxymethylated trimethylated chitosan oligomer (TMO51) produced with 15 equivalents of chloroacetic acid having 47 % 6-O-Caboxymethylation	^{1}H NMR, ^{13}C NMR, FTIR
U11CMTMO	Gu11G conjugated to CMTMO7.5 having 1-3 % Gu11G ligand	^{1}H NMR
Chitosan oligomer anthraldehyde	Chitosan oligomer labelled with 9-anthraldehyde	UV/fluorescence spectroscopy, TLC
Chitosan polymer anthraldehyde	Chitosan polymer labelled with 9-anthraldehyde	UV/fluorescence spectroscopy, TLC
TMO anthraldehyde	Trimethylated chitosan oligomer labelled with 9-anthraldehyde	^{1}H NMR, UV/fluorescence spectroscopy, TLC
TMC anthraldehyde	Trimethylated chitosan polymer labelled with 9-anthraldehyde	^{1}H NMR, UV/fluorescence spectroscopy, TLC

Table 3.1 – Chitosan products

Label	Description	Characterisation
TMOFAM	Trimethylated chitosan oligomer (DTM 44 %) labelled with 5/6-carboxyfluorescein	^{1}H NMR, TLC, UV, fluorescence spectroscopy
CMTMOFAM	6-O-carboxymethyl trimethyl chitosan oligomer (DTM 51.8 %) labelled with 5/6-carboxyfluorescein	^{1}H and ^{13}C NMR, TLC, UV and fluorescence spectroscopy
u11CMTMOFAM	Gu11G conjugated to 6-O-carboxymethyl trimethyl chitosan oligomer (DTM 51.8 %) labelled with 5/6-carboxyfluorescein	^{1}H NMR, TLC, UV and fluorescence spectroscopy
u7CMTMOFAM	u7 conjugated to 6-O-carboxymethyl trimethyl chitosan oligomer (DTM 51.8 %) labelled with 5/6-carboxyfluorescein	^{1}H NMR, TLC, UV and fluorescence spectroscopy
u11CMTMO-OG	Gu11G conjugated to 6-O-carboxymethyl trimethyl chitosan oligomer (DTM 29.4 %) labelled with Oregon Green	^{1}H NMR, TLC, UV and fluorescence spectroscopy

Chapter 4

Trimethylated Chitosans as Non-Viral Gene Delivery Vectors: Cytotoxicity and Transfection Efficiency

4.1 Introduction

Having synthesised and characterised the library of trimethylated chitosan derivatives (described in Chapter 3) it was essential to establish their cytotoxicity and transfection efficiency. Many cationic polymers proposed as non-viral vectors have also been found to be toxic (Gebhart & Kabanov, 2001, Morgan et al., 1989). The toxicity of polycationic amino acids was found to be related to the monomer with cytotoxicity in the order ornithine > lysine > arginine (Morgan et al., 1989). Fischer et al. (2003) ranked the toxicity of cationic polymers in this way: PEI = PLL > poly(diallyl-dimethyl-ammonium chloride) (DADMAC) > diethylaminoethyl-dextran (DEAE-dextran) > poly(vinyl pyridinium bromide) (PVPBr) > PAMAM (dendrimer generation 3) > cationic human serum albumin (cHSA) > native human serum albumin (nHSA). Most studies report that chitosan displays low toxicity (Illum, 1998, Rao & Sharma, 1997, Richardson et al., 1999b). However, Carreno-Gomez and Duncan (1997) found that HCl chitosan (100 – 130 kDa) salts were relatively toxic (IC_{50} = 0.21 ± 0.04 mg/ml) in the presence of serum. Toxicity was found to be dose, time and molecular weight-dependant (Carreno-Gomez & Duncan, 1997, Morgan et al., 1989).

4.1.1 Mechanism of Polycation Induced Toxicity

Very early studies showed that PLL caused agglutination of cells through interaction with the membrane of adjacent cells (Katchalsky, 1964). They also found that rather than just neutralising the surface potential of the cell, with increasing concentration of PLL it increases to high positive values (Katchalsky, 1964). This indicates that the polymer chain was perpendicular to the membrane (Katchalsky, 1964). The toxicity of polycationic amino acids was not altered by inhibition of microtubule or microfilament formation, so it was concluded that toxicity was plasma membrane-dependent (Morgan et al., 1989).

There are many mechanisms by which polycations could induce toxicity due to interaction with negatively charged cell components and proteins (Fischer et al., 2003). It has been shown by many that toxicity of polycations is related to polymer molecular weight, this is true for PLL (Choksakulnimitr et al., 1995) and DEAE-dextran (Fischer et al., 2003). However, branched PEI was found to display similar toxicity across a range of molecular weights (600-1000, 60 and 25 kDa) in COS-1 and Calu-3 cells

(Florea et al., 2002a). In the same study it was concluded that PEI, DADMAC and PLL were highly plasma membrane damaging, evidenced by their ability to release haemoglobin from red blood cells (Fischer et al., 2003). It is however still unclear exactly what leads to cationic polymer-mediated membrane damage (Fischer et al., 2003, Vepa et al., 1997). It seems therefore, that the toxicity of a given type/group of polymers must be determined individually using more than one cell type.

4.1.2 Cytotoxicity Assessment

Several methods have been used to assess cytotoxicity of drugs and polymers. These include: [^{3}H]thymidine and [^{3}H]leucine incorporation (Morgan et al., 1989, Sgouras & Duncan, 1990), lactate dehydrogenase release (Choksakulnimitr et al., 1995, Vepa et al., 1997), sodium 39-[1-(phenylaminocarbonyl)-3, 4-tetrazolium]-bis-(4-methoxy-6-nitro)benzenesulfonic acid (XTT) assay (Scudiero et al., 1988). A rapid and facile assay was developed by Mosmann (1983) to measure the cytotoxicity of anticancer agents which uses MTT (Section 2.3.2). This method has also been used extensively to study the cytotoxicity of many polymers (Fischer et al., 2003, Sgouras & Duncan, 1990). When the MTT assay was compared to [^{3}H]thymidine and [^{3}H]leucine incorporation or counted cell numbers in HepG2 and CCRF (lymphoblastoid leukaemia) cells, PLL cytotoxicity showed good correlation with IC_{50} values determined using the different methods (Sgouras & Duncan, 1990). However, the different cell lines displayed different IC_{50} values, the suspension culture being more susceptible to toxicity, indicating that toxicity is cell line-dependant (Sgouras & Duncan, 1990). The reproducibility, speed and ease of the MTT assay, along with its common use in the literature led to its choice for the determination of chitosan derivative toxicity.

It is interesting to consider the relationship between polycation cytotoxicity and transfection efficiency. Using the MTT method Florea et al. (2002) showed that transfection efficiency of PEI (0.4 - 34.4 μg/ml) correlated well with the toxicity in Calu-3 cells, but did not correspond with toxicity in COS-1 cells. However, Van de Wetering et al. (1997) also showed that poly(2-(dimethylamino)ethyl methacrylate) (p(DMEAMA)) transfection of COS-7 and OVCAR-3 cell lines also showed a correlation with cytotoxicity. When studying a library of linear poly(amidoamine)s (PAA) Hill et al. (1999) found them to be largely non-toxic (IC_{50} > 400 μg/ml). However, only those PAAs that showed some toxicity were able to transfect A549 cells

(lung carcinoma epithelial cells) (Hill et al., 1999). Richardson et al. (2001) showed that PAAs with IC_{50} = 4-5 mg/ml in B16F10 cells (Richardson et al., 1999a) were able to produce transfection comparable to PEI in HepG2 cells.

4.1.3 Transfection Efficiency Assessment

In vitro transfection assays commonly use a reporter gene plasmid construct. The two most commonly used constructs encode for β-galactosidase (Ferkol et al., 1996, van de Wetering et al., 1997, Zanta et al., 1997) or luciferase (Boussif et al., 1995, Ferkol et al., 1996, Plank et al., 1992, Wagner et al., 1990). β-galactosidase expression can be detected using 5-bromo-4-chloro-3-indolyl β-D-galactoside (X-Gal) as a substrate which is enzymatically converted to a blue compound. Thus cells expressing β-galactosidase can be counted and this is a particularly useful tool (Ferkol et al., 1996). Luciferase expression is measured by the enzymatic oxidation of luciferin (Section 2.3.6) in a bioluminescent reaction (Promega, 2003b). The detection of luciferase is a quicker and more sensitive method than the detection of β-galactosidase. These advantages led to the choice of luciferase as the reporter gene for use in the transfection experiments reported here.

4.1.4 Study Aims and Objectives

The initial aim of this study was to investigate the effect of increasing trimethylation of chitosan oligomers and chitosan polymers on cytotoxicity, over both 6 and 24 h incubations, using the MTT assay. MCF-7 (breast cancer epithelia) cells were chosen as a model because it was thought that they would be useful to investigate the applicability of trimethylated chitosan derivatives for cancer gene therapy. This cell line has been shown to express uPAR (Chapter 5) making them a useful model to also study targeted-chitosan gene delivery. COS-7 (African Green Monkey kidney fibroblast) cells were also used as a model as this cell line is commonly used to study transfection (Akinc et al., 2003, Akuta et al., 2002, Cherng et al., 1996) thus allowing comparison of the data generated here with the literature. This cell line was also shown to express uPAR (Chapter 5). For the cytotoxicity experiments an incubation time of 6 h was chosen to measure the toxicity of the derivatives over the exposure time used in the *in vitro* transfection studies. In other experiments the 24 h incubation time was chosen to mimic an increased tissue-therapeutic contact time, which might be expected *in vivo* where

clearance would be likely to take longer. Furthermore, the 24 h exposure was also chosen as the cells would still be within an exponential growth phase in this period meaning that any toxicity, due to inhibition of proliferation and/or cell death, would be clearly visible in the MTT assay.

It was hypothesised that increasing DTM would increase the gene delivery efficiency of the chitosan derivatives but would also detrimentally affect cell viability. The purpose of this study was therefore to define an optimum derivative with regards to both cytotoxicity and transfection efficiency that could be further developed as a targeted non-viral delivery system.

4.2 Materials and Methods

4.2.1 Materials

The chitosan oligomer (3-6 kDa) and the chitosan polymer (~100 kDa) were both modified as described in Sections 3.2.1 and 3.2.2 to produce the library of trimethylated oligomers and polymers used in these studies (listed in Table 4.1). The plasmid pGL3 luc was prepared and characterised as described in Section 2.3.7.

4.2.2 Evaluation of Cytotoxicity

Some of the cytotoxicity studies were undertaken in collaboration with a visiting student whom I supervised, Susanne Roth.

The MTT assay was used to assess cytotoxicity essentially as described in Section 2.3.3. Chitosan derivatives and PEI were dissolved in DMEM at concentrations ranging from 20 to 10,000 μg/ml (100 μl/well) and after a 6 h or 24 h exposure the cell viability was determined by MTT assay after 24 h. The viability of cells exposed to chitosan derivatives was compared to that of cells treated with DMEM only. The pH of solutions applied to cells did not vary significantly from that of DMEM alone.

To examine the cytotoxicity of polyplexes, vector : pGL3 luc polyplexes were made (as described in Section 4.2.3) and polyplex-containing media (20 μl) was added to each well and the cells incubated either for 6 or 24 h as outlined above. Again toxicity was assessed by MTT assay after 24 h. Where possible an IC_{50} value was calculated using Bio-Graph software, with curve fitting according to the Hill equation (Equation 4.1) using Rmax fixed at 100 and Rmin at 0, weighted for standard error as described by Zhang et al. (2004).

Table 4.1 – Characteristics of chitosan derivatives

Label	Trimethyl group (mol %)[z]	Estimated Mw (kDa)*
TMO20	20	3.5-7.0
TMO44	44	3.6-7.2
TMO55	55	3.6-7.3
TMO94	94	3.8-7.5
TMC36	36	~119
TMC57	57	~121
TMC76	76	~123
TMC93	93	~125

* - Mw calculated from the starting molecular weight given by the manufacturer i.e. 3-6 kDa (oligomer) and ~100 kDa (polymer). Using these values the derivatised chitosan molecular weight was calculated using the equation below. The value z (% of glucosamine monomer units that are trimethylated) was quantified by ^{1}H NMR (Section 3.3.1).

		% of monomer		Mw of derivative
% x N-acetyl glucosamine Mw	=	0.03	x	203
% x trimethyl glucosamine Mw	=	z	x	206
% x dimethyl glucosamine Mw	=	(100-0.03-z)	x	189

Sum = Estimated Mw

Equation 4.2

$$y = Rmin + (Rmax - Rmin)/(1+(x/IC_{50})^P \quad \text{Equation 4.1}$$

$$\text{Cell Viability} = 0 + (100 - 0)/(1+([\text{derivative}]/IC_{50})^P$$

The Rmax and Rmin values were fixed at these values as an a priori decision assuming that the data should fit between these values, i.e. at low concentrations the polymer would not exhibit toxicity and that toxicity would increase with increasing concentration. It is realised that this is not always the case in practice but these criteria were adopted to allow comparison of the IC_{50} values for chitosans having different degrees of trimethylation and also to allow comparison of the IC_{50} values obtained for the different cell lines. This technique also adds the confidence limits of the curve fit rather than simply giving an IC_{50} value derived from a simple line drawn between two points as is often used in other studies. In experiments where toxicity, even at the highest concentration, was not sufficient to achieve an IC_{50} value, the data could not be fitted to the Hill equation (or if the residual S.D. was greater than 0.1) curve fits were abandoned. To compare between the toxicity of polyplexes and that of the vector alone, statistical analysis was made using repeated measures ANOVA followed by Bonferroni post hoc test for pairs of data.

4.2.3 Preparation and Characterisation of Polyplexes

To form polyplexes of pGL3 luc with both chitosan derivatives and PEI the cationic vector solutions were prepared in DMEM (0.1 mg/ml) (NB in the absence of serum). These solutions (300 μg) were added to a vial containing pDNA (30 μg) to give a 10:1 ratio (vector : pDNA w/w). A 10:1 w/w ratio of vector : pDNA corresponds to N : P ratios of approximately 16 for trimethylated derivatives and 72 for PEI. This mixture was then vortexed at a low speed (to avoid pDNA shearing) for 20 s and then left for 20 min to allow polyplexes to form. To ensure that polyplexes had formed the mixture was electrophoresed on an agarose gel (0.7 %) containing ethidium bromide (0.25 μg/ml) (Section 2.3.8).

4.2.4 Transfection of COS-7 and MCF-7 Cells

Cells were seeded ($1x10^5$ cells/well) in a 24 well plate and grown overnight in DMEM supplemented with 10 % FCS and penicillin/streptomycin (100 Units/ml, 100 μg/ml) at 37 °C 5 % CO_2. An hour prior to the start of the transfection experiment, the media was removed and replaced with DMEM alone (without serum or antibiotics),

and the plates returned to the incubator. To start the experiment, polyplex-containing media (200 µl) was added slowly to each well to give a pGL3 luc final concentration of 2 µg/well. Experiments were conducted in quadruplicate. The plates were incubated for 6 h and transfection was performed in the absence of serum. The polyplex-containing medium was then removed and replaced with complete cell culture medium (200 µl). The plates were incubated for a further 48 h to allow protein expression. At the end of this time the media was removed and cell lysis buffer (200 µl) added to each well. Each well was then scraped with a rubber policeman to provide cell lysates which were then transferred to eppendorf tubes. The lysate was then cleared by centrifugation (10 min at 13000 RCF), the supernatant collected and assayed for protein content using the BCA assay (see Section 2.3.5) and for luciferase activity (see Section 2.3.6). Luciferase activity is expressed as relative light units (RLU)/mg protein.

4.3 Results

4.3.1 Cytotoxicity of Quaternised Chitosan Derivatives

All the chitosan derivatives were less toxic than PEI over the concentration range examined (PEI $IC_{50} \leq 30$ µg/ml, Table 4.2), in both cell lines tested. TMCs showed greater effects on cell viability when compared with TMOs of a similar DTM (Table 4.2). Different slopes of fitted curves were observed for the different DTM of TMC after 6 h incubation in MCF-7 cells (Fig. 4.1). Conversely, more similar curves were seen in COS-7 cells (Fig. 4.2). At low concentrations of TMC36 and TMC57 there appeared to be an increase in COS-7 cell viability (Fig. 4.2b). As the DTM increased there was a general trend that the gradient of the slope increased (Figs. 4.1 and 4.2). After an incubation of 24 h the slope gradients were more consistent between the two cell lines (Figs. 4.3 and 4.4). A curve could not be fitted to the TMC36 cytotoxicity measured after 24 h incubation in the COS-7 cells, as the cell viability reduced initially but then increased dramatically at 500 µg/ml (Fig. 4.4b). Interestingly, an apparent increase in cell viability in MCF-7 cells after a 6 h incubation with TMOs was also detected (Fig. 4.5a), which was not replicated in COS-7 cells (Fig. 4.5b). In both cell lines only TMO94 was sufficiently toxic after a 6 h incubation to allow an IC_{50} value to be estimated (Fig. 4.5). After a 24 h incubation IC_{50} values could be estimated for TMO55 and TMO94 in both cell lines (Fig. 4.6). Cell viability was seen to decrease when exposed to chitosan derivatives having an increasing DTM.

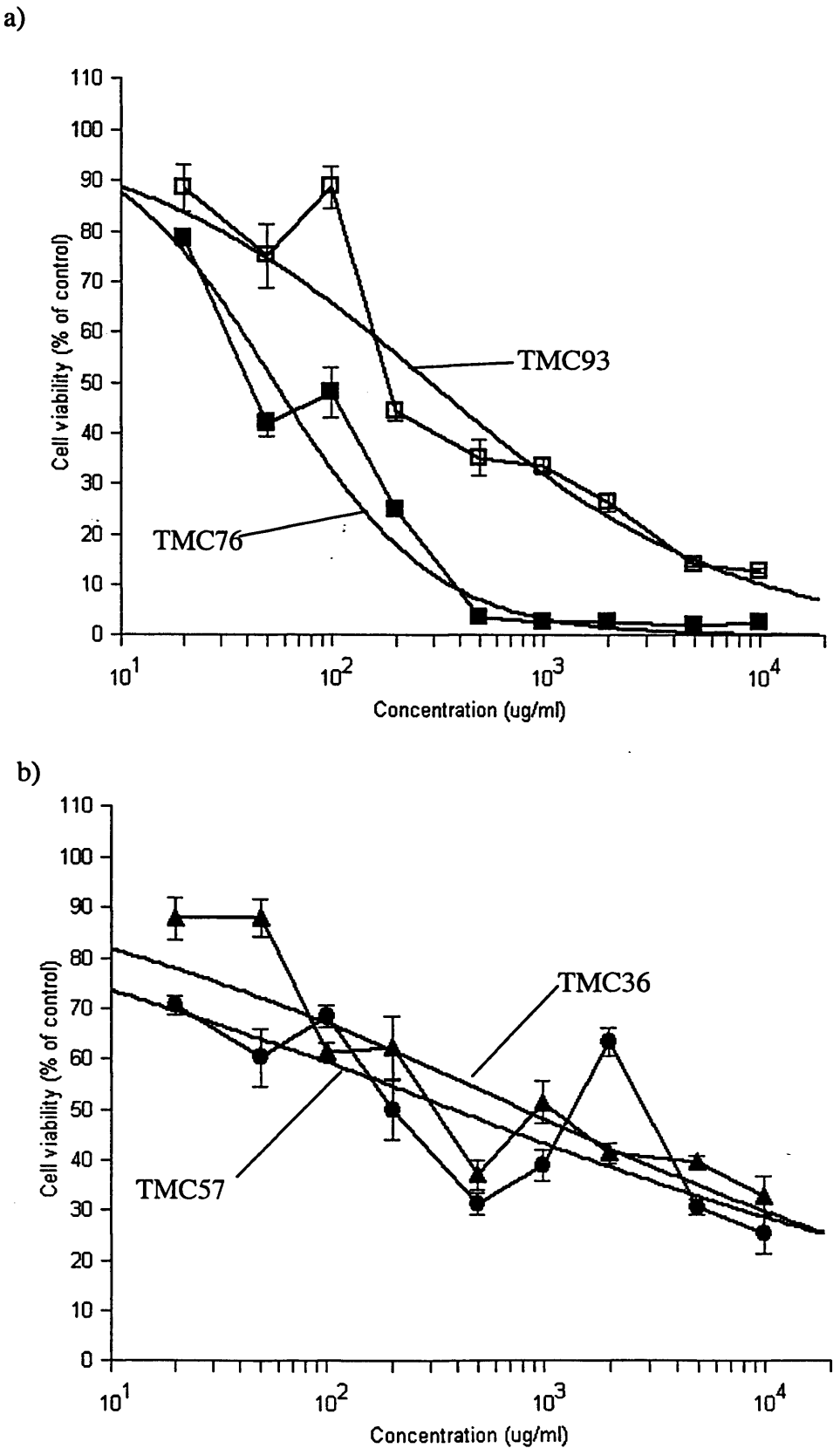

Figure 4.1 – Cytotoxicity of TMC after 6 h incubation on MCF-7 cells

Effect of trimethylated chitosan polymer on the viability of MCF-7 cells after a 6 h incubation. a) ■TMC76, □TMC93, b) ▲TMC36, ● TMC57. Data represent mean (n=6) ± S.E.M and the curves were fitted as described (Section 4.2.2).

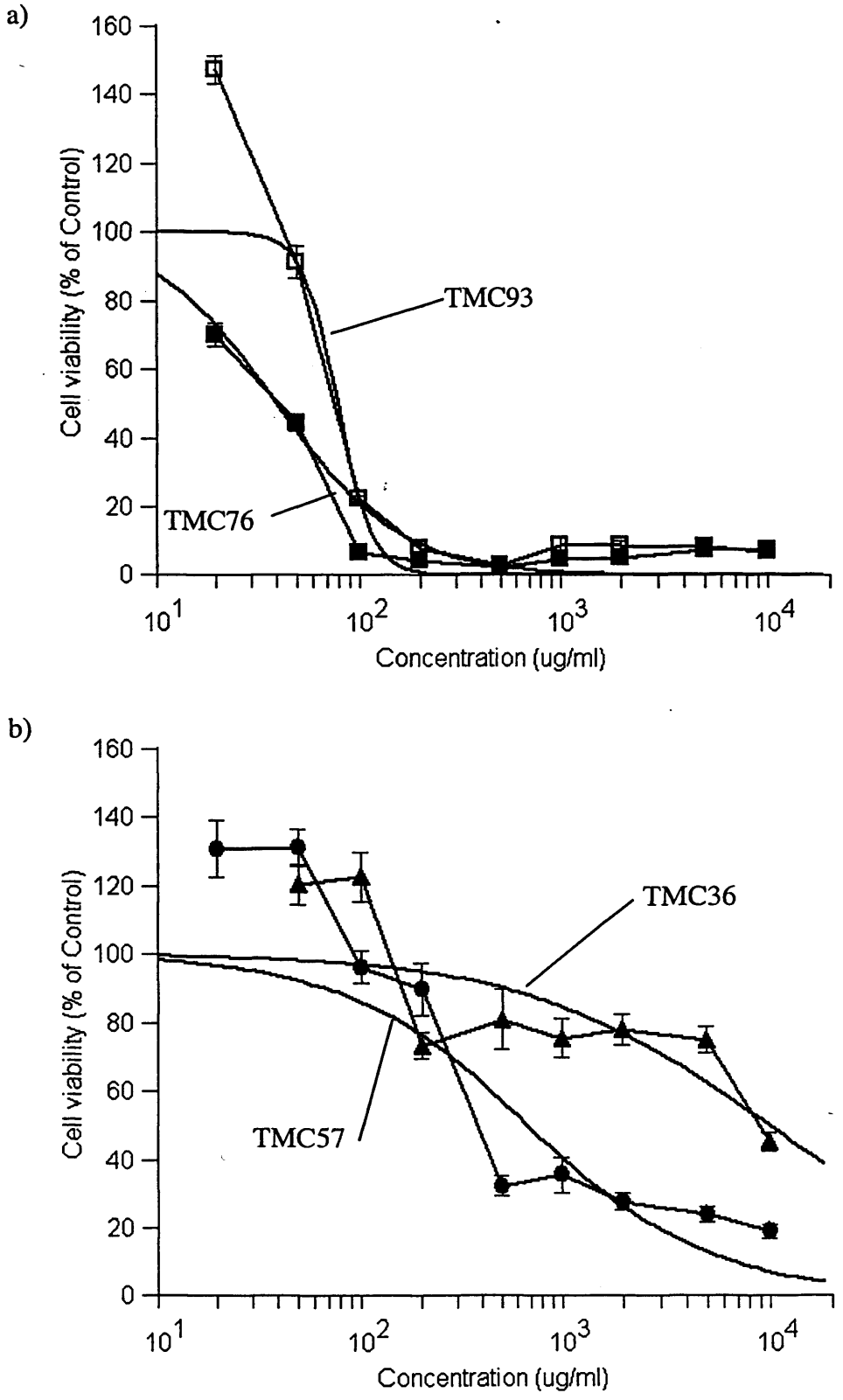

Figure 4.2 – Cytotoxicity of TMC after 6 h incubation on COS-7 cells

Effect of trimethylated chitosan polymer on the viability of COS-7 cells after a 6 h incubation. a) ■TMC76, □TMC93, b) ▲TMC36, ● TMC57. Data represent mean (n=6) ± S.E.M and the curves were fitted as described (Section 4.2.2).

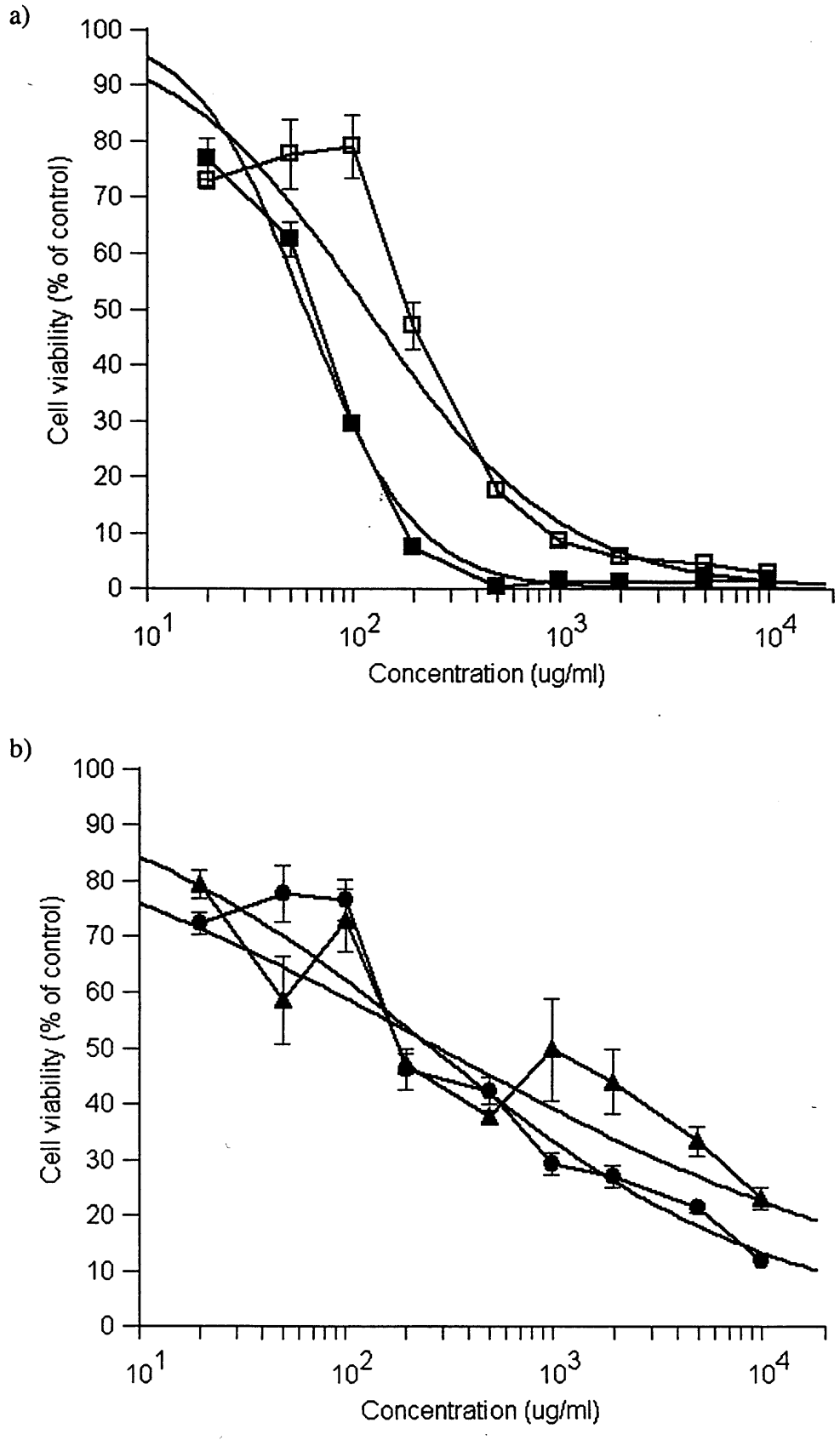

Figure 4.3 – Cytotoxicity of TMC after 24 h incubation on MCF-7 cells

Effect of trimethylated chitosan polymer on the viability of MCF-7 cells after a 6 h incubation. a) ■TMC76, □TMC93, b) ▲TMC36, ● TMC57. Data represent mean (n=6) ± S.E.M and the curves were fitted as described (Section 4.2.2).

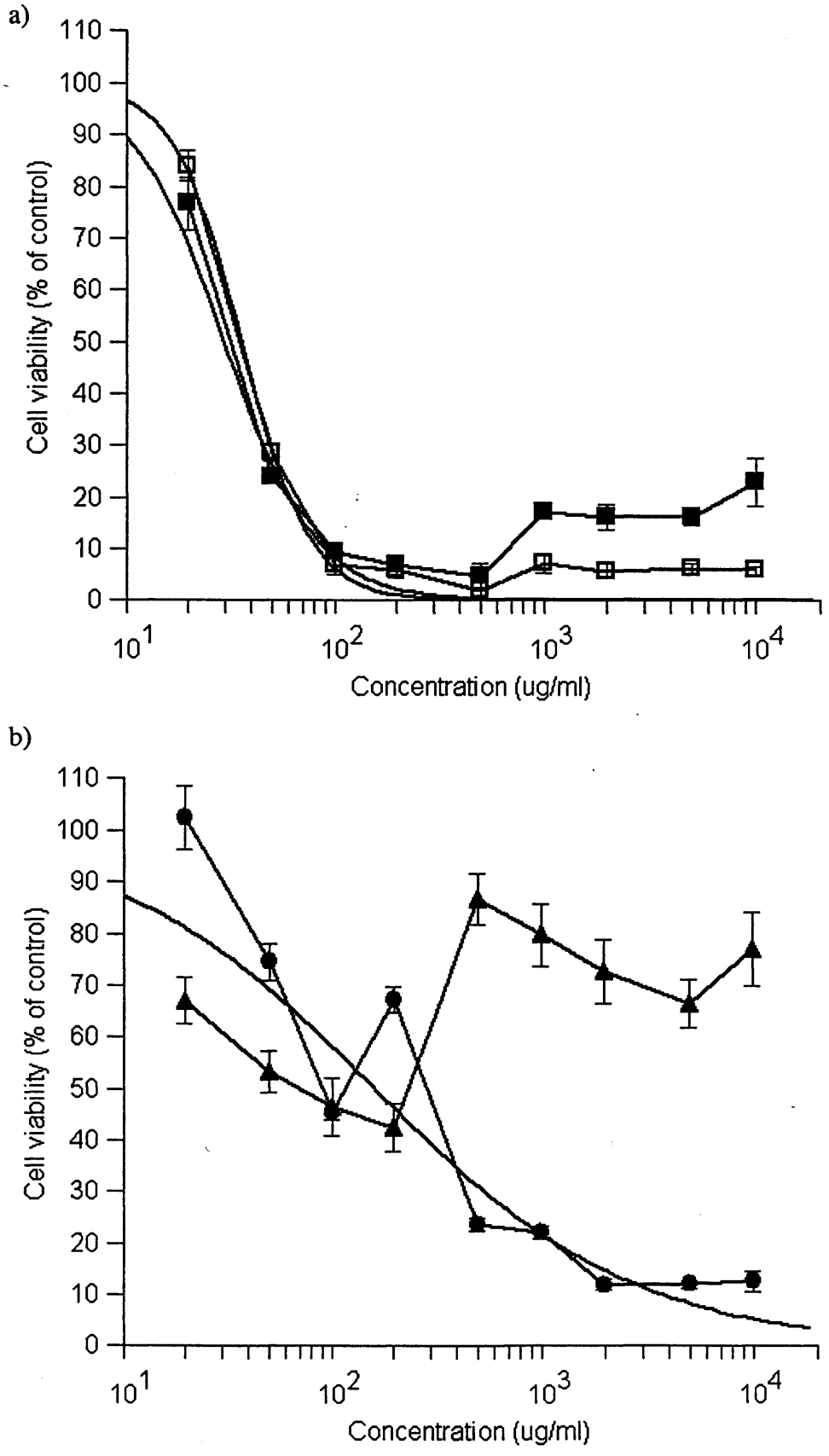

Figure 4.4 – Cytotoxicity of TMC after 24 h incubation on COS-7 cells

Effect of trimethylated chitosan polymer on the viability of COS-7 cells after a 6 h incubation. a) ■TMC76, □TMC93, b) ▲TMC36, ● TMC57. Data represent mean (n=6) ± S.E.M and curves were fitted as described (Section 4.2.2).

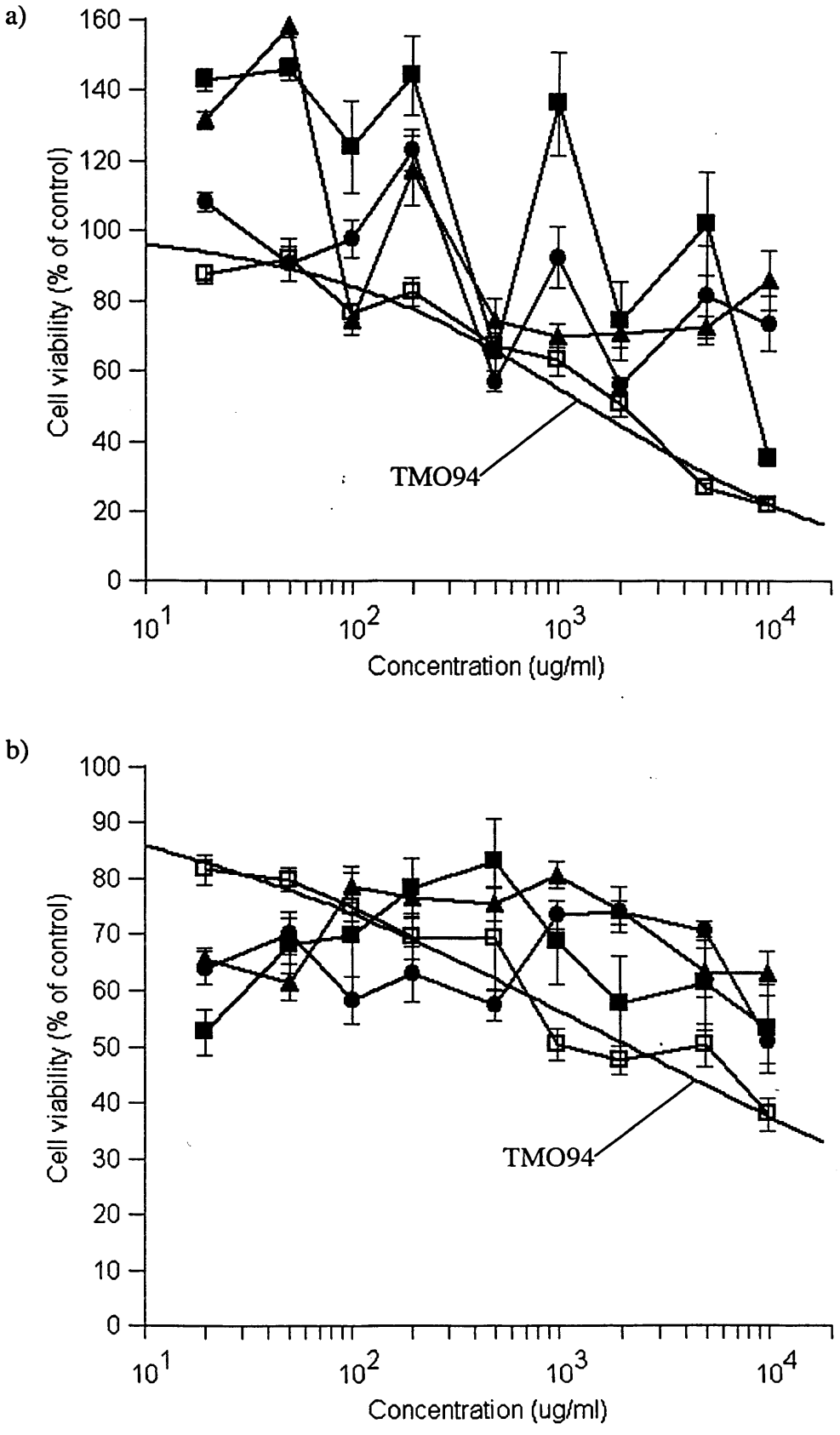

Figure 4.5 – Cytotoxicity of TMO after 6 h incubation

Effect of trimethylated chitosan oligomer on the viability of a) MCF-7 and b) COS-7 cells after a 6 h incubation : ▲TMO20, ●TMO44, ■TMO55, □TMO94. Data represent mean (n=6) ± S.E.M and curves were fitted as described (Section 4.2.2).

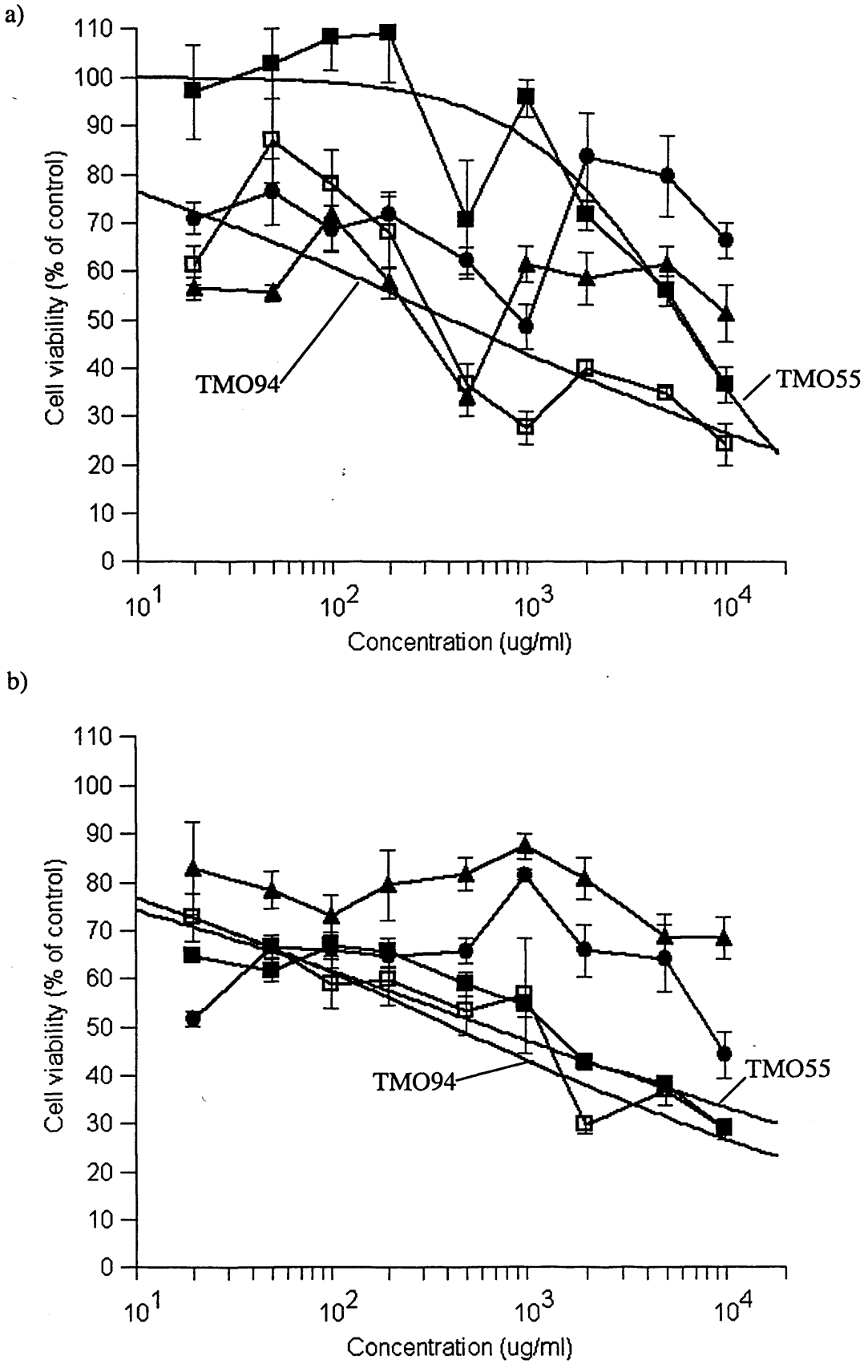

Figure 4.6 – Cytotoxicity of TMO after 24 h incubation

Effect of trimethylated chitosan oligomer on the viability of a) MCF-7 and b) COS-7 cells after a 24 h incubation: ▲TMO20, ●TMO44, ■TMO55, □TMO94. Data represent mean (n=6) ± S.E.M and curves were fitted as described (Section 4.2.2).

Table 4.2 – Summary of the Cytotoxicity of TMO and TMC

Product Label	Exposure time (h)	IC_{50} (µg/ml) MCF -7	COS-7
TMO20	6	> 10000	> 10000
	24	> 10000	> 10000
TMO44	6	> 10000	> 10000
	24	> 10000	> 10000
TMO55	6	> 10000	> 10000
	24	5959 ± 943	661 ± 205
TMO94	6	1402 ± 210	2207 ± 381
	24	417 ± 210	430 ± 116
TMC36	6	823 ± 324	10100 ± 5620
	24	285 ± 100	> 10000
TMC57	6	393 ± 259	676 ± 329
	24	265 ± 53	161 ± 50
TMC76	6	55 ± 10	40 ± 87
	24	59 ± 30	30 ± 8
TMC93	6	293 ± 68	79 ± 16
	24	118 ± 28	36 ± 3
PEI (25kDa)	6	< 20	30
	24	< 20	< 20

The IC_{50} values were calculated for the cytotoxicity data (see Figs. 4.1 – 4.6) using the Hill equation as described in the methods (Section 4.2.2).

This was true in both MCF-7 and COS-7 cells (Figs. 4.1-4.6) and was observed for both the polymer (Figs. 4.1-4.4) and the oligomer (Figs. 4.5 and 4.6).There was an almost linear decrease in IC_{50} values seen with increasing degree of chitosan polymer trimethylation up to 76 % DTM (Fig. 4.7).

At degrees of trimethylation lower than 94 % the oligomeric chitosan derivatives showed no appreciable toxicity at any of the concentrations tested after 6 h exposure (Fig. 4.5). At the highest TMO concentration the solution became more viscous and any toxicity seen was thought to be due to removal of cells when removing the derivative solution. The extent of toxicity seen was different in the two cell lines with chitosan derivatives generally (but not in all cases) being more toxic towards COS-7 cells (Table 4.2).

4.3.2 Effect of Polyplex Formation on Cytotoxicity

The effect of the chitosan derivatives alone on cell viability was compared to the effect of their polyplexes with pGL3 luc. MCF-7 cells showed an increase in cell viability when exposed to polyplexes made with the lowest DTM of both polymer (DTM = 36 %) and oligomer (DTM = 20 %) (Fig. 4.8a). In contrast, for COS-7 cells treated with TMO20 derived polyplexes there was no difference in cell viability, although cells treated with polyplexes made from TMC36 showed a dramatic decrease in cell viability (Fig. 4.8b). Complexation of TMO55 with pDNA led to a decrease in the viability of MCF-7 cells, but caused no significant difference in the viability of COS-7 cells (Fig. 4.8). Both cell lines had similar responses to TMC76 derived polyplexes and the polyplexes had less effect on cell viability than the cationic vector alone (Fig. 4.8). At the highest DTM there was only a significant difference in MCF-7 cells incubated with TMO94, here the cationic material alone was more toxic than polyplexes (Fig. 4.8). PEI-derived polyplexes had the same effect on cell viability in both cell lines and the polyplexes (PEI : pGL3 luc 10:1 w/w) were less toxic than PEI (Fig. 4.8).

4.3.4 Confirmation of Quaternised Chitosan : pGL3 luc Polyplex Formation

To investigate the ability of chitosan derivatives to complex pDNA adequately, solutions of the derivatives and plasmid were subjected to agarose gel electrophoresis using gels containing ethidium bromide (Section 2.3.8).

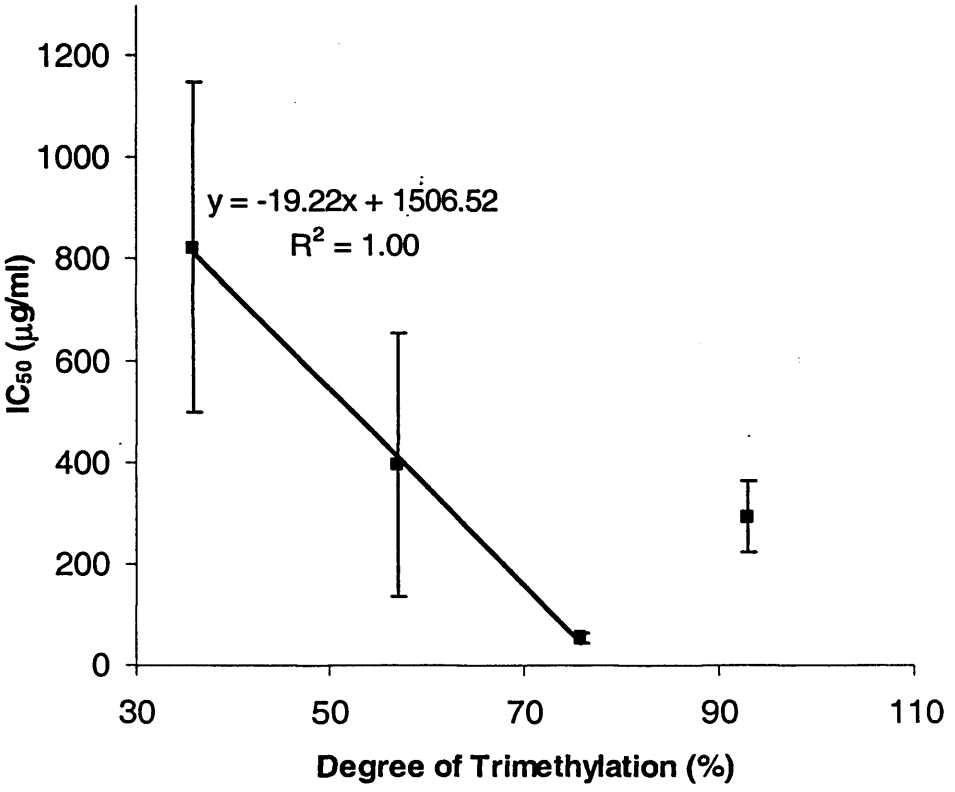

Figure 4.7 – Effect of the DTM of TMC on cytotoxicity

Correlation between the IC50 values observed and the degree of polymer trimethylation using MCF-7 cells (6 h incubation). The trendline was drawn through TMC36, TMC57 and TMC76. Data represent the IC_{50} derived from the curve fit, n=54 (± S.E.M).

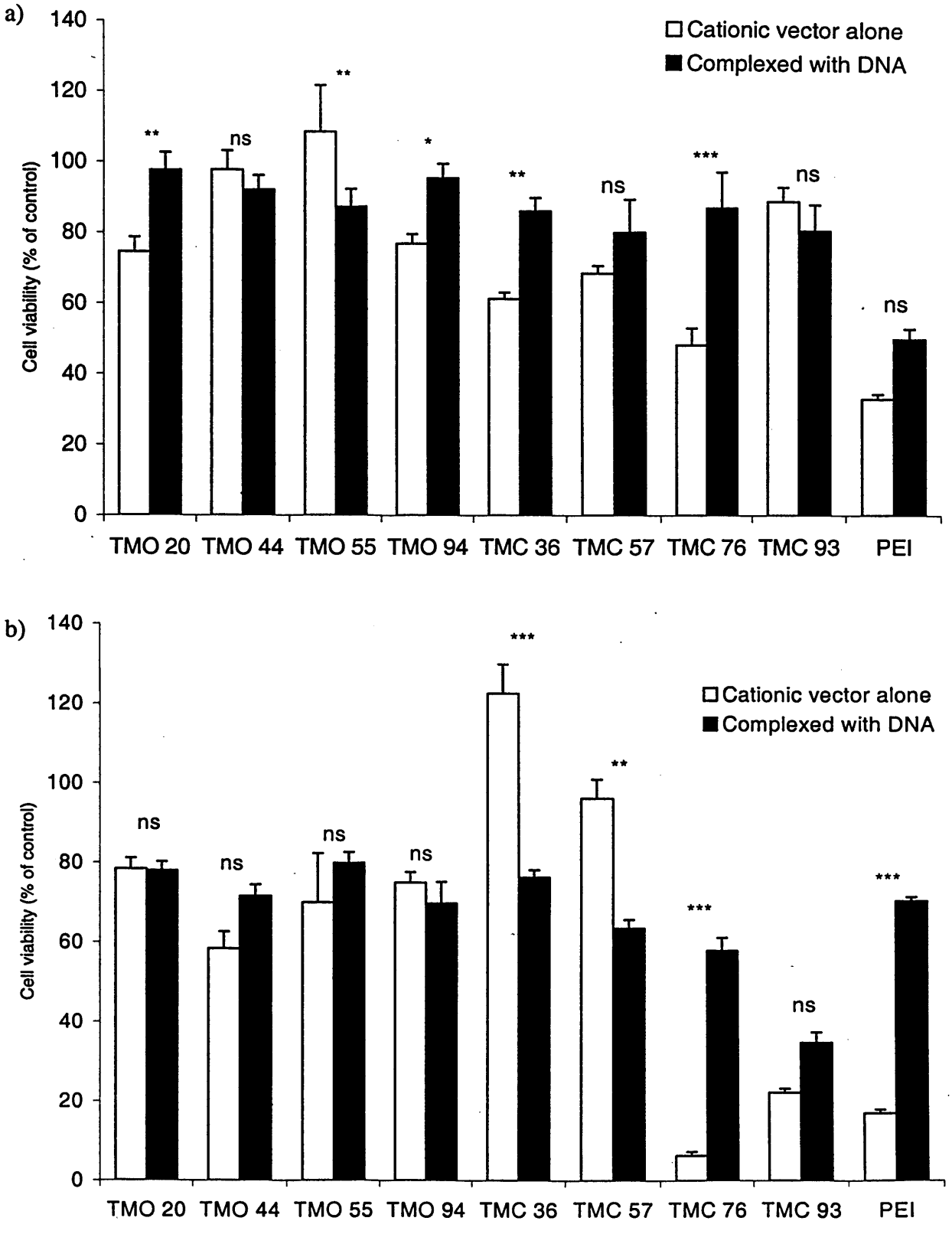

Figure 4.8 – Effect of vector or polyplexes on cell viability

Viability of MCF-7 (a) and COS-7 (b) cells when incubated for 6 h with cationic vector alone (0.1 mg/ml) or their polyplexes with pGL3luc applied at the same concentration as free derivatives (10 :1 w/w derivative : pDNA). Data represent mean (n=6) ± S.E.M. Statistical differences between polyplexes and vector alone are reported as : * $p < 0.05$, ** $p < 0.01$, *** $p < 0.001$, ns = no significant difference; $p > 0.05$ (repeated measures ANOVA with Bonferroni post hoc test)

All derivatives were able to form polyplexes at a 10:1 ratio (w/w chitosan derivative : pDNA), evidenced by the prevention of migration under electrophoretic conditions (Fig. 4.9). These results indicate that in an aqueous environment, such as cell culture medium, the quaternised chitosan derivatives are able to condense pDNA. The extent of pDNA condensation was similar to that observed for PEI used to form polyplexes at the same polymer : plasmid ratio (Fig. 4.9).

4.3.4 Transfection of COS-7 and MCF-7 Cells Using Chitosan Derivatives

The pGL3 luc containing polyplexes formed with both TMO and TMC derivatives produced appreciable transfection in both COS-7 (Fig. 4.10a) and MCF-7 (Fig. 4.10b) cells. Maximum transfection efficiency was observed using the TMO derivative having a 44 % DTM in both cell lines. In contrast, the transfection efficiency of TMC containing polyplexes had a biphasic effect in relation to the DTM. There were two optima, corresponding to polyplexes prepared with TMC having a DTM of 57 % and 93 %.

Polyplexes prepared using TMO44 applied to COS-7 cells produced a level of transfection that was 40 % of that seen for PEI-derived polyplexes in COS-7 cells. However, in MCF-7 cells the TMO44 polyplexes produced a 16-fold higher transfection than PEI-derived polyplexes. TMCs with degrees of trimethylation of 57 and 93 % gave 23- and 50-fold increase, respectively, over PEI transfection efficiency in MCF-7 cells.

4.4 Discussion

The quaternised trimethyl chitosan derivatives synthesised in Chapter 3 were studied here to assess the influence of quaternary amine groups on cell viability and transfection efficiency. Through the use of oligomeric and polymeric chitosan the effect of molecular weight was also studied. Increasing trimethylation confers more permanent positive charge to the polymer/oligomer and also extends the pH range over which the polymer/oligomer is soluble. In addition, this effect probably increases the interaction of the chitosan derivative with pDNA thus improving the formulation profile. The latter is thought to be due to the increased solubility of the quaternised amine as well as the permanent positive charge, independent of pH.

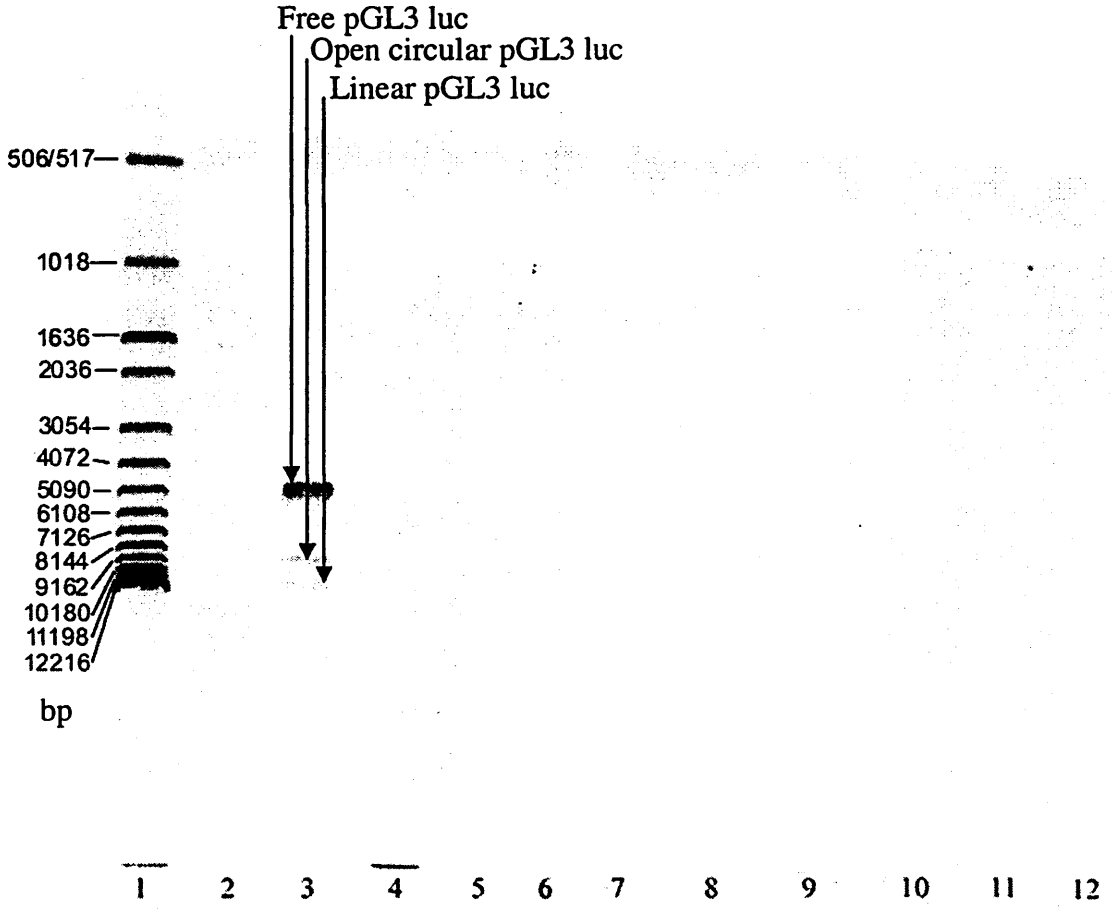

Figure 4.9 – Analysis of polyplexes by agarose gel

Ethidium bromide agarose gel electrophoresis of complex solutions (10:1 w/w derivative : pDNA) applied to cells. Lane: 1) 1kb DNA ladder, 2) Blank (DMEM), 3) pGL3 luc DNA, 4) TMO20/DNA, 5) TMO44/DNA, 6) TMO55/DNA, 7)TMO94/DNA, 8) TMC34/DNA, 9) TMC57/DNA, 10) TMC76/DNA, 11) TMC93/DNA, 12) PEI/DNA. The gel was imaged using a Typhoon 9410 Variable Mode Imager.

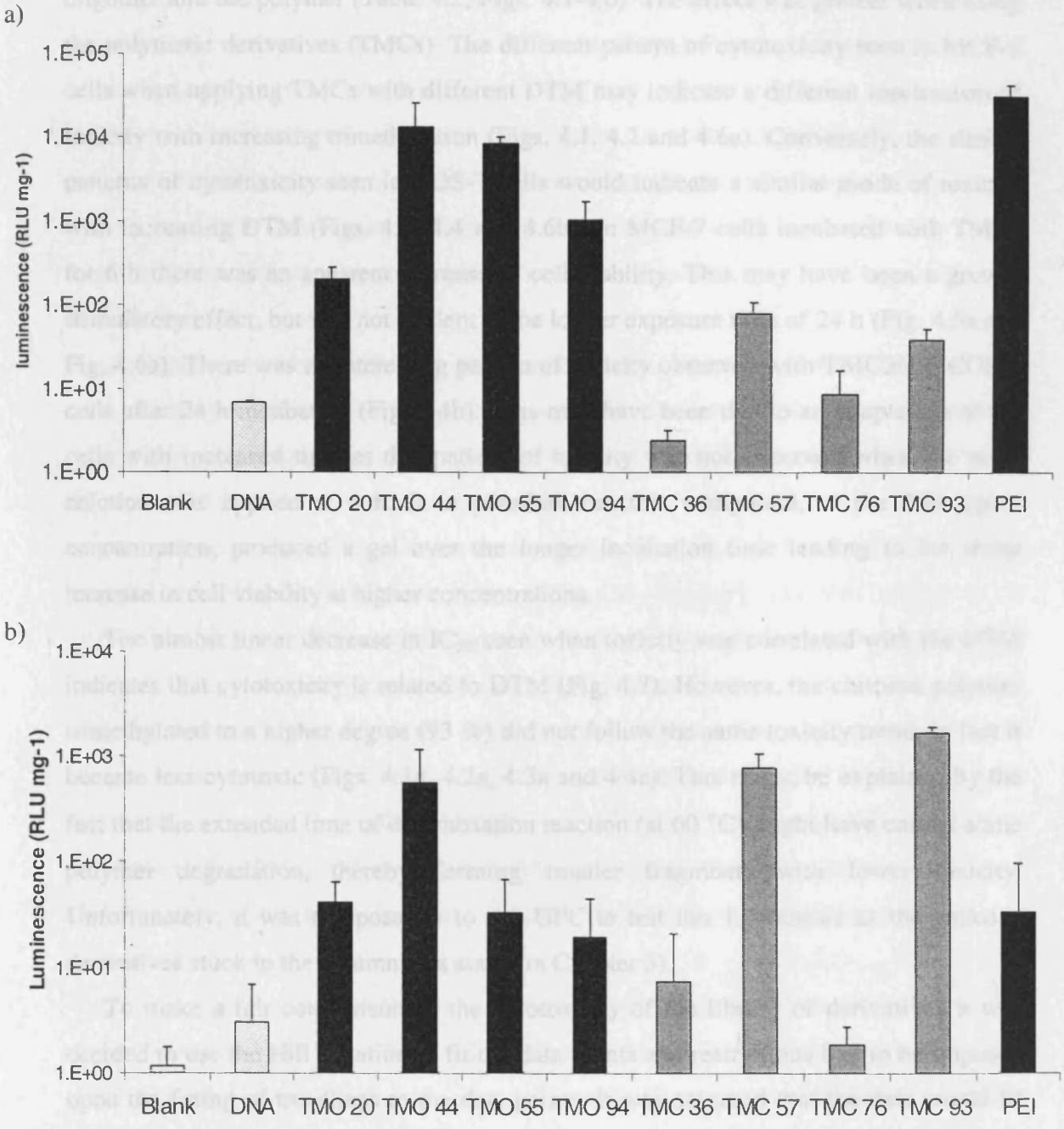

Figure 4.10 – Effect of the DTM of chitosan on transfection efficiency

Transfection efficiencies of chitosan derivatives and PEI in COS-7 (a) and MCF-7 (b) cells. Ratio cationic vector/ DNA 10 :1 (w/w). Average transfection efficiencies are expressed as relative light units (RLU)/ mg protein. Data represent mean (n=4) ± S.D.

It was shown in this study that increasing the DTM increased the toxicity of both the oligomer and the polymer (Table 4.2, Figs. 4.1-4.6). The effect was greater when using the polymeric derivatives (TMCs). The different pattern of cytotoxicity seen in MCF-7 cells when applying TMCs with different DTM may indicate a different mechanism of toxicity with increasing trimethylation (Figs. 4.1, 4.2 and 4.6a). Conversely, the similar patterns of cytotoxicity seen in COS-7 cells would indicate a similar mode of toxicity with increasing DTM (Figs. 4.3, 4.4 and 4.6b). In MCF-7 cells incubated with TMOs for 6 h there was an apparent increase in cell viability. This may have been a growth stimulatory effect, but was not evident at the longer exposure time of 24 h (Fig. 4.5a and Fig. 4.6a). There was an interesting pattern of toxicity observed with TMC36 in COS-7 cells after 24 h incubation (Fig. 4.4b). This may have been due to an adaptation of the cells with increased time as this pattern of toxicity was not observed when the same solution was applied at 6 h. It is possible that this compound, at the 500 μg/ml concentration, produced a gel over the longer incubation time leading to the sharp increase in cell viability at higher concentrations.

The almost linear decrease in IC_{50} seen when toxicity was correlated with the DTM indicates that cytotoxicity is related to DTM (Fig. 4.7). However, the chitosan polymer trimethylated to a higher degree (93 %) did not follow the same toxicity trend, in fact it became less cytotoxic (Figs. 4.1a, 4.2a, 4.3a and 4.4a). This might be explained by the fact that the extended time of derivatisation reaction (at 60 °C) might have caused some polymer degradation, thereby forming smaller fragments with lower toxicity. Unfortunately, it was not possible to use GPC to test this hypothesis as the chitosan derivatives stuck to the columns (as stated in Chapter 3).

To make a fair comparison of the cytotoxicity of the library of derivatives it was decided to use the Hill equation to fit the data points and restrictions had to be imposed upon the fitting of trendlines to the data points. It was assumed that the data would fit between 100 % viability and 0 %. To ensure appropriate curve fits the residual S.D. must be less than 0.1. Therefore, for data indicating lack of toxicity it was not possible to use this method to calculate an IC_{50} value. Further experiments at higher concentrations were not undertaken as it was reasoned that firstly, a concentration of > 10 mg/ml would be much higher than cells would normally be exposed to in gene delivery experiments and secondly, the viscosity of chitosan solutions at higher concentrations increases and this in turn would produce other kinds of effects that

would contribute to the toxicity observed. Ideally it would have been better to study the toxicity of trimethylated chitosan at a larger range of lower concentrations but time did not permit these experiments and it was felt that sufficient data points had been obtained to clearly illustrate the general trends.

In this study chitosan oligomers were shown to be less cytotoxic than chitosan polymers. Clearly illustrating the effect of molecular weight. This is hypothesised to be due to the fewer contact points each individual oligomeric chain can have with the negatively charged membrane or components, as suggested by Katchalsky (1964) for PLL derivatives.

A comparison of the effect on cell viability of the chitosan derivatives alone, and that of their polyplexes gives a greater insight into the complicated issue of toxicity. Application of chitosan derivatives to the cells caused toxicity which was probably due to interaction with the plasma membrane. It was expected that in polyplexes the cationic charge would be partially counter-balanced by the pGL3 luc phosphate negative charges, resulting in a lower toxicity. This was however, not the case with all derivatives (Fig. 4.8). This may be due to the internalisation of the polyplexes (therefore having intracellular interactions with negatively charged components) or because the chitosan derivative conformation in the polyplex is different to that of the unpolyplexed chitosan derivative. This change in conformation promotes more interactions with membrane components (Koping-Hoggard et al., 2003) i.e. because the derivatives have interacted with pDNA to form a polyelectrolyte complex there are a greater number of cationic charges in a single mass, creating multiple contact points upon the cell membrane.

However, this study has shown that toxicity is not a simple issue. Some polyplexes showed increased cytotoxicity whilst others showed decreased cytotoxicity (Fig. 4.8). This may be a temporal phenomenon, with toxic effects appearing later after DNA dissociation has occurred. This effect might be expected to differ between the two cell lines and would certainly differ for the different degrees of chitosan trimethylation. Cherng et al. (1996) also found that polyplexes of pDNA with pDMAEMA were less toxic than the cationic polymer alone, whilst Hill et al. (1999) showed that when a PAA (poly(methylene-bis-acrylamide-2 methyl piperazine); Mw 8.5 kDa) was used to make polyplexes their cytotoxicity increased. Overall, these studies show that the chitosan derivatives studied here are relatively non-toxic when compared with PEI, the most popular 'gold standard' (Merdan et al., 2002) cationic polymer used to mediate

transfection (Table 4.2). If the cytotoxicity of the chitosan derivatives studied here is related to the comparative study of Fischer et al. (2003), the TMOs having a DTM of up to 44 % displayed IC_{50} values of > 10 mg/ml would be equivalent to human serum albumin in terms of toxicity (IC_{50} > 10 mg/ml) i.e. they are equivalent to the least toxic compound tested by Fischer et al. (2003). Even the most toxic TMO with DTM of 94 % (24 h; IC_{50} ~0.4 mg/ml) would be ranked less toxic than PVPBr (24 h; IC_{50} = 246 μg/ml).

Increasing the time of exposure to chitosan derivative decreased cell viability in both cell lines at all the DTM where toxicity was apparent. This effect was even more evident with PEI, which even at 20 μg/ml was highly toxic after a 24 h incubation with both cell lines. This may be due to the internalisation of the polycation thereby causing intracellular effects in addition to the initial plasma membrane effect. It is noteworthy that most of the oligomeric chitosan derivatives were still not toxic over the longer exposure period (Table 4.2). This is in agreement with Richardson et al. (1999b) who studied chitosan oligomers over 72 h. In the comparison of the cytotoxicity of polyplexes with that of the derivative alone it is expected that decreased cytotoxicity would be found with oligomer derivatives due to the increased ability of the cell to expel the dissociated (from pDNA) oligomer more easily than the polymer.

The trimethyl chitosan derivatives used in these studies were initially chosen as it had been shown in earlier experiments that they outperform native chitosan in gene transfection studies in COS-1 and Caco-2 cells (Thanou et al., 2002). From gel electrophoresis studies performed here it was shown that all the chitosan derivatives were able to complex pDNA at the polymer : pGL3 luc ratio studied (10:1) and prevent its migration through an agarose gel (Fig. 4.9). Further analysis by agarose gel and photon correlation spectroscopy (PCS) of polyplexes is described in Chapter 6.

The breast cancer epithelial cell line, MCF-7, used in these studies was shown to be transfected effectively (Fig. 4.8). These novel data indicate that MCF-7 breast cancer cells can be transfected using a non-viral vector such as trimethylated chitosans. However, not all derivatives were able to deliver pGL3 luc efficiently (Fig. 4.10). The TMO44, TMC57 and TMC93 derivatives gave the best delivery in MCF-7 cells and in all cases transfection efficiency surpassed that seen using PEI. The results seen in COS-7 cells were rather different. In this case all the TMO derivatives produced

substantial transfection. The TMC57 and TMC93 derivatives gave transfection efficiencies that were 11- and 5-fold, respectively, higher than that seen for the pGL3 luc alone in COS-7 cells (Fig. 4.10). A bell shaped curve was seen for transfection efficiency in both cell lines (Fig. 4.10) and the optimum transfection was observed using TMO with a DTM of 44 % (Fig. 4.10). This observation is in good agreement with studies involving chitosans where the optimum polyplexes were made at the chitosan pKa of 6.2-6.5 (Sato et al., 2001). This is particularly encouraging as this TMO derivative showed little or no toxicity in both cell lines (Table 4.2). When Hill et al. (1999) studied linear PAA transfection and toxicity, they found that only the PAAs (poly(methylene-bis-acrylamide-2 methyl piperazine) and poly(methylene-bis-acrylamide-dimethyl ethylenediamine)) were able to mediate transfection. However, both PAAs displayed greater toxicity than that seen for TMO44 (Hill et al., 1999). In a comparison of relative transfection efficiency the PAA ISA23 (poly(2-methylpiperazine) 2,2'-bis(acrylamido)-acetic acid) gave similar transfection efficiency to PEI in Hep G2 cells (Richardson et al., 2001).

Although higher transfection efficiency of MCF-7 cells with TMO44, TMC57 and TMC93 derivatives was seen, the transfection seen here with chitosan derivatives in COS-7 cells was noticeably lower than that obtained using PEI (Fig. 4.10). PEI was slightly more toxic in MCF-7 cells than in COS-7 cells (Table 4.2), which could be an explanation for the disparity in the relative efficiencies of the derivatives to PEI between cell lines.

It should be noted that in this study only one ratio of derivative : DNA was considered. This approach was seen as the foundation to allow fair comparison of toxicity and transfection efficiency across the library of cationic vectors. However, this approach does have limitations. In the transfection studies some of the vectors might be more efficient at a different polymer : pGL3 luc ratio. In the case of the linear PEI (marketed as Ex-Gen 500) the suggested starting ratio for use is 6:1 (N : P) and that this can be improved with study optimisation for each cell type (Elmadbouh et al., 2004, Gebhart & Kabanov, 2001). This study has more than a 10-fold higher ratio to create PEI polyplexes. However, it should be noted that the PEI used here was less efficient than Ex-Gen 500 and previous experiments in our labs showed that the PEI : pGL3 luc ratio used transfected cells consistently. Whereas higher w/w ratios of the chitosan derivatives : pGL3 luc gave better transfection in many cases, transfection with PEI-

derived polyplexes would have been abolished at the same w/w ratio. Therefore, a compromise of a ratio of 10:1 polymer : pGL3 luc w/w was chosen for this study.

It has long been known that there are many factors that govern cationic polymer transfection efficiency and the effect of cationic polymers on cell viability. These studies confirm the complexities of these effects and shed some further light on the questions:

1) Does the size, oligomer or polymer, influence toxicity and transfection efficiency?

2) Does increasing permanent charge increase toxicity?

3) Does charge have an effect on transfection efficiency?

1) Trimethylated chitosan derivatives seem to have a dependence on molecular weight for both toxicity and transfection efficiency. This finding is in conflict with data presented by Huang et al. (2004) who investigated the cytotoxicity of different molecular weight chitosans using A549 cells. They found that chitosan molecular weight did not affect cell viability (Huang et al., 2004). However, this study was performed at pH 6.2, the molecular weights studied were not less than 100 kDa, the cell line and polymer were different (Huang et al., 2004).

2) Increasing the DTM on the chitosan backbone was seen here to increase the toxicity of the derivatives. However, when compared to other cationic polymers the chitosan derivatives are still less toxic (Fischer et al., 2003).

3) Modifying the permanent cationic charge on the chitosan backbone had an effect on transfection and the optimum DTM appears to be approximately 50 %. The difference between cell lines may prove to be an asset allowing researchers to preferentially transfect desired cell types with appropriate vectors (Fang et al., 2001, Huang et al., 2004, Lee et al., 2001). From this study it appears that new polymeric materials and derivatives need to be tested individually to assess their toxicity and transfection efficiency.

4.5 Conclusions

Trimethylated chitosan derivatives are significantly less cytotoxic than PEI and their effect on the cell viability is dependent on the DTM. Three derivatives, one oligomer (TMO44) and two polymer (TMC57 and TMC93) produce pGL3 luc-containing

complexes that were able to produce higher levels of transfection than PEI in MCF-7 cells.

A degree of quaternisation of 44 % on the oligomeric chitosan backbone gave the optimum derivative for transfection. It was postulated that, due to the results seen here, and the favourable transfection profile of chitosan polyplexes formed at chitosan's pKa approximately 50 % DTM would be the optimum derivative with regards to transfection and cytotoxicity. Therefore a trimethyl chitosan oligomer with 52 % DTM was synthesised for use in all further studies (Chapters 5 and 6).

Before further development of the vector for targeted gene delivery it was first necessary to establish an appropriate model using cells expressing uPAR. These studies are described in the next chapter.

Chapter 5

Characterisation of uPA-Expressing Cell Lines and Use of the Prostate Cancer (DU145) and Leukaemic (U937) Cell Lines to Study the Binding and Uptake of Free and Conjugated u7 and u11 Peptide Constructs

5.1 Introduction

The development of novel, targeted delivery systems requires validated cell models to enable establishment of *in vitro* proof of receptor targeting. To study the proposed uPAR targeted delivery system, cells expressing uPAR had to be identified. The presence of uPAR was investigated by Western Blotting. Cell lines identified positive may be suitable for the subsequent studies on uPAR-targeted gene delivery systems.

As mentioned in Section 1.4, uPAR is reported to be over-expressed in a wide variety of cancers including breast, prostate, colon and in acute myelogenous leukaemia and monocytic leukaemia (Blasi & Carmeliet, 2002, Ramage et al., 2003). The histiocytic lymphoma monocyte cell line (U937) has been widely used to determine the structure and function of uPAR (Abi-Habib et al., 2004, American Diagnostica, 2004, Cubellis et al., 1986, Deng et al., 1996, Muehlenweg et al., 2000, Picone et al., 1989, Quax et al., 1998, Rajagopal & Kreitman, 2000, Ramage et al., 2003, Schmiedeberg et al., 2002, Wang et al., 1994).

For these studies it was considered important to identify cell lines that could be used as models for breast and prostate cancer. MCF-7 cells are known to express uPAR (Rajagopal & Kreitman, 2000). They studied the binding of ^{125}I-labelled ATF-PE38 (a fusion protein between the amino terminal fragment of uPA and a truncated pseudomonas exotoxin which is cytotoxic) in these cells. They found that MCF-7 cells have $4.6 \times 10^3 \pm 4.3 \times 10^2$ binding sites/cell and consequently the fusion protein was highly toxic (low IC_{50} value) (Rajagopal & Kreitman, 2000). In contrast, LNCaP (prostate cancer) were shown to have low uPAR expression leading to poor cell killing by the fusion protein (Rajagopal & Kreitman, 2000). This particular study led to the procurement of MCF-7 and other breast and prostate cancer cell lines used by Tenovus Cancer Research (Cardiff) for this study. In total, twelve cell lines were tested for the expression of uPAR. These included resistant MCF-7 cell lines developed by Tenovus Cancer Research which have been shown to be more invasive than the wild type MCF-7 cell line (Hiscox et al., 2005) with the theory that the increased invasiveness may be related to uPAR expression.

Western blot analysis is commonly used as a technique (Ausubel et al., 1994) to detect protein expression in a cell. This led to the choice of this technique as the primary test for the characterisation and selection of cell lines expressing the receptor. Several monoclonal and polyclonal antibodies are available that detect uPAR (American

Diagnostica, 2004). The polyclonal rabbit α-uPAR antibody (399R; American Diagnostica) was selected as it has been widely used to detect uPAR (Stahl & Mueller, 1994, Wang et al., 1994). Although Western Blotting gives an indication of the level of a specific protein within a cell, it does not discriminate between the location or functional activity of the protein.

Ligand-receptor interactions are best studied using competition or displacement assays. First it was necessary to assess the binding and affinity of the peptides u7 and u11, proposed as potential ligands to target TMO polyplexes. To do this, a competition assay using fluorescent uPA (uPA-FITC) available commercially (American Diagnostica) was developed. The displacement assays described here examined the ability of peptide ligands to displace uPA-FITC from uPAR on U937 and DU145 cells (Rang et al., 1996). Having studied peptide binding to uPAR it was important to assess whether the peptide-PEG conjugates still showed affinity for the receptor. Again displacement assays using uPA-FITC were used. As chemical conjugation may affect the binding site of the ligand (e.g. steric hindrance) such studies are important.

The conjugation of PEG to proteins and peptides has been widely used to increase their residence time in the body and increase stability (Reviewed in Harris et al., 2001, Roberts et al., 2002, Veronese et al., 1985). In non-viral gene delivery systems PEG conjugation has been studied as both a 'stealth' technique (i.e. to prolong circulation time and reduce RE uptake), and to reduce the toxicity of cationic vectors (Kursa et al., 2003, Merdan et al., 2003, Ogris et al., 2003). Here, the aim was to investigate the effect of conjugation of a polymer on the binding of peptides derived from the binding region of uPA, without the additional confounding effect of non-specific binding due to cationic charge (i.e. that found in trimethylated chitosan). The mono-functional properties of mPEG make it an interesting polymer for study as it should produce conjugates containing one peptide : one PEG, with the peptide at the end of the polymer. It was also considered that peptide-PEG-TMO conjugates may be made later using hetero-bi-functional PEG to space the peptide away from the polyplex, thus enabling a better binding of the peptide to the receptor.

As the ultimate goal of this project was to increase the uptake of a non-viral gene delivery system through receptor-mediated endocytosis, it was considered essential to develop a method to assess the endocytic uptake of the peptide-CMTMO in cells

expressing uPAR. Fluorescently labelled conjugates were prepared for this purpose and their synthesis and characterisation has already been described in Chapter 3. Cellular uptake was monitored using flow cytometry and fluorescent microscopy.

Fluorescein and Oregon Green were used in these studies as fluorescent labels. Fluorescein is a relatively cheap, commonly used fluorophore with high fluorescent output and the excitation/emission wavelengths are suitable for use with most instruments. It has the disadvantage that is reported to be highly pH sensitive, showing marked quenching at acidic pH (Geisow et al., 1981). Oregon Green has a similar high output with compatible excitation/emission wavelengths, but this probe is less pH-sensitive (Delmotte & Delmas, 1999). A disadvantage of this probe is that it is more expensive.

To summarise, the aims of the studies presented in this Chapter were:

- To define cell lines expressing uPAR
- Develop *in vitro* models for the assessment of potential ligands for the receptor.
- To establish uPAR binding of u7, u11 and their PEG conjugates
- To assess the cellular interaction (at 4 °C and 37 °C) of u7 and u11 CMTMO conjugates in cell lines which express uPAR

5.2 Methods

To investigate the levels of uPAR, Western blotting was performed on a panel of cell lines: Caco-2 (human colon carcinoma), COS-1 (African green monkey kidney fibroblast), COS-7 (COS-1 transformed with SV40), DU145 (human prostate epithelial carcinoma), MCF-7 (human breast epithelial carcinoma), MCF-7 S+t (MCF-7 cells resistant to tamoxifen), MCF-7 DR (MCF-7 resistant to both tamoxifen and gefitinib), PC3 (human epithelial prostate carcinoma), T47D wt (human breast epithelial carcinoma tumour wild type), T47D TR (T47D resistant to tamoxifen), U937 (human leukaemia histiocytic lymphoma monocyte) and U937 PMA (U937 stimulated with PMA to become macrophage like). The production of cell lysates and Western blotting was conducted as described in Chapter 2 (Section 2.3.9).

The fluorescent chitosan derivatives were synthesised and characterised as described in Chapter 3. The chitosan compounds used in the studies described here are listed in Table 5.1.

Table 5.1 – The fluorescent chitosan derivatives and their peptide conjugates

Label	Description
Oligo-9-anthraldehyde	Chitosan oligomer labelled with 9-anthraldehyde
Chitosan-9-anthraldehyde	Chitosan polymer labelled with 9-anthraldehyde
TMO-9-anthraldehyde	Trimethylated chitosan oligomer labelled with 9-anthraldehyde
TMC-9-anthraldehyde	Trimethylated chitosan polymer labelled with 9-anthraldehyde
CMTMO-FAM	5/6-carboxyfluorescein modified (1.7 % FAM) CMTMO, 51.8 % DTM, 30 % CM
U7-CMTMO-FAM	~1 % u7 peptide conjugated to 5/6-carboxyfluorescein modified (0.11 % FAM) CMTMO, 51.8 % DTM 30 % CM
U11-CMTMO-FAM	1-3 % Gu11G peptide conjugated to 5/6-carboxyfluorescein modified (0.19 % FAM) CMTMO, 51.8 % DTM 30 % CM
CMTMO-OG	CMTMO (DTM 29.4 %, 15 % CM) labelled with Oregon Green (0.53 % OG)
U11-CMTMO-OG	~1 % Gu11G conjugated to CMTMO (DTM 29.4 %, 15 % CM) labelled with Oregon Green (% OG not determined)

5.2.1 Effect of pH and Concentration on FAM, OG and FITC Fluorescence

As it is important to interpret cellular uptake data, the effect of pH and concentration on FAM, OG and FITC fluorescent output was assessed. Potassium phosphate buffers of pH 7.4, 6.4 and 5.5 were used to model the extracellular, endosomal and lysosomal pH respectively. These buffers were prepared by adjusting the pH of a 0.1 M solution of KH_2PO_4 (25 ml) with NaOH (0.1 M) and making to 100 ml with ddH_2O (giving 0.05 M solutions).

The fluorophores FAM (6.6 μM), OG (2.3 μM) and FITC (257 μM) were dissolved/diluted in ddH_2O. Fluorophore solutions of increasing concentration were prepared in the buffers in triplicate and pipetted (100 μl) into a black 96 well plate which was read in the fluorescent plate reader. Data is expressed as the mean (n = 3) ± SD.

5.2.2 Synthesis and Characterisation of Activated mPEG

In order to synthesise peptide-PEG conjugates it was first necessary to activate mPEG (CH_3-O-[CH_2-CH_2-O-]$_n$$CH_2$-$CH_2$-OH). Two methods were assessed for this activation; a succinimidyl carbonate (Hermanson, 1996) and a *p*-nitrophenol chloroformate method (Veronese et al., 1985). These techniques are described below.

5.2.2.1 Synthesis and Characterisation of SC-mPEG

mPEG (Mw 5000 Da, Fluka) was reacted with N,N'-disuccinimidyl carbonate (DSC) to produce an activated mPEG (Fig. 5.1). mPEG (1 mMole) was dissolved in dry dioxane, DSC (6 mMole) and 4-(dimethylamino)pyridine (DMAP; 6 mMole) were dissolved in dry acetone (adapted from Hermanson, 1996). The mPEG and DSC were then mixed at r.t. (1 min), and DMAP was added slowly to catalyse the reaction. The reaction was allowed to proceed for 6 h and the product was precipitated by diethyl ether (5-10 volumes). To purify the succinimidyl carbonate mPEG (SC-mPEG) the precipitated product was re-dissolved in acetone (5 ml) and again precipitated with diethyl ether (5-10 volumes) twice. The product was then dried under vacuum at r.t., and stored at 4 °C. To further purify the product the SC-mPEG (0.3 g) was dissolved in MeOH (2 ml) and chromatography performed using a Sephadex LH-20 column eluted in MeOH.

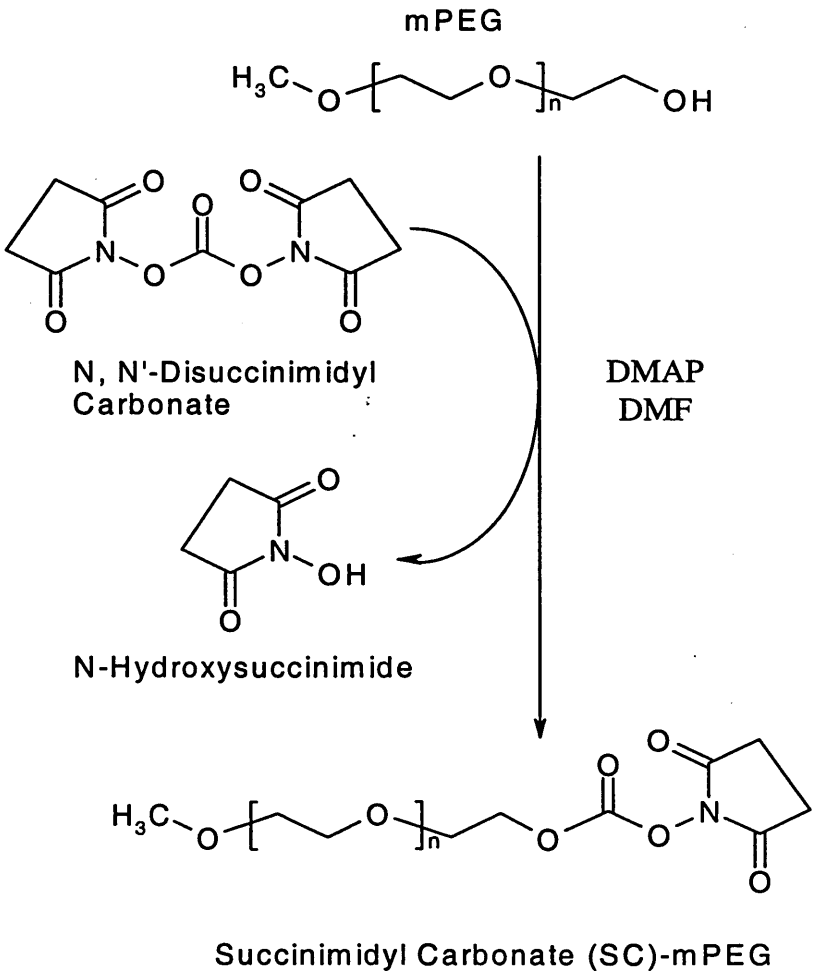

Figure 5.1 – Production of an activated mPEG using disuccinimidyl carbonate

mPEG was modified using the reaction depicted here over 6 h to produce an activated succinimidyl carbonate PEG (SC-mPEG) (adapted from Hermanson, 1996)

The eluted fractions (5 ml) were collected and analysed by TLC (K6 silica gel TLC plate, mobile phase = acetonitrile : water (80:20 v/v)). After the solvent front had travelled at least 6 cm the plate was removed from the tank and dried in the fume hood. The plate was then dipped in phosphomolybdic acid containing K_2CrO_4 and dried. The spots observed, due to oxidation, showed those fractions that contained SC-mPEG. The SC-mPEG product was characterised using GPC and ^{1}H NMR.

5.2.2.2 Synthesis and Characterisation of PNP-mPEG

A second method was also studied as a means to activate mPEG. This used *p*-nitrophenol chloroformate (PNP) (Veronese et al., 1985). In this case mPEG (1 mMole) was dissolved in acetonitrile. PNP (3 mMole) and triethylamine (TEA; 3 mMole) were then dissolved in acetonitrile and added to the mPEG solution. This was left to react for 48 h at r.t. (Fig. 5.2). The reaction was stopped by precipitation of the product (PNP-MPEG) with diethyl ether (5-10 volumes). The product was isolated by centrifugation (3000 RCF, 15 min) and the supernatant discarded. To purify the product, the pellet was re-dissolved in acetonitrile and re-precipitated with ether (5-10 volumes) then centrifuged (3000 RCF, 15 min). The supernatant was discarded and the isolated product was dried under vacuum overnight. Analysis of this product by ^{1}H NMR showed unreacted PNP, to remove this the PNP-mPEG (0.3 g) was then dissolved in MeOH and further purified using a Sephadex LH-20 column which was eluted with MeOH. Eluted fractions (10 ml) were collected. As before, fractions were analysed by TLC (K6 (254) TLC plate, mobile phase = acetonitrile : water (80: 20 v/v)). In this case it was possible to visualise PNP (due to its absorbance in UV and therefore quenching of TLC plate fluorescence). Fractions (5-7) showed a spot at the origin (i.e. not due to free PNP which migrated down the plate). These fractions were characterised by UV and ^{1}H NMR spectroscopy and also by organic (THF) GPC to determine the presence of dimers.

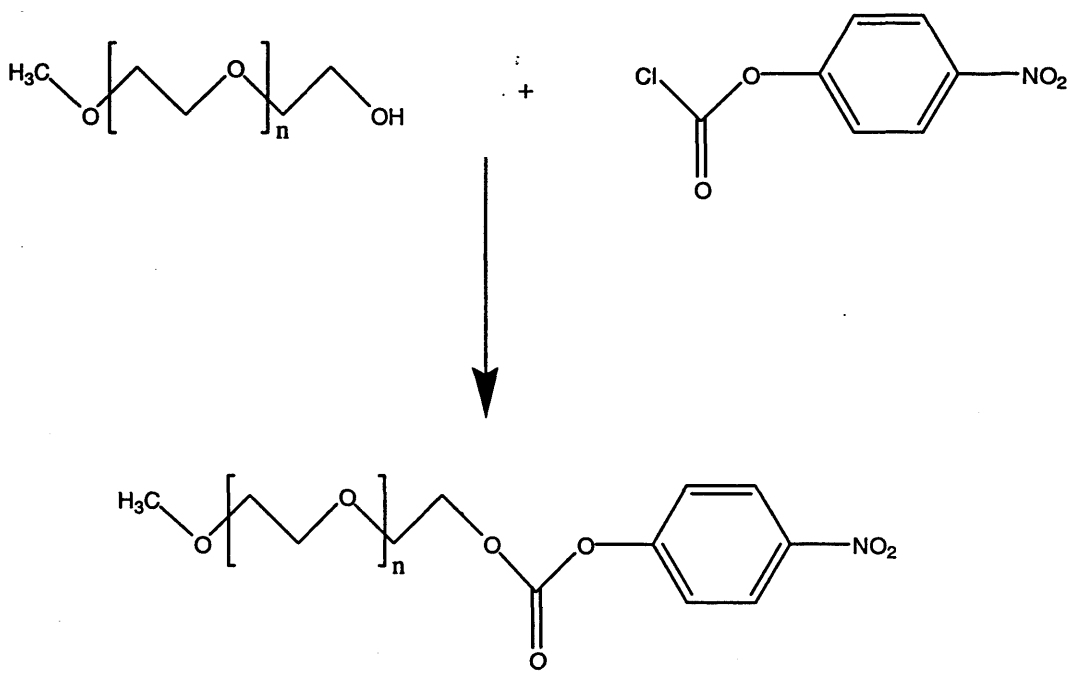

Figure 5.2 – Production of a PNP activated mPEG

Reaction scheme of a PNP with mPEG to produce PNP-mPEG

5.2.3 Reaction of PNP-mPEG with Peptides

Due to the lower dimer content found in PNP-mPEG compared to SC-mPEG, PNP-mPEG was used to prepare peptide-PEGs. Following activation, PNP-mPEG was reacted with peptides (Fig. 5.3) at a 1:5 PNP-mPEG : peptide ratio. To verify that a peptide could be conjugated with PNP-mPEG and to assess the most appropriate solvent for conjugation, the model peptide GlyPheGly (GFG) was dissolved in DMSO or PBS. This peptide solution was added to a similar (DMSO or PBS) solution of PNP-mPEG. The reaction was performed under nitrogen at r.t. for 48 h. The GFG-mPEG derivative prepared in PBS was transferred to a dialysis membrane (2 kDa Mw cut-off) and dialysed against ddH_2O until no UV absorbance (400 nm; due to PNP) could be detected in the dialysate. This product was then lyophilised to constant weight. The GFG-mPEG prepared in DMSO was precipitated with 10 volumes diethyl ether and centrifuged (3000 RCF, 10 min, 4 °C). The supernatant was discarded and the pellet was then washed in diethyl ether/ethanol (10 ml) followed by isolation using centrifugation (3000 RCF, 10 min) twice. The final product was isolated by drying in a rotary evaporator. This product was then re-dissolved in ddH_2O (5 ml) and dialysed as above. The GFG-mPEG products prepared in the different solvents were characterised by ^1H NMR, UV spectroscopy and aqueous GPC.

The peptides u7 and u11 were conjugated in PBS to PNP-MPEG using the method outlined above (Fig. 5.3). They were also purified in the same manner. Additionally, PEG-peptide conjugates were made using NHS-PEG-FAM. This was reacted with Gu11G and Scrambled u11 in a 1:1 reaction. Peptides were dissolved in DMF and added to DMF solutions (10 mg/ml) of NHS-PEG-FAM in round bottom flasks under stirring. The reaction was covered with foil to prevent light and allowed to proceed overnight at room temperature. Precipitation of the product was made with 10 volumes of diethyl ether. The product was isolated by centrifugation (3000 RCF for 10 min) and the supernatant was discarded. The reaction was followed by TLC and the products were characterised by ^1H NMR and aqueous GPC.

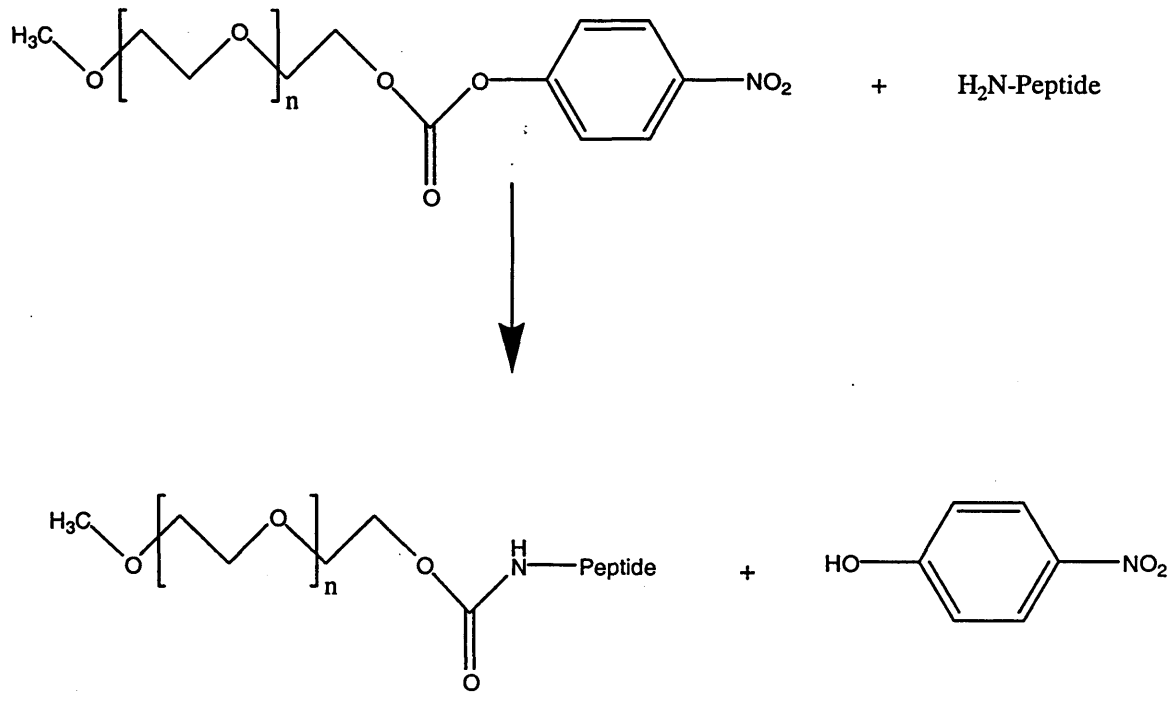

Figure 5.3 - Conjugation of peptides with PNP-mPEG

Reaction of peptides, through their N-terminal amino acid, with PNP-mPEG

5.2.4 Investigation of Ligand-Conjugate Interaction with uPAR Expressing Cells Using Flow Cytometry

5.2.4.1 Flow Cytometric Assessment of the Binding of uPA-FITC

Several preliminary flow cytometry experiments were performed using MCF-7 and DU145. The cells were incubated with uPA-FITC (1.5 - 6 nM) for up to 3 h and cell-associated fluorescence assessed by flow cytometry. However, the shift in cell-associated fluorescence observed was very small. In order to perform accurate displacement assays a higher number of receptors/cell was considered to be necessary. Therefore, the U937 cell line was obtained and used to establish a flow cytometry method which could be used to assess the interaction of the peptides and their conjugates with uPAR.

The preliminary studies with MCF-7, DU145 and U937 cells were performed in collaboration with an MPharm project student, Maria Harvey, whom I supervised. The method used was as follows.

Aqueous solutions were prepared of PBS (pH 7.4), glycine HCl buffer (0.05 M glycine HCl, 0.1 M NaCl, pH 3), HEPES (0.5 M HEPES, 0.1 M NaCl, pH 7.4) and PBS containing 0.1 % w/v bovine serum albumin (BSA). First, U937 cells were removed from the incubator, centrifuged (200 RCF, 5 min, r.t.) and re-suspended in ice cold glycine buffer (10 ml) as an acid wash to remove bound uPA. This was neutralised after a 1 min incubation with ice cold HEPES buffer (10 ml). This cell-suspension was then centrifuged (200 RCF, 5 min, 4 °C) and re-suspended in ice cold PBS/BSA to give a concentration of 2.5 x 10^6 cells/ml and 200 µl were aliquoted in eppendorfs (i.e. 5 x 10^5 cells/eppendorf).

The cells were then incubated with uPA-FITC (6 nM) at 4 °C for 1, 2 or 3 h. At each time point the cells were centrifuged (6000 RCF, 4 °C, 2 min) and the supernatant discarded. The cell pellet was re-suspended in PBS (200 µl) and analysed for uPA-FITC binding by flow cytometry (FACSCalibur flow cytometer) as described in Section 2.3.4.

To study the effect of uPA-FITC concentration on cell binding, cell association was assessed using a concentration range of 0.15-15 nM and an incubation of 1 or 3 h (4 °C). The effect of acid washing (for the removal of bound uPA) on cell-associated fluorescence was compared after a 1 h incubation with uPA-FITC on cells that had been treated with and without acid washes. Finally, cell binding and uptake of uPA-FITC (1.5 nM) was followed at several time points up to 1 h at 4 °C and 37 °C.

5.2.4.2 Displacement of uPA-FITC from U937 Cells by uPA, Peptides and Peptide Conjugates

Having characterised the binding of uPA-FITC to U937 cells it was now possible to conduct displacement/competition experiments to assess the affinity of the potential peptide ligands u7 and u11. Firstly, U937 cells were incubated with uPA-FITC (1.5 nM) in the presence of increasing concentrations of uPA (0.05-80 nM) for 1 h (4 °C). To do this the cells were aliquoted into eppendorfs and the eppendorfs centrifuged (6000 RCF, 4 °C, 2 min). The supernatant was removed and the cells re-suspended in PBS/BSA containing uPA-FITC (1.5 nM) and a range of concentrations of uPA (0.05-80 nM). After 1 h incubation at 4 °C the eppendorfs were centrifuged (6000 RCF, 4 °C, 2 min). The supernatants were discarded and the cell pellets re-suspended in PBS and analysed by flow cytometry.

The ability of the peptides (Gu11G, u7, Scrambled u11 and Scrambled u7) in the concentration range of 1 nM – 1 mM to displace uPA-FITC (1.5 nM) was then assessed using the same method. Following this, the ability of peptide-PEG conjugates to displace uPA-FITC was assessed using the same method. Data are expressed as the averaged geometric mean of 10000 events (unless otherwise stated).

5.2.4.3 Flow Cytometry Assessment of the Binding/Uptake of Fluorescently Labelled Peptide-CMTMO Conjugates by U937 Cells

The cellular binding (4 °C) and uptake (37 °C) of peptide-targeted trimethylated chitosan conjugates labelled with fluorescein (u7-CMTMO-FAM, u11-CMTMO-FAM and CMTMO-FAM as control) was assessed using flow cytometry, first in the U937 cells. U937 cells were prepared as described above (without an acid wash) and the fluorescently labelled conjugates (1 mg/ml or 0.1 mg/ml) incubated with the cells. Their cell-association (4 °C and 37 °C) was assessed at several time points up to 1 h. Subsequently, the cell-association of the u11-CMTMO-OG (0.001 mg/ml – 0.1 mg/ml) conjugate (compared with CMTMO-OG) was also assessed in U937 cells at time points up to 1 h (4 °C and 37 °C).

5.2.4.4 Flow Cytometry Assessment of the Uptake of Fluorescently Labelled Peptide-CMTMO Conjugates by DU145 Cells

Subsequently, preliminary studies were also carried out to determine the binding and uptake of fluorescently labelled peptide-CMTMO conjugates (u7-CMTMO-FAM and u11-CMTMO-FAM) in the prostate cancer cell line, DU145. This work was carried out in collaboration with an MPharm IV student, Helen Pritchett, whom I supervised.

DU145 cells were seeded in 6 well plates (3 x 10^5 cells/well) and were allowed to grow for 24 h. Then, one set of plates was transferred to the fridge (4 °C) for 5 min. Media was removed from the wells of both the 37 °C and 4 °C plates and the cells were washed with DMEM (1 ml; stored at corresponding temperature). Then DMEM containing the fluorescent conjugates (0.1 mg/ml, 1 ml/well at appropriate temperature) was added to each well. The cells were incubated for time periods between 0 and 60 min. At each time point the conjugate containing medium was removed and the cells were washed 3 times in ice cold PBS. The cells were then scraped from the well surface in PBS (1 ml) using a rubber policeman and the resultant cell suspension was transferred to an eppendorf tube with a pipette. All the eppendorfs were centrifuged (6000 RCF, 4 °C, 2 min) and the supernatants discarded. The cell pellets were re-suspended in PBS (200 µl) and analysed by flow cytometry. Due to the lower FAM loading present in u11-CMTMO-FAM and u7-CMTMO-FAM compared with the CMTMO-FAM, CMTMO-FAM was incubated with the cells at a concentration of 1.18 µg/ml i.e. the same FAM concentration. This ensured that an equivalent concentration of FAM was present in the CMTMO-FAM control compared to the peptide-CMTMO-FAM solutions. This allowed a direct comparison of the cell-associated fluorescence. Data are expressed as the mean (n = 2) of the geometric mean of 10000 events.

Studies were also performed to analyse the uptake of u11-CMTMO-OG (0.1 mg/ml) in DU145 cells using the same method as that outlined above.

5.2.5 Epifluorescent Microscopy

5.2.5.1 Visualisation of Trimethylchitosan 9-Anthraldehyde Cell Association and Uptake

The uptake of chitosan and trimethylated chitosan 9-anthraldehyde conjugates by COS-7 cells was visualised using epifluorescent microscopy. These studies were performed in collaboration with an MPharm IV student, Lee Jones, whom I supervised.

COS-7 cells were seeded onto 13 mm diameter coverslips placed in 12 well plates at a seeding density of 1 x 10^5 cells/ml. The cells were allowed to adhere over 24 h. Then the fluorescent derivatives (0.1 mg/ml) were added in DMEM and incubated with the cells for 1 h at 37 °C. Following this incubation, the medium was removed and the cells were washed in PBS three times. The cells were then fixed in paraformaldehyde (3 % in PBS) for 30 min before the coverslips were lifted from the plate. They were then rinsed, first in PBS and then in ddH_2O. The coverslips were then mounted onto slides using

Dako mounting medium and they were sealed with clear nail polish. Duplicate slides were made and stored at 4 °C in the dark before imaging with the fluorescent microscope.

5.2.5.2 Visualisation of u11-CMTMO-FAM and u11-CMTMO-OG

In parallel to the flow cytometry experiments described above, cells were also prepared for epifluorescent microscopy to visualise the intracellular distribution of u11-CMTMO-FAM and u11-CMTMO-OG. The DU145 cells were seeded on glass bottom cell culture dishes (3 x 10^5 cells/well) and allowed to adhere for 24 h. The derivatives were then added in DMEM (0.1 mg/ml) to the cells and incubated for times between up to 1 h. In the case of u11-CMTMO-FAM, a glass bottom culture dish was removed from the incubator at each time point, rinsed three times in 1 ml of warmed (37 °C) PBS then immediately imaged using the fluorescent microscope. Due to the small amount of u11-CMTMO-OG available, a glass bottom culture dish was incubated with u11-CMTMO-OG and cells imaged at several time points up to 1 h whilst still in the conjugate containing media. After 1 h incubation, the medium containing u11-CMTMO-OG was removed and the cells were washed three times with PBS and then imaged again.

5.3 Results

5.3.1 Effect of pH and Concentration on Probe Fluorescence

Both FAM and FITC showed pH-dependent quenching (Fig. 5.4). FAM showed marked fluorescence quenching as pH decreased (Fig. 5.4a). At the highest FAM concentration at pH 5.5 the fluorescence output was 27 % of the value seen for the equivalent concentration at pH 7.4. FITC showed a similar pH-dependent effect with the fluorescence output at pH 5.5 being 30 % of the value seen for the equivalent concentration at pH 7.4 (Fig. 5.4b). OG showed much less quenching due to pH. The fluorescence at pH 5.5 was 89 % of the fluorescence of the equivalent concentration at pH 7.4 (Fig. 5.4c).

The effect of concentration on fluorescent output can be seen in the data plotted for FITC as the fluorescence curve plateaus at higher concentration (Fig. 5.4b). Due to the lower concentrations of the fluorophores (OG and FAM) this is not as evident in these plots.

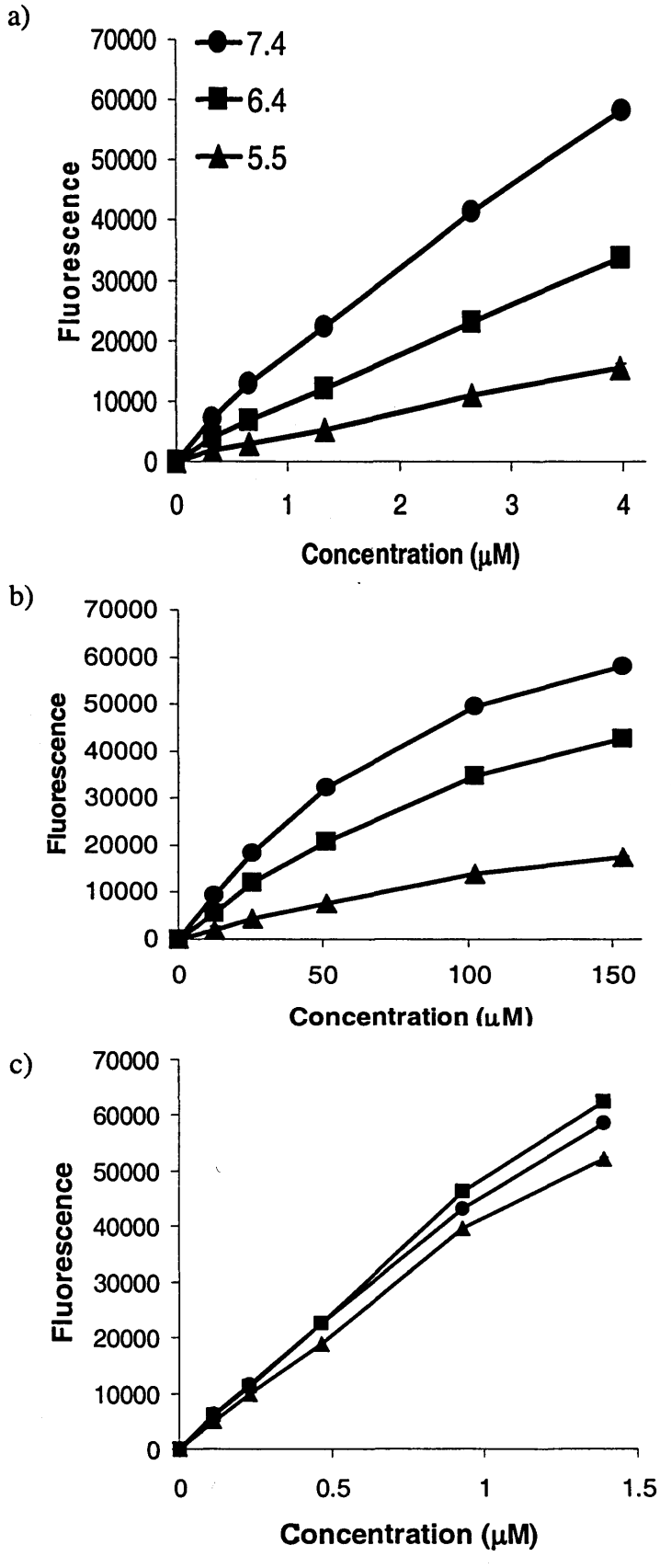

Figure 5.4 – Effect of pH and concentration on probe fluorescence

The effect of pH and concentration on the fluorescence of: a) FAM, b) FITC, c) OG. Data represent mean (n = 3) ± S.D.

5.3.2 Peptide Conjugation to mPEG

The activation of mPEG with DSC was confirmed by ^{1}H NMR (Fig. 5.5). However, mPEG-PEGm dimers were formed in this reaction and were present even after purification chromatography on a Sephadex LH-20 GPC column. This was apparent from the shoulder in the GPC chromatogram shown in Fig. 5.6. The degree of substitution was calculated from the integration of ^{1}H NMR using Equation 5.1 as 47 %. Meaning the activated mPEG would only be able to yield 47 % peptide-mPEG conjugate if the subsequent reaction with peptides was 100 % efficient.

$$\left(\frac{\left[\frac{\int c}{4} \right]}{\left[\frac{\int a}{3} \right]} \right) \times 100 = \% \text{ mPEG activation with DSC} \qquad \text{Equation 5.1}$$

The activation of mPEG with PNP was also successful (Fig. 5.7), and there was less dimer impurity as shown by GPC (Fig. 5.8). The extent of derivatisation was assessed by UV spectroscopy using the equation $A = \varepsilon cl$ with ε being 17500 for PNP at 405 nm (Rotrekl et al., 1999, Veronese et al., 1985). Derivatisation was determined to be 90 %. Due to its greater purity and extent of activation PNP-mPEG was chosen for peptide conjugation. The degree of modification with GFG in PBS was assessed by ^{1}H NMR integration of peaks corresponding to phenol (δ 7.1 – 7.3 ppm) and those corresponding to the methyl end group of mPEG (δ 3.3 ppm) (see Equation 5.2). Conjugation of GFG with PNP-mPEG in PBS gave 62.7 % GFG-mPEG (the remainder being PNP-mPEG or mPEG) whereas reaction in DMSO gave a slightly lower reaction efficiency producing 53.9 % GFG-mPEG.

$$\left(\frac{\left[\frac{\Sigma \int 7.1\text{-}7.3 \text{ ppm}}{5} \right]}{\left[\frac{\int 3.3 \text{ ppm}}{3} \right]} \right) \times 100 = \% \text{ conjugation with PNP-mPEG} \qquad \text{Equation 5.2}$$

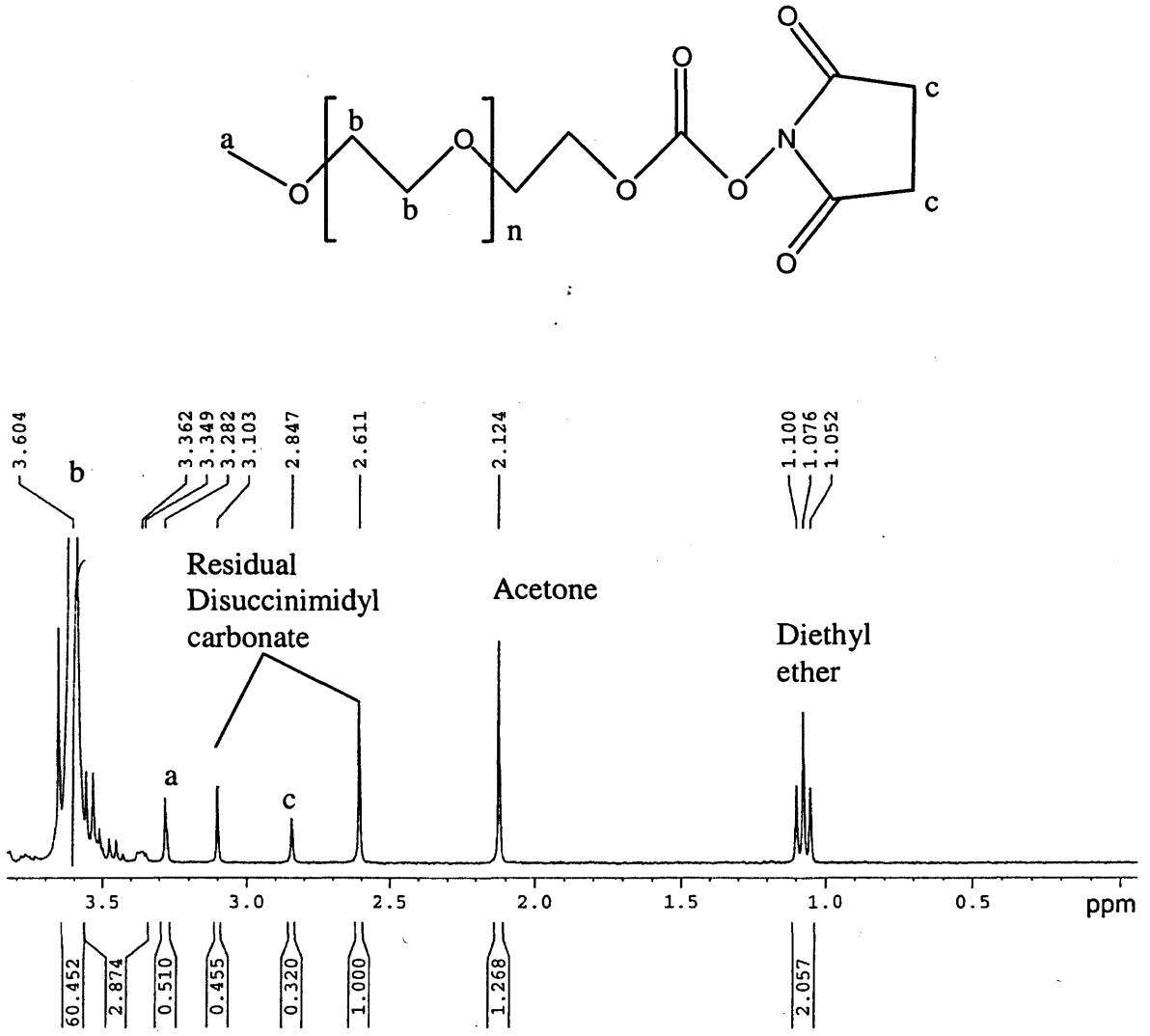

Figure 5.5 – ^{1}H NMR spectra of SC-mPEG

A ^{1}H NMR of SC-PEG showing a = methoxy terminal PEG group at δ 3.35 ppm, c = succinimidyl carbonate activation at δ 2.85 ppm.

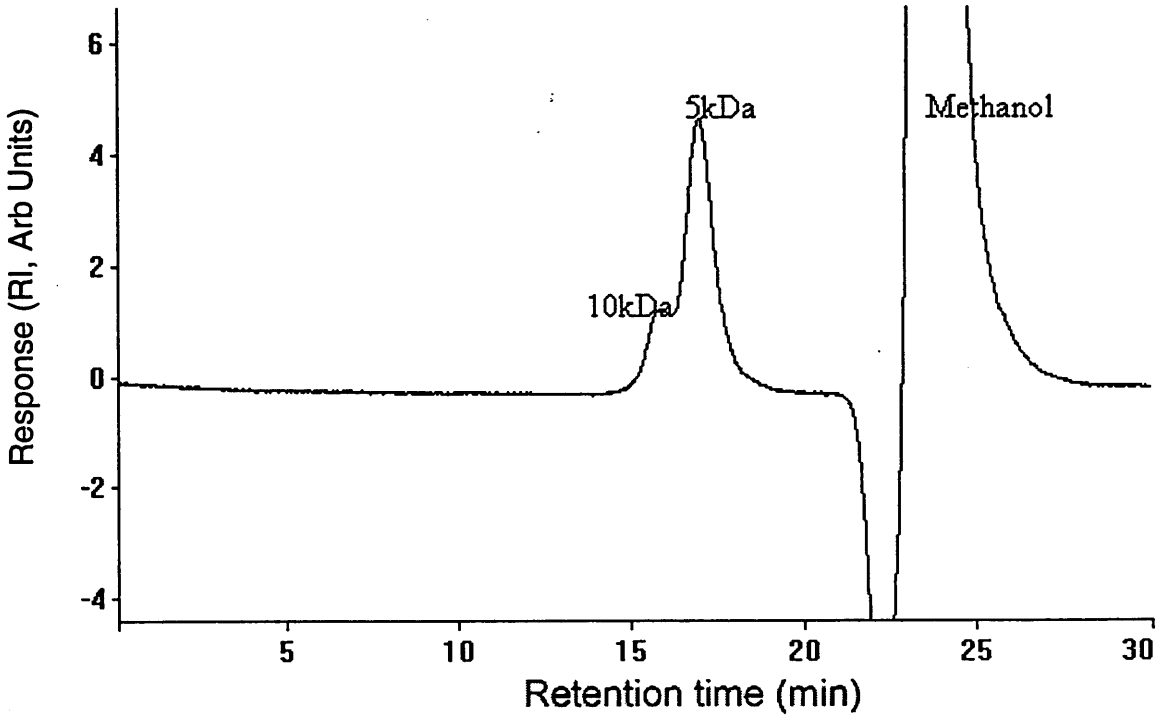

Figure 5.6 – GPC analysis of SC-mPEG

Analysis of SC-mPEG by aqueous GPC (PBS, 1 ml/min, detection by RI) following its separation from small molecules using Sephadex LH-20.

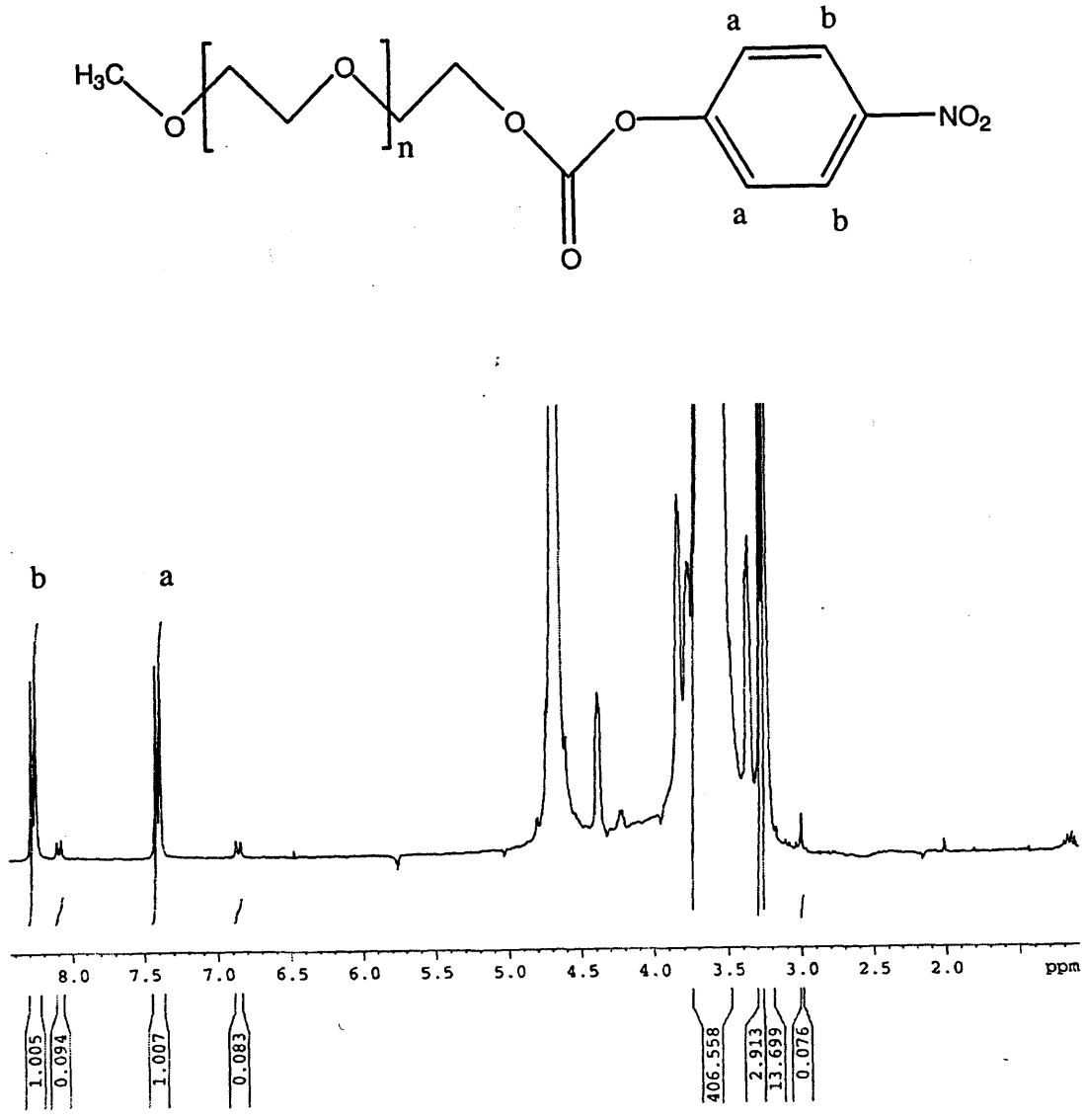

Figure 5.7 – ^{1}H NMR spectra of PNP-mPEG

A ^{1}H NMR spectra of PNP-mPEG showing the introduction of PNP at a) δ 7.4 and b) 8.3 ppm.

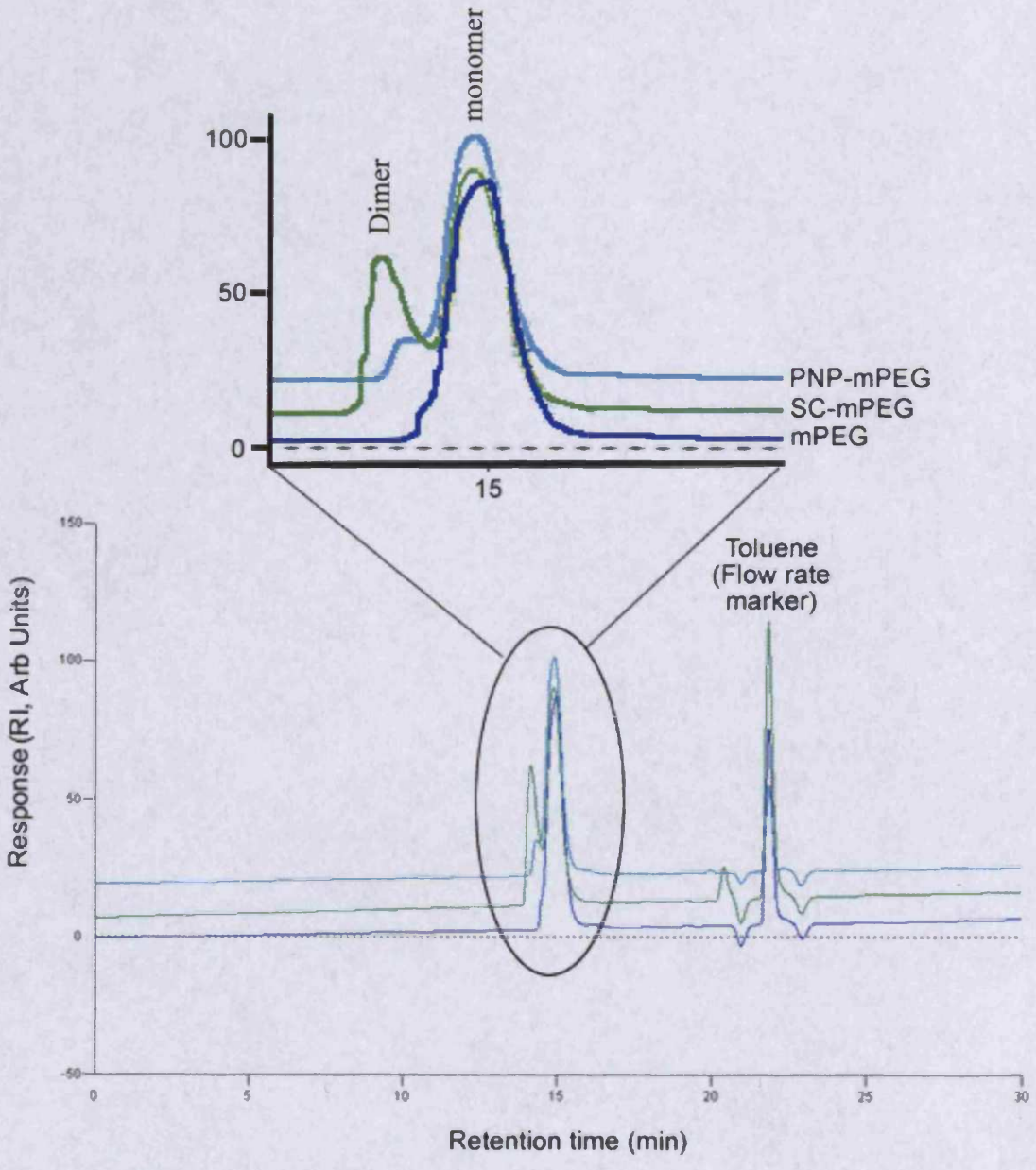

Figure 5.8 – GPC characterisation of mPEGs activated using PNP or DSC

The GPC was run using THF as eluent (1 ml/min) and with RI detection.

The reaction of u7 and u11 with PNP-mPEG yielded 59 % u7-mPEG and 59 % u11-mPEG from integration of ^{1}H NMR, although due to the small quantities produced this is an approximation.

The reaction of NHS-PEG-FAM with Gu11G and Scrambled u11 was successful and the extent of derivatisation was estimated from the integration of ^{1}H NMR (Fig. 5.9). This estimation gave peptide loading values for Gu11G-PEG-FAM of ~75 % and that of Scrambled u11-PEG-FAM was ~93 %. However, as FAM proton signals were not clear this was calculated relative to the PEG backbone signal and is therefore only a rough estimate due to the difference in size between peptide peaks and that of the PEG backbone.

5.3.3 Determination of uPAR Content in a Panel of Cell Lines by Western Blotting

Preliminary Western blot experiments conducted using the polyclonal α-uPAR primary antibody showed the presence of uPAR in COS-7 cells, but not in Caco-2 cells (results not shown). Western blot experiments were conducted using polyclonal α-uPAR, cell lysates of COS-1, COS-7, MCF-7 and Caco-2 cells standardised for protein content were loaded onto the gel in duplicate. uPAR was detected in all cell lines (Fig. 5.10a). A second band was also apparent in this experiment at approximately 40 kDa. In a repeat of this experiment the two bands were again present (Fig. 5.10b). Comparison of uPAR levels in MCF-7, MCF-7 S+t, T47D wt, DU145, T47D TR and MCF-7 DR cells showed greater levels of uPAR in DU145 cells than in any of the other cell lines analysed in this experiment (Fig. 5.11).

After these experiments a monoclonal α-uPAR antibody was purchased (American Diagnostica Product #3937). The binding of this antibody was assessed using PMA-differentiated U937 cells (U937 PMA). When differentiated these cells become macrophage-like adherent cells (Picone et al., 1989). From this experiment it can be seen that at a 1:2000 primary antibody dilution there was less non-specific binding and detection up to 10 μg loaded protein was retained (Fig. 5.12). Using this dilution of primary antibody a series of experiments was performed analysing lysates of U937, U937 PMA, Caco-2, DU145, COS-7, MCF-7, PC-3 and COS-1 cell lines. Initially a concentration of 30 μg protein/lane was applied for all cell lines, uPAR bands were seen most prominently in U937 PMA.

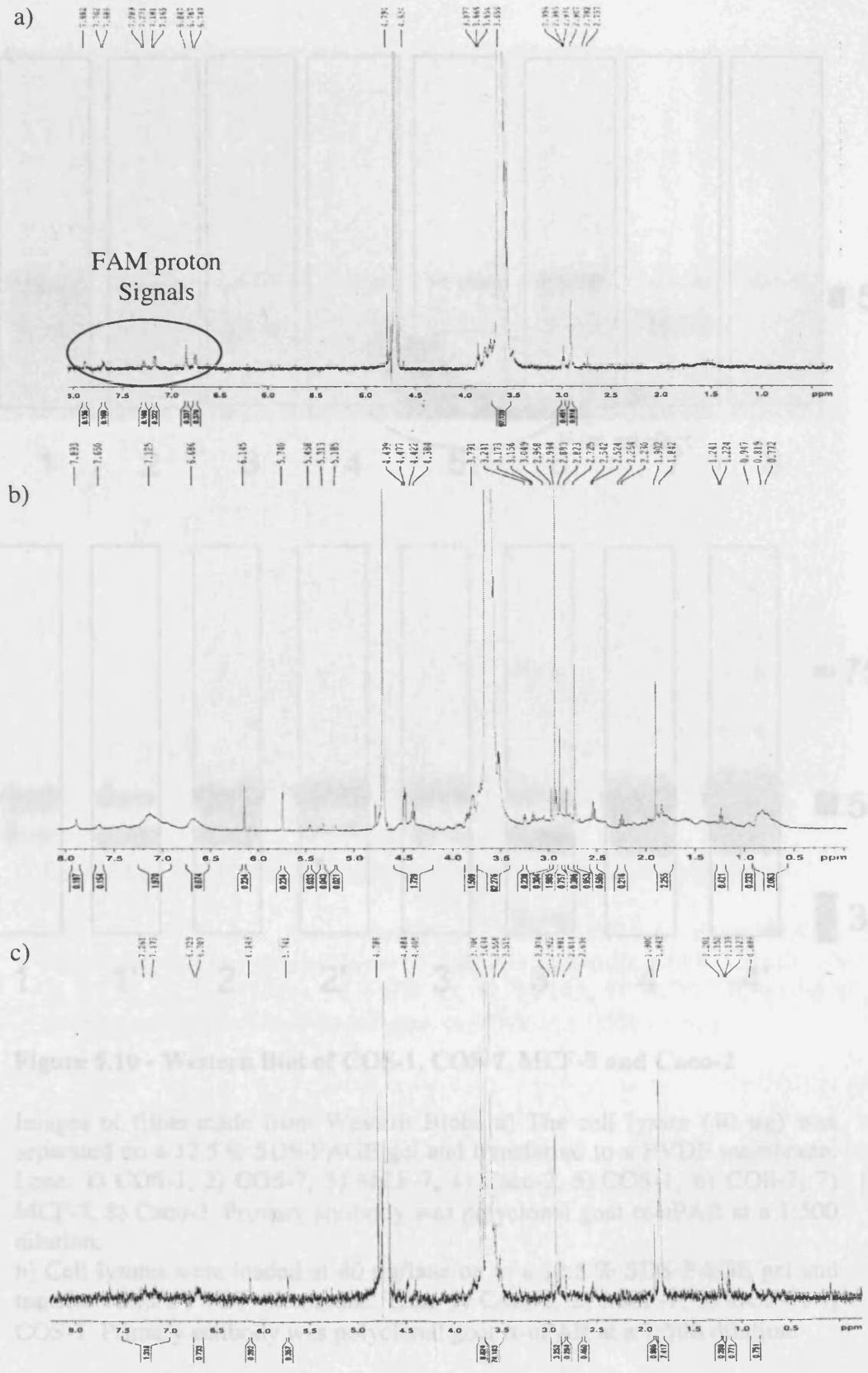

Fig 5.9 - ^{1}H NMR spectra for a) PEG-FAM, b) u11-PEG-FAM and c) Scrambled u11-PEG-FAM

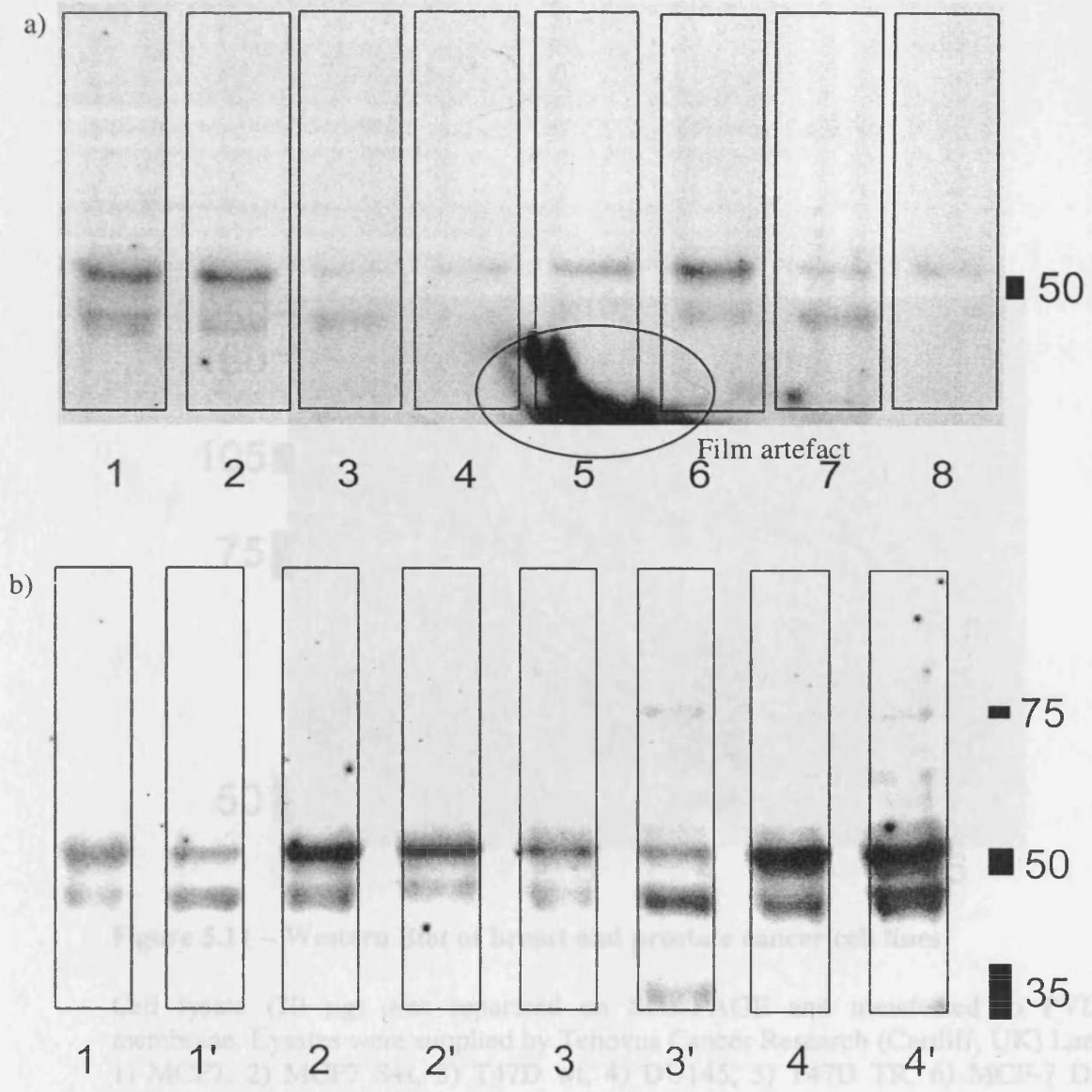

Figure 5.10 - Western Blot of COS-1, COS-7, MCF-7 and Caco-2

Images of films made from Western Blots. a) The cell lysate (40 µg) was separated on a 12.5 % SDS-PAGE gel and transferred to a PVDF membrane. Lane: 1) COS-1, 2) COS-7, 3) MCF-7, 4) Caco-2, 5) COS-1, 6) COS-7, 7) MCF-7, 8) Caco-2. Primary antibody was polyclonal goat α-uPAR at a 1:500 dilution.
b) Cell lysates were loaded at 40 µg/lane on to a 12.5 % SDS-PAGE gel and transferred to a PVDF membrane. Lane 1) Caco-2, 2) MCF-7, 3) COS-7, 4) COS-1. Primary antibody was polyclonal goat α-uPAR at a 1:500 dilution.

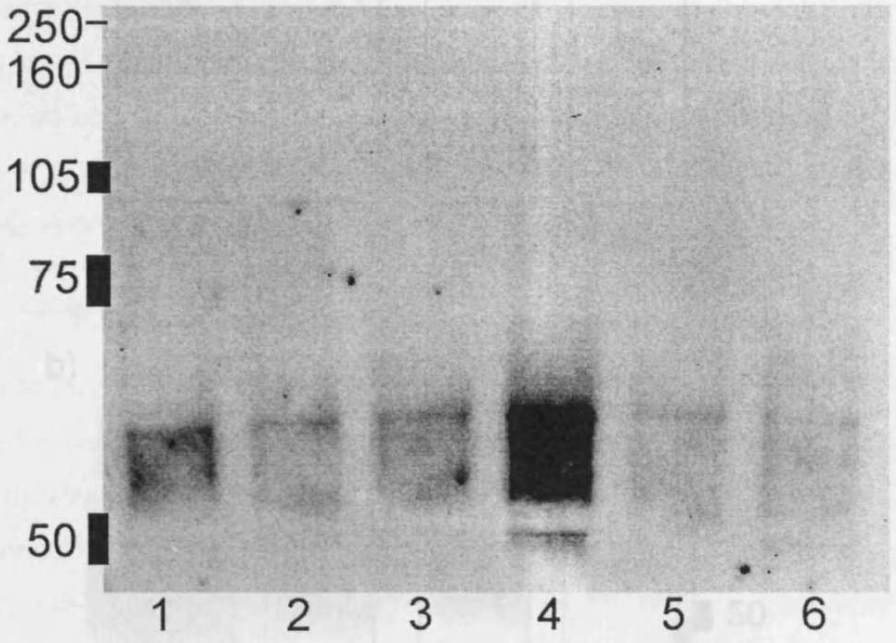

Figure 5.11 – Western Blot of breast and prostate cancer cell lines

Cell lysate (20 μg) was separated on SDS-PAGE and transferred to PVDF membrane. Lysates were supplied by Tenovus Cancer Research (Cardiff, UK) Lane: 1) MCF7, 2) MCF7 S+t, 3) T47D wt, 4) DU145, 5) T47D TR, 6) MCF-7 DR. Primary antibody was polyclonal goat α-uPAR at a 1:500 dilution.

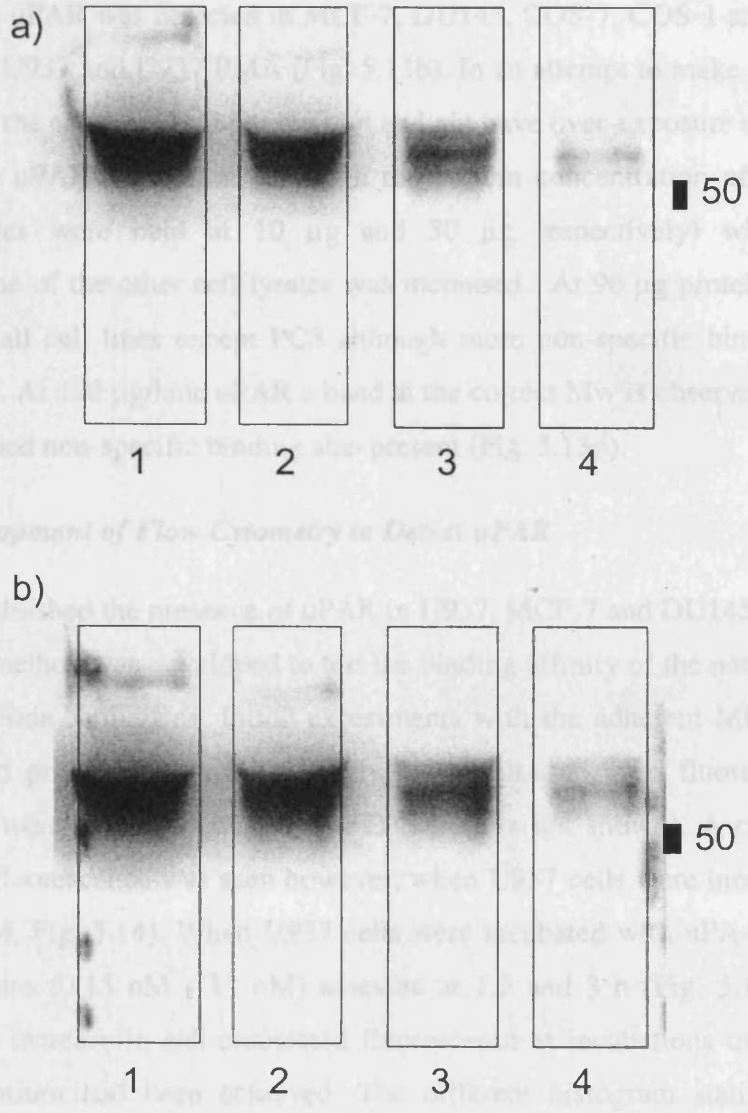

Figure 5.12 – Effect of protein loading and mAb concentration on detection of uPAR in PMA differentiated U937 cells

a) 1:1000 dilution of primary antibody, b) 1:2000 dilution of primary antibody. Lanes: 1) 80 µg protein loaded, 2) 40 µg protein loaded, 3) 20 µg protein loaded, 4) 10 µg protein loaded.

Again there is the possibility of two bands although there is less distinction between them with uPAR being present throughout this molecular weight range (40-55 kDa, Fig. 5.13a). The presence of uPAR was also detected in U937 cells and faintly in MCF-7 cells at this concentration (Fig. 5.13a). At an increased concentration of 60 μg protein/lane uPAR was detected in MCF-7, DU145, COS-7, COS-1 and at an increased intensity in U937 and U937 PMA (Fig. 5.13b). In an attempt to make a fair comparison between all the cell lines in the same blot and not have over-exposure of the film (in cell lines where uPAR expression was high the protein concentration of U937 PMA and U937 lysates were held at 10 μg and 30 μg respectively) whilst the protein concentration of the other cell lysates was increased. At 90 μg protein/lane uPAR can be seen in all cell lines except PC3 although more non-specific binding is occurring (Fig. 5.13c). At 120 μg/lane uPAR a band at the correct Mw is observed in all cell lines, with increased non-specific binding also present (Fig. 5.13d).

5.3.4 Development of Flow Cytometry to Detect uPAR

Having established the presence of uPAR in U937, MCF-7 and DU145 cell lines, a flow cytometry method was developed to test the binding affinity of the natural ligand (uPA) and the peptide-conjugates. Initial experiments with the adherent MCF-7 and DU145 cells proved problematic and little increase in cell-associated fluorescence was seen when they were incubated with uPA-FITC (results not shown). A clear shift in cell-associated fluorescence was seen however, when U937 cells were incubated with uPA-FITC (6 nM, Fig. 5.14). When U937 cells were incubated with uPA-FITC at different concentrations (0.15 nM - 15 nM) assessed at 1,2 and 3 h (Fig. 5.15), there was no appreciable increase in cell-associated fluorescence at incubations over 1 h indicating that equilibrium had been achieved. The different histogram statistics reported by CellQuest© software (mean, geometric mean and median) were compared and a similar trend was observed (Fig. 5.15a). From these, the geometric mean was chosen as the most appropriate statistic and all subsequent data is reported using this statistic. This choice is due to both the log plot of FL1 in flow cytometry experiments and the normal distribution of the histogram (Fig. 5.14).

A plateau of the cell-associated fluorescence was seen as the concentration of uPA-FITC increased (Fig. 5.15b).

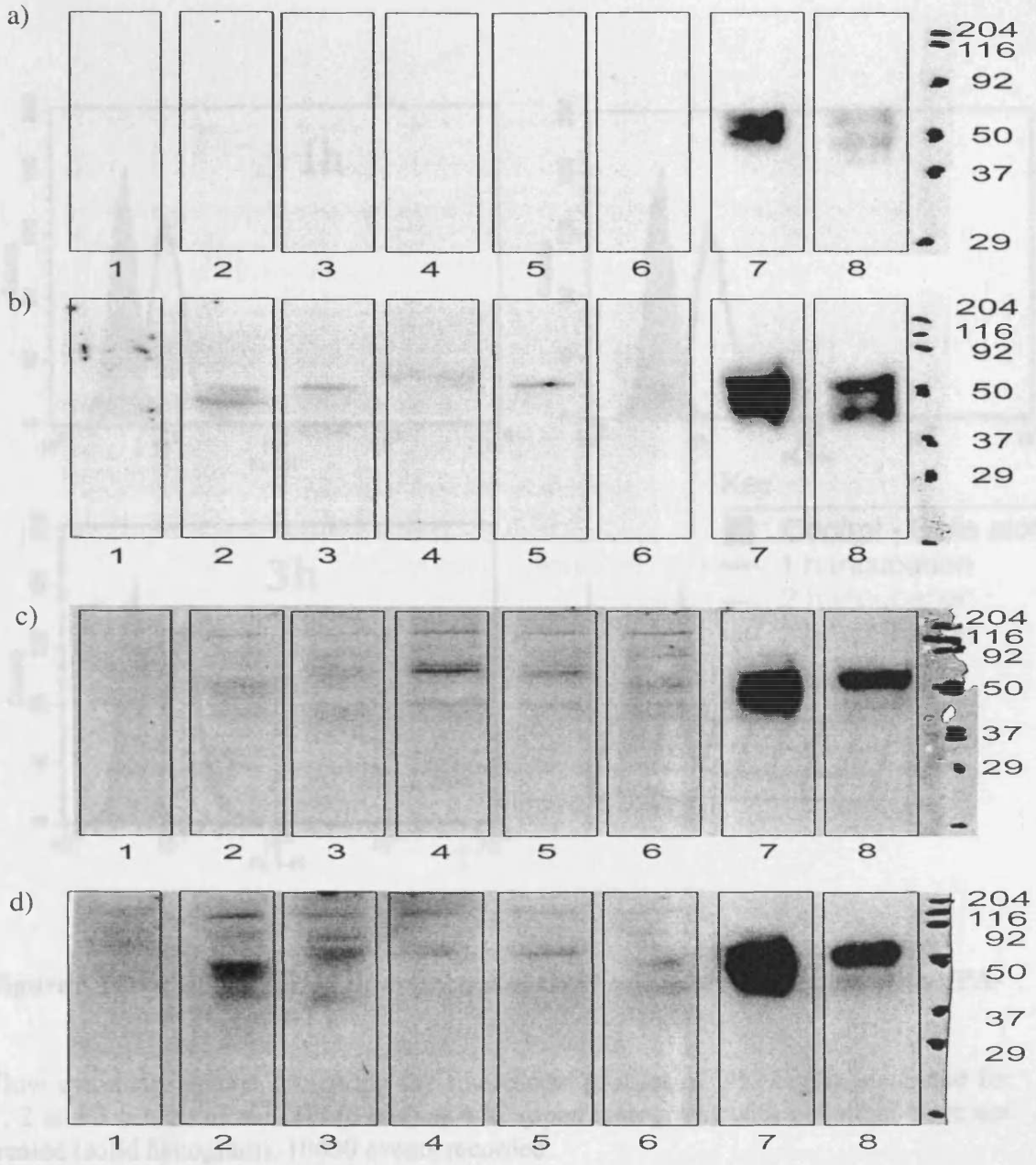

Figure 5.13 – Analysis of cell lines by Western blot for relative uPAR expression

Western Blot of all cell lines at: a) 30 µg protein/lane, b) 60 µg protein/lane: 1) PC3, 2) MCF7, 3) DU145, 4) COS7, 5) COS1, 6) CACO2, 7) U937 PMA stimulated, 8) U937. In blots c) and d) U937 PMA was applied at 10 µg protein/lane and U937 was applied at 30 µg protein/lane. The other cell lines were applied at c) 90 µg protein/lane and d) 120 µg protein/lane.

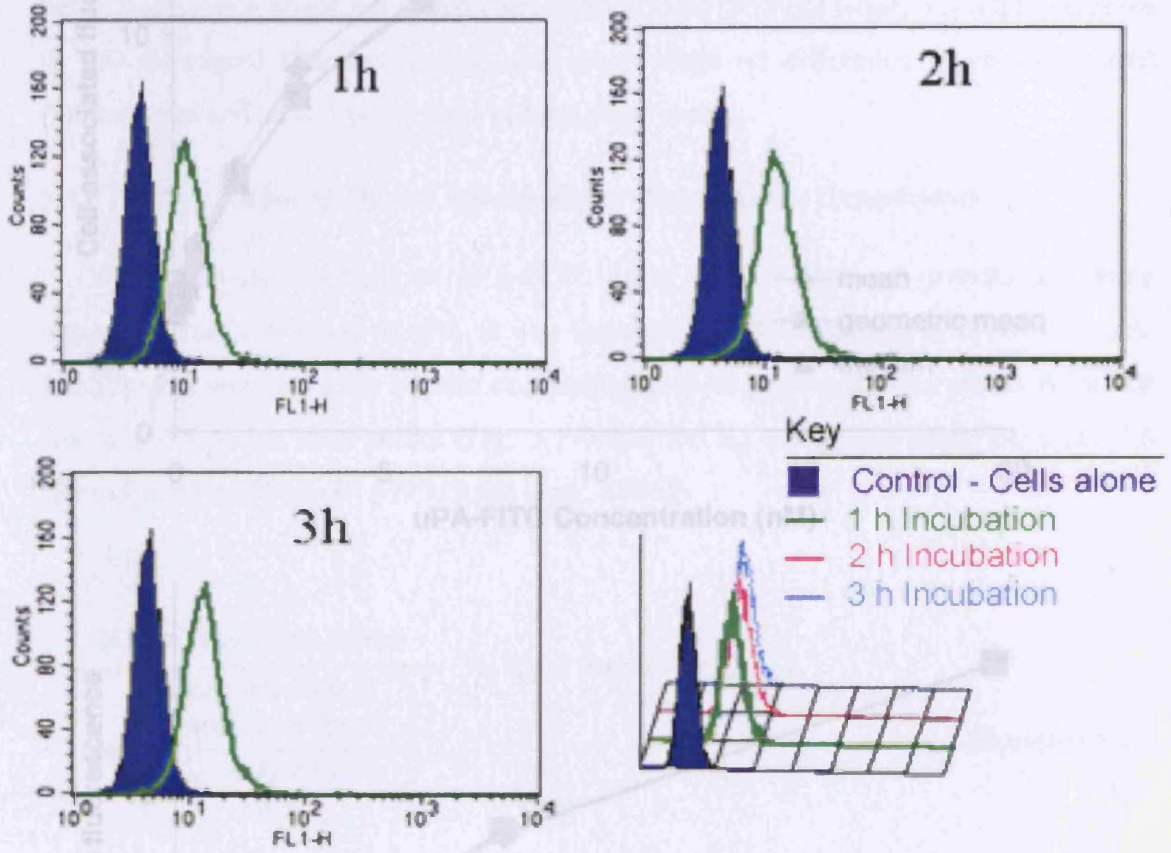

Figure 5.14 – Cell-associated fluorescence of U937 cells after incubation with uPA-FITC for 1-3 h

Flow cytometry results comparing the fluorescent profiles of U937 cells incubated for 1, 2 and 3 h with uPA-FITC (6 nM) at 4 °C (open histogram) with cells that were not treated (solid histogram). 10000 events recorded.

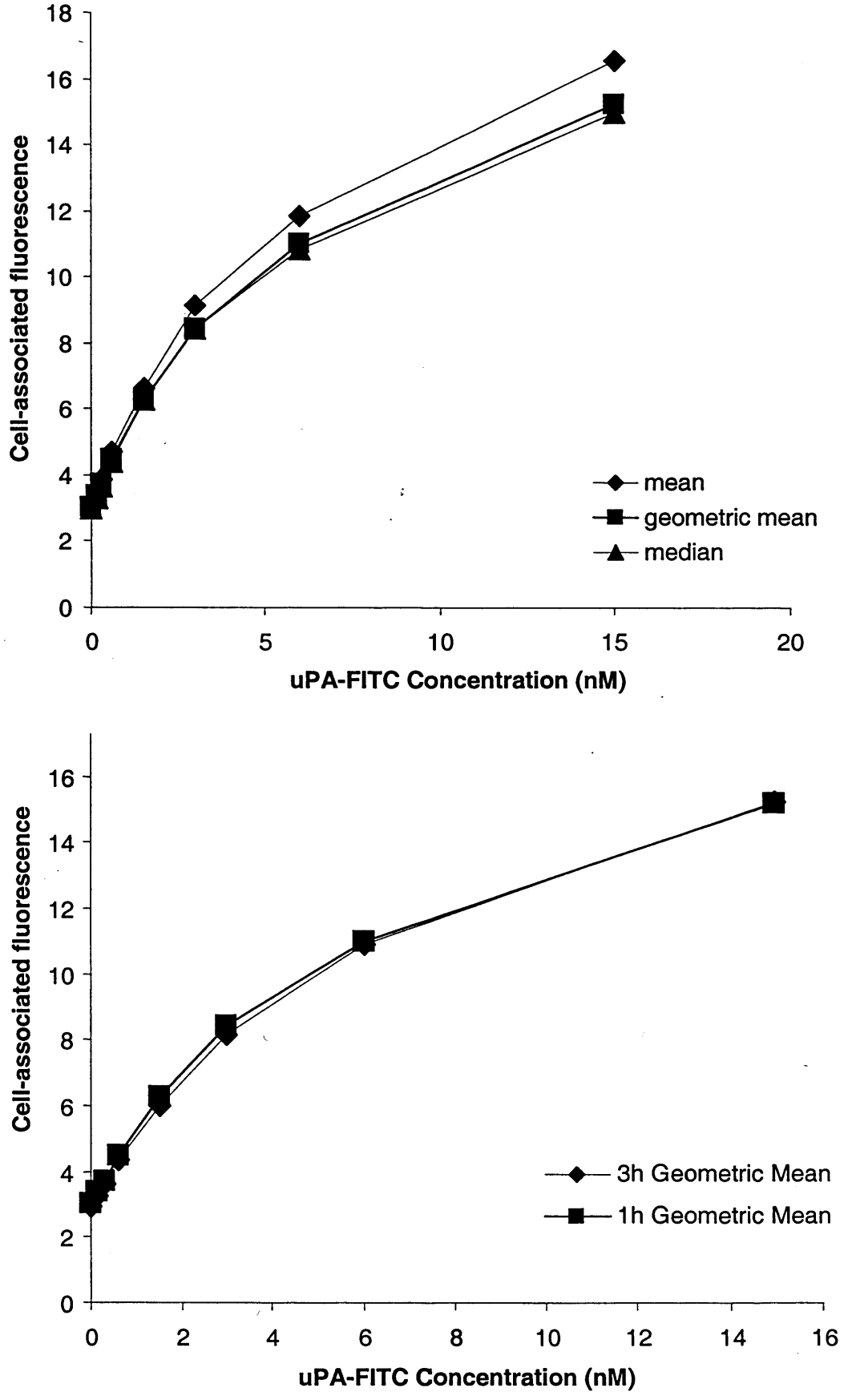

Figure 5.15 – Effect of addition of uPA-FITC on U937 cell-associated fluorescence

Flow cytometry assessment of uPA-FITC concentration dependent binding at 4 °C to U937 cells. Panel a) shows a 1 h comparison of mean, geometric mean and median values. Panel b) shows a comparison of 3h and 1 h geometric means. 10000 events recorded.

The uptake of uPA-FITC in U937 cells over 1 h was assessed at 4 °C and 37 °C, it was seen to increase almost linearly at 37 °C, but to plateau at 4 °C after 40 min (Fig. 5.16).

In the comparison of cells treated with or without an acid wash (to remove bound uPA) there was a slight but statistically insignificant (Student t-test, $p > 0.05$) decrease in cell-associated fluorescence i.e. acid wash made no difference to cell-associated fluorescence and so it was not used in later experiments.

5.3.5 Determination of Ligand Affinity Using Displacement Experiments

When the displacement of uPA-FITC from U937 cells was investigated using increasing concentrations of uPA, it was found that 97 % inhibition of uPA-FITC cell-binding was seen when the highest concentration of uPA (80 nM) was added. A Hill fit was applied to the data points (Fig. 5.17) and the K_d calculated using Equation 5.3 (from Cheng and Prusoff, 1973 (Rang et al., 1996)).

$$\frac{IC_{50}\text{ of displacing ligand}}{1 + \left(\dfrac{\text{Concentration of fluorescent ligand}}{K_d\text{ of fluorescent ligand}}\right)} = K_d\text{ of displacing ligand} \qquad \text{Equation 5.3}$$

$$\frac{IC_{50}\text{ of displacing ligand (determined from the Hill Fit)}}{1 + \left(\dfrac{\text{Concentration of uPA-FITC}}{K_d\text{ of uPA-FITC}}\right)} = K_d\text{ of displacing ligand}$$

Using this equation it was assumed that the K_d of uPA-FITC was 1.5 nM as the manufacturer recommends this concentration for FACS experiments and it is within the range of K_d values reported by others (American Diagnostica, 2002). Using the fluorescent ligand at its K_d simplifies the above equation to give the IC_{50} value calculated from the Hill fit divided by 2 = K_d. This gives the K_d of uPA to be 0.43 – 0.54 nM.

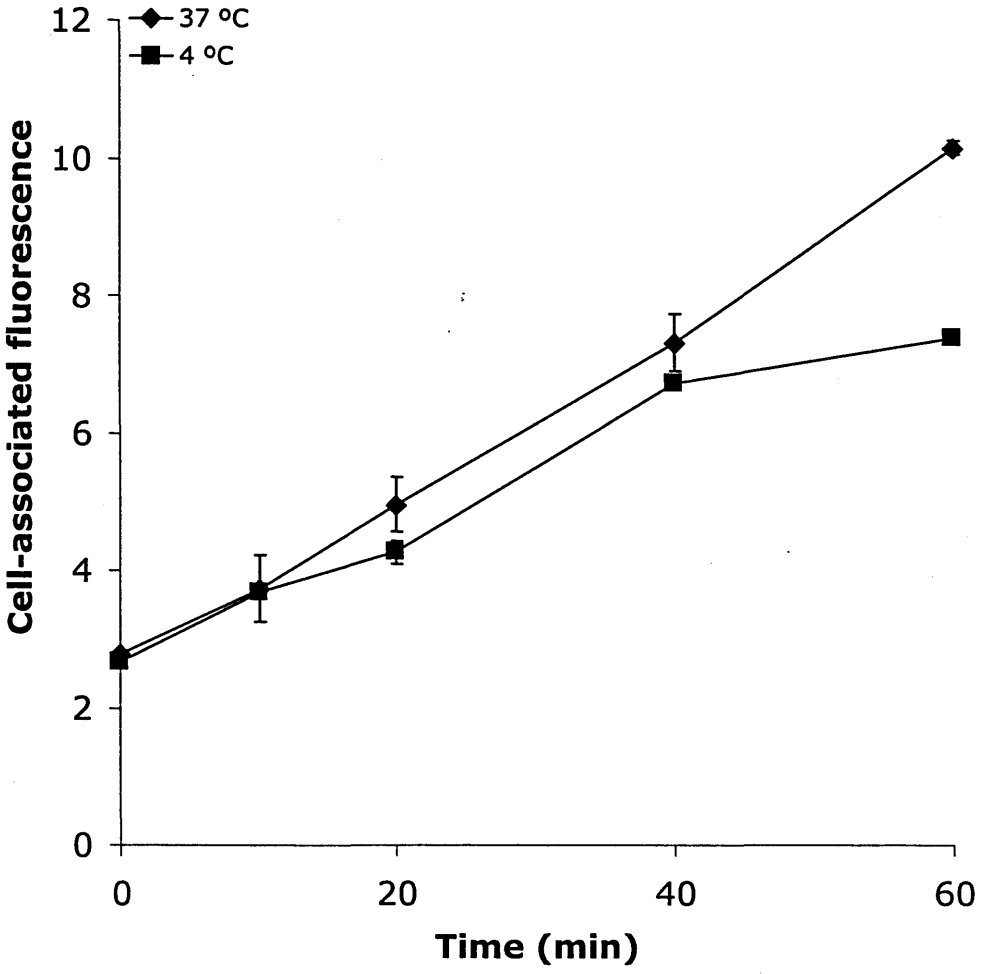

Figure 5.16 – Effect of temperature and time on uPA-FITC binding/uptake in U937 cells

Flow cytometry assessment of the uptake of uPA-FITC (1.5 nM) at 37 °C and 4 °C over 1 h. 10000 events recorded, data represent mean (n = 3) ± S.D.

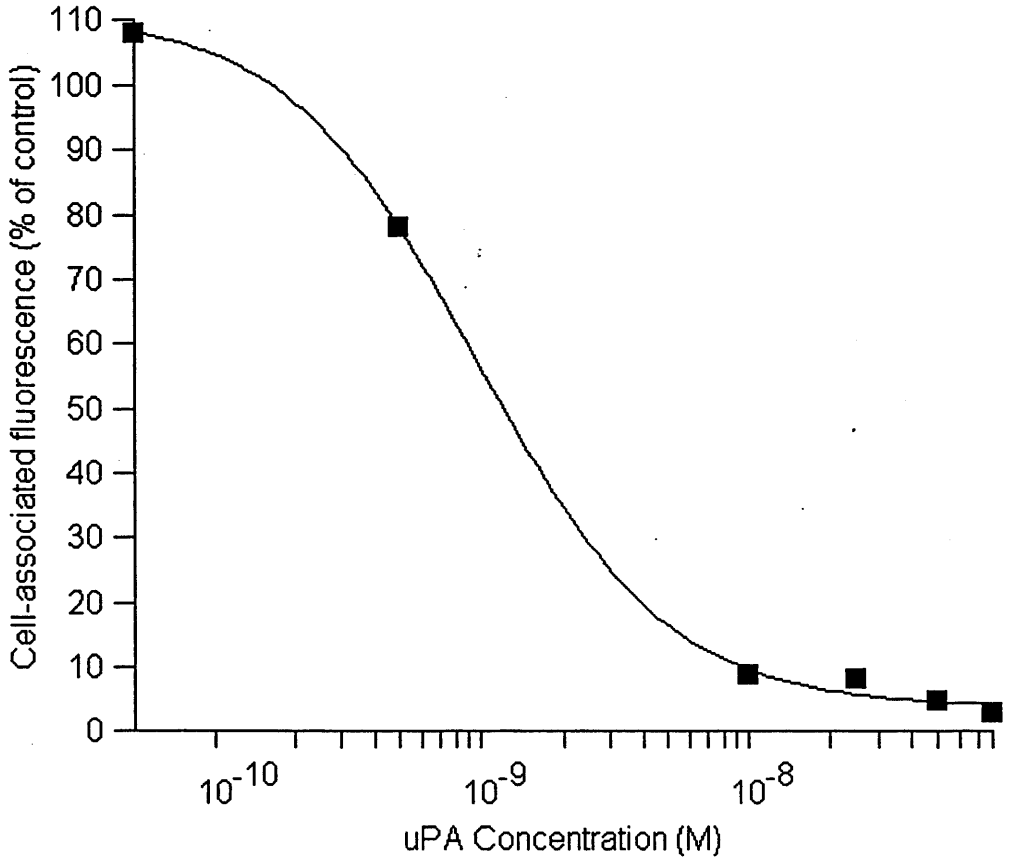

Figure 5.17 – Displacement of uPA-FITC from U937 by uPA

Flow cytometry analysis of the displacement of uPA-FITC (1.5 nM) from U937 cells by increasing concentrations of uPA, measured after a 1 h incubation at 4 °C. 10000 events collected. Curve shows the Hill fit.

When u7 or Gu11G were used as competing ligands in a similar uPA-FITC displacement assay, no uPA-FITC displacement was seen in the case of u7 (Fig. 5.18a). However, Gu11G did displace uPA-FITC with 80 % inhibition achieved at a Gu11G concentration of 0.1 mM (Fig. 5.18b). Using the IC_{50} calculated from the Hill fit, the K_d of Gu11G was calculated to be 1.3 – 1.4 μM. uPA-FITC displacement from U937 cells at 4 °C was studied in the presence of peptide-PEG conjugates. No displacement was seen for any of the peptide-PEG conjugates (Fig. 5.19). However, flow cytometry analysis of u11-PEG-FAM cell uptake showed that this conjugate was taken up significantly more ($p < 0.05$) than the Scrambled u11-PEG-FAM conjugate after a 1 h incubation (Fig. 5.20). Cell-associated fluorescence increased with incubation time for the u11-PEG-FAM conjugate but not for the Scrambled u11-PEG-FAM conjugate.

5.3.6 Uptake of u7- and u11- Containing CMTMO-FAM Conjugates

The cell-association of the cationic peptide-CMTMO-FAM conjugates (1 mg/ml) were assessed in U937 cells at 4 and 37 °C (Fig. 5.21a). Over and above the initial, considerable binding, a significant conjugate uptake was seen after 10 min for u11-CMTMO-FAM. After 20 min this uptake was 5.9-fold higher than that seen with cells incubated with the untargeted CMTMO-FAM (Fig. 5.21a). The uptake appeared to plateau after 20 min at this concentration. When CMTMO-FAM conjugates were incubated with U937 cells at a ten-fold lower conjugate concentration (0.1mg/ml) a similar increase in cell-associated fluorescence was observed (Fig. 5.21b). At both concentrations there was no difference between the cell-associated fluorescence at 4 and 37 °C.

Following these encouraging results, the cell-association of u7-CMTMO-FAM and u11-CMTMO-FAM with the adherent cell line DU145 was investigated. The pattern of uptake was similar to that seen in U937 cells with u11-CMTMO-FAM cell uptake being greater than that seen for CMTMO-FAM or u7-CMTMO-FAM. However, in this case there was little plateau in the cell-associated fluorescence seen at 37 °C over the 1 h incubation period (Fig. 5.22).

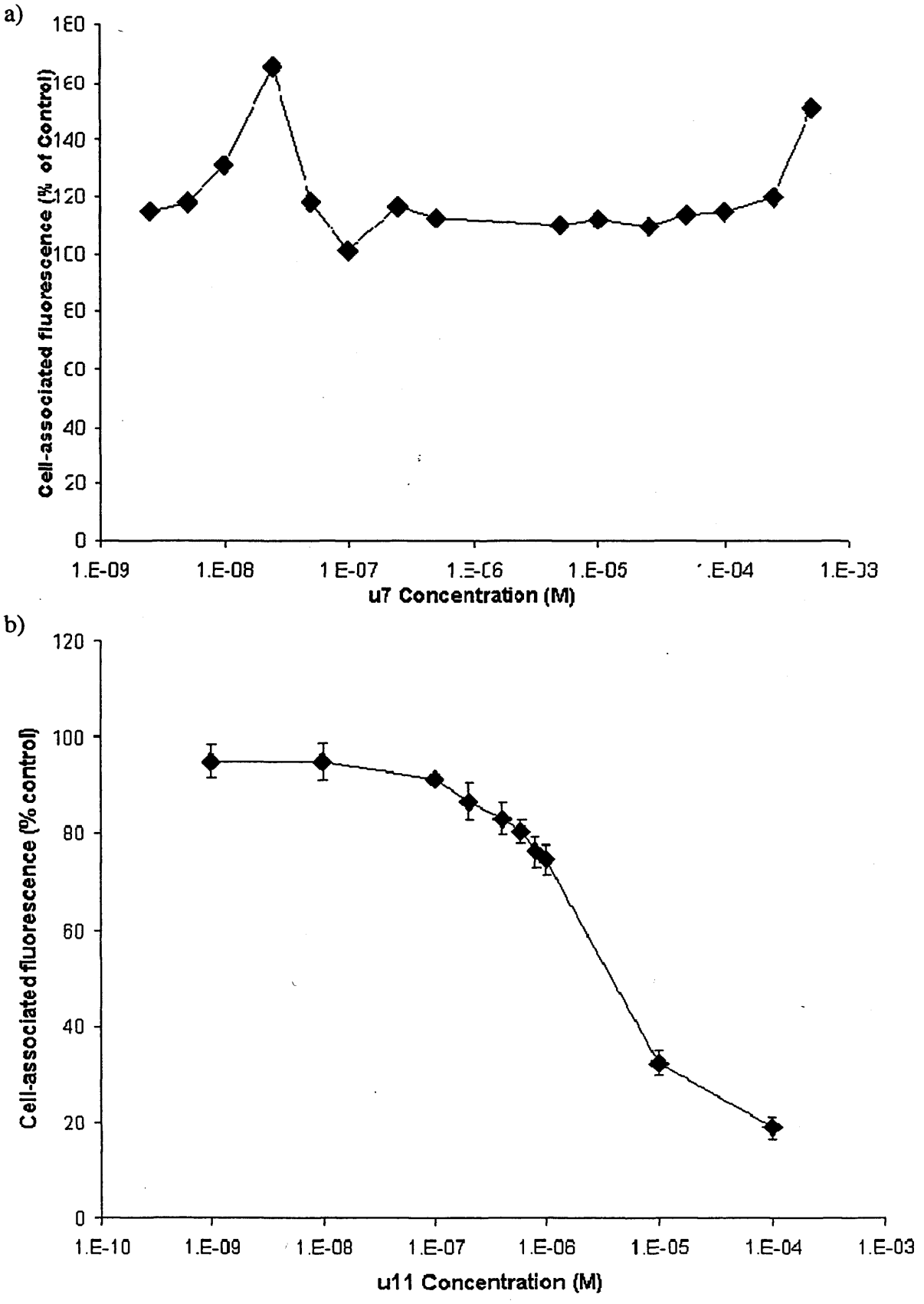

Figure 5.18 – Displacement of uPA-FITC by peptides

Flow cytometry assessment of peptide ligand displacement of uPA-FITC from U937 cells at 4 °C. a) u7, 10000 events collected b) Gu11G 10000 events collected, data represent mean; n = 3, ± S.D. Control cells were incubated with uPA-FITC in the absence of any displacing ligand.

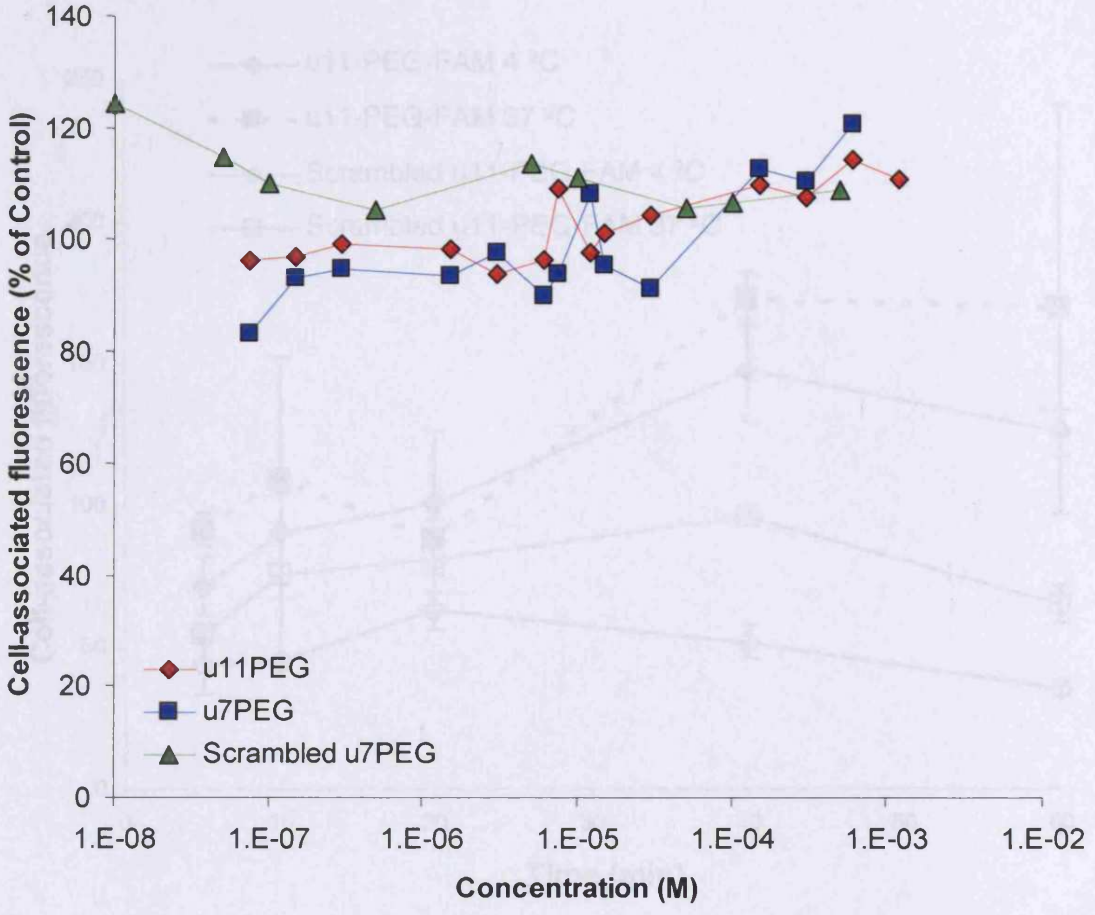

Figure 5.19 – Displacement of uPA-FITC by peptide-mPEG conjugates

Flow cytometry analysis of the displacement of uPA-FITC from U937 cells by peptide-PEG derivatives at 4 °C. 10000 events collected. Control cells were incubated with uPA-FITC in the absence of any competing ligand.

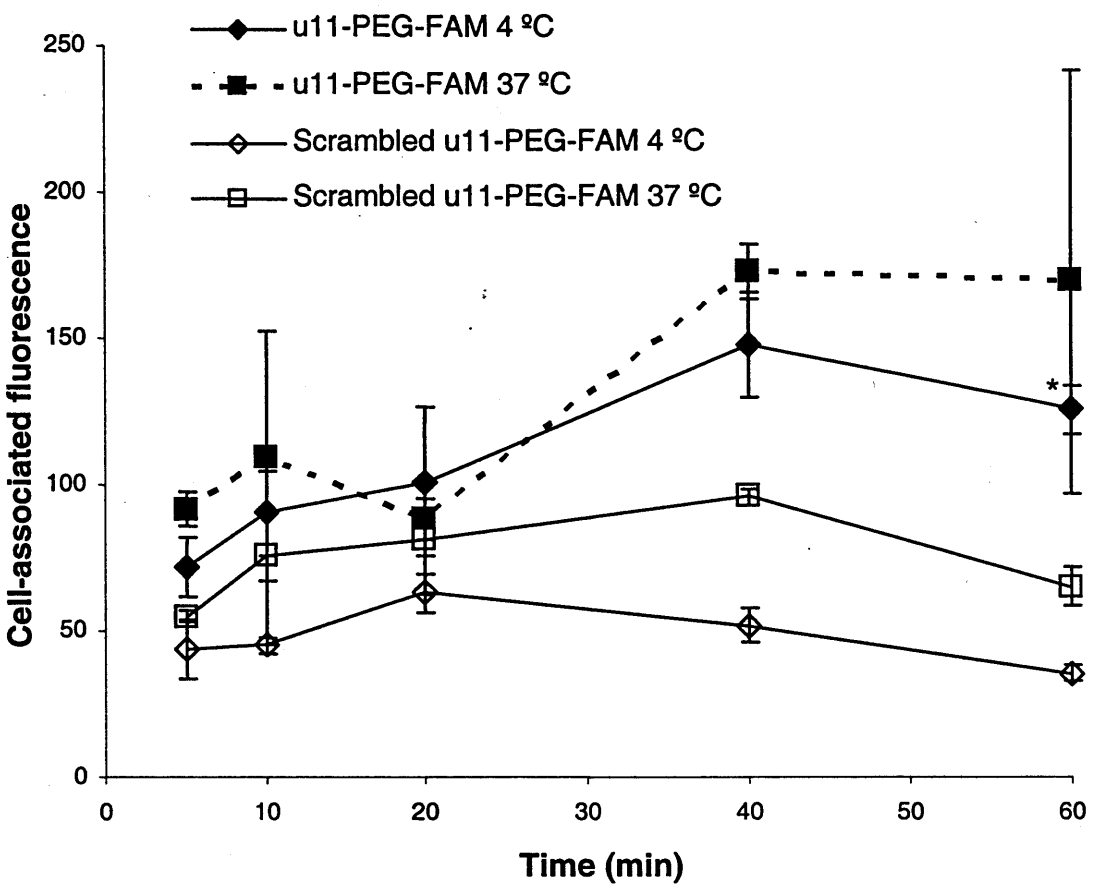

Figure 5.20 – Binding and uptake of peptide-PEG-FAM by U937 cells

Flow cytometry analysis of the binding (4 ºC) and uptake (37 ºC) of u11-PEG-FAM and Scrambled u11-PEG-FAM at 4 and 37 ºC. 10000 events were collected. The data represent mean (n = 3) ± S.D. * The data are statistically different compared to the Scrambled u11-PEG-FAM 4 ºC, student t-test ($p < 0.05$).

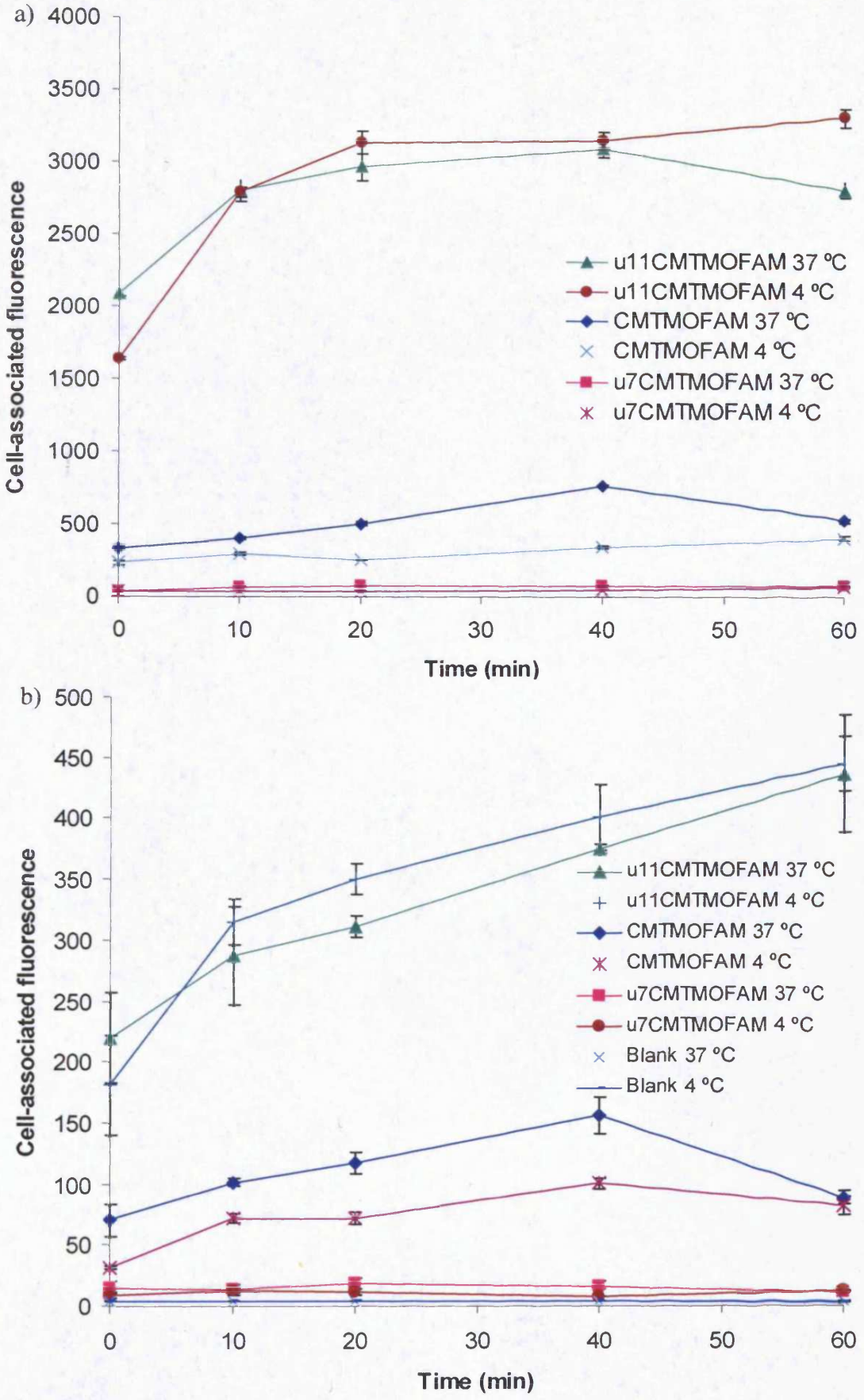

Figure 5.21 – Binding and uptake of peptide-CMTMO-FAM by U937 cells

Flow cytometry analysis of the binding (4 °C) and uptake (37 °C) of fluorescently labelled trimethylated chitosan oligomers in U937 cells a) 1 mg/ml, data represent mean (n=3) ± S.D. b) 0.1mg/ml, data represent mean (n = 6) ± S.D.

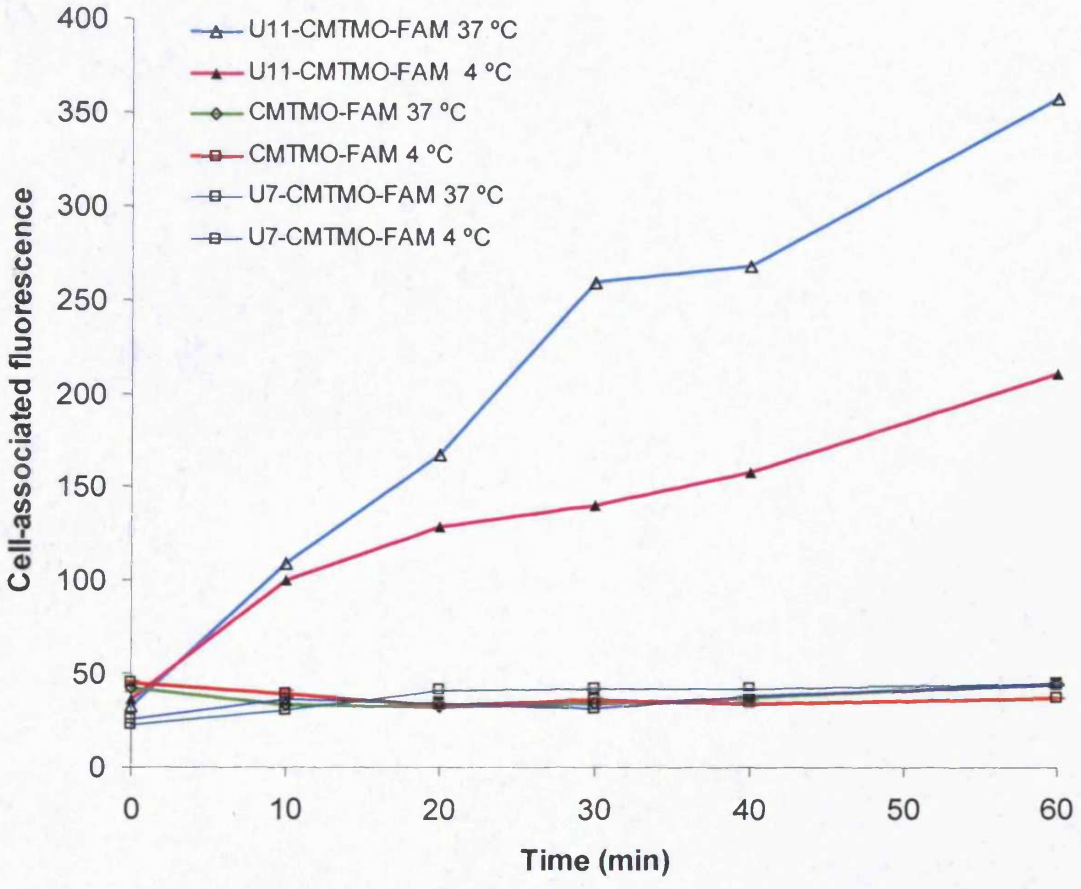

Figure 5.22 – Binding (4 °C) and uptake (37 °C) of peptide-CMTMO-FAM by DU145 cells

Flow cytometry analysis of the uptake of fluorescently labelled trimethylated chitosan oligomers at 0.1 mg/ml. 10000 events collected, data represent mean (n = 2).

Again there was a significant increase in cell-associated fluorescence in cells incubated with u11-CMTMO-FAM compared to all the other conjugates, but there was a significant difference between the cell-association seen at 37 °C and at 4 °C ($p < 0.05$, ANOVA with Bonferroni post hoc test). In a subsequent experiment the concentration of CMTMO-FAM was adjusted so that the same concentration of FAM was compared (Fig. 5.23) and this confirmed the lack of difference between u7-CMTMO-FAM and CMTMO-FAM. In this experiment, if anything, presence of the u7 peptide reduced the cell-association of CMTMO-FAM (Fig. 5.23).

5.3.7 Displacement of u11-CMTMO-FAM by uPA or Gu11G

To investigate the specificity of the binding of u11-CMTMO-FAM competition studies (1 h incubation) were performed using uPA and u11 (Fig. 5.24). uPA inhibited the binding of u11-CMTMO-FAM in a dose-dependent manner. An initial decrease in u11-CMTMO-FAM binding was observed with 0.15 nM uPA displacing 22 % of the u11-CMTMO-FAM cell-associated fluorescence. The highest concentration of uPA (3 nM) displaced 25 % of u11-CMTMO-FAM cell-associated fluorescence. Gu11G only showed inhibition of the binding of u11-CMTMO-FAM at its highest concentration (50 μm) which displaced 40 % of the fluorescent ligand (Fig. 5.24b). As only 25 % inhibition was achieved with the highest concentration of uPA, and cell-associated fluorescent output from cells incubated with u11-CMTMO-FAM (0.1 mg/ml) was 100-fold higher than untreated cells, the concentration of u11-CMTMO-FAM was decreased. The concentration range of uPA applied was the same and a similar inhibition of binding was achieved (20 %), although the curve has been shifted to the right (Fig. 5.25).

When U937 cells were incubated with u11-CMTMO-OG (Fig. 5.26a) (OG shows minimal pH sensitivity) there was a very similar uptake profile to that seen with u11-CMTMO-FAM (Fig. 5.21). Cell binding/uptake of u11-CMTMO-OG was dependent on concentration and no difference between 4 °C and 37 °C binding/uptake was observed ($p > 0.05$). DU145 cells showed a similar uptake profile with u11-CMTMO-OG (Fig. 5.26b) to that seen with u11-CMTMO-FAM (Fig. 5.22) with increasing cell-associated fluorescence with increasing time (Fig. 5.26b). There was a clear difference in cell-associated fluorescence after 30 min incubation between 4 °C and 37 °C.

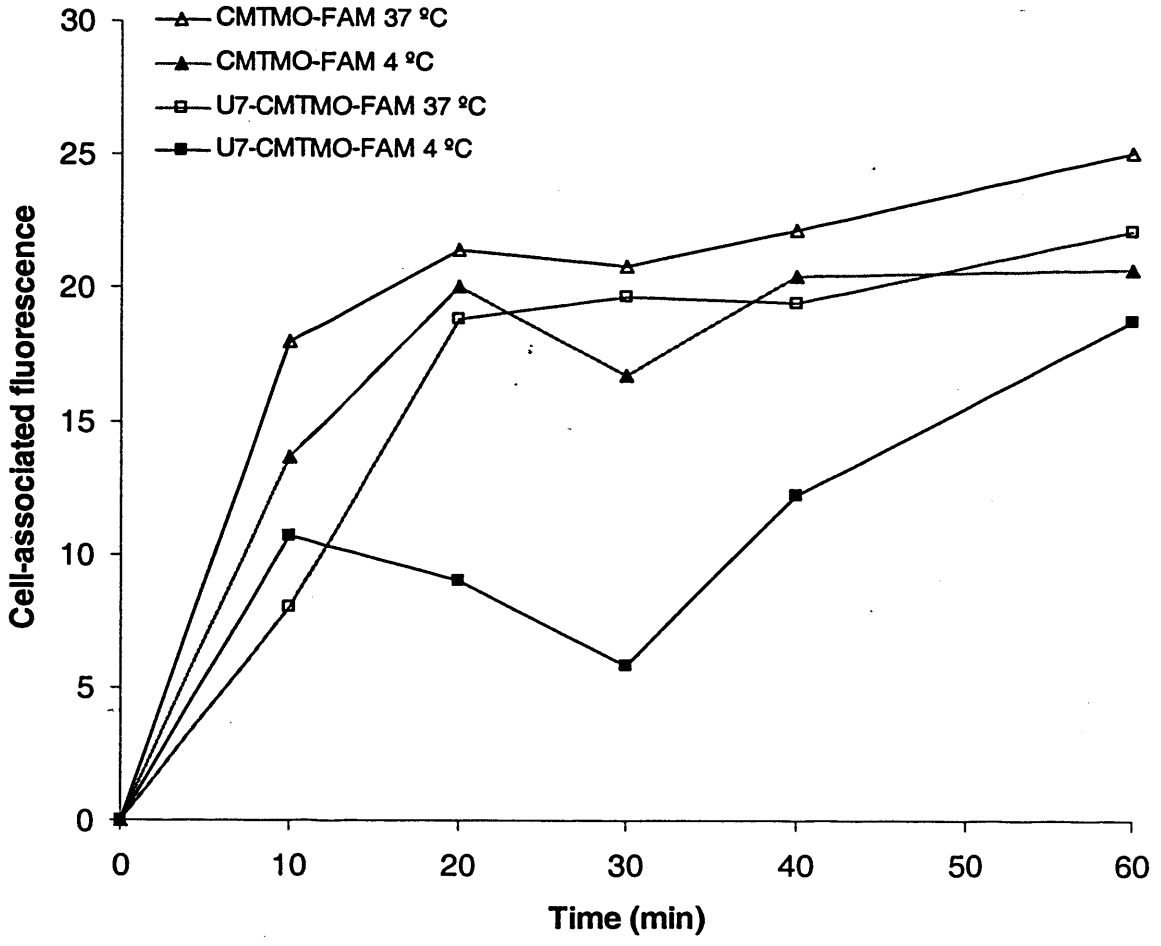

Figure 5.23 – Cell-association (4 °C and 37 °C) of u7-CMTMO-FAM compared to CMTMO-FAM

Flow cytometry analysis of the binding and uptake of fluorescently labelled trimethylated chitosan oligomers. CMTMOFAM (11.8 µg/ml) concentration adjusted to FAM concentration in u7-CMTMO-FAM. 10000 events were collected. The normalised data represent mean (n = 2).

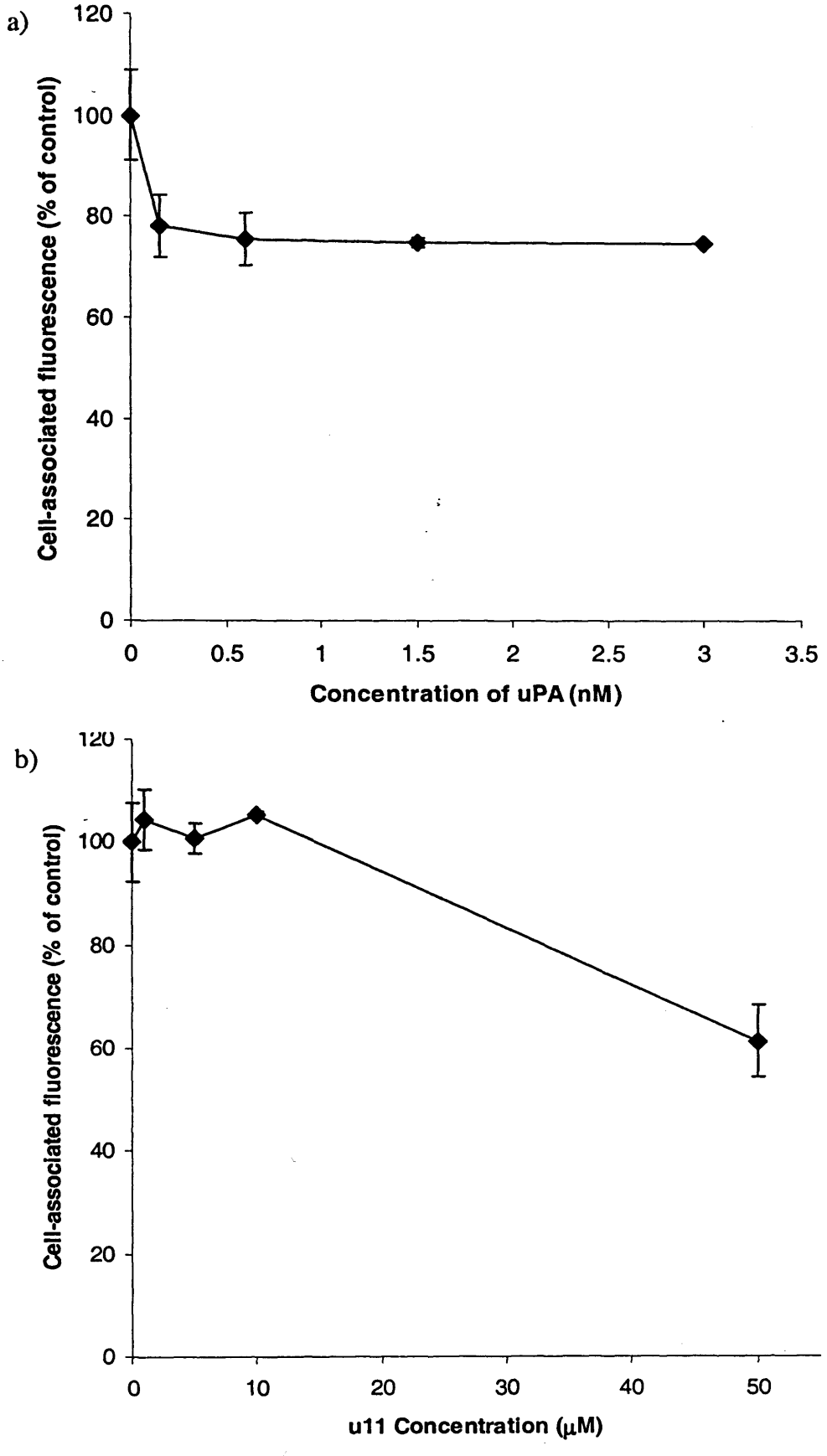

Figure 5.24 – Effect of uPA and Gu11G on binding of u11-CMTMO-FAM (0.1 mg/ml) to DU145 cells (1 h)

Flow cytometry analysis of the displacement of u11-CMTMO-FAM (0.1 mg/ml) from DU145 cells at 4 °C by a) uPA data represent mean (n = 4) ± S.D and b) u11 data represent mean (n = 3) ± S.D.

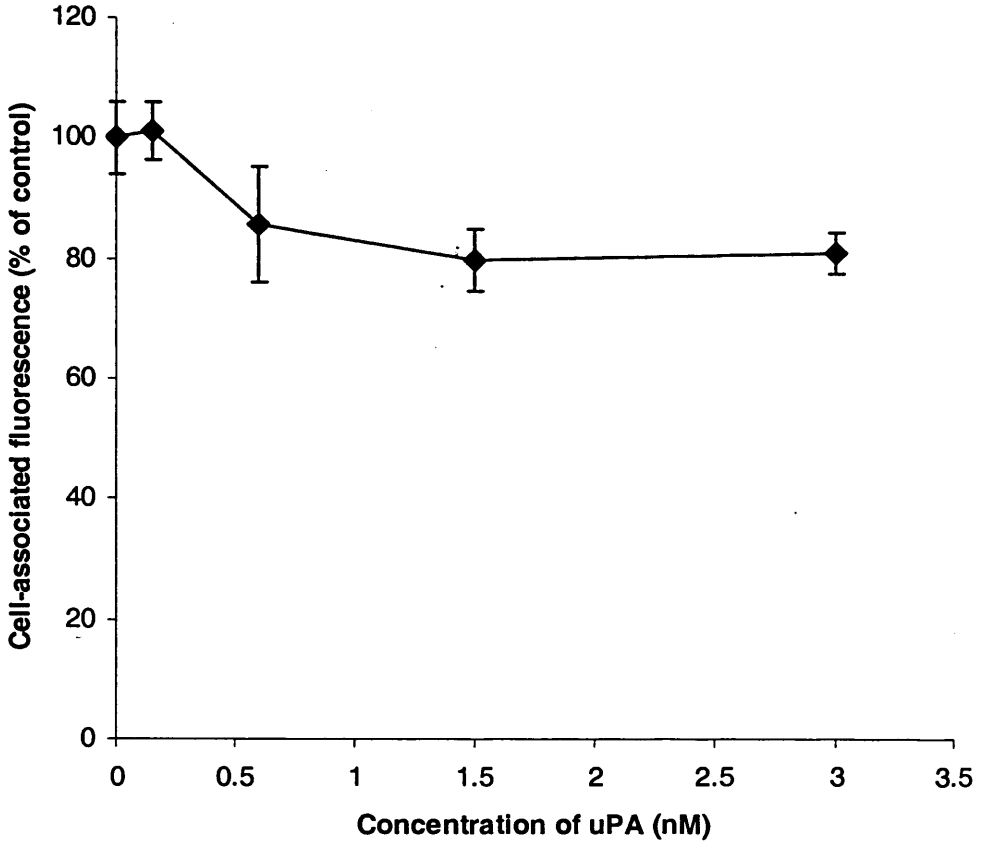

Figure 5.25 – Displacement of u11-CMTMO-FAM (0.01 mg/ml) from DU145 cells by uPA

Flow cytometry analysis of the cell-associated fluorescence of DU145 cells incubated at 4 °C for 1 h with u11-CMTMO-FAM (0.01 mg/ml) and increasing concentrations of uPA. Data represent mean (n = 5) ± S.D.

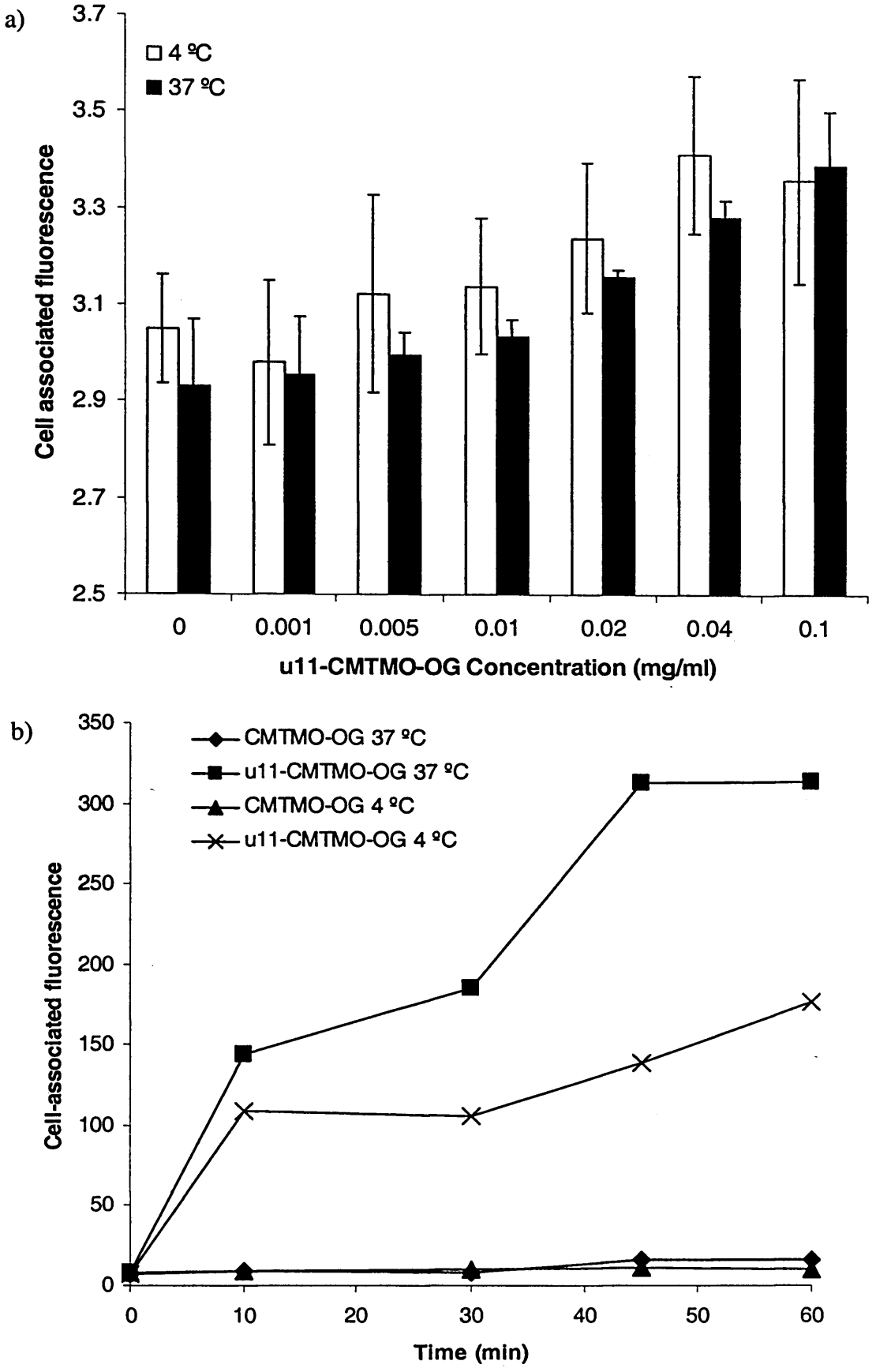

Figure 5.26 – Binding (4 °C) and uptake (37 °C) of u11-CMTMO-OG by DU145 cells

Flow cytometry assessment of a) the uptake of u11-CMTMO-OG in U937 cells at different concentrations after 1 h incubation, data represent mean (n = 3) ± SD; b) the uptake of u11-CMTMO-OG (0.1 mg/ml) in DU145 cells up to 1 h. Data represent mean (n = 2).

5.3.8 Fluorescence Microscopy of DU145 Cells Incubated with Chitosan Conjugates

Preliminary experiments were undertaken with COS-7 cells, these cells were incubated with chitosan-9-anthraldehyde and trimethylchitosan-9-anthraldehyde. Fluorescent labelling of the plasma membrane was seen but as this fluorophore had a broad emission spectra no further studies were made (results not shown).

DU145 cells showed no distinct auto-fluorescence in the absence of ligand (Fig. 5.27a) but cells incubated with u11-CMTMO-FAM conjugate which had been immediately rinsed with PBS three times showed a clear indication of cell binding (Fig. 5.27b). The probe was randomly distributed across the cells (Fig. 5.27b). After 10 min many cells showed localised, discreet staining of the cell membrane and also of projections from the cells (Fig. 5.27c). There was minimal intracellular staining at this time point (Fig. 5.27d). After 30 min there was still intense staining of localised regions of the cell membrane and cellular projections (Fig. 5.28e). However, after 1 h some intracellular fluorescence was also visible (Fig. 5.27f). When u11-CMTMO-OG was used as a probe in DU145 cells, similar labelling was seen after 30 and 60 min, but more defined, vesicle-like (endocytic) compartments were visible (Fig. 5.28).

5.4 Discussion

The first aim of this study was to identify cell lines expressing uPAR that could subsequently be used to study targeted gene delivery. Western blotting showed that four cell lines: U937 PMA, U937, MCF-7 and DU145 cells express high levels of uPAR. The detection of two uPAR related bands in some blots could indicate either 1) different levels of glycosylation (Behrendt et al., 1990), or 2) a cleaved receptor (Montuori et al., 2002). If different degrees of glycosylation were present this would undoubtedly affect the affinity of ligands for the receptor. The presence of receptor fragments would not correlate with ligand uptake due to its cleavage from the membrane. As the cells were rinsed with PBS before lysis in a buffer containing peptidase inhibitors (leupeptin, pepstatin A, aprotinin and PMSF) it would be expected that uPAR degredation would not occur during lysate preparation. This could indicate that the first case (glycosylation variants were produced in the cells) was more likely. The U937 cells were used for these studies as they have been widely reported to express uPAR (Cubellis et al., 1989, Cubellis et al., 1986, Ploug et al., 1991, Rajagopal & Kreitman, 2000) and they served as a useful positive control for Western blotting experiment and in subsequent ligand-binding experiments.

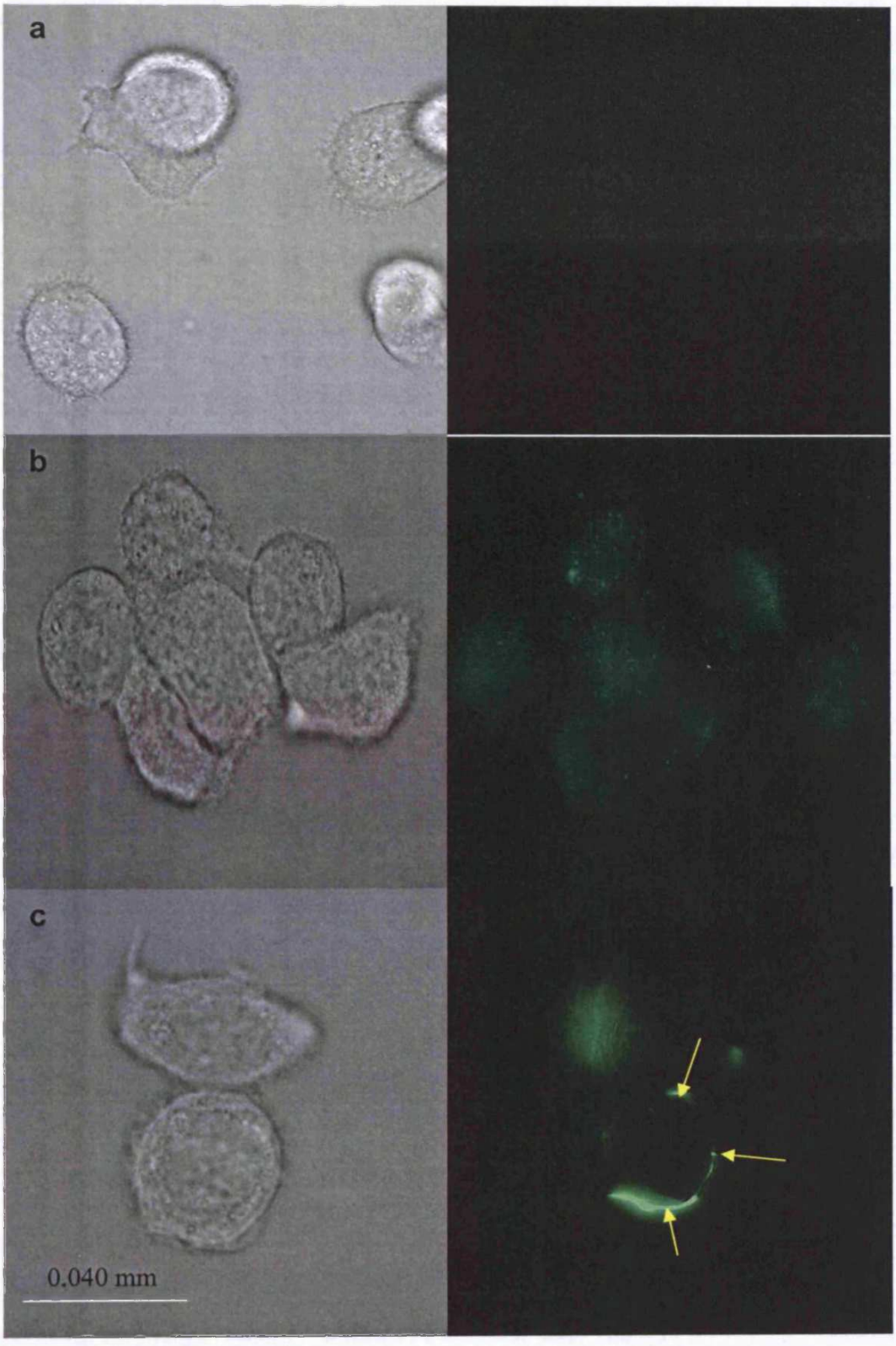

Figure 5.27 – Fluorescent images of DU145 cells incubated with u11-CMTMO-FAM

The left hand panel shows phase contrast images and the right hand panel shows fluorescent images of: panel a) shows cells where no probe was added, panel b) shows cells after u11-CMTMO-FAM was added and cells immediately washed, panel c) shows cells after a 10 min incubation with u11-CMTMO-FAM. The yellow arrows indicate discrete areas of membrane binding.

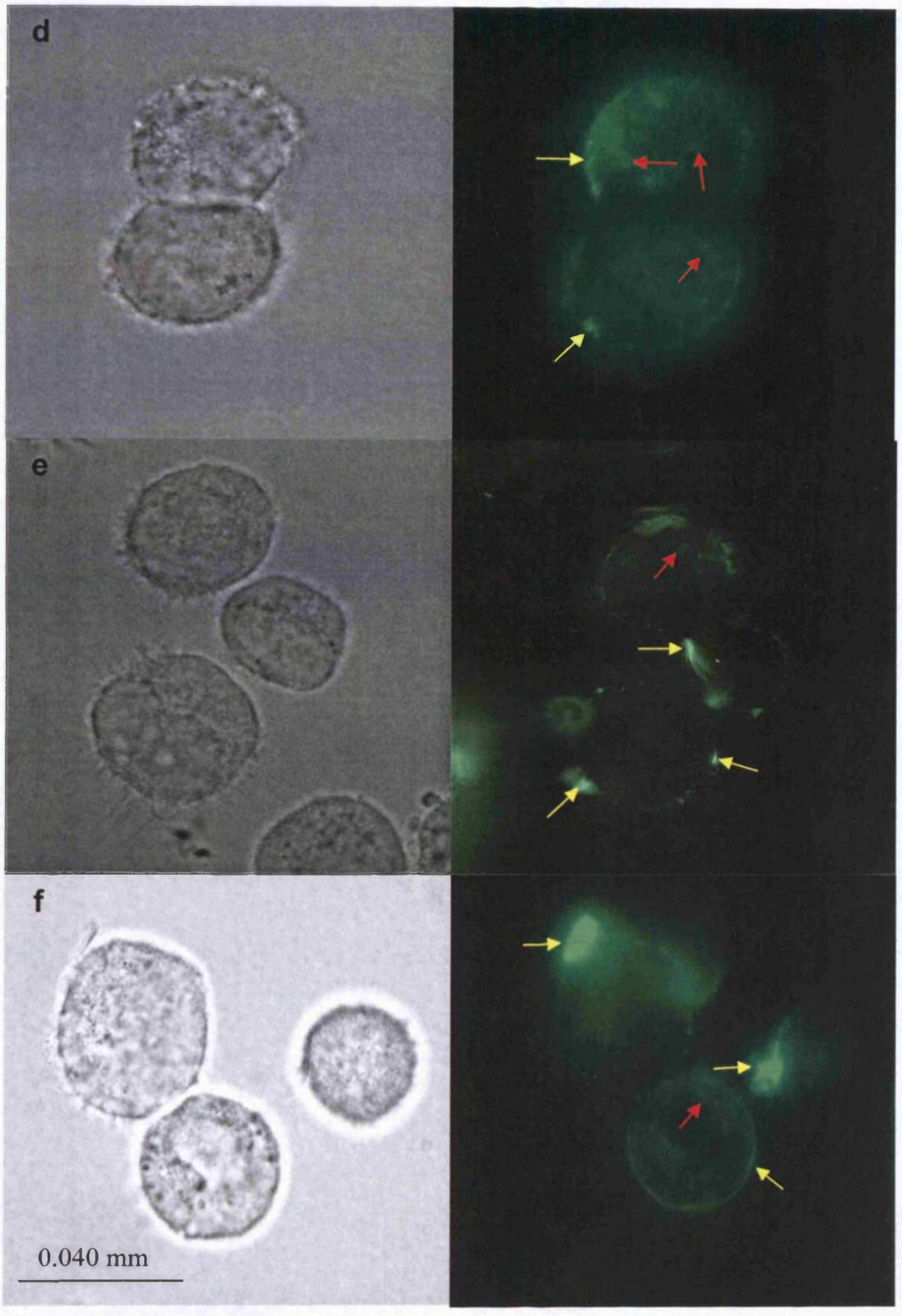

Figure 5.27 continued

Panel d) shows cells after a 10 min incubation with u11-CMTMO-FAM. Panel e) shows cells after a 30 min incubation with u11-CMTMO-FAM. Panel f) shows cells after a 60 min incubation with u11-CMTMO-FAM. The yellow arrows indicate discrete areas of membrane binding and the red arrows indicate possible intracellular localisation.

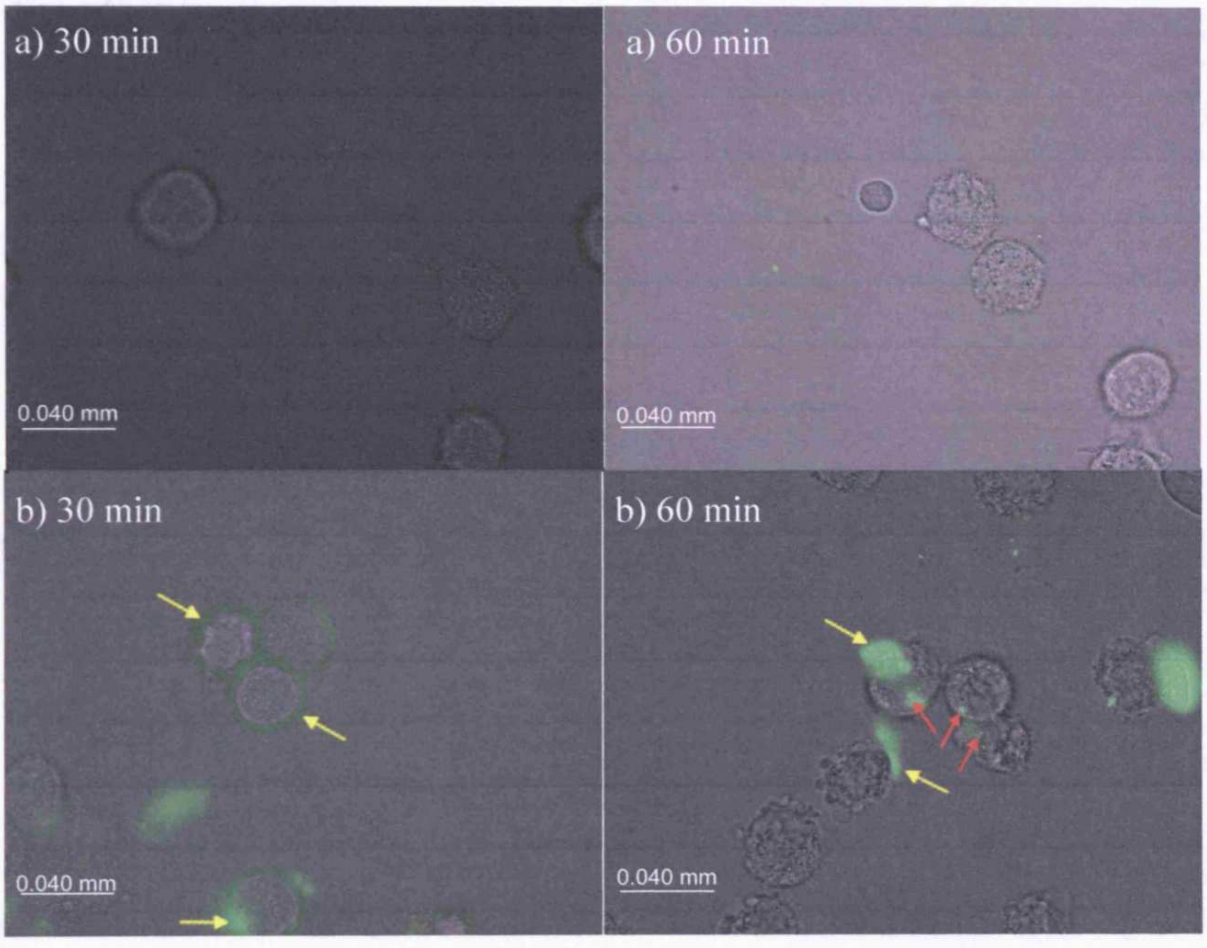

Figure 5.28 – Fluorescent microscopy of DU145 incubated with u11-CMTMO-OG

A phase contrast image has been combined with the fluorescent image. Images of a) CMTMO-OG and b) u11-CMTMO-OG. Binding of the targeted conjugate on the membrane (yellow arrows) in discrete areas was seen as were endosome-like compartments (red arrows).

In addition, U937 cells are easily manipulated as they grow in suspension and multiply quickly. The differentiated U937 PMA cells were not studied in ligand-binding experiments as this macrophage line could exhibit phagocytic uptake and it was thought that this might complicate the cell uptake pattern seen. As the ultimate goal of this project was targeted gene delivery for the treatment of breast and prostate cancer a panel of these cell lines was investigated.

Having established that U937 and DU145 cell lines express uPAR, investigation of the ligands and conjugates for uPAR was possible. As uPA-FITC is available commercially and its K_d is reported (American Diagnostica, 2002), the K_d of the displacing ligands could be calculated. To test/confirm the reported K_d of uPA (i.e. uPA-FITC), competition studies were conducted using uPA-FITC in the presence of uPA. The uPA K_d obtained (0.43 – 0.54 nM) is within the range reported (Roldan et al., 1990). However, care should be taken in the interpretation of the K_d values gained as there is a range of values reported for the K_d of uPA: 0.5 nM (Cubellis et al., 1986), 0.2 nM – 10 nM (Roldan et al., 1990), 1 nM (Blasi & Carmeliet, 2002), 1.5 nM (American Diagnostica, 2002). Also, the affinity of uPA may be altered by the FITC conjugation. This introduces a more lipophillic characteristic to the protein and may also alter the protein conformation. The binding kinetics of uPA-FITC were not further determined. The value of 1.5 nM used was resolved to be accurate enough for subsequent comparison and it was established that uPA-FITC could be used at 1.5 nM for future displacement experiments. This is because it would be close to the K_d of uPA-FITC, a preferred condition for displacement assays.

If the different levels of uPAR glycosylation seen in the Western blot experiments were present in ligand binding experiments this might affect uPA-FITC and potential ligand binding affinity. However, lack of heterogeneity in an individual experiment seen in the results obtained here suggests that any variability in uPAR glycosylation is not in the ligand binding domain.

Competition studies allow a library of molecules to be screened and their affinity for a specific receptor to be assessed. The binding affinity of Gu11G was considerably lower (K_d = 1.3 – 1.4 μM) than that of uPA (K_d = 0.43 – 0.54 nM). This affinity was also lower than the reported K_d (~0.4 nM) of a non-natural 9-mer peptide developed through combinatorial chemistry by Ploug et al. (2001). Nevertheless, it was considered

that a ligand (like u11) derived from uPA would be more likely to induce endocytosis and thus be better for polyplex targeting.

The reduction in uPA-FITC binding to 80 % of the control value when the highest concentration of Gu11G was added confirms that this peptide sequence plays an important role in the binding of uPA to uPAR. This observation is in agreement with Apella et al. (1987). The loss of secondary and tertiary structure, along with other putative binding amino acids could account for the reduced affinity of Gu11G for uPAR. The advantages of the use of a peptide fragment for polyplex-receptor targeting have already been discussed at length in Section 1.3.2.4, and in addition it would be expected that there would be more than one peptide per polyplex (Chapter 6). The latter would promote a polyvalent interaction, increasing the binding to cells (Chiu et al., 2004). Use of a peptide is particularly attractive as the 'small' ligand should interfere less with polyplex formation and be less antigenic than a larger protein. The peptide ligand does not have the catalytic activity of the whole protein and it is easier to synthesise than larger fragments or the whole protein (making the construct more cost effective).

The endocytosis of trimethylated chitosan has not so far been studied (to the author's knowledge). FITC-chitosan nanoparticle uptake by A549 cells has been reported (Huang et al., 2002) and it was found that uptake was time- and concentration-dependent. Nanoparticle uptake was still occurring after 4 h incubation. Extensive non-specific labelling of the cell membrane by FITC-chitosan nanoparticles was also observed.

As was observed earlier (Fig. 5.4), the pH sensitivity of FAM fluorescence indicated that when FAM-conjugates are internalised into endosomes progressing to lysosomes there would have been a significant quenching of the fluorescence due to a decrease in the compartment pH because of the proton pump driven acidification of these vesicles.

The comparison of cell-association at 4 °C and 37 °C is commonly used to distinguish between membrane binding (4 °C) and the overall cell-uptake (37 °C); the difference between the two being the endocytic uptake (Duncan & Lloyd, 1978, Duncan et al., 1986). It is generally accepted that endocytosis does not occur at 4 °C as it is an energy requiring process (Stryer, 1995). The increased association at 37 °C is commonly thought to be due to internalisation. However, a general rule of thumb is that an increase in 10 °C doubles the reaction rate (derived from the Arrhenius equation, (Solomons, 1996)) this would also affect the cell-binding. This is one explanation for the similarity

in the increase in cell-associated fluorescence in DU145 cells treated with u11-CMTMO-FAM or u11-CMTMO-OG at 37 °C over that at 4 °C i.e. that the increased cell-associated fluorescence at 37 °C is due to increased membrane interaction with u11-CMTMO-FAM or u11-CMTMO-OG and not internalisation. However, if this were the case it would surely be true in the U937 cell line. The other explanation is that CMTMO buffers the endocytic compartment and therefore there is no quenching of the cell-associated fluorescence in u11-CMTMO-FAM.

The synthesis of activated PEG derivatives showed evidence of dimer formation. The activated PEG-ester probably reacts with terminal hydroxyl groups of mPEG. This side reaction was unexpected and it also proved problematic. The dimer impurity could not be separated using GPC. There was reduced dimer formation when mPEG was activated with PNP. The separation of peptide-PEG derivatives from unreacted material also proved difficult. Due to lack of time and the poor binding found in preliminary experiments, the synthesis of PEG-peptide conjugates was not pursued but separation may have been possible using affinity chromatography.

The NHS-PEG-FAM proved valuable in terms of giving a positive increase in cell-associated fluorescence when conjugated to Gu11G, this was not observed using Scrambled u11-PEG-FAM (Fig. 5.20). This further indicates that Gu11G may specifically interact with uPAR and the binding observed is not just a cell-membrane binding effect mediated by the peptide isoelectric point or lipophillicity (partition coefficient) as these effects would be similar for the Scrambled peptide conjugate. However, the lack of inhibition of uPA-FITC binding by the peptide-PEG derivatives was puzzling. This could have been due to the presence of a heterogeneous mixture i.e. PEG-peptide, mPEG and PNP-mPEG.

It is however interesting, that the uptake observed using u11-PEG-FAM in U937 cells was not as striking as that seen using u11-CMTMO-FAM or u11-CMTMO-OG. This may indicate that either the hyper-mobile PEG backbone was interfering with the conformation of the peptide or wrapping around it and restricting its access to the binding pocket of uPAR. Alternatively CMTMO might enhance the affinity of the peptide for the receptor. Both uPA and uPAR are known to be heavily glycosylated and this could account for the greater affinity for the receptor of the u11-CMTMO conjugates compared to the u11-PEG conjugate due to interactions between the

saccharide chains. The loading of peptide ligand units on PEG was calculated to be approximately one for every two PEG chains, in u11-CMTMO-FAM it was calculated to be between one per oligomer and one for every three oligomers. This would not therefore account for the much lower binding of u11-PEG-FAM. The number of moles of each conjugate applied were also similar.

The binding of the u11-CMTMO-FAM conjugates in U937 cells was prodigious. The binding/uptake of u11-CMTMO-FAM in U937 cells was saturated at 1 mg/ml after 20 min indicating a limit to the number of receptors available. The uptake rate is decreased at 0.1 mg/ml in U937 cells but was not saturated. In DU145 cells uptake appears to continue at 37 °C after 1 h incubation, this is greater than that seen at 4 °C. The uptake of u11-CMTMO-FAM in U937 cells is higher than that in DU145 cells, this is consistent with the higher expression of uPAR. Non-specific binding, assessed using CMTMO-FAM, was lower than expected. The conjugate was expected to have an overall positive charge, increasing its interaction with cell membranes due to their negative charge (Fischer et al., 2003, Mislick & Baldeschwieler, 1996). This charge could have been tested using zeta potential measurements but due to a limited amount of compound this was not performed.

The deficient endocytosis, i.e. little or no difference between 4 °C binding and 37 °C uptake, of u11-CMTMO-FAM (Fig. 5.23) and u11-CMTMO-OG (Fig. 5.24a) in U937 cells may be due to a fused gene between mixed lineage leukaemia translocated to 10 and phosphatidylinositol-binding clathrin assembly protein (Cottier et al., 2004). This fusion may decrease clathrin-dependent endocytosis in this cell line. However, endocytosis of uPAR has been reported in U937 cells (Conese et al., 1994, Nykjaer et al., 1997). Although to a lower extent than in LB6 clone 19 (murine cell line expressing uPAR) (Conese et al., 1994). Endocytosis of uPAR has been more thoroughly studied in cell lines apart from U937, e.g. HT1080 (human fibrosarcoma) cells (Czekay et al., 2001), Madin-Darby canine kidney epithelial cells (Vilhardt et al., 1999), LB6 (murine) clone 19 cells (Nykjaer et al., 1997). Low uptake of u7-CMTMO-FAM further showed that this peptide was unsuitable as a targeting ligand for future investigation. This is in disagreement with the work presented by Drapkin et al. (2000).

The encouraging uptake of u11 targeted derivatives led to this being developed for further experiments described in Chapter 6. The displacement of only 25 % of the fluorescence due to u11-CMTMO-FAM by uPA was disappointing, although it could point to the conjugate having a higher affinity than the peptide alone. The fact that only 25 % inhibition was found when the concentration of u11-CMTMO-FAM was decreased 10-fold could indicate this. Although the shift in the curve indicates that this is likely to be the extent of specific binding. As 40 % inhibition was achieved with 50 μM Gu11G it seems likely that the conjugate is targeting the uPA receptor. Further experiments with increased concentrations of either uPA or Gu11G were not possible due to lack of u11-CMTMO-FAM.

Non-specific binding could have played a part in the cellular binding of peptide-CMTMO conjugates. uPA-FITC displacement experiments were not performed as it was considered that the conjugate may have bound to uPA-FITC rather than competing for the receptor. Whilst this would have been an interesting investigation, assessment of the uptake of the conjugate using fluorescent derivatives was deemed more important.

Although flow cytometry gives valuable information on the uptake of fluorescent ligands, and is a powerful method due to the large number of cells analysed, but little can be said of where the fluorescent derivative goes within the cell. This prompted study of the fluorescent conjugates by fluorescent microscopy. The localised binding seen in fluorescent microscopy was very interesting and could indicate the clustering of receptors in lipid rafts after binding the peptide. This would be consistent with reports of uPAR endocytosis in conjunction with LDLRP and other co-receptors (Conese et al., 1994, Czekay et al., 2001) and was similar to that seen in histochemistry experiments by Myohanen et al. (1993). Further investigation into the mechanisms involved using co-localisation studies, inhibitors and confocal microscopy would be intriguing. A limitation to the study performed here is that polyplexes formed with u11-CMTMO were not tested, this would undoubtedly have an effect on the binding and internalisation of the ligand.

In conclusion, these studies confirmed that uPAR is expressed on U937, U937 PMA, MCF-7 and DU145 cells making them a useful model for the binding and endocytosis studies conducted here and the transfection studies conducted later in Chapter 6.

Cell-uptake of Gu11G-conjugates in cells expressing uPAR has been demonstrated. This indicates that u11-CMTMO is suitable for further development of a targeted therapy. u7 was not found to inhibit the binding of uPA-FITC and neither were u7-PEG conjugates. The peptide-conjugate u11-CMTMO has been taken forward for development of a targeted polyplex formulation discussed in the next chapter.

Chapter 6

Development of a Novel Synthetic Gene Delivery System Using a uPAR-Targeted Conjugate

6.1 Introduction

In Chapter 4 TMO was shown to produce good transfection efficiency and to be significantly less cytotoxic when compared to PEI. As the breast and prostate cell lines (MCF-7 and DU145) were shown to express uPAR (Chapter 5), and Gu11G, u11-CMTMO-FAM, u11-CMTMO-OG and u11-PEG-FAM were shown to target uPAR (Chapter 5) it was now possible to examine the concept of a multi-component uPAR-targeted polyplex. In this chapter it is proposed that u11-CMTMO can form part of a uPAR targeted polyplex. From the results presented in Chapter 4, and those of Sato et al. (2001) that showed that optimum transfection was achieved with complexes formed at the pKa of chitosan, it was hypothesised that a DTM of approximately 50 % would produce the most effective transfection reagent. Therefore, a TMO with a DTM of 51.8 % was synthesised (Chapter 3) and used in this chapter to prepare u11-CMTMO polyplexes.

6.1.1 Targeted Synthetic Gene Delivery

As has been discussed (Section 1.5.3.2) many attempts have been made to design polyplexes that can be targeted to specific receptors/cells. They have shown varying degrees of success. Efficient targeted gene delivery has been reported using transferrin-targeted HPMA-PLL-based polyplexes that showed an approximately 15-fold increase in transfection of K562 cells compared with PLL polyplexes (Dash et al., 2000). Interestingly, no decrease in transfection efficiency with HPMA coated PLL-based polyplexes compared with PLL-polyplex mediated transfection was seen in this study (Dash et al., 2000). Perhaps the most substantial increase in transfection efficiency reported was that seen using galactose-targeted PEI polyplexes (Zanta et al., 1997). However, this increase was observed using PEI polyplexes prepared using a 2:1 N/P ratio (Zanta et al., 1997). This ratio is lower than that normally used. A similar formulation did not produce this increase, it actually decreased it (Kunath et al., 2003b) this may be due to the more optimal N/P ratios studied.

Trastuzumab, which has found success in the treatment of HER2 positive breast cancer (Leyland-Jones et al., 2003), has also been conjugated to PEI for use as a targeted gene delivery vector (Chiu et al., 2004). A 20-fold increase in transfection efficiency in Sk-Br-3 (HER2 expressing cells) was detected over that found with PEI polyplexes at a 10:1 N/P ratio (Chiu et al., 2004). This increase could be competed with

free trastuzumab, and was not found in a cell line expressing low levels of HER2 (MDA-MB-231) (Chiu et al., 2004). It was estimated that each polyplex would contain 475 DNA molecules and 3185 trastuzumab molecules based on the size of each component and the size of the polyplex (250 nm), and it was proposed that this would lead to polyvalent interactions which would increase cellular uptake (Chiu et al., 2004).

In peptide-mediated targeting, phage display derived peptides have been widely used (Arap et al., 2002, Jost et al., 2001, Maruta et al., 2003, Nilsson et al., 2000, Trepel et al., 2002). Parker et al. (2005) found a 10.4-fold higher uptake of pDNA in HUVEC cells using SIGYPLP (a phage display derived peptide) targeted PLL particles. This increased uptake did not translate into an increased expression in the HUVEC cell line. This could have been due to the slow growth of the cells, and therefore limited access to the nucleus, but increased expression was seen in faster growing cell lines such as B16F10 (Parker et al., 2005). These SIGYPLP-pHPMA-coated PLL polyplexes produced increased transfection compared with that found using pHPMA-coated PLL polyplexes. This transfection efficiency was further increased by addition of chloroquine (approximately 100-fold) (Parker et al., 2005). Further to their work on non-viral gene delivery successful re-targeting of adenovirus using SIGYPLP-pHPMA coating was reported (Parker et al., 2005).

A targeted liposomal formulation is currently being investigated clinically (Phase I). This vector is comprised of a DOTAP/DOPE (1:1) liposome coated with a single chain anti-transferrin antibody fragment and it contains the wild type gene for p53 (Marshall, 2005). Pre-clinical studies showed high transfection efficiency of prostate, breast, head, neck and pancreatic tumour cells but not normal fibroblasts (Marshall, 2005). *In vivo* tumour growth was inhibited in pre-clinical studies when the liposome was delivered systemically and used in combination with standard chemotherapy or radiotherapy (Marshall, 2005).

6.1.2 Factors Affecting Polyplex Formation and Methods of Polyplex Characterisation

It is apparent that non-specific, cation-mediated interaction with the cell membrane can be lost when the polyplex contains additional polymers or targeting residues (van Steenis et al., 2003). The transfection mechanism used by targeted polyplexes can also be very different due to internalisation through RME. Therefore, although targeted vectors may not yet have achieved the remarkable increases in transfection efficiency

expected, the fact that they may achieve cell-specific uptake potentially makes them a more effective therapy.

There are many factors that influence the size and shape of complexes formed. These include: the polymer identity (PEI, PLL etc.), size and shape of polymer, nucleotide size and form (oligonucleotide, open plasmid, coiled plasmid, nicked plasmid), temperature of polyplex formation, volume of the solutions used, order of solution addition, salt concentration and solution pH (as discussed in Section 1.4.2.1).

Several methods have been used to investigate the formation of polyplexes. The EtBr exclusion assay works on the basis that cation complexed DNA prevents or reduces the intercalation of EtBr with DNA and therefore reduces its fluorescence (Ex 510 nm, Em 590 nm) (Barrett et al., 2004, Kunath et al., 2003a). Assessment of polyplexes using agarose gel electrophoresis is a commonly used technique where polyplex migration is retarded in the gel (Akinc et al., 2003, Blessing et al., 1998, Chen et al., 1994). This enables study of a range of plasmid : pDNA ratios simultaneously to determine the lowest ratio which forms a polyplex. Polyplex size is often assessed using PCS, particle size is determined by the Brownian motion of the particle in solution; its speed being inversely proportional to the size of the polyplex (Brown et al., 2000, Dash et al., 1997, Jillavenkatesa et al., 2005, Thanou et al., 2002). Care should be taken in the interpretation of PCS spectra as a multimodal distribution of particle sizes may not be determined (Frantzen et al., 2003).

Many studies use DNA as a model for the plasmid that would ultimately be used in transfection studies e.g. *λ Hind III*, salmon testes DNA or calf thymus DNA (Jones et al., 2000, Kim et al., 2003, Kim et al., 2001, Kunath et al., 2003a, Richardson et al., 1999b, Richardson et al., 2001). Others have investigated polyplex formation using the plasmid to be transfected e.g. pCMV CAT (Lee et al., 1998) and pGL3 luc (Kunath et al., 2003a). The advantage of using model DNA is that it is commercially available and cheap. The use of the transfection plasmid may be more expensive or time consuming but gives a more reliable representation of the polyplex which would be formed in transfection experiments.

6.1.3 Ideal Characteristics of Polyplexes

The reproducible production of uniform, small polyplexes is a complicated procedure that is thought necessary for efficient delivery of nucleic acids. This profile is

sought for a variety of reasons. *In vitro* this profile is sought due to the array of endocytic pathways available for < 200 nm nanoparticles to enter the cell (Hashizume et al., 2000, Rejman et al., 2004, Slepnev & Camilli, 1998). However, the formation of large particles, due to aggregates, has been found to increase *in vitro* transfection through their postulated sedimentation onto cells (Ogris et al., 1998). Whereas, the small particles (30 – 60 nm) stay in solution and only come into contact with the cells through Brownian motion (Ogris et al., 1998). Cherng et al. (1996) found that the optimum pDMAEMA derived polyplex size was 140 – 170 nm for the transfection of COS-7 cells.

In vivo a small polyplex is additionally required due to the need to extravasate from the blood stream to enter interstitial spaces for subsequent uptake into tumour cells. Capillary fenestra allow extravasation of small particles (up to approximately 200 nm) (Takakura et al., 1998, Takakura et al., 2002). Small size also minimises RE capture by macrophages and prevents deposition in the lung due to entrapment in alveoli (Cannon & Swanson, 1992, Freitas, 2003). In contradiction to this theory, Kursa et al. (2003) found that large (1 μm) complexes produced efficient tumour localisation of luciferase expression with transferrin targeted PEI polyplexes. This localisation is puzzling, but could be due to the EPR effect (Section 1.3.1).

The positively charged TMO may be expected to interact with serum proteins. This would interfere with polyplex formation. However, it was found that serum did not decrease transfection efficiency of COS-1 cells (Thanou et al., 2002). Although the lack of decrease in transfection efficiency could be due to the previously mentioned effect of polyplex sedimentation onto the cells. Temperature undoubtedly could have an effect on polyplex formation but this is not a widely studied parameter. Where reported at all it is only mentioned briefly indicating that polyplexes were produced at r.t. (Fischer et al., 2001). In order to achieve efficient polyplex formation it has been recommended that polymer-containing solution is added to the DNA. This method of preparation gave a 10-fold higher transfection efficiency over that seen using polyplexes formed by the reverse method (Boussif et al., 1995). Here it was anticipated that the addition of a peptide-conjugated component to the system would have an effect on polyplex formation as similar effects have been reported when peptide- or PEG- cation conjugates have been used (Kursa et al., 2003).

6.1.4 Parameters Considered and Actions Taken in Preparation of u11-Targeted Polyplexes

It is now well known that a number of factors affect the nature of the polyplexes formed and their stability in biological solutions (e.g. culture medium, serum etc.). The parameters discussed above were considered and the actions taken are listed here.

1) For the transfection studies described in this thesis branched PEI was selected as a positive control. PEI displays a high transfection efficiency making it an accepted reference standard (Boussif et al., 1995).
2) To understand, and therefore interpret, the final result of a transfection (which has several barriers to overcome as discussed in Section 1.4.2.1.2) studies were made into the size, stability and shape of polyplexes produced with TMO and when u11-CMTMO was included in the formulation. These studies were performed using PCS, agarose gel electrophoresis and TEM.
3) It was decided that, in order to have an accurate model of the complexes formed with the plasmid, and therefore give the best prediction of polyplex formation, the reporter plasmid used in transfection experiments (pGL3 luc) should be used in the formulation studies.
4) Polyplexes were formed in DMEM. This meant that that because the polyplexes were formed in a physiological salt solution they could be applied directly to the cells. The same polyplex formulations that were applied to cells were also characterised by agarose gel and PCS. This would also ensure that the polyplexes were not disrupted by dilution or salt change when added to the cells, and what was measured in the characterisation experiment was an accurate model of the formulation to which the cells were exposed.
5) Serum was excluded from the solution used in the formation of the complexes to avoid any interaction and therefore destabilisation or interference with polyplex formation. It is also possible that polyplexes would have interacted with serum producing another confounding factor. Therefore, serum was excluded from the solutions incubated on the cells. Although this is not an accurate representation of the *in vivo* environment, it was considered that the polyplexes should be applied under the same conditions as those used for fluorescent targeted CMTMOs (Chapter 5). In addition, the reduction of variables was expected to benefit the study through optimising the vector in the absence of serum.

6) Polyplexes were formed at r.t. in media that had been allowed to equilibrate with room temperature. Polymer containing solutions were added to DNA solutions. A single step and a two step mixing process were investigated in an emulation of the experiments performed by Kursa et al. (2003). This was performed to increase the probability of the ligand being localised to the surface of the polyplex.

In summary the aims of this chapter were: to optimise the formation of polyplexes with TMO51 and then in a multi-component system using pGL3 luc, TMO51 and u11-CMTMO or pGL3 luc, PEI and u11-CMTMO; to determine the effect of the parameters measured in non-biological systems (i.e. size, stability and shape) on the transfection efficiency found *in vitro*; and finally, to optimise this multi-component system in order to achieve increased expression of luciferase over control polyplexes.

6.2 Methods

Polyplexes were prepared essentially as described in Section 4.2.3, pGL3 luc was aliquoted into bijous and cationic vector solution, (or mixture when u11-CMTMO included) (in DMEM) added at the specified ratios (Table 6.1) and vortexed for 10 s. Polyplexes were allowed to form for 20 min before application to the cells. In addition, a two step polyplex formation procedure was also developed to preferentially incorporate u11-CMTMO on the polyplex surface (Fig. 6.1). To form polyplexes, pGL3 luc (27 μg) was aliquoted into bijous (5 ml vessels). Cationic vector (PEI or TMO51) solutions (in DMEM) at the specified ratios (Table 6.1) were then added and the mixture was vortexed, at low speed to avoid pDNA shearing, for 10 s. After a 5 min incubation at r.t. the u11-CMTMO solution (in DMEM) was added to the bijou at the specified ratios (Table 6.1) and a further vortex of 10 s performed. These mixtures were then allowed to incubate at r.t. for a further 15 min before application to cells.

The polyplexes formed in this way were analysed by agarose gel electrophoresis as described in Section 2.3.8 and by PCS as described in Section 2.3.12.

Transmission electron microscopy (TEM) was also performed in Electron Microscopy facilities in Imperial College, London. First, copper grids coated with collagen and carbon (supplied by Imperial College) were negatively charged in a moderate vacuum. Then a drop (10 μl) of polyplex containing (10:1 TMO: pGL3 luc) solution was applied. The grid was blotted with filter paper and negatively stained with 1 % uranyl acetate twice for 1 min.

Table 6.1 - Formulations used in the investigation of uPAR targeted polyplexes

Procedure	Ratio of cation : pGL3 luc (w/w) TMO51	PEI	u11-CMTMO	Gu11G
1 step	0.01 - 30	-	-	-
1 step	-	1 - 2	-	-
1 step	-	-	3 - 9	-
1 step	1	-	5	-
2 step	-	10	-	0.5 – 5
2 step	1 – 10	-	2.5 – 5	-
2 step	-	2	2 – 5	-

In 2 step procedures the polycation (PEI or TMO51) is added in the first step and the targeting group (u11-CMTMO or Gu11G) is added in the second step

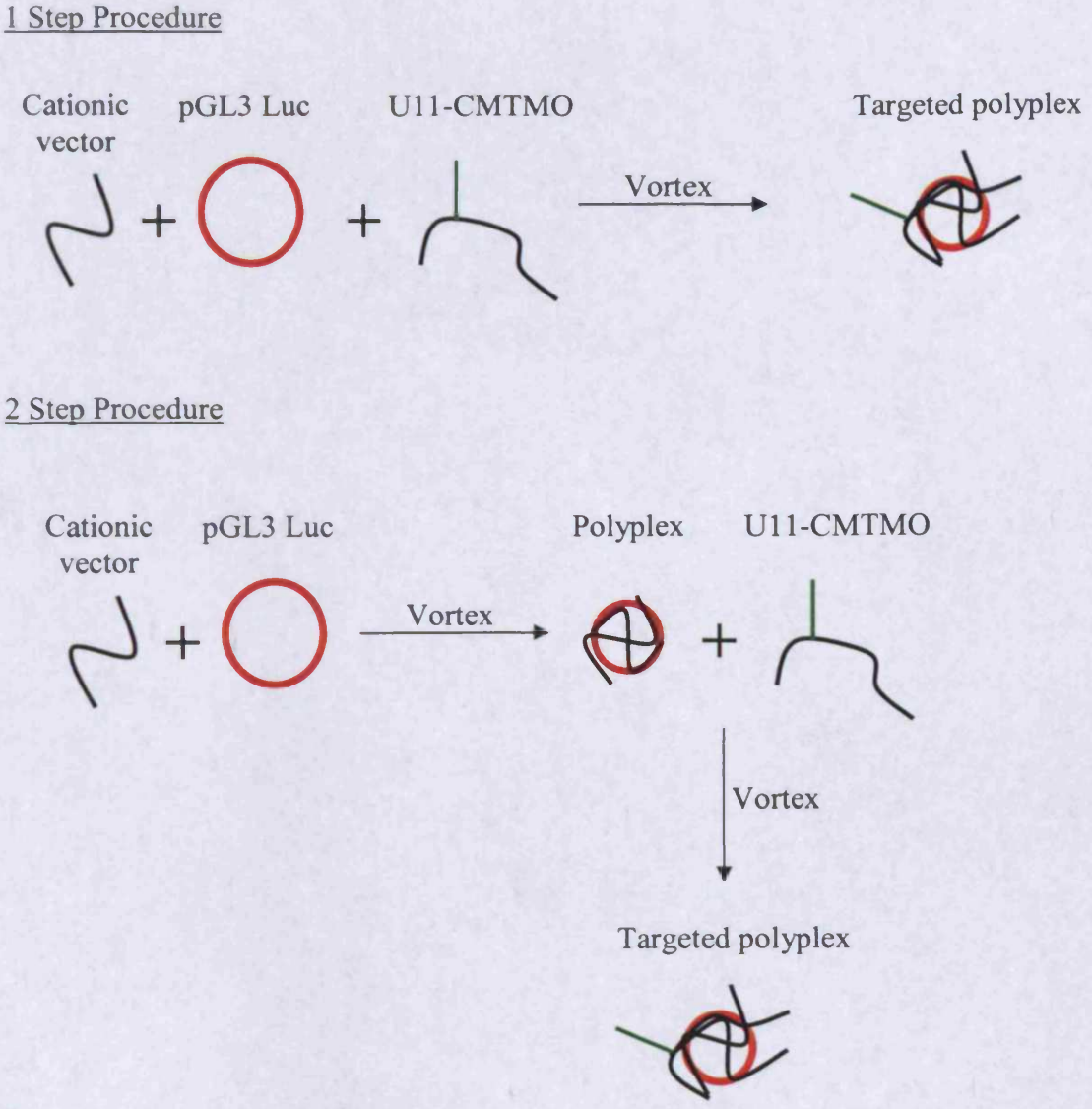

Figure 6.1 – Strategies for the preparation of u11-CMTMO-targeted polyplexes

Uranyl acetate staining was performed by dipping the grid in 1 % uranyl acetate left for 1 min, then in ddH_2O and the excess solution removed with filter paper and the grid left in the air to dry. Samples were prepared in triplicate. The TEM was a TECAN at 120 kV and images were collected with a TECAN CCD camera (Tietz) and analysed with TEM Software.

Luciferase expression was measured through luminescence measurements as described in Section 2.3.6.

6.3 Results

6.3.1 Characterisation of TMO51 : pGL3 luc and PEI : pGL3 luc Polyplexes

Retardation of the TMO51 : pGL3 luc polyplex (ratio 2:1 w/w) at the point of application was seen (Fig. 6.2). Inhibition of pGL3 luc migration was also seen at much lower ratios, with very slight retardation at 0.1:1 and a more significant retardation at 0.5:1 (Fig. 6.2). PCS analysis showed that the polyplexes formed at a ratio of 0.01:1, 1:1, 2:1 and 10:1 had an average size of 581, 688, 286 and 119 nm respectively (Fig. 6.3). Polyplex size (10:1 TMO51 : pGL3 luc w/w) observed by TEM was similar to that seen by PCS (Fig. 6.4). In addition TEM showed that these polyplexes were spherical, onion like structures with sizes between 45 and 160 nm.

The effect of the volume of TMO51 solution added to plasmid solution, at the same TMO : pGL3 luc ratio (w/w), was studied by PCS. The most efficiently packed polyplexes were produced with the largest volume of polymer solution added to the smallest volume of pDNA solution (Table 6.2).

Polyplex formation with PEI was also studied using agarose gel electrophoresis and a ratio of 1.25:1 (w/w; 9:1 N/P) did not completely retard pGL3 luc. However, at 1.5:1 (w/w; 10.8:1 N/P) and 1.75:1 (w/w; 12.6:1 N/P) complete plasmid retardation was found (data not shown). At these ratios of PEI poor transfection efficiency was observed, at a 2:1 (w/w) ratio superior transfection efficiency was achieved.

6.3.2 Characterisation of u11-CMTMO : pGL3 luc Polyplexes

Having established that polyplexes were formed at a 2:1 ratio with TMO51 : pGL3 luc a study of polyplexes formed with u11-CMTMO : pGL3 luc was made (Fig. 6.5). Analysis using agarose gel showed increasing retardation of pGL3 luc with an increasing concentration of u11-CMTMO (Fig. 6.5). However, complete polyplex formation was not found at any of the u11-CMTMO/polyplex ratios studied (Fig. 6.5).

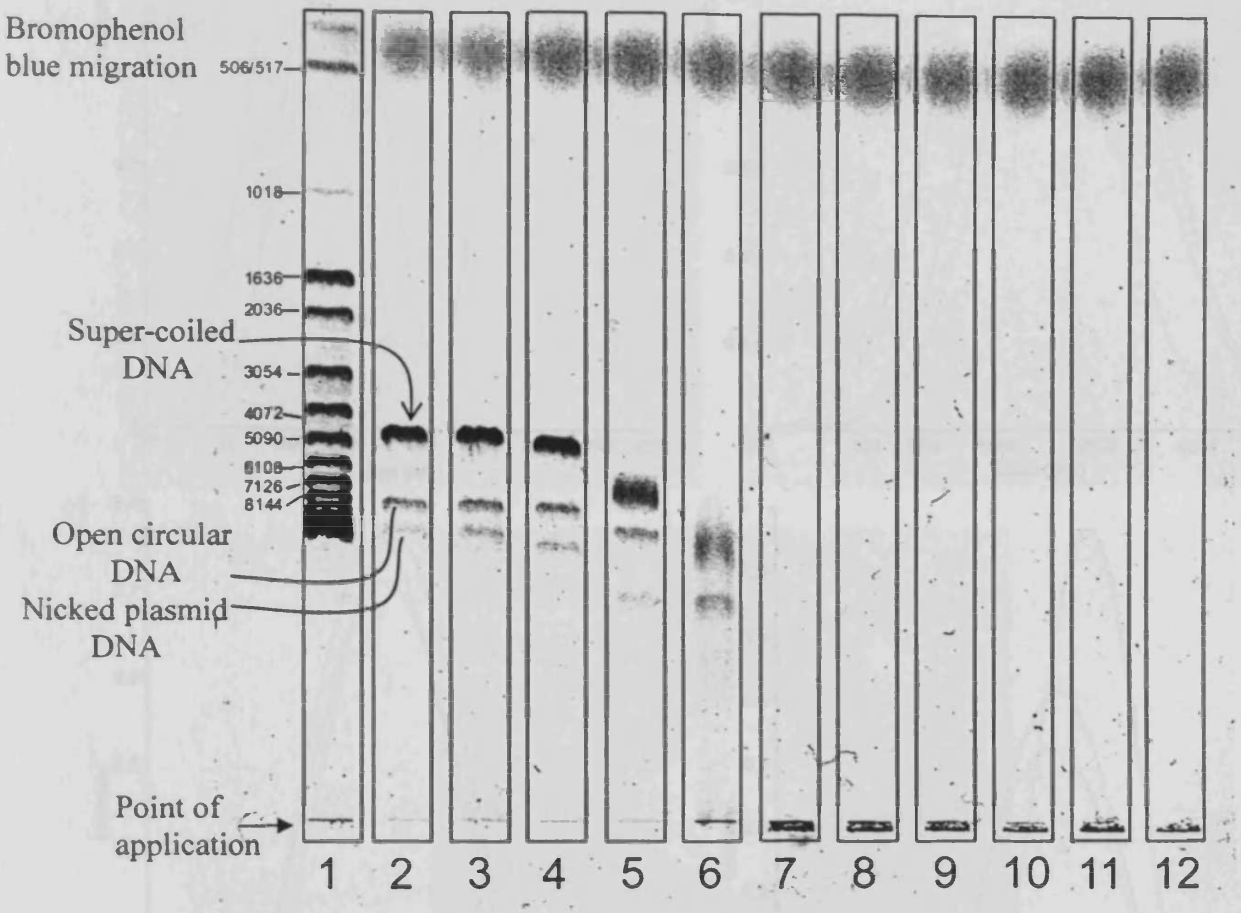

Figure 6.2 – Polyplex analysis by agarose gel electrophoresis

The data show polyplexes produced with increasing ratio of TMO51: pGL3 luc (w/w).
Lanes show:
1) 1 kb ladder (Invitrogen),
2) pGL3 luc,
3) 0.01:1 TMO51 : pGL3 luc,
4) 0.1:1 TMO51 : pGL3 luc,
5) 0.5:1 TMO51 : pGL3 luc,
6) 1:1 TMO51 : pGL3 luc,
7) 2:1 TMO51 : pGL3 luc,
8) 3:1 TMO51 : pGL3 luc,
9) 4:1 TMO51 : pGL3 luc,
10) 14:1 TMO51 : pGL3 luc,
11) 20:1 TMO51 : pGL3 luc,
12) 30:1 TMO51 : pGL3 luc.

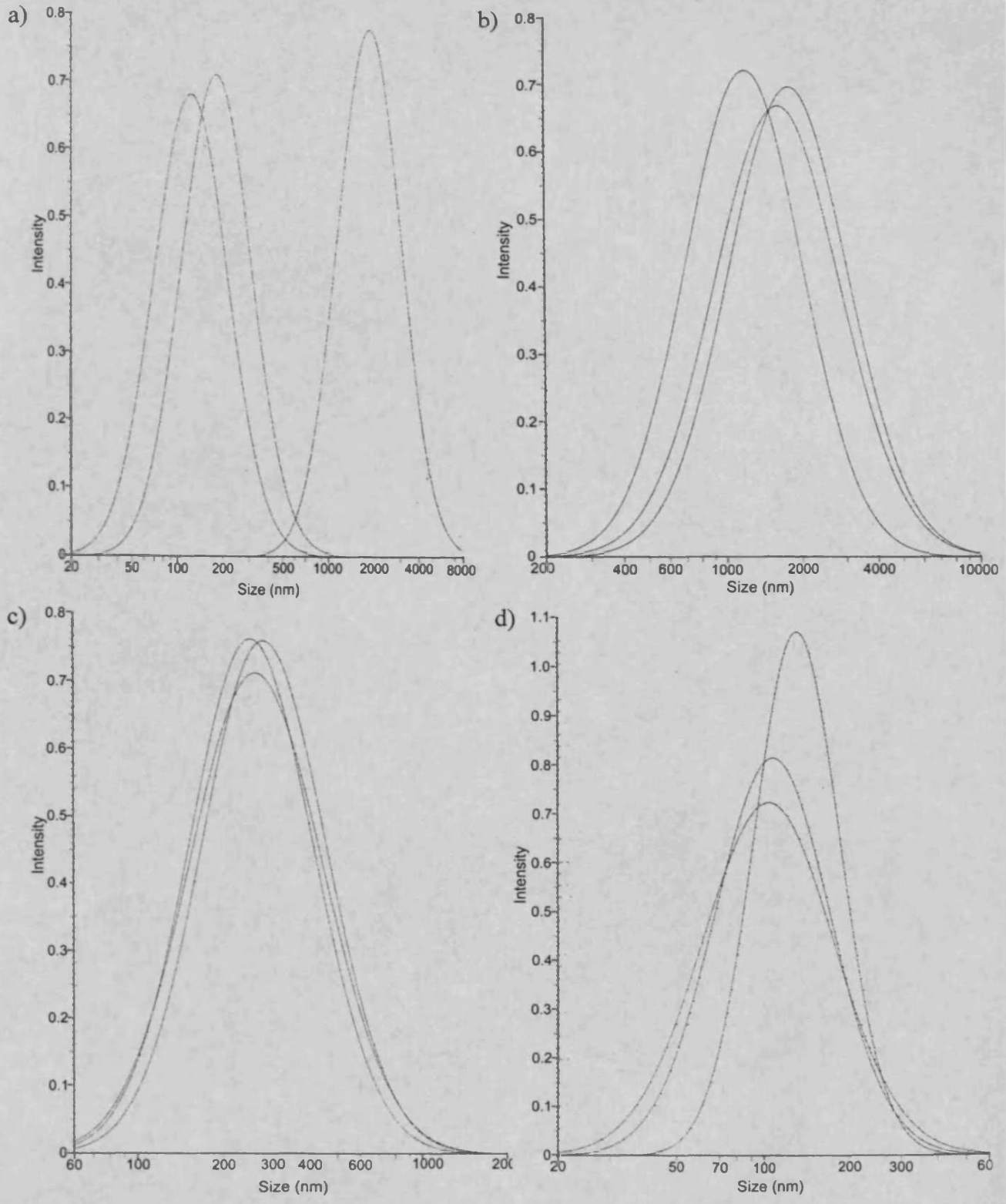

Figure 6.3 – Size of TMO51 : pGL3 polyplexes measured by PCS

These data show the size distribution of polyplexes of TMO : pGL3 luc assessed by PCS. Charts show triplicate curves for polyplexes prepared at TMO51 : pGL3 luc ratios:
a) 0.01:1 TMO51 : pGL3 luc,
b) 1:1 TMO51 : pGL3 luc,
c) 2:1 TMO51 : pGL3 luc,
d) 10:1 TMO51 : pGL3 luc
(note different size scales).

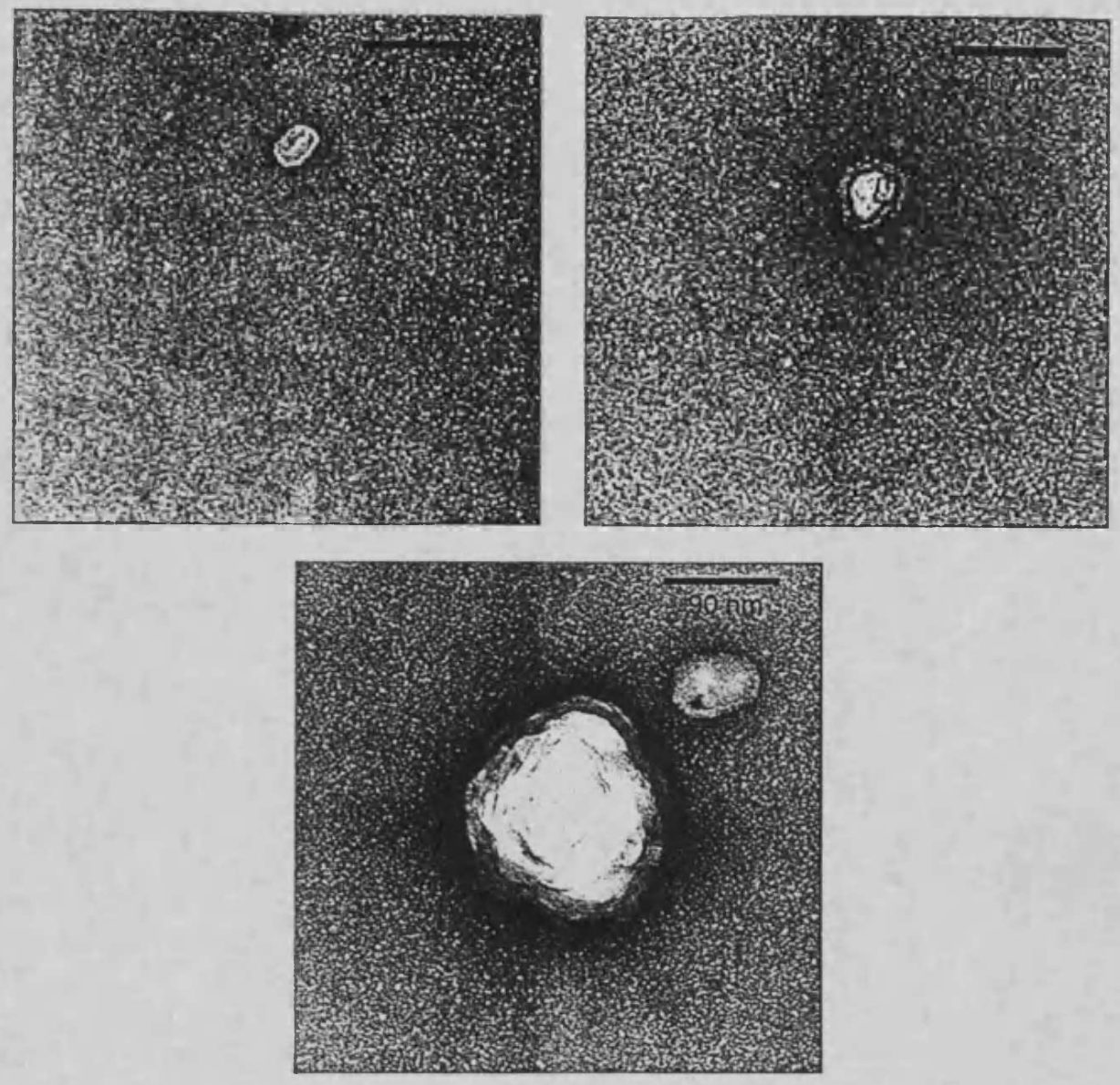

Figure 6.4 TEM pictures of polyplexes formed with TMO51: pGL3 luc

Negatively stained pictures of TMO : pGL3 luc (10:1 w/w) polyplexes having approximate sizes of 45-160 nm. Pictures represent a sample taken from triplicate experiments.

Table 6.2 – Effect of solution volume on polyplex size assessed by PCS

Volume of TMO (µl)	Volume of pGL3 luc (µl)	Average Size (nm)
10	10	1240.2
100	10	692.1
300	10	511.4

Solutions were made to 2 ml immediately prior to PCS analysis, data represent mean (n = 3).

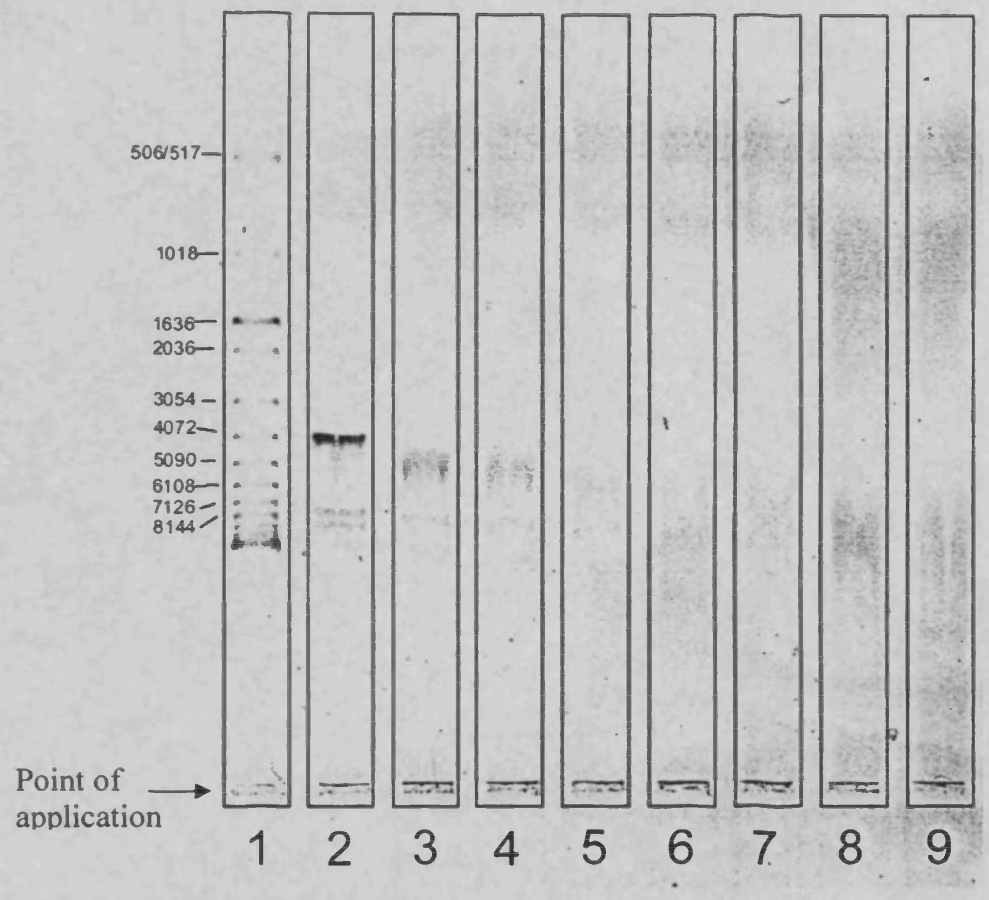

Figure 6.5 – Agarose gel analysis of u11-CMTMO : pGL3 luc polyplexes

Analysis of polyplexes produced with increasing ratio of u11-CMTMO : pGL3 luc (w/w). Lanes show:
1) 1 kb DNA ladder (Invitrogen),
2) pGL3 luc,
3) 3:1 u11-CMTMO : pGL3,
4) 4:1 u11-CMTMO : pGL3,
5) 5:1 u11-CMTMO : pGL3,
6) 6:1 u11-CMTMO : pGL3,
7) 7:1 u11-CMTMO : pGL3,
8) 8:1 u11-CMTMO : pGL3,
9) 9:1 u11-CMTMO : pGL3

6.3.3 Gu11G-Coated PEI : pGL3 luc Polyplexes

The transfection efficiency of peptide (Gu11G) coated PEI : pGL3 luc polyplexes was assessed, Gu11G was used in a non-covalent manner as a coating on PEI complexes. This resulted in a decrease in luciferase expression compared with that found for uncoated PEI : pGL3 luc polyplexes in MCF-7 cells (Fig. 6.6a) at all concentrations of Gu11G tested.

In COS-1 cells there was also a decrease in luciferase expression at 1, 2 and 10 μg/well Gu11G (Fig. 6.6b). However, when polyplexes were co-incubated with 3 μg/well of Gu11G, there is an apparent increase in expression, although this was not statistically significant. Repetition of this experiment with the inclusion of COS-7 cells allowed for a comparison to be made between the three cell lines similar levels and patterns of luciferase expression were found (Fig. 6.7). Again, a decrease in transfection efficiency was apparent in all three cell lines (Fig. 6.7).

6.3.4 Transfection of COS-7, DU145 and MCF-7 with TMO51 Polyplexes and u11-CMTMO Coated TMO51 Polyplexes.

In transfection experiments on COS-7, DU145 and MCF-7 cells, poor transfection efficiency with TMO : pGL3 luc at a 2:1 ratio was seen in all cell lines (Fig. 6.8). The addition of u11-CMTMO in either a 1 step procedure or a 2 step procedure reduced the efficiency of transfection, although the 2 step procedure appeared to decrease transfection efficiency by a smaller amount.

From previous experiments (Chapter 4) a higher ratio of TMO (10:1) gave superior transfection efficiencies. The two step transfection protocols on COS-7, DU145 and MCF-7 cells using this ratio of TMO : pGL3 luc and coating of the polyplexes with u11-CMTMO gave no significant difference in transfection efficiency compared to TMO alone ($p>0.05$ ANOVA) (Fig. 6.9).

6.3.5 Characterisation of u11-CMTMO-Coated TMO51 Polyplexes

All polyplexes were efficiently retarded in agarose gel electrophoresis (Fig. 6.10). An increase in polyplex size was seen when u11-CMTMO was used to coat TMO51 polyplexes. When u11-CMTMO was included at a 2:1 (u11-CMTMO : pGL3 luc, w/w) ratio complexes were 89 % larger (Fig. 6.11b), at a 5:1 ratio complexes were 59 % larger (Fig. 6.11c).

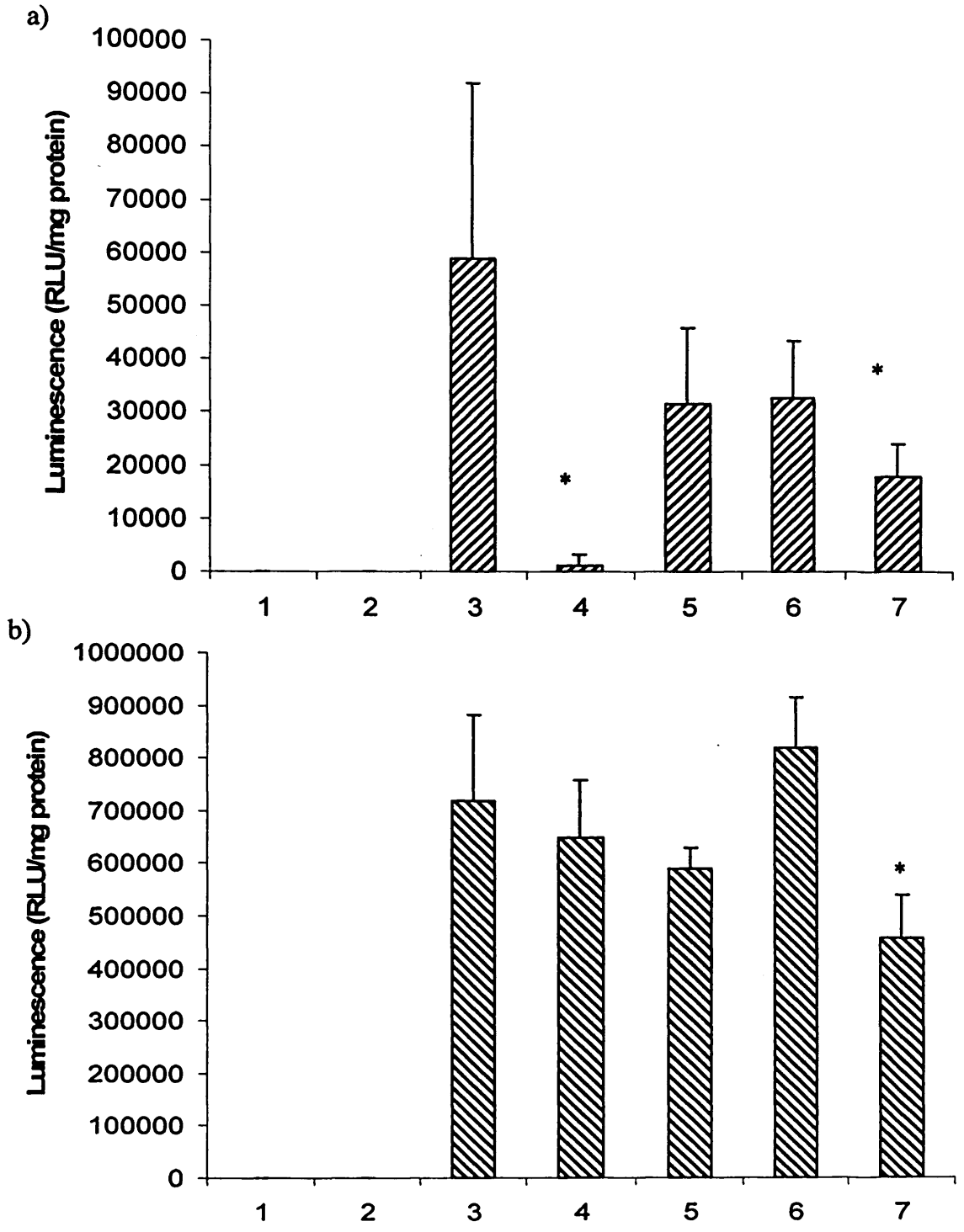

Figure 6.6 – Investigation of the ability of Gu11G-coated PEI : pGL3 luc polyplexes to transfect MCF-7 and COS-1 cells

The data shown represent the transfection of a) MCF-7 cells, b) COS-1 cells. The histogram key represents:
1) cells alone,
2) naked pGL3 luc,
3) PEI : pGL3 luc (10:1)
4) PEI : pGL3 luc (10:1) + 1 μg/well Gu11G 2 step,
5) PEI : pGL3 luc (10:1) + 2 μg/well Gu11G 2 step,
6) PEI : pGL3 luc (10:1) + 3 μg/well Gu11G 2 step,
7) PEI : pGL3 luc (10:1) + 10 μg/well Gu11G 2 step.
The data represents mean ± SD (n =4), * statistically significant difference compared to PEI ($p < 0.05$, ANOVA followed by Bonferroni post hoc test).

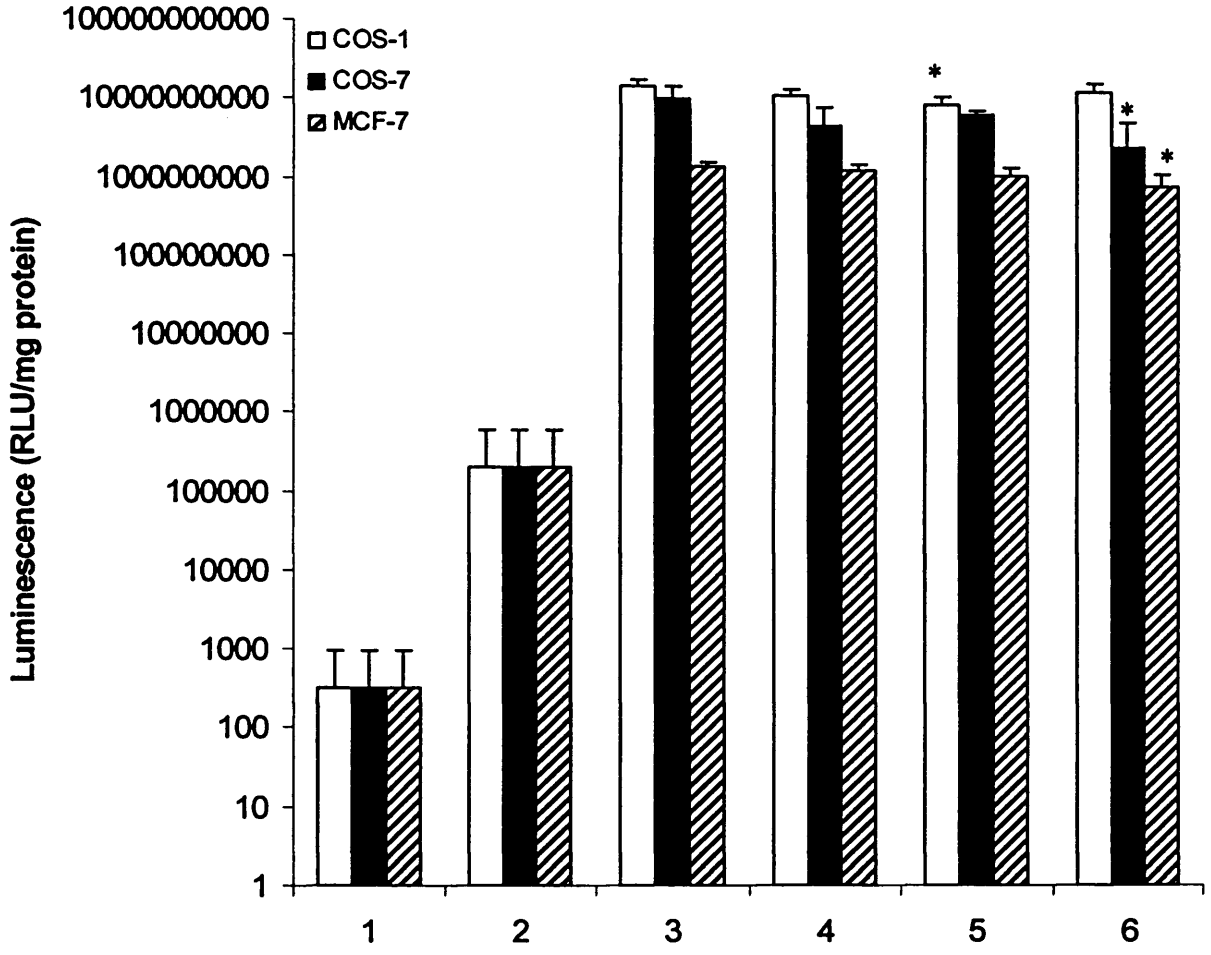

Figure 6.7 – Comparison of the transfection efficiency achieved in COS-1, COS-7 and MCF-7 cells transfected with Gu11G-coated PEI polyplexes

The histogram key represents:
1) cells alone,
2) naked pGL3 luc,
3) PEI : pGL3 luc (10:1)
4) PEI : pGL3 luc (10:1) + 1 μg/well Gu11G 2 step,
5) PEI : pGL3 luc (10:1) + 2 μg/well Gu11G 2 step,
6) PEI : pGL3 luc (10:1) + 3 μg/well Gu11G 2 step.
Data represents mean ± SD (n = 4), * statistically significant difference compared to PEI : pGL3 luc ($p < 0.05$, ANOVA followed by Bonferroni post hoc test).

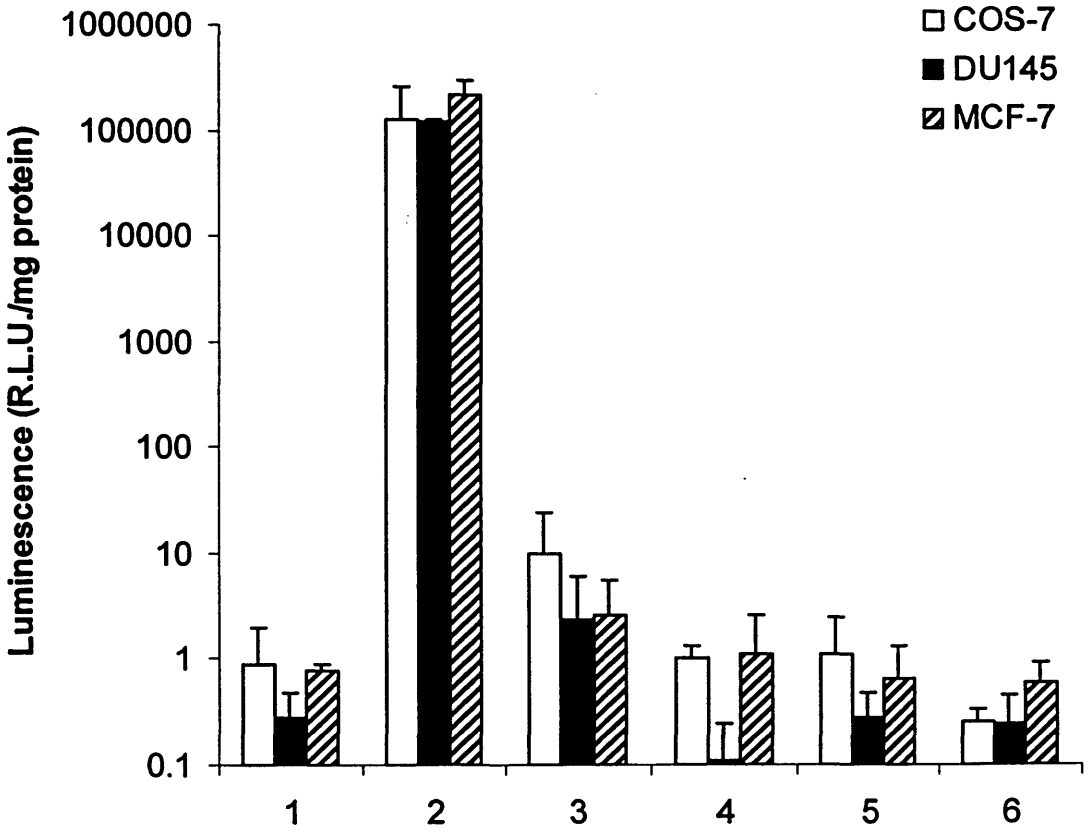

Figure 6.8 – Transfection efficiency of COS-7, DU145 and MCF-7 cells transfected with u11-CMTMO-coated TMO51 polyplexes

Luciferase activity of cells transfected with:
1) Naked pGL3 luc,
2) PEI: pGL3 luc (2:1),
3) TMO: pGL3 luc (2:1),
4) TMO: u11-CMTMO: pGL3 luc (1:5:1) 1 step,
5) TMO: u11-CMTMO: pGL3 luc (1:5:1) 2 steps,
6) TMO: u11-CMTMO: pGL3 luc (1.5:2.5:1) 2 steps.
Data represents mean ± SD (n = 4).

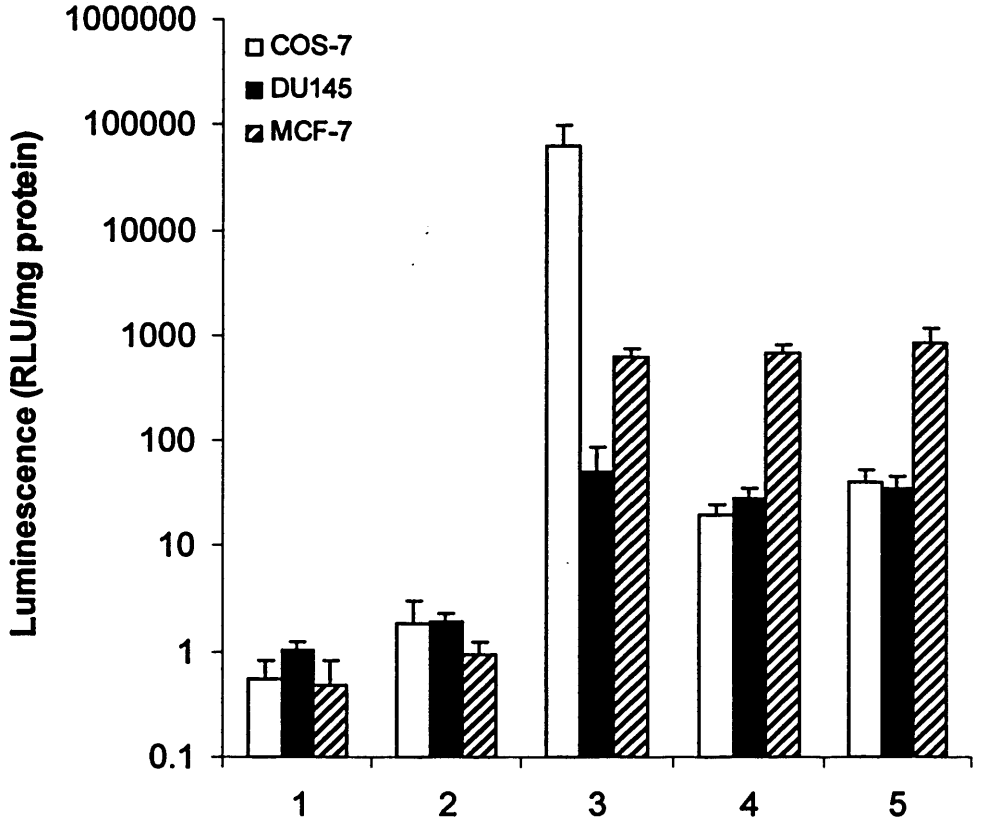

Figure 6.9 – Transfection efficiency of COS-7, DU145 and MCF-7 cells transfected with u11-CMTMO-coated TMO51 polyplexes

Data show the luciferase activity of cells transfected with:
1) cells alone
2) naked pGL3 luc
3) TMO51: pGL3 luc (10:1)
4) TMO51: u11-CMTMO: pGL3 luc (10:2:1)
5) TMO51: u11-CMTMO: pGL3 luc (10:5:1)
All formulations were produced in a two step procedure. Data represents mean ± SEM (n = 6).

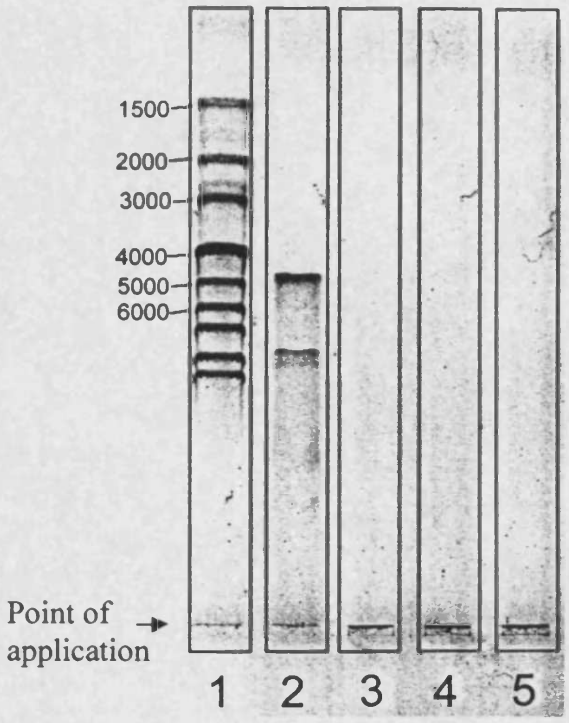

Figure 6.10 – Agarose gel analysis of u11-CMTMO-coated TMO polyplexes

Lane key:
1) 1 kb DNA ladder (New England Biolabs),
2) pGL3 luc,
3) TMO51: pGL3 luc (10:1),
4) TMO51: u11-CMTMO: pGL3 luc (10:2:1),
5) TMO51: u11-CMTMO: pGL3 luc (10:5:1).
All formulations were produced in a 2 step procedure.

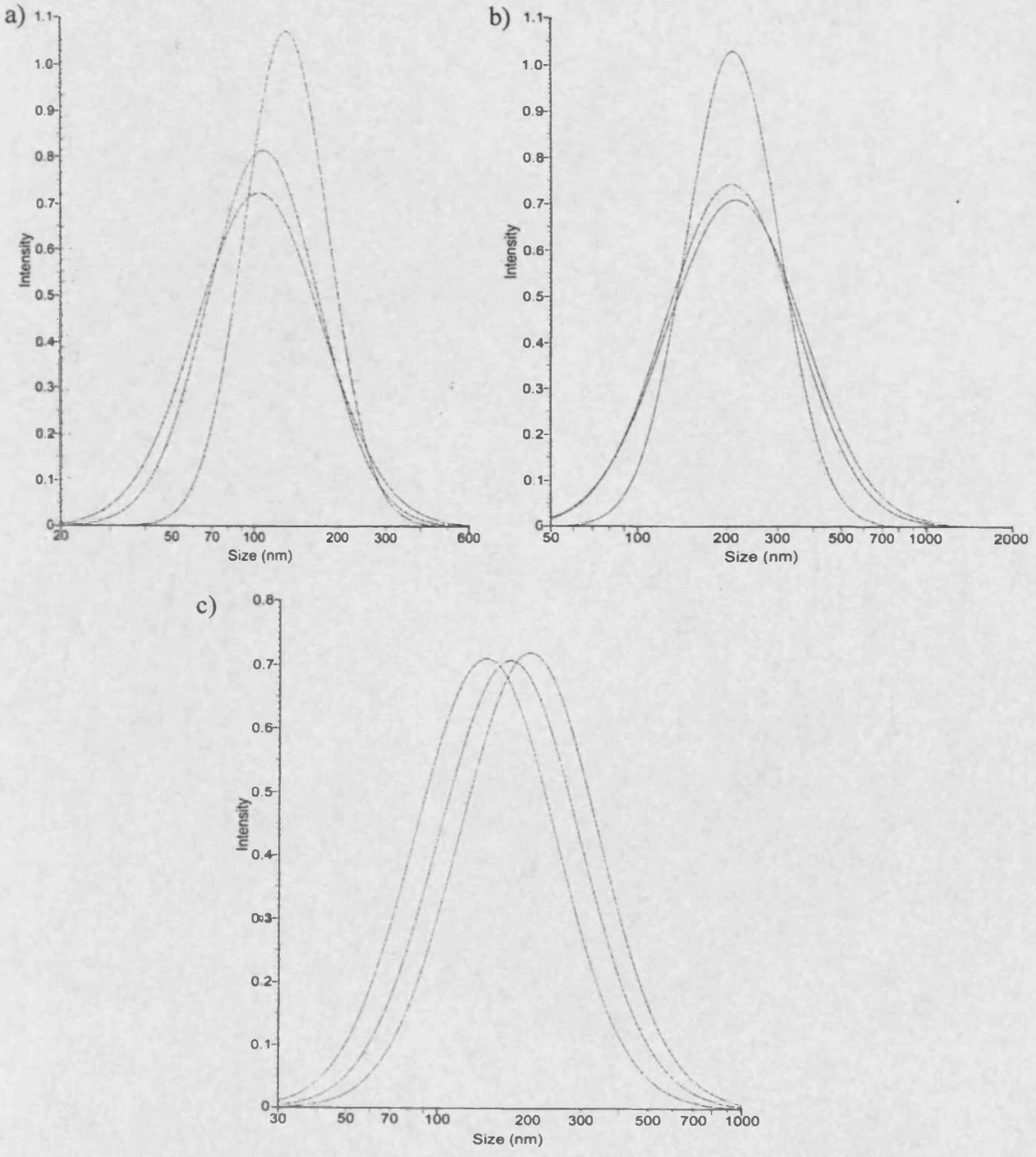

Figure 6.11 – Analysis of u11-CMTMO-coated TMO polyplex size by PCS

Data show the size distribution of:
a) TMO51: pGL3 luc (10:1) average size 119 nm,
b) TMO51: u11-CMTMO: pGL3 luc (10:2:1) average size 225 nm,
c) TMO51: u11-CMTMO: pGL3 luc (10:5:1) average size 189 nm
Formulations were produced in a 2 step procedure. Note size scale (triplicate results).

6.3.6 Transfection of COS-7, DU145 and MCF-7 with u11-CMTMO-Coated PEI Polyplexes

u11-CMTMO-coated polyplexes of PEI : pGL3 luc were also studied. The transfection efficiency of these coated complexes were not significantly different to those seen for PEI polyplexes ($p>0.05$ ANOVA) (Fig. 6.12).

6.3.7 Characterisation of u11-CMTMO-Coated PEI Polyplexes

All polyplexes were retarded in agarose gel electrophoresis (Fig. 6.13). The size of polyplexes produced with PEI also increased in size when u11-CMTMO was used as a coating. When u11-CMTMO was included at a 2:1 (u11-CMTMO : pGL3 luc, w/w) ratio complexes were 5 % larger (Fig. 6.14b) and at a 5:1 ratio complexes were 50 % larger (Fig. 6.14c).

6.4 Discussion

In the first steps of polyplex optimisation the aim was to produce small polyplexes with little excess surface charge. The use of N/P ratios is an arbitrary measurement and is difficult to assess effectively. The number of phosphate groups available for interaction is likely to be less than half of those present due to the duplex nature of DNA. The charge on the amine groups present (apart from quaternised groups) is affected by the pH of the solution (microenvironment) and the pKa of the amine. Therefore w/w ratios were used, as for a polymer with peptide substitution and as a multi-component system this was simpler.

Through agarose gel analysis it was found that polyplexes were formed at a low w/w ratio of TMO51 : pGL3 (0.5:1). At a lower ratio (0.01:1 TMO51 : pGL3 luc) PCS showed two populations, this indicates that polyplexes had formed (Fig. 6.3a) but that the solution was unstable and large aggregates formed. The size of polyplexes at a 2:1 ratio measured by PCS was larger than 200 nm (Fig. 6.4) indicating that clathrin-coated vesicles would not be available for the endocytosis of the polyplex, but that endocytosis through caveolae would still be possible (Rejman et al., 2004). At a higher ratio smaller complexes were formed although the inclusion of u11-CMTMO increased the size of these to greater than 200 nm (Fig. 6.11). This potential restriction of the endocytic pathway to caveolae may be responsible for the reduction in transfection efficiency. However, this restriction to caveolae may be a beneficial aspect to RME as Rejman et al. (2004) found that 500 nm particles were not directed to late endosomal or lysosomal compartments in B16F10 (murine melanoma) cells.

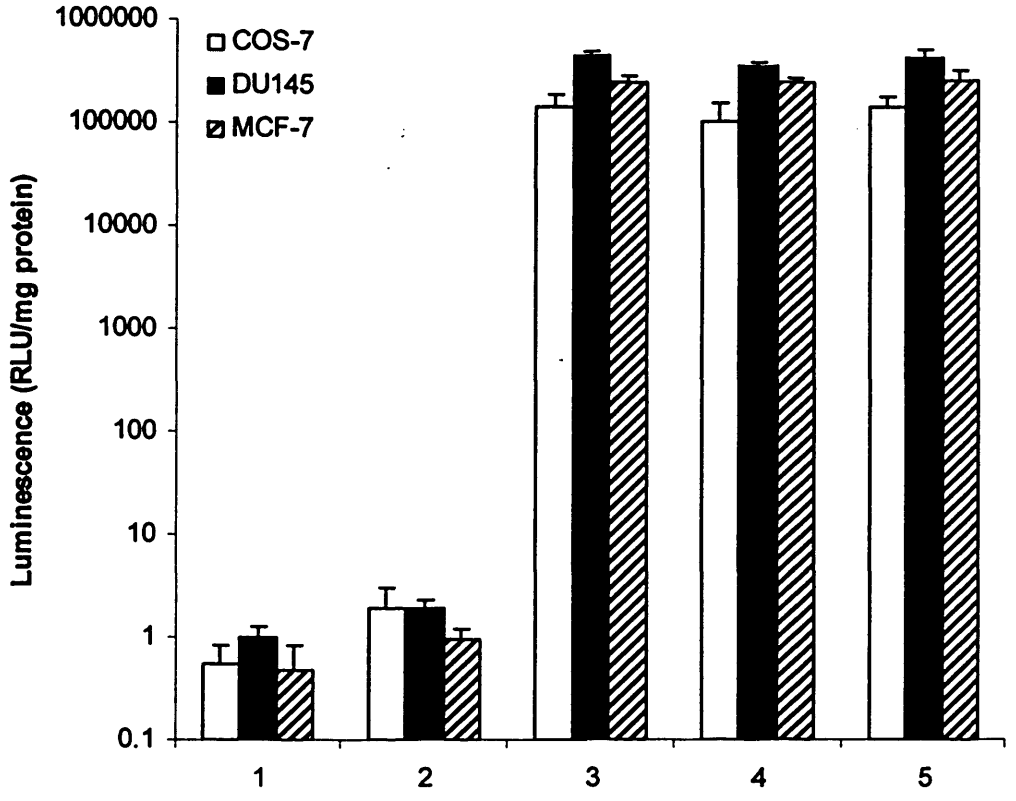

Figure 6.12 – Transfection efficiency of COS-7, DU145 and MCF-7 cells transfected with u11-CMTMO-coated PEI polyplexes

Luciferase activity of cells transfected with:
1) cells alone,
2) naked pGL3 luc,
3) PEI: pGL3 luc (2:1),
4) PEI: u11-CMTMO: pGL3 luc (2:2:1),
5) PEI: u11-CMTMO: pGL3 luc (2:5:1).
Formulation were produced in a 2 step procedure. Data represents mean ± SEM (n = 6).

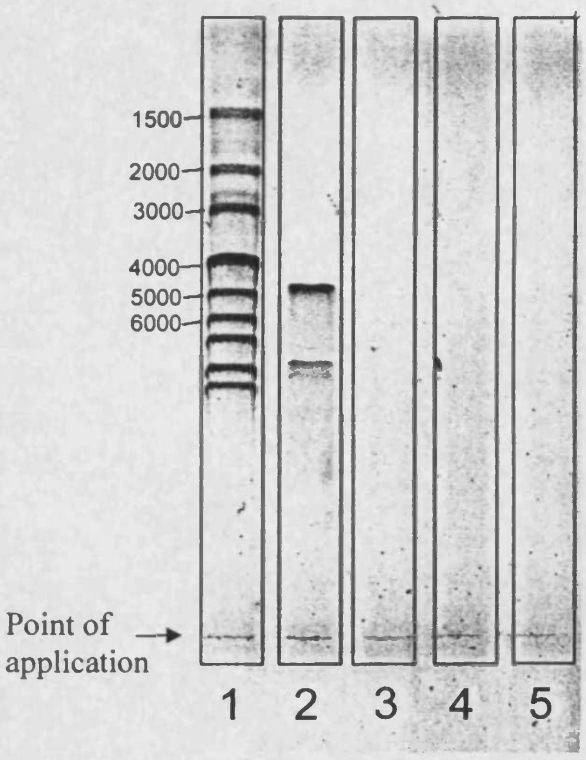

Figure 6.13 – Agarose gel analysis of u11-CMTMO-coated PEI polyplexes

Lane Key:
1) 1 kb DNA ladder (New England Biolabs),
2) pGL3 luc,
3) PEI: pGL3 luc (2:1),
4) PEI: u11-CMTMO: pGL3 luc (2:2:1),
5) PEI: u11-CMTMO: pGL3 luc (2:5:1).
Formulations were produced in a 2 step procedure.

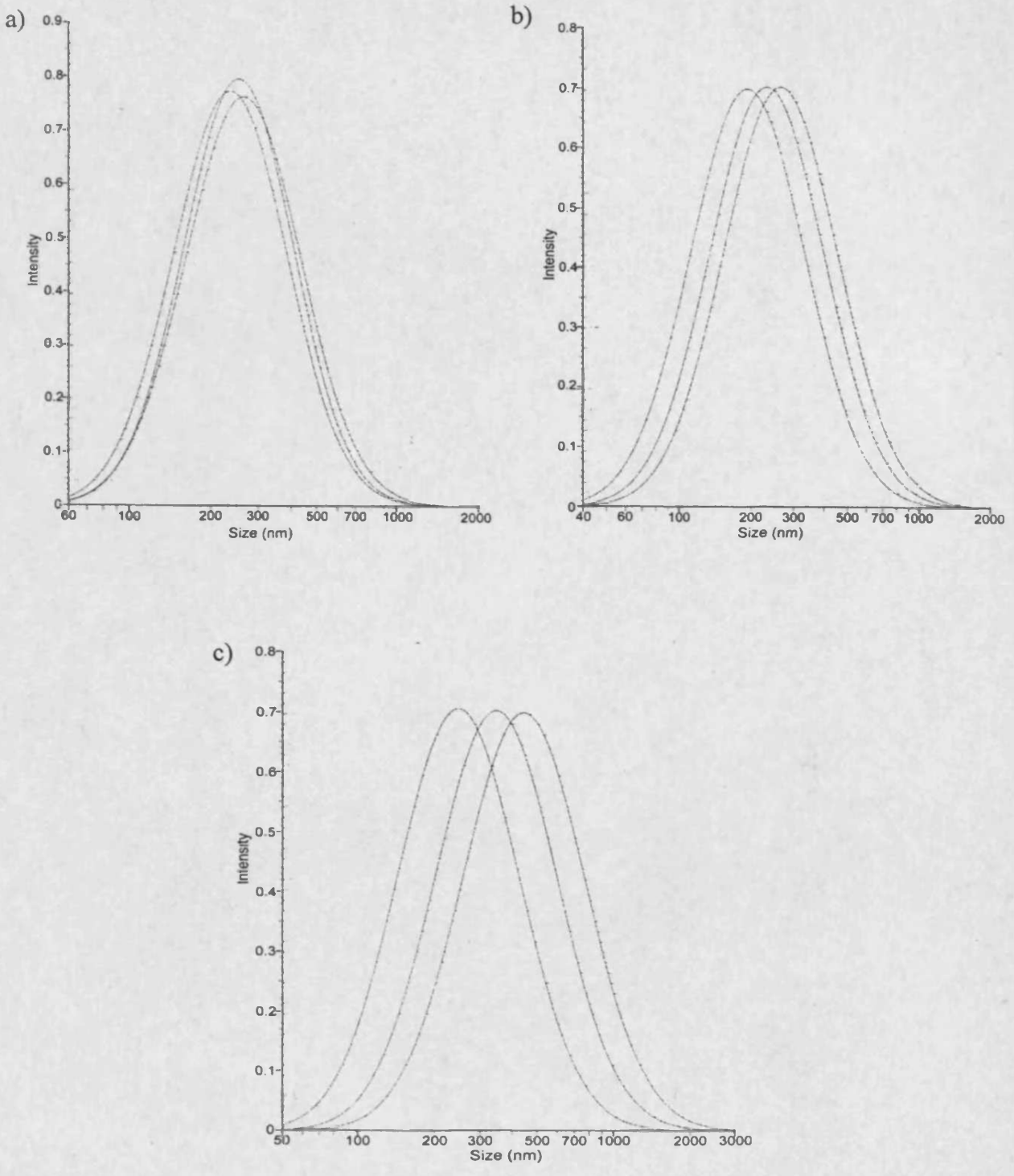

Figure 6.14 – Size of ull-CMTMO-coated PEI polyplexes assessed by PCS

Data show the size distribution of:
a) PEI: pGL3 luc (2:1) average size = 254 nm,
b) PEI: u11-CMTMO: pGL3 luc (2:2:1) average size = 268 nm,
c) PEI: u11-CMTMO: pGL3 luc (2:5:1) average size = 382 nm
Formulations were produced in a 2 step procedure. Note size scale (triplicate experiments).

The non-covalent inclusion of the peptide in a polyplex formulation reduced the cell lysate luminescence upon exposure to luciferin when compared to control polyplexes produced with PEI. This infers that there is less luciferase produced in the cells. This is an assumption, other possibilities exist: the peptide could inhibit luciferase, or quench the light emitted in the chemiluminescent reaction. Assuming that these are not the case, as these effects have not been reported previously (to the author's knowledge) and are deemed unlikely, the reduced luminescence is therefore due to lower luciferase expression. It is important to consider which step in the transfection process has been compromised.

It is possible that the reduction in transfection efficiency caused by peptide addition is due to reduced vector uptake. This could be due to:

1) less efficient packing of the plasmid (thereby giving larger polyplexes),
2) peptide coverage of the polyplex surface, reducing non-specific ionic interaction with the cell surface,
3) free peptide competing for the receptor,
4) any combination of the above mentioned effects.

At the outset it was hoped that covalent attachment of the peptide to CMTMO would enable formulation of a polyplex to improve tumour targeting. It was hypothesised that the peptide would be on the surface of the polyplex and not be buried inside it. The two step strategy for polyplex formation was developed to increase the probability that the peptide would locate to the surface. Production of a polyplex using TMO (or PEI) as a first step, followed by addition of u11-CMTMO was considered a better way to achieve small complexes. The polyplexes achieved were ~ 200 nm with u11-CMTMO coated TMO polyplexes and ~ 300 nm with u11-CMTMO coated PEI polyplexes. This size is smaller than that reported by others (1 μm; Kursa et al. 2003), larger than that reported by some (100 nm; Kunath et al. 2003a) but was similar to that reported by the majority (Suh et al., 2002, Zauner et al., 1998, Zhou et al., 2002).

As 1-3 mol % (peptide to glucosamine monomer) Gu11G (Chapter 3) was determined as conjugated to CMTMO this equates to 0.3 - 0.8 peptide per oligomer (average oligomer length = 27). Purification of u11-CMTMO so that 1 peptide per oligomer chain was present through affinity chromatography may have been possible. This was not pursued due to the polydisperse nature of the oligomer in the first instance and the time needed to develop this method in the second instance. u11-CMTMO

solution was investigated as a complexing agent alone as it was considered that the solution would be an heterogenous mixture of CMTMO and u11-CMTMO (Fig. 6.5) but it was found that at 5x the ratio needed to achieve complete complex formation with TMO51, there was still free plasmid. This finding led to the development of the two step strategies.

PEI is reported to produce complexes of less than 100 nm measured using PCS (Kircheis et al., 2001b) so this polymer was used to decrease the size when u11-CMTMO was used to coat polyplexes. u11-CMTMO-coated PEI polyplexes were also used to allow comparison with u11-CMTMO-coated TMO51 polyplexes. This would exclude the potential problem of TMO51 being too tightly complexed with pGL3 luc and not releasing it when inside the cell. At the concentration of PEI used in these experiments and in the physiological medium (i.e. salt concentration) polyplexes were larger than those produced with TMO51 (Figs. 6.11 and 6.14). A linear PEI rather than the branched form used in these studies may have produced polyplexes smaller than 200 nm when coated with u11-CMTMO.

The procedure used to introduce the targeting ligand may be further improved through the use of a different conjugation strategy, that of conjugation post polyplex formation, which has been used by several groups (Blessing et al., 2001, Kursa et al., 2003, Lee et al., 2002). These strategies involve the formation of polyplexes followed by the subsequent conjugation of the ligand to the polyplex. Lee et al. (2002) use the streptavidin molecule to coat PEI polyplexes, followed by biotin-PEG-EGF which binds to the streptavidin in a high affinity interaction. The strategy used by Blessing et al (2001) is that of polyplex formation using PEI containing thiol groups followed by conjugation of vinyl sulphone-PEG-EGF. Kursa et al (2003) formed polyplexes with PEI, which were then modified by the conjugation of heterobifunctional PEG, this is then further modified with transferrin.

There are several experiments that could be performed to elucidate the lack of increased transfection with the u11-CMTMO-coated formulation applied in these experiments. Regrettably, due to lack of time, it was not possible to investigate which steps could have been improved. Exploration of the endocytic pathway would have been interesting. This could have been done using inhibitors of caveolae-dependent endocytosis such as genistein and filipin (Rejman et al., 2004). The endocytic pathway could have been further defined using inhibitors of clathrin-mediated endocytosis such

as amantadine and phenylarsine oxide (Ruckert et al., 2003) or chlorpromazine (Ippoliti et al., 2000).

It may have been that there was similar or increased uptake of ligand coated conjugates but that the peptide directed the polyplex for lysosomal degradation. Experiments using chloroquine to prevent lysosome acidification may have increased transfection efficiency, this was true of ATF-Lys polyplexes prepared by Sun et al. (Sun et al., 2004). This was also true using a ATF-saporin chimera which showed greater toxicity in cells treated with bafilomycin A or chloroquine (Ippoliti et al., 2000). The uptake could have been investigated with labelled oligomer or DNA. Unfortunately there wasn't sufficient fluorescently labelled oligomer to study this.

The effect of serum on transfection efficiency was not studied at this stage as this would provide a more complex environment to study, although more physiologically relevant. In effect this may have reduced uptake because there was a lack of co-factors used in uPAR endocytosis. However, as u11-CMTMO-FAM, u11-CMTMO-OG and u11-PEG-FAM uptake had occurred in cells incubated without serum in previous experiments (Chapter 5) it was considered that similar conditions should be used in gene delivery experiments. A point to note is that fluorescent uptake was studied over 1 h and in transfection experiments cells were incubated with polyplexes for 6 h, greater uptake would probably be seen over this longer time period.

The nuclear envelope is regarded as one of the rate limiting steps in transfection (Banks et al., 2003). Dividing cells are easier to transfect than those in a quiescent state due to the disruption of the nuclear envelope. This could aid in the use of non-viral therapy as a selective treatment of cancer because one of the main attributes of cancer cells is their rapid division. In the experiments presented here cells were at 70-90 % confluence and could have been at any stage in the cell cycle, the addition of a cell cycle inhibitor e.g. aphidicolin to halt the cells at G1 before transfection would have enabled the study of this parameter (Mortimer et al., 1999).

The release of pDNA from the polyplex is a parameter that must occur before transcription of the plasmid can be performed and that may be required in the cytosol before plasmid entry into the nucleus (Dean et al., 2005). In the future I expect this step will be engineered to ensure it occurs at the right moment. It may involve the use of a layering approach such as that attempted here in the two step procedure.

A comparison between the untargeted vector and that coated with a peptide conjugate is a harsh contrast. A more favourable comparison would probably have been

seen between polyplexes coated with u11-CMTMO and polyplexes coated with CMTMO, this experiment was not performed. Use of scrambled u11-CMTMO as a coating would have provided a better control experiment as the scrambled peptide would have been expected to interfere with polyplex formulation to a similar extent as u11-CMTMO but would not have produced RME. Although increased transfection efficiency over that seen with the polycation alone was not seen, the significant restoration of transfection to that achieved with the polycation alone is an encouraging result as was reported by Parker et al. (2005). Initially, the uptake of the u11-CMTMO coated complexes could be studied by flow cytometry and fluorescent microscopy with fluorescently labelled TMO, u11-CMTMO and/or DNA. Using three labels with different excitation/emission wavelengths would enable the trafficking of each component to be studied. Unfortunately many instruments are not able to excite at different wavelengths and fluorophores often emit over a broad wavelength causing problems in interpreting data obtained. However, the potential of this approach remains. Confocal microscopy would give more reliable data on the actual position of fluorophores in the cell than epifluorescent microscopy, this would aid in the determination of the route of endocytosis. Co-localisation experiments using markers for endocytic compartments would also aid in the elucidation of the endocytic pathway.

Purification of the complexes from free TMO and u11-CMTMO would be beneficial. This is a difficult challenge to overcome, removing free TMO and u11-CMTMO whilst: a) not disrupting the polyplex ensuring that the pDNA is well packed, b) not losing pDNA or being able to characterise the amount of pDNA in the final solution reliably, c) not losing polyplexes due to adherence on the column/vessel used to purify the polyplex.

Competition experiments could have been made using u11 and uPA to determine that the uptake of coated polyplexes was specific. Transfection experiments using cells expressing low/no uPAR, knockouts or stably transfected cells, would further support a specific uptake mechanism. As has been outlined in this discussion, there are many experiments which would shed further light on the whole process of ligand-targeted transfection, this is addressed in Chapter 7.

In conclusion, although it was not possible to increase the transfection efficiency observed with u11CMTMO-coated polyplexes over that of the cationic vectors alone, it was possible to restore transfection efficiency to the level found with a non-targeted and therefore non-specific vector. This would be expected to produce improved cancer therapy through the specificity of the formulation.

Chapter 7

General Discussion

The interest in non-viral gene delivery has exploded in recent years, demonstrated by the volume of published research. Polyplex gene delivery has now progressed to clinical trials, with a PEI/DNA polyplex (Ohana et al., 2004). This project describes a rationally designed, uPAR targeted non-viral gene delivery system with the aim to use it in anti-cancer therapy. It is one of the few, if not the only example of an endogenous ligand derived oligopeptide targeted non-viral vector. The uPA receptor is a novel target, Gu11G is a novel peptide derived from the binding region of uPA and the conjugation of this peptide with a polymeric structure such as 6-O-carboxymethyl trimethylchitosan oligomer is unique.

7.1 Non-Viral Gene Therapy: a Perspective

An effective gene therapy for the treatment of cancer has many levels of control that can be used to eliminate toxicity and promote tumour regression. At the level of the vector, which is where this thesis has concentrated, it is desirable to achieve targeted, efficient delivery of the gene. This presented the first choice, which receptor to target? In this thesis the uPA receptor was identified as a novel, over-expressed receptor with a high affinity ligand, the binding region of which had been identified.

Consideration of the pharmacokinetic/pharmacodynamics of the non-viral delivery system were made. It was considered that, if administered intravenously, the polyplex would be localised in the tumour due to the EPR effect. Uptake by the RES may have occurred. Although, this uptake would need to be assessed *in vivo*. If, as in many cases, the polyplex was administered intra-tumourally it would be retained at the site of injection. Although 100 % cancer cell uptake would be advantageous it is unrealistic without large doses, which would also give non-specific cell uptake. It is expected that the u11-CMTMO-coated polyplexes would increase specific uptake and improve internalisation.

This brings us to the next stage of transfection, the escape from the endosome. This step has been investigated by groups using: endosomolytic polymers (Cho et al., 2003, Richardson et al., 1999, Richardson et al., 2001); endosome escaping polymers PLL (Zauner et al., 1998) and PEI (Ogris & Wagner, 2002); and membrane disrupting peptides (Wagner, 1999). Trimethylated chitosan could behave like chitosan which was found to have membrane perturbing properties (Erbacher et al., 1998) and therefore it may not need an additional endosomolytic component.

Following endosomal escape the vector must deliver the gene through the cytosol to the nucleus. Macromolecule movement within the cell is severely hampered and the diffusion rate of 2 kbp DNA is > 100 times slower in cytosol than in water (Lechardeur et al., 2005). The entry of complexes to the nucleus has also been identified as the rate limiting step in transfection (Banks et al., 2003). To overcome this challenge the use of nuclear localisation signals (NLS), adapted from viruses, has been investigated (reviewed in Bremner et al., 2001). This has produced conflicting results with Zanta et al. (1999) finding that the attachment of a single NLS to DNA increased transfection 10-1000 fold, yet, more recently Van der Aa (2005) failed to achieve any increase when conjugating a NLS to DNA. However, cancer gene therapy may benefit from the difficulty in accessing the nucleus of non-dividing cells, at mitosis the nuclear envelope is disassembled. This would allow the complex access to the nucleus, in the rapidly dividing cell environment found in cancer, at a higher rate than in 'normal' cells. This would give greater transfection efficiency in cancer cells over that found in normal cells and would therefore increase the therapeutic potential of the delivery system.

Release of the gene from the vector must occur, whether this happens before or after nuclear import. This is a parameter which requires further study. PEI/DNA complexes have been shown to be transcribed when directly injected into the nucleus (Pollard et al., 1998). In this case it may be that the DNA is relaxed and transcribed from the polyplex by topoisomerase in a similar way as that which occurs in the normal transcription process.

Another area of DNA localisation in the cell is in mitochondria. Although a less widely researched area, the delivery of DNA to mitochondria through the use of mitochondrotropic DQAsomes has been studied (Weissig et al., 1998). Dequalinium™, which is a dicationic amphiphile, interacts with DNA to form DQAsomes. These DQAsomes have been found to escape endosomes and localise in mitochondria (D'Souza et al., 2003). This technique is mainly being investigated for the treatment of mitochondrial diseases such as neuromuscular disease due to mitochondrial DNA deletions but could equally be utilised for other gene therapies (Torchilin et al., 2002).

Following localisation in the nucleus the gene is under the control of promoter regions regulating the transcription of proteins from the cell DNA. The use of tumour specific promoters forms the basis of several efforts (Wang & Liu, 2003) and has been fundamental in the development of the PEI polyplex in clinical trials (Ohana et al., 2004).

Having reached the point where the gene has been transcribed the question of which gene to transcribe is pertinent. Many gene therapy clinical trials for the treatment of cancer have used tumour suppressor genes (130 of 688) with the p53 gene making up half of these (62) (Edelstein, 2005). Indeed the first approved gene therapy in China uses an adenoviral delivery of wild type p53/radiotherapy combination and a similar p53 containing virus is being developed in the USA (Lane, 2004, Surendran, 2004). However, for complete regression this gene would need to be expressed in all cancer cells. A more promising therapy may be GDEPT, the first reported example was in 1991 (Huber et al., 1991). This technique has resulted in three examples reaching phase III clinical trials (reviewed in Dachs et al., 2005). All three of these trials used the transgene for thymidine kinase followed by administration of gancyclovir (Edelstein, 2005). Ideally, under the control of a tumour specific promoter, a non-native enzyme is produced which catalyses the activation of pro-drug to a toxic metabolite which kills the cancer cell and surrounding tumour by the bystander effect.

Increasingly it is apparent that, to achieve the true promise of gene therapy with a non-viral vector, a multi-component product must be developed (Parker et al., 2003, Zuber et al., 2001). The individual strands which are being developed and optimised independently must be drawn together in an complex system containing all the necessary components.

7.2 Trimethylated Chitosan as a Non-Viral Vector

The primary reasons for the choice of trimethylated chitosan were that it was described as an efficient, non-toxic vector (Thanou et al., 2002). This was investigated and the effect of trimethylation on chitosan toxicity defined (Kean et al., 2005). These factors remain true but there is, as described above, so much more to the transfection process than the vector. It is not enough to consider that the vector packs the DNA efficiently, or is not toxic. As a plasmid DNA vector, trimethylated chitosan oligomer holds promise due to its minimal cytotoxicity. The release of DNA from TMO polyplexes may be the most difficult step in the transfection process. If this were addressed through a triggerable event such as cytosomal, endosomal or nuclear enzymatic hydrolysis then another piece of the transfection process would be expedited. The development of improved non-viral vectors is currently a hot topic; the research presented here and elsewhere has shown that some vectors are more effective in

particular cell types. The disease being treated will also undoubtedly affect the efficiency of the vector, and therefore influence the choice of vector to be used. The notion that one vector will emerge as the most appropriate for all diseases/applications is unlikely. Trimethylated chitosan is another tool to be used, it has both a good transfection profile and is modifiable, allowing the attachment of ligands, NLS, endosome disrupting peptides etc. A comparative study between vectors using each vector's optimised (for that cell line and plasmid) complex ratio would be a useful guide for future scientists. The recent addition of luciferase as a standard (i.e. luminescence standardised against a luciferase enzyme standard curve and normalised for total cell protein) in transfection assays allows for a more accurate comparison to be made between vectors in different papers (Akinc et al., 2005, Forrest et al., 2004, Forrest & Pack, 2002).

7.3 Is uPAR the Correct Target for Cancer Gene Therapy?

Whilst this project was being pursued uPAR was targeted with a recombinant gene product coding the amino-terminal fragment of uPA (amino acids 1-135) with 10 lysine residues following it for gene complexion (Sun et al., 2004). This study showed a doubling in transfection efficiency over non-targeted complexes in uPAR transfected human lung carcinoma cells (Sun et al., 2004). The crystal structure of a soluble form of uPAR crystallised with a non-natural peptide (AE147) was also solved during the PhD (Llinas et al., 2005) and even more recently the crystal structure of the uPA-uPAR complex was reported (Huai et al., 2006). This research, along with that presented here, shows that uPAR is a viable target for anti-cancer therapy. To achieve a more efficient delivery system it may be necessary to incorporate two ligands, uPAR may be an ideal candidate for this approach due to its requirement for an endocytic partner. An ideal partner ligand would be one derived from binding region of apolipoprotein E that binds to low density lipoprotein receptor related protein which is associated with uPAR endocytosis (Raussens et al., 2000, Raussens et al., 2002). AE147 ((L)Lys-(L)Ser-(L)Asp-(L)β-cyclohexyl-alanine-(L)Phe-(D)Ser-(D)Lys-(L)Tyr-(L)Leu-(L)Trp-(L)Ser-(L)Ser-(L)Lys) is a peptide containing D-amino acids and a substituted alanine (Llinas et al., 2005). This peptide has a higher affinity (16.4 nM) for the receptor than that determined for Gu11G (1.3-1.4 μM) in the research presented in this thesis (Llinas et al., 2005). Other peptides developed by Ploug et al. (2001) had a higher affinity for

uPAR but were not used in the crystallisation studies reported by Llinas et al. (2005), the reason for this is unclear. The use of one of these peptides should be considered in future experiments to increase the affinity of the conjugate for the receptor but its endocytosis must first be established.

7.4 Developing a Targeted Non-viral Vector

Complex formation did not seem to be the problem in formulating a targeted non-viral gene delivery vector in the experiments presented. The confirmation of polyplex formation and size measurements indicate that this was not the factor responsible for decreased/unchanged transfection efficiency. In jumping from showing ligand binding and conjugate binding to transfection efficiency many steps have not been investigated: DNA binding and uptake; endosomal escape; nuclear localisation. Unfortunately this means that the stage at which transfection could be enhanced cannot be deduced. The use of a much reduced aa sequence from the endogenous ligand may have reduced the affinity for the receptor too far. However, the synthesis of this short sequence is simpler and has less antigenic potential than a longer sequence.

The Gu11G-CMTMO may not have associated with the polyplexes efficiently. Therefore free Gu11G-CMTMO in the transfection solution would compete with that in polyplexes for the receptor, thereby reducing polyplex uptake. These problems were not addressed in this thesis and further investigation may result in the elimination of the difficulty in achieving increased transfection efficiency.

Some success has been seen in peptide targeted non-viral gene delivery. Parker et al. (2005) found increased transfection efficiency over a HPMA-coated PLL : pDNA polyplex in both a SIGYPLP (HUVEC binding) and an RGD peptide targeted delivery system. Both of these peptides had been developed by phage display technology. As was achieved in this study, restoration of transfection to the levels achieved with the un-coated vector was reported (Parker et al., 2005). In 1999 increased transfection in MRC5 fibroblast like normal lung cells was reported when an RGD was attached to PEI (Erbacher et al., 1999). A novel peptide (CNGRC) targeting CD13/aminopeptidase-N developed through phage display (Pasqualini et al., 1995) has also been successful in increasing tumour gene expression (12-fold) mediated with a PEI construct *in vivo* (Moffatt et al., 2005). Another novel peptide mediated delivery system targeting human airway epithelia identified by phage display (THALWHT) increased *in vitro* gene

delivery, although the receptor being targeted was not identified (Jost et al., 2001). RGD targeted delivery is probably the most widely investigated peptide mediated delivery system (Anwer et al., 2004, Harvie et al., 2003, Kunath et al., 2003, Suh et al., 2002). Expression of the integrin receptor, which binds RGD peptides, is increased in angiogenic tumour vasculature but it is also widespread in the normal vasculature and would mean that the vector would have non-specific uptake. Inhibition of tumour growth *in vivo* using RGD coated pegylated liposomes containing doxorubicin has been reported, although increased liver uptake was also seen (Schiffelers et al., 2003). As the association of uPAR with integrins has been reported, RGD peptides could be also be used as a co-ligand to increase vector specificity and uptake.

7.5 uPAR Targeted Drug Delivery

Although it was decided to concentrate on the development of a non-viral gene delivery system this thesis presents the basis for a novel drug delivery platform using Gu11G-CMTMO. The uptake and binding specificity of this conjugate were demonstrated using fluorescein and Oregon Green which are similar in structure to many drug molecules (Wang et al., 2003). This may form the basis for a future polymer targeted drug delivery system, although drug release from the carrier was not studied and would need optimisation. Whether CMTMO would be the most appropriate oligomer (or polymer) for this application is unclear, the toxicity of this derivative was not tested but was expected to be lower or similar to that of TMO with the same degree of trimethylation. Realistically, a less cationic polymer construct would probably be safer. This could still be based upon the chitosan backbone with pendant drug groups attached to the polymer using hydrolysable/enzymatically degradable linkers (reviewed by Duncan, 2002, Duncan, 2003). The benefits of retaining the chitosan backbone are: the natural abundance of this polymer, meaning that any new therapy based upon it would be cost effective; the number of points available for modification – an amine on every (almost, depending on degree of deacetylation) monomer; the polysaccharide nature - a biologically well tolerated structure (although with modification the toxicity would have to be measured).

The higher affinity ligand AE147 developed by Ploug et al. (2001) may improve the efficacy of the conjugate for uPAR expressing cells and should be studied as an

improved vector. The possible degradation of the peptide, Gu11G, was not studied in this research. It was expected that any normal degradation of the free peptide would be hindered by its conjugation. AE147-conjugate would probably have an even higher stability in serum than that of a natural peptide due to the D-amino acids and substituted alanine residue.

7.6 Conclusions

The modification of chitosan has been successful in many respects. It has been shown that uPAR targeted delivery using a peptide derived from the binding region of the endogenous ligand is feasible, as shown by increased binding of Gu11G-CMTMO-FAM, Gu11G-CMTMO-OG and Gu11G-PEG-FAM. The translation of this conjugate into an improved (over that achieved with the cationic vector alone) non-viral gene delivery system would require more study.

7.7 Future Work

An improved understanding and possibly an improved formulation may be achieved through:

A) With regard to the carrier

- Investigation of trimethyl chitosan metabolism using chitosanase or lysozyme. Degradation of trimethyl chitosan means that elimination from the body would be more likely

B) With regard to the ligand

- Use of AE147 as a targeting ligand. This higher affinity ligand may confer higher uPAR affinity to the conjugate

C) With regard to the conjugate

- Investigation of chitosan protection/deprotection using *tert*-butoxycarbonyl or 9-fluorenylmethoxycarbonyl followed by conjugation of peptides by their C-terminal aa. C-terminal conjugation may increase the ligand affinity for uPAR
- Further characterisation of 6-O-carboxymethylation, use of $ClCH_2{}^{14}COOH$. The production of radiolabelled CMTMO would enable study of uptake and *in vivo*

distribution of the conjugate. The degree of 6-O-carboxymethylation could be assessed through the radioactivity of the derivative

- Further characterisation of peptide conjugation, use of ^{14}C peptides. The production of radiolabelled peptide-CMTMO conjugate would enable study of uptake and *in vivo* distribution of the conjugate. The degree of peptide conjugation could also be assessed through the radioactivity of the derivative
- Purification of polyplex using centrifugation or dialysis (assessment of pDNA content using radiolabelled pDNA).

Steps which could be followed in the investigation of the current formulation and/or improved formulations are outlined in the flow chart in Fig. 7.1.

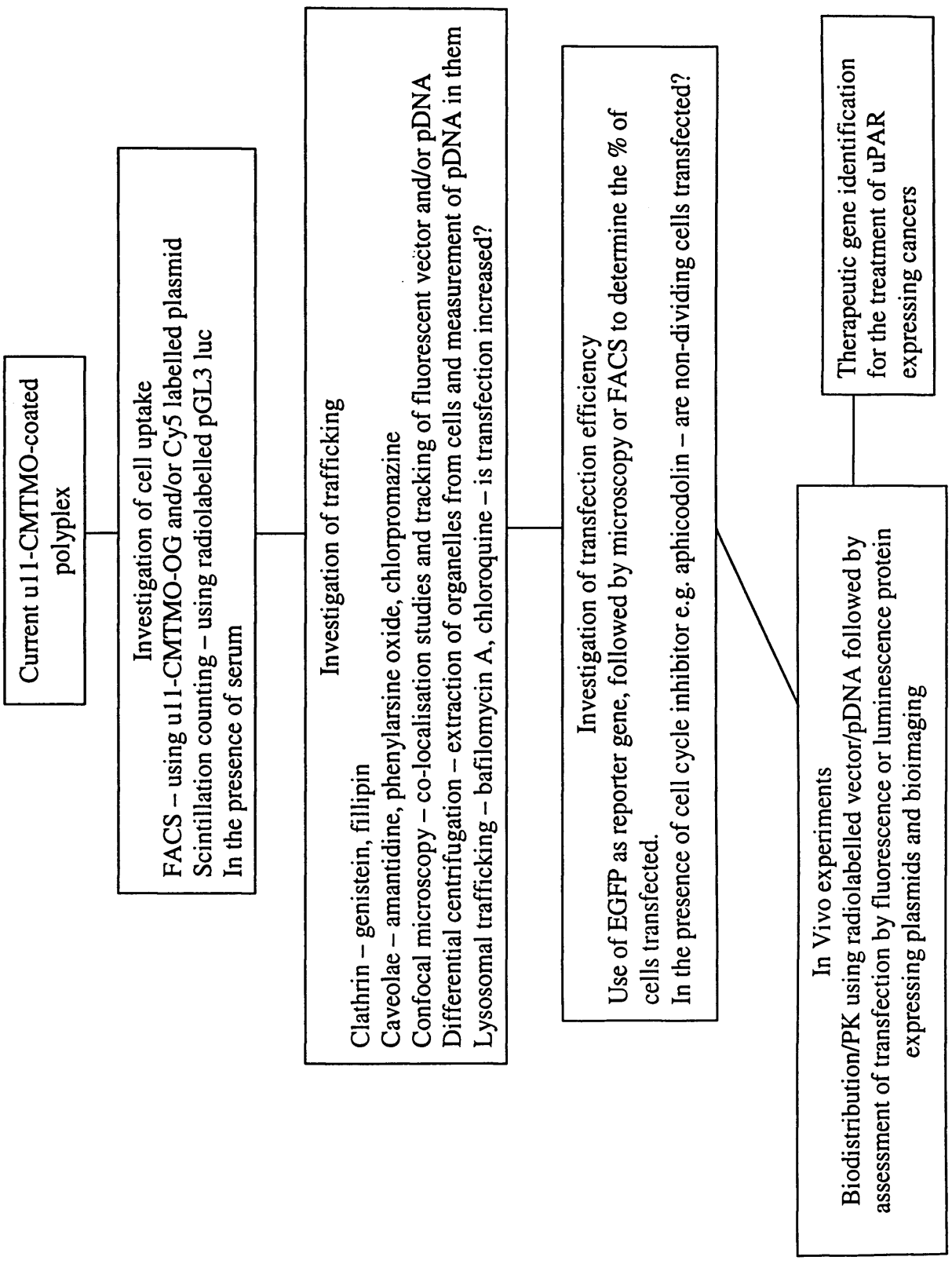

Figure 7.1 – Future research directions

Bibliography

Bibliography

R.J. Abi-Habib, S. Liu, T.H. Bugge, S.H. Leppla, A.E. Frankel, A urokinase-activated recombinant diphtheria toxin targeting the granulocyte-macrophage colony-stimulating factor receptor is selectively cytotoxic to human acute myeloid leukemia blasts. Blood, 104(7) (2004) 2143-8.

E. Abraham, M.R. Gyetko, K. Kuhn, J. Arcaroli, D. Strassheim, J.S. Park, S. Shetty, S. Idell, Urokinase-type plasminogen activator potentiates lipopolysaccharide-induced neutrophil activation. J. Immunol., 170(11) (2003) 5644-51.

C.H. Ahn, S.Y. Chae, Y.H. Bae, S.W. Kim, Biodegradable poly(ethylenimine) for plasmid DNA delivery. J. Control. Release, 80(1-3) (2002) 273-82.

A. Akinc, D.M. Lynn, D.G. Anderson, R. Langer, Parallel synthesis and biophysical characterization of a degradable polymer library for gene delivery. J. Am. Chem. Soc., 125(18) (2003) 5316-23.

A. Akinc, M. Thomas, A.M. Klibanov, R. Langer, Exploring polyethylenimine-mediated DNA transfection and the proton sponge hypothesis. J. Gene. Med., 7(5) (2005) 657-63.

T. Akuta, A. Eguchi, H. Okuyama, T. Senda, H. Inokuchi, Y. Suzuki, E. Nagoshi, H. Mizuguchi, T. Hayakawa, K. Takeda, M. Hasegawa, M. Nakanishi, Enhancement of phage-mediated gene transfer by nuclear localization signal. Biochem. Biophys. Res. Commun., 297(4) (2002) 779-786.

T.M. Allen, Ligand-targeted therapeutics in anticancer therapy. Nat. Rev. Cancer, 2(10) (2002) 750-763.

T.M. Allen, P.R. Cullis, Drug delivery systems: entering the mainstream. Science, 303(5665) (2004) 1818-22.

American Diagnostica, uPA-FITC (124FITC) Information booklet. 2002, American Diagnostica.

American Diagnostica, American Diagnostica Catalogue. 2004, American Diagnostica.

P.A. Andreasen, R. Egelund, H.H. Petersen, The plasminogen activation system in tumor growth, invasion, and metastasis. Cell. Mol. Life Sci., 57(1) (2000) 25-40.

K. Anwer, G. Kao, A. Rolland, W.H. Driessen, S.M. Sullivan, Peptide-mediated gene transfer of cationic lipid/plasmid DNA complexes to endothelial cells. J. Drug Target., 12(4) (2004) 215-21.

E. Appella, E.A. Robinson, S.J. Ullrich, M.P. Stoppelli, A. Corti, G. Cassani, F. Blasi, The Receptor-Binding Sequence of Urokinase - a Biological Function for the Growth-Factor Module of Proteases. J. Biol. Chem., 262(10) (1987) 4437-4440.

W. Arap, R. Pasqualini, E. Ruoslahti, Cancer treatment by targeted drug delivery to tumor vasculature in a mouse model. Science, 279(5349) (1998) 377-80.

W. Arap, W. Haedicke, M. Bernasconi, R. Kain, D. Rajotte, S. Krajewski, H.M. Ellerby, D.E. Bredesen, R. Pasqualini, E. Ruoslahti, Targeting the prostate for destruction through a vascular address. Proc. Natl. Acad. Sci. U. S. A., 99(3) (2002) 1527-1531.

ATCC, Mammalian cell culture information, 2003, http://www.lgcpromochem.com/atcc/

F.M. Ausubel, R. Brent, R.E. Kingston, D.D. Moore, J.G. Seidman, J.A. Smith, K. Struhl, eds. Current protocols in molecular biology. 1994, John Wiley & Sons Inc: New York.

K.D. Bagshawe, Antibody-directed enzyme prodrug therapy for cancer: its theoretical basis and application. Mol. Med. Today, 1(9) (1995) 424-31.

K. Bajou, C. Maillard, M. Jost, R.H. Lijnen, A. Gils, P. Declerck, P. Carmeliet, J.M. Foidart, A. Noel, Host-derived plasminogen activator inhibitor-1 (PAI-1) concentration is critical for in vivo tumoral angiogenesis and growth. Oncogene, 23(41) (2004) 6986-90.

N.H. Bander, E.J. Trabulsi, L. Kostakoglu, D. Yao, S. Vallabhajosula, P. Smith-Jones, M.A. Joyce, M. Milowsky, D.M. Nanus, S.J. Goldsmith, Targeting metastatic prostate cancer with radiolabeled monoclonal antibody J591 to the extracellular domain of prostate specific membrane antigen. J. Urol., 170(5) (2003) 1717-21.

G.A. Banks, R.J. Roselli, R. Chen, T.D. Giorgio, A model for the analysis of nonviral gene therapy. Gene Ther., 10(20) (2003) 1766-75.

L.B. Barrett, M. Berry, W.B. Ying, M.N. Hodgkin, L.W. Seymour, A.M. Gonzalez, M.L. Read, A. Baird, A. Logan, CTb targeted non-viral cDNA delivery enhances transgene expression in neurons. J. Gene. Med., 6(4) (2004) 429-38.

N. Behrendt, E. Ronne, M. Ploug, T. Petri, D. Lober, L.S. Nielsen, W.D. Schleuning, F. Blasi, E. Appella, K. Dano, The human receptor for urokinase plasminogen activator. NH2-terminal amino acid sequence and glycosylation variants. J. Biol. Chem., 265(11) (1990) 6453-60.

J.M. Benns, R.I. Mahato, S.W. Kim, Optimization of factors influencing the transfection efficiency of folate-PEG-folate-graft-polyethylenimine. J. Control. Release, 79(1-3) (2002) 255-69.

F. Blasi, uPA, uPAR, PAI-I: key intersection of proteolytic, adhesive and chemotactic highways? Immunol. Today, 18(9) (1997) 415-417.

F. Blasi, P. Carmeliet, uPAR: a versatile signalling orchestrator. Nat. Rev. Mol. Cell Biol., 3(12) (2002) 932-43.

T. Blessing, J.S. Remy, J.P. Behr, Monomolecular collapse of plasmid DNA into stable virus-like particles. Proc. Natl. Acad. Sci. U. S. A., 95(4) (1998) 1427-31.

T. Blessing, M. Kursa, R. Holzhauser, R. Kircheis, E. Wagner, Different strategies for formation of pegylated EGF-conjugated PEI/DNA complexes for targeted gene delivery. Bioconj. Chem., 12(4) (2001) 529-37.

O. Boussif, F. Lezoualc'h, M.A. Zanta, M.D. Mergny, D. Scherman, B. Demeneix, J.P. Behr, A versatile vector for gene and oligonucleotide transfer into cells in culture and in vivo: polyethylenimine. Proc. Natl. Acad. Sci. U. S. A., 92(16) (1995) 7297-301.

K.H. Bremner, L.W. Seymour, C.W. Pouton, Harnessing nuclear localization pathways for transgene delivery. Curr. Opin. Mol. Ther., 3(2) (2001) 170-7.

I. Brigger, C. Dubernet, P. Couvreur, Nanoparticles in cancer therapy and diagnosis. Adv. Drug Del. Rev., 54(5) (2002) 631-51.

G. Brooks, Gene Therapy, Pharmaceutical Press, London, 2002.

D.A. Brown, E. London, Functions of lipid rafts in biological membranes. Annu. Rev. Cell Dev Biol., 14(1) (1998) 111-136.

M.D. Brown, A. Schatzlein, A. Brownlie, V. Jack, W. Wang, L. Tetley, A.I. Gray, I.F. Uchegbu, Preliminary characterization of novel amino acid based polymeric vesicles as gene and drug delivery agents. Bioconj. Chem., 11(6) (2000) 880-891.

M.D. Brown, A.G. Schatzlein, I.F. Uchegbu, Gene delivery with synthetic (non viral) carriers. Int. J. Pharm., 229(1-2) (2001) 1-21.

H. Buning, M.U. Ried, L. Perabo, F.M. Gerner, N.A. Huttner, J. Enssle, M. Hallek, Receptor targeting of adeno-associated virus vectors. Gene Ther., 10(14) (2003) 1142-51.

Cancer Research UK, Cancer Research UK, 2005, http://www.cancerresearchuk.org/

G.J. Cannon, J.A. Swanson, The macrophage capacity for phagocytosis. J. Cell Sci., 101(Pt 4) (1992) 907-13.

B. Carreno-Gomez, R. Duncan, Evaluation of the biological properties of soluble chitosan and chitosan microspheres. Int. J. Pharm., 148(2) (1997) 231-240.

M.V. Carriero, S. Del Vecchio, P. Franco, M.I. Potena, F. Chiaradonna, G. Botti, M.P. Stoppelli, M. Salvatore, Vitronectin binding to urokinase receptor in human breast cancer. Clin. Cancer Res., 3(8) (1997) 1299-308.

M. Cavazzana-Calvo, S. Hacein-Bey, G. de Saint Basile, F. Gross, E. Yvon, P. Nusbaum, F. Selz, C. Hue, S. Certain, J.L. Casanova, P. Bousso, F.L. Deist, A. Fischer, Gene therapy of human severe combined immunodeficiency (SCID)-X1 disease. Science, 288(5466) (2000) 669-72.

V. Chan, H.-Q. Mao, K.W. Leong, Chitosan-induced perturbation of dipalmitoyl-sn-glycero-3-phosphocholine membrane bilayer. Langmuir, 17(12) (2001) 3749-3756.

E. Check, Harmful potential of viral vectors fuels doubts over gene therapy. Nature, 423(6940) (2003) 573-4.

I. Chemin, D. Moradpour, S. Wieland, W.B. Offensperger, E. Walter, J.P. Behr, H.E. Blum, Liver-directed gene transfer: a linear polyethlenimine derivative mediates highly efficient DNA delivery to primary hepatocytes in vitro and in vivo. J. Viral Hepat., 5(6) (1998) 369-75.

J. Chen, S. Gamou, A. Takayanagi, N. Shimizu, A novel gene delivery system using EGF receptor-mediated endocytosis. FEBS Lett., 338(2) (1994) 167-9.

J.Y. Cherng, P. van de Wetering, H. Talsma, D.J. Crommelin, W.E. Hennink, Effect of size and serum proteins on transfection efficiency of poly ((2-dimethylamino)ethyl methacrylate)-plasmid nanoparticles. Pharm. Res., 13(7) (1996) 1038-42.

A. Chilkoti, M.R. Dreher, D.E. Meyer, D. Raucher, Targeted drug delivery by thermally responsive polymers. Adv. Drug Del. Rev., 54(5) (2002) 613-30.

O. Chisholm, G. Symonds, Transfection of myeloid cell lines using polybrene/DMSO. Nucleic Acids Res., 16(5) (1988) 2352.

S.J. Chiu, N.T. Ueno, R.J. Lee, Tumor-targeted gene delivery via anti-HER2 antibody (trastuzumab, Herceptin) conjugated polyethylenimine. J. Control. Release, 97(2) (2004) 357-69.

Y.W. Cho, J.D. Kim, K. Park, Polycation gene delivery systems: escape from endosomes to cytosol. J. Pharm. Pharmacol., 55(6) (2003) 721-34.

Y.H. Choi, F. Liu, J.S. Park, S.W. Kim, Lactose-poly(ethylene glycol)-grafted poly-L-lysine as hepatoma cell-tapgeted gene carrier. Bioconj. Chem., 9(6) (1998) 708-18.

S. Choksakulnimitr, S. Masuda, H. Tokuda, Y. Takakura, M. Hashida, In vitro cytotoxicity of macromolecules in different cell culture systems. J. Control. Release, 34(3) (1995) 233-241.

G. Chung-Faye, D. Palmer, D. Anderson, J. Clark, M. Downes, J. Baddeley, S. Hussain, P.I. Murray, P. Searle, L. Seymour, P.A. Harris, D. Ferry, D.J. Kerr, Virus-directed, enzyme prodrug therapy with nitroimidazole reductase: a phase I and pharmacokinetic study of its prodrug, CB1954. Clin. Cancer Res., 7(9) (2001) 2662-8.

M. Conese, D. Olson, F. Blasi, Protease nexin-1-urokinase complexes are internalized and degraded through a mechanism that requires both urokinase receptor and alpha 2-macroglobulin receptor. J. Biol. Chem., 269(27) (1994) 17886-92.

K. Corsi, F. Chellat, L. Yahia, J.C. Fernandes, Mesenchymal stem cells, MG63 and HEK293 transfection using chitosan-DNA nanoparticles. Biomaterials, 24(7) (2003) 1255-1264.

M. Cottier, A. Tchirkov, B. Perissel, M. Giollant, L. Campos, P. Vago, Cytogenetic characterization of seven human cancer cell lines by combining G- and R-banding, M-FISH, CGH and chromosome- and locus-specific FISH. Int. J. Mol. Med., 14(4) (2004) 483-95.

M.V. Cubellis, M.L. Nolli, G. Cassani, F. Blasi, Binding of single-chain prourokinase to the urokinase receptor of human U937 cells. J. Biol. Chem., 261(34) (1986) 15819-22.

M.V. Cubellis, P. Andreasen, P. Ragno, M. Mayer, K. Dano, F. Blasi, Accessibility of receptor-bound urokinase to type-1 plasminogen activator inhibitor. Proc. Natl. Acad. Sci. U. S. A., 86(13) (1989) 4828-32.

R.P. Czekay, T.A. Kuemmel, R.A. Orlando, M.G. Farquhar, Direct binding of occupied urokinase receptor (uPAR) to LDL receptor-related protein is required for endocytosis of uPAR and regulation of cell surface urokinase activity. Mol. Biol. Cell, 12(5) (2001) 1467-1479.

G.U. Dachs, J. Tupper, G.M. Tozer, From bench to bedside for gene-directed enzyme prodrug therapy of cancer. Anticancer Drugs, 16(4) (2005) 349-59.

P.R. Dash, V. Toncheva, E. Schacht, L.W. Seymour, Synthetic polymers for vectorial delivery of DNA: characterisation of polymer-DNA complexes by photon correlation spectroscopy and stability to nuclease degradation and disruption by polyanions in vitro. J. Control. Release, 48(2-3) (1997) 269-276.

P.R. Dash, M.L. Read, K.D. Fisher, K.A. Howard, M. Wolfert, D. Oupicky, V. Subr, J. Strohalm, K. Ulbrich, L.W. Seymore, Decreased Binding to Proteins and Cells of Polymeric Gene Delivery Vectors Surface Modified with a Multivalent Hydrophilic Polymer and Retargeting through Attachment of Transferrin. J. Biol. Chem., 275(6) (2000) 3793-3802.

G. De Petro, D. Tavian, A. Copeta, N. Portolani, S.M. Giulini, S. Barlati, Expression of urokinase-type plasminogen activator (u-PA), u-PA receptor, and tissue-type PA messenger RNAs in human hepatocellular carcinoma. Cancer Res., 58(10) (1998) 2234-9.

D.A. Dean, D.D. Strong, W.E. Zimmer, Nuclear entry of nonviral vectors. Gene Ther., 12(11) (2005) 881-90.

B. Degryse, C.F.M. Sier, M. Resnati, M. Conese, F. Blasi, PAI-1 inhibits urokinase-induced chemotaxis by internalizing the urokinase receptor. FEBS Lett., 505(2) (2001) 249-254.

C. Delmotte, A. Delmas, Synthesis and fluorescence properties of Oregon Green 514 labeled peptides. Bioorg. Med. Chem. Lett., 9(20) (1999) 2989-94.

G. Deng, S.A. Curriden, S. Wang, S. Rosenberg, D.J. Loskutoff, Is plasminogen activator inhibitor-1 the molecular switch that governs urokinase receptor-mediated cell adhesion and release? J. Cell Biol., 134(6) (1996) 1563-71.

W.A. Denny, Prodrug strategies in cancer therapy. Eur. J. Med. Chem., 36(7-8) (2001) 577-95.

T.L. Doering, W.J. Masterson, G.W. Hart, P.T. Englund, Biosynthesis of glycosyl phosphatidylinositol membrane anchors. J. Biol. Chem., 265(2) (1990) 611-4.

G. Dolivet, J.L. Merlin, M. Barberi-Heyob, C. Ramacci, P. Erbacher, R.M. Parache, J.P. Behr, F. Guillemin, In vivo growth inhibitory effect of iterative wild-type p53 gene transfer in human head and neck carcinoma xenografts using glucosylated polyethylenimine nonviral vector. Cancer Gene Ther., 9(8) (2002) 708-714.

A. Domard, M. Rinaudo, C. Terrassin, New method for the quaternization of chitosan. Int. J. Biol. Macromol., 8(2) (1986) 105-107.

A. Domard, M. Domard, Chitosan: Structure-properties Relationship and Biomedical Applications, in: S. Dimitriu (Ed.), Polymeric Biomaterials, Marcel Dekker, 2002, pp. 187-210

P.T. Drapkin, C.R. O'Riordan, S.M. Yi, J.A. Chiorini, J. Cardella, J. Zabner, M.J. Welsh, Targeting the urokinase plasminogen activator receptor enhances gene transfer to human airway epithelia. J. Clin. Invest., 105(5) (2000) 589-96.

G.G. D'Souza, R. Rammohan, S.M. Cheng, V.P. Torchilin, V. Weissig, DQAsome-mediated delivery of plasmid DNA toward mitochondria in living cells. J. Control. Release, 92(1-2) (2003) 189-97.

C. Dufes, J.M. Muller, W. Couet, J.C. Olivier, I.F. Uchegbu, A.G. Schatzlein, Anticancer drug delivery with transferrin targeted polymeric chitosan vesicles. Pharm. Res., 21(1) (2004) 101-7.

R. Duncan, J.B. Lloyd, Pinocytosis in the rat visceral yolk sac. Effects of temperature, metabolic inhibitors and some other modifiers. Biochim. Biophys. Acta, 544(3) (1978) 647-55.

R. Duncan, L.C. Seymour, L. Scarlett, J.B. Lloyd, P. Rejmanova, J. Kopecek, Fate of N-(2-hydroxypropyl)methacrylamide copolymers with pendent galactosamine residues after intravenous administration to rats. Biochim. Biophys. Acta, 880(1) (1986) 62-71.

R. Duncan, Polymer-Drug Conjugates: Targeting cancer, in: V. Muzykantov,V.P. Torchilin (Ed.), Biomedical Aspects of Drug Targeting, Kluwer Academic Publishers, Norwell, Massachusetts, 2002, pp. 193-209

R. Duncan, The dawning era of polymer therapeutics. Nat. Rev. Drug Discov., 2(5) (2003) 347-60.

R. Duncan, Targeting and Intracellular Delivery of Drugs, in: R.A. Meyers (Ed.), Encyclopedia of Molecular Cell Biology and Molecular Medicine, Wiley-VCH, Weinheim, 2005, pp. 163-204

H.F. Dvorak, J.A. Nagy, J.T. Dvorak, A.M. Dvorak, Identification and characterization of the blood vessels of solid tumors that are leaky to circulating macromolecules. Am. J. Pathol., 133(1) (1988) 95-109.

M. Edelstein, Gene Therapy Clinical Trials Worldwide, 2005, http://www.wiley.co.uk/wileychi/genmed/clinical/

I. Elmadbouh, P. Rossignol, O. Meilhac, R. Vranckx, C. Pichon, B. Pouzet, P. Midoux, J.B. Michel, Optimization of in vitro vascular cell transfection with non-viral vectors for in vivo applications. J. Gene. Med., 6(10) (2004) 1112-24.

B.F. El-Rayes, P.M. LoRusso, Targeting the epidermal growth factor receptor. Br. J. Cancer, 91(3) (2004) 418-24.

A.O. Eniola, S.D. Rodgers, D.A. Hammer, Characterization of biodegradable drug delivery vehicles with the adhesive properties of leukocytes. Biomaterials, 23(10) (2002) 2167-77.

P. Erbacher, S.M. Zou, T. Bettinger, A.M. Steffan, J.S. Remy, Chitosan-based vector/DNA complexes for gene delivery: Biophysical characteristics and transfection ability. Pharm. Res., 15(9) (1998) 1332-1339.

P. Erbacher, J.S. Remy, J.P. Behr, Gene transfer with synthetic virus-like particles via the integrin-mediated endocytosis pathway. Gene Ther., 6(1) (1999) 138-45.

Familydoctor, Prostate cancer, 2005, http://www.familydoctor.co.uk/htdocs/PROSTATE/PROSTATE_specimen.html

N. Fang, V. Chan, H.Q. Mao, K.W. Leong, Interactions of phospholipid bilayer with chitosan: effect of molecular weight and pH. Biomacromolecules, 2(4) (2001) 1161-8.

T. Ferkol, J.C. Perales, F. Mularo, R.W. Hanson, Receptor-mediated gene transfer into macrophages. Proc. Natl. Acad. Sci. U. S. A., 93(1) (1996) 101-105.

Fermentas, ExGen 500, 2005, http://www.fermentas.com/catalog/transfection/exgeninvitro.htm

D. Fischer, T. Bieber, S. Brusselbach, H.-P. Elasser, T. Kissel, Cationized human serum albumin as a non-viral vector system for gene delivery? Characterization of complex formation with plasmid DNA and transfection efficiency. Int. J. Pharm., 225(1-2) (2001) 97-111.

D. Fischer, Y. Li, B. Ahlemeyer, J. Krieglstein, T. Kissel, In vitro cytotoxicity testing of polycations: influence of polymer structure on cell viability and hemolysis. Biomaterials, 24(7) (2003) 1121-31.

K. Fischer, V. Lutz, O. Wilhelm, M. Schmitt, H. Graeff, P. Heiss, T. Nishiguchi, N. Harbeck, H. Kessler, T. Luther, V. Magdolen, U. Reuning, Urokinase induces proliferation of human ovarian cancer cells: characterization of structural elements required for growth factor function. FEBS Lett., 438(1-2) (1998) 101-5.

B.I. Florea, C. Meaney, H.E. Junginger, G. Borchard, Transfection efficiency and toxicity of polyethylenimine in differentiated Calu-3 and nondifferentiated COS-1 cell cultures. AAPS Pharmsci., 4(3) (2002a) E12.

B.I. Florea, P.G.M. Ravenstijn, H.E. Junginger, G. Borchard, *N*-trimethylated oligomeric chitosan (TMO) protects plasmid DNA from DNase 1 degradation and promotes transfection efficiency *in vitro*. S.T.P. Pharma Sciences, 12(4) (2002b) 243-249.

J. Folkman, Y. Shing, Angiogenesis. J. Biol. Chem., 267(16) (1992) 10931-4.

M.L. Forrest, D.W. Pack, On the Kinetics of Polyplex Endocytic Trafficking: Implications for Gene Delivery Vector Design. Mol. Ther., 6(1) (2002) 57-66.

M.L. Forrest, G.E. Meister, J.T. Koerber, D.W. Pack, Partial acetylation of polyethylenimine enhances in vitro gene delivery. Pharm. Res., 21(2) (2004) 365-71.

R.J. Francis, S.K. Sharma, C. Springer, A.J. Green, L.D. Hope-Stone, L. Sena, J. Martin, K.L. Adamson, A. Robbins, L. Gumbrell, D. O'Malley, E. Tsiompanou, H. Shahbakhti, S. Webley, D. Hochhauser, A.J. Hilson, D. Blakey, R.H. Begent, A phase I trial of antibody directed enzyme prodrug therapy (ADEPT) in patients with advanced colorectal carcinoma or other CEA producing tumours. Br. J. Cancer, 87(6) (2002) 600-7.

C.B. Frantzen, L. Ingebrigtsen, M. Skar, M. Brandl, Assessing the accuracy of routine photon correlation spectroscopy analysis of heterogeneous size distributions. AAPS PharmSciTech, 4(3) (2003) E36.

R.A. Freitas, Chapter 15.4 Systemic Nanorobot Distribution and Phagocytosis, (Ed.), Nanomedicine, Volume IIA: Biocompatibility, Landes Bioscience, Georgetown, Texas, 2003, pp.

S. Gao, J. Chen, X. Xu, Z. Ding, Y.H. Yang, Z. Hua, J. Zhang, Galactosylated low molecular weight chitosan as DNA carrier for hepatocyte-targeting. Int. J. Pharm., 255(1-2) (2003) 57-68.

D. Gavrilov, O. Kenzior, M. Evans, R. Calaluce, W.R. Folk, Expression of urokinase plasminogen activator and receptor in conjunction with the ets family and AP-1 complex transcription factors in high grade prostate cancers. Eur. J. Cancer, 37(8) (2001) 1033-40.

C.L. Gebhart, A.V. Kabanov, Evaluation of polyplexes as gene transfer agents. J. Control. Release, 73(2-3) (2001) 401-16.

M.J. Geisow, P. D'Arcy Hart, M.R. Young, Temporal changes of lysosome and phagosome pH during phagolysosome formation in macrophages: studies by fluorescence spectroscopy. J. Cell Biol., 89(3) (1981) 645-52.

S. Ghosh, R. Brown, J.C.R. Jones, S.M. Ellerbroek, M.S. Stack, Urinary-type Plasminogen Activator (uPA) Expression Localization Are Regulated by a3b1 Integrin in Oral Keratinocytes. J. Biol. Chem., 275(31) (2000a) 23869-76.

S. Ghosh, S.M. Ellerbroek, Y. Wu, M.S. Stack, Tumor cell-mediated proteolysis: regulatory mechanisms and functional consequences. Fibrinolysis Proteolysis, 14(2-3) (2000b) 87-97.

W.T. Godbey, M.A. Barry, P. Saggau, K.K. Wu, A.G. Mikos, Poly(ethylenimine)-mediated transfection: a new paradigm for gene delivery. J. Biomed. Mater. Res., 51(3) (2000) 321-8.

L. Goretzki, B.M. Mueller, Receptor-mediated endocytosis of urokinase-type plasminogen activator is regulated by cAMP-dependent protein kinase. J. Cell Sci., 110(Pt 12) (1997) 1395-402.

W. Guo, R.L. Lee, Receptor-targeted gene delivery via folate-conjugated polyethylenimine. AAPS Pharmsci., 1(4) (1999) E19.

H. Han, D.J. Bearss, L.W. Browne, R. Calaluce, R.B. Nagle, D.D. Von Hoff, Identification of differentially expressed genes in pancreatic cancer cells using cDNA microarray. Cancer Res., 62(10) (2002) 2890-6.

T. Hara, Y. Aramaki, S. Takada, K. Koike, S. Tsuchiya, Receptor-mediated transfer of pSV2CAT DNA to a human hepatoblastoma cell line HepG2 using asialofetuin-labeled cationic liposomes. Gene, 159(2) (1995) 167-74.

Harcourtschool, Cell compartments, 2005, http://www.harcourtschool.com/glossary/science/define/gr5/nucleus5ae.html

J.M. Harris, N.E. Martin, M. Modi, Pegylation: a novel process for modifying pharmacokinetics. Clin. Pharmacokinet., 40(7) (2001) 539-51.

P. Harvie, B. Dutzar, T. Galbraith, S. Cudmore, D. O'Mahony, P. Anklesaria, R. Paul, Targeting of lipid-protamine-DNA (LPD) lipopolyplexes using RGD motifs. J. Liposome Res., 13(3-4) (2003) 231-47.

M. Hashida, M. Nishikawa, F. Yamashita, Y. Takakura, Cell-specific delivery of genes with glycosylated carriers. Adv. Drug Del. Rev., 52(3) (2001) 187-196.

H. Hashizume, P. Baluk, S. Morikawa, J.W. McLean, G. Thurston, S. Roberge, R.K. Jain, D.M. McDonald, Openings between defective endothelial cells explain tumor vessel leakiness. Am. J. Pathol., 156(4) (2000) 1363-80.

R. Hejazi, M. Amiji, Chitosan based delivery systems: Physiochemical properties and pharmaceutical applications, in: S. Dimitriu (Ed.), Polymeric Biomaterials, Marcel Dekker, 2002, pp. 213-236

G.T. Hermanson, Bioconjugate Techniques, Academic Press, London, 1996.

I.R. Hill, M.C. Garnett, F. Bignotti, S.S. Davis, In vitro cytotoxicity of poly(amidoamine)s: relevance to DNA delivery. Biochim. Biophys. Acta, 1427(2) (1999) 161-74.

S. Hiscox, L. Morgan, T.P. Green, D. Barrow, J. Gee, R.I. Nicholson, Elevated Src activity promotes cellular invasion and motility in tamoxifen resistant breast cancer cells. Breast Cancer Res. Treat., (2005) 1-12.

M. Huang, Z. Ma, E. Khor, L.Y. Lim, Uptake of FITC-chitosan nanoparticles by A549 cells. Pharm. Res., 19(10) (2002) 1488-94.

M. Huang, E. Khor, L.Y. Lim, Uptake and cytotoxicity of chitosan molecules and nanoparticles: effects of molecular weight and degree of deacetylation. Pharm. Res., 21(2) (2004) 344-53.

B.E. Huber, C.A. Richards, T.A. Krenitsky, Retroviral-mediated gene therapy for the treatment of hepatocellular carcinoma: an innovative approach for cancer therapy. Proc. Natl. Acad. Sci. U. S. A., 88(18) (1991) 8039-43.

P.E. Huber, M.J. Mann, L.G. Melo, A. Ehsan, D. Kong, L. Zhang, M. Rezvani, P. Peschke, F. Jolesz, V.J. Dzau, K. Hynynen, Focused ultrasound (HIFU) induces localized enhancement of reporter gene expression in rabbit carotid artery. Gene Ther., 10(18) (2003) 1600-7.

M.A. Hudson, L.M. McReynolds, Urokinase and the urokinase receptor: association with in vitro invasiveness of human bladder cancer cell lines. J. Natl. Cancer Inst., 89(10) (1997) 709-17.

L. Illum, Chitosan and its use as a pharmaceutical excipient. Pharm. Res., 15(9) (1998) 1326-31.

R. Ippoliti, E. Lendaro, P.A. Benedetti, M.R. Torrisi, F. Belleudi, D. Carpani, M.R. Soria, M.S. Fabbrini, Endocytosis of a chimera between human pro-urokinase and the plant toxin saporin: an unusual internalization mechanism. FASEB J., 14(10) (2000) 1335-44.

T. Ishii, Y. Okahata, T. Sato, Mechanism of cell transfection with plasmid/chitosan complexes. Biochim. Biophys. Acta-Biomembr., 1514(1) (2001) 51-64.

C.A. Jansma, M. Thanou, H.E. Junginger, G. Borchard, Preparation and characterization of 6-O-carboxymethyl-N-trimethyl chitosan derivative as a potential carrier for targeted polymeric gene and drug delivery. STP Pharma Sci., 13(1) (2003) 63-67.

C. Jeuniaux, M.F. Voss-Foucart, Chitin biomass and production in the marine environment. Biochem. Syst. Ecol., 19(5) (1991) 347-356.

A. Jillavenkatesa, S. Dapkunas, L.-S.H. Lum, Particle Size Characterisation Practical Guide, 2005, http://www.msel.nist.gov/practiceguides/SP960_1.pdf

N.A. Jones, I.R. Hill, S. Stolnik, F. Bignotti, S.S. Davis, M.C. Garnett, Polymer chemical structure is a key determinant of physicochemical and colloidal properties of polymer-DNA complexes for gene delivery. Biochim. Biophys. Acta, 1517(1) (2000) 1-18.

P.J. Jost, R.P. Harbottle, A. Knight, A.D. Miller, C. Coutelle, H. Schneider, A novel peptide, THALWHT, for the targeting of human airway epithelia. FEBS Lett., 489(2-3) (2001) 263-9.

W. Kafienah, F. Al-Fayez, A.P. Hollander, M.D. Barker, Inhibition of cartilage degradation: a combined tissue engineering and gene therapy approach. Arthritis Rheum., 48(3) (2003) 709-18.

A. Katchalsky, Polyelectrolytes and their biological interactions, in: T. Shedlowsky (Ed.), Connective tissue: Intercellular macromolecules, Little, Brown and Co., Boston, 1964, pp. 9-41

T. Kawano, T. Okuda, H. Aoyagi, T. Niidome, Long circulation of intravenously administered plasmid DNA delivered with dendritic poly(L-lysine) in the blood flow. J. Control. Release, 99(2) (2004) 329-37.

C.Y. Ke, C.J. Mathias, M.A. Green, Folate-receptor-targeted radionuclide imaging agents. Adv. Drug Del. Rev., 56(8) (2004) 1143-60.

T. Kean, S. Roth, M. Thanou, Trimethylated chitosans as non-viral gene delivery vectors: Cytotoxicity and transfection efficiency. J. Control. Release, 103(3) (2005) 643-53.

T. Kiang, J. Wen, H. Lim, K.W. Leong. Degree of deacetylation of chitosan: effect on gene transfection efficiency in vivo. in *Proc. Int. Symp. Control. Release Bioact. Mater.* 2002. Seoul, Korea.

T.H. Kim, J.E. Ihm, Y.J. Choi, J.W. Nah, C.S. Cho, Efficient gene delivery by urocanic acid-modified chitosan. J. Control. Release, 93(3) (2003) 389-402.

Y.H. Kim, S.H. Gihm, C.R. Park, K.Y. Lee, T.W. Kim, I.C. Kwon, H. Chung, S.Y. Jeong, Structural characteristics of size-controlled self-aggregates of deoxycholic acid-modified chitosan and their application as a DNA delivery carrier. Bioconj. Chem., 12(6) (2001) 932-938.

R. Kircheis, A. Kichler, G. Wallner, M. Kursa, M. Ogris, T. Felzmann, M. Buchberger, E. Wagner, Coupling of cell-binding ligands to polyethylenimine for targeted gene delivery. Gene Ther., 4(5) (1997) 409-18.

R. Kircheis, L. Wightman, A. Schreiber, B. Robitza, V. Rossler, M. Kursa, E. Wagner, Polyethylenimine/DNA complexes shielded by transferrin target gene expression to tumors after systemic application. Gene Ther., 8(1) (2001a) 28-40.

R. Kircheis, L. Wightman, E. Wagner, Design and gene delivery activity of modified polyethylenimines. Adv. Drug Del. Rev., 53(3) (2001b) 341-58.

H. Kobayashi, M. Schmitt, L. Goretzki, N. Chucholowski, J. Calvete, M. Kramer, W.A. Gunzler, F. Janicke, H. Graeff, Cathepsin B efficiently activates the soluble and the tumor cell receptor-bound form of the proenzyme urokinase-type plasminogen activator (Pro-uPA). J. Biol. Chem., 266(8) (1991) 5147-52.

D.B. Kohn, M. Sadelain, J.C. Glorioso, Occurrence of leukaemia following gene therapy of X-linked SCID. Nat. Rev. Cancer, 3(7) (2003) 477-88.

M. Koping-Hoggard, I. Tubulekas, H. Guan, K. Edwards, M. Nilsson, K.M. Varum, P. Artursson, Chitosan as a nonviral gene delivery system. Structure-property relationships and characteristics compared with polyethylenimine in vitro and after lung administration in vivo. Gene Ther., 8(14) (2001) 1108-21.

M. Koping-Hoggard, Y.S. Mel'nikova, K.M. Varum, B. Lindman, P. Artursson, Relationship between the physical shape and the efficiency of oligomeric chitosan as a gene delivery system in vitro and in vivo. J. Gene. Med., 5(2) (2003) 130-41.

J.F. Kukowska-Latallo, E. Raczka, A. Quintana, C. Chen, M. Rymaszewski, J.R. Baker, Jr., Intravascular and endobronchial DNA delivery to murine lung tissue using a novel, nonviral vector. Hum. Gene Ther., 11(10) (2000) 1385-95.

M.N.V.R. Kumar, A review of chitin and chitosan applications. Reactive & Functional Polymers, 46(1) (2000) 1-27.

K. Kunath, T. Merdan, O. Hegener, H. Haberlein, T. Kissel, Integrin targeting using RGD-PEI conjugates for in vitro gene transfer. J. Gene. Med., 5(7) (2003a) 588-99.

K. Kunath, A. von Harpe, D. Fischer, T. Kissel, Galactose-PEI-DNA complexes for targeted gene delivery: degree of substitution affects complex size and transfection efficiency. J. Control. Release, 88(1) (2003b) 159-72.

M. Kursa, G.F. Walker, V. Roessler, M. Ogris, W. Roedl, R. Kircheis, E. Wagner, Novel shielded transferrin-polyethylene glycol-polyethylenimine/DNA complexes for systemic tumor-targeted gene transfer. Bioconj. Chem., 14(1) (2003) 222-31.

D. Lane, Anthony Dipple Carcinogenesis Award. p53 from pathway to therapy. Carcinogenesis, 25(7) (2004) 1077-81.

F. Lanza, G.L. Castoldi, B. Castagnari, R.F. Todd, 3rd, S. Moretti, S. Spisani, A. Latorraca, E. Focarile, M.G. Roberti, S. Traniello, Expression and functional role of urokinase-type plasminogen activator receptor in normal and acute leukaemic cells. Br. J. Haematol., 103(1) (1998) 110-23.

J.D. Lathia, L. Leodore, M.A. Wheatley, Polymeric contrast agent with targeting potential. Ultrasonics, 42(1-9) (2004) 763-8.

E.C. Lattime, S.L. Gerson, Gene Therapy of Cancer, Academic Press, London, 1999.

D. Lechardeur, A.S. Verkman, G.L. Lukacs, Intracellular routing of plasmid DNA during non-viral gene transfer. Adv. Drug Del. Rev., 57(5) (2005) 755-67.

L. Leclercq, M. Boustta, M. Vert, A Physico-chemical Approach of Polyanion-Polycation Interactions Aimed at Better Understanding the In Vivo Behaviour of Polyelectrolyte-based Drug Delivery and Gene Transfection. J. Drug Target., 11(3) (2003) 129-138.

H. Lee, T.H. Kim, T.G. Park, A receptor-mediated gene delivery system using streptavidin and biotin-derivatized, pegylated epidermal growth factor. J. Control. Release, 83(1) (2002) 109-19.

K.Y. Lee, I.C. Kwon, Y.H. Kim, W.H. Jo, S.Y. Jeong, Preparation of chitosan self-aggregates as a gene delivery system. J. Control. Release, 51(2-3) (1998) 213-20.

M. Lee, J.W. Nah, Y. Kwon, J.J. Koh, K.S. Ko, S.W. Kim, Water-soluble and low molecular weight chitosan-based plasmid DNA delivery. Pharm. Res., 18(4) (2001) 427-431.

N.R. Lemoine, Risks and benefits of gene therapy for immunodeficiency: a reality check. Gene Ther., 9(23) (2002) 1561-1562.

S.R. Leong, L. DeForge, L. Presta, T. Gonzalez, A. Fan, M. Reichert, A. Chuntharapai, K.J. Kim, D.B. Tumas, W.P. Lee, P. Gribling, B. Snedecor, H. Chen, V. Hsei, M. Schoenhoff, V. Hale, J. Deveney, I. Koumenis, Z. Shahrokh, P. McKay, W. Galan, B. Wagner, D. Narindray, C. Hebert, G. Zapata, Adapting pharmacokinetic properties of a humanized anti-interleukin-8 antibody for therapeutic applications using site-specific pegylation. Cytokine, 16(3) (2001) 106-19.

B. Leyland-Jones, K. Gelmon, J.P. Ayoub, A. Arnold, S. Verma, R. Dias, P. Ghahramani, Pharmacokinetics, safety, and efficacy of trastuzumab administered every three weeks in combination with paclitaxel. J. Clin. Oncol., 21(21) (2003) 3965-71.

S. Li, Y. Tan, E. Viroonchatapan, B.R. Pitt, L. Huang, Targeted gene delivery to pulmonary endothelium by anti-PECAM antibody. Am. J. Physiol.-Lung Cell. Mol. Physiol., 278(3) (2000) L504-11.

D. Liu, J. Aguirre Ghiso, Y. Estrada, L. Ossowski, EGFR is a transducer of the urokinase receptor initiated signal that is required for in vivo growth of a human carcinoma. Cancer Cell, 1(5) (2002) 445-57.

P. Llinas, M. Helene Le Du, H. Gardsvoll, K. Dano, M. Ploug, B. Gilquin, E.A. Stura, A. Menez, Crystal structure of the human urokinase plasminogen activator receptor bound to an antagonist peptide. EMBO J., 24(9) (2005) 1655-63.

C. Luparello, M. Del Rosso, In vitro anti-proliferative and anti-invasive role of aminoterminal fragment of urokinase-type plasminogen activator on 8701-BC breast cancer cells. Eur. J. Cancer, 32A(4) (1996) 702-7.

J. Luten, J.H. van Steenis, R. van Someren, J. Kemmink, N.M. Schuurmans-Nieuwenbroek, G.A. Koning, D.J. Crommelin, C.F. van Nostrum, W.E. Hennink, Water-soluble biodegradable cationic polyphosphazenes for gene delivery. J. Control. Release, 89(3) (2003) 483-97.

K.D. Mack, R. Wei, A. Elbagarri, N. Abbey, M.S. McGrath, A novel method for DEAE-dextran mediated transfection of adherent primary cultured human macrophages. J. Immunol. Methods, 211(1-2) (1998) 79-86.

H. Maeda, T. Konno, K. Iwai, S. Maki, S. Tashiro, [Tumor selective drug delivery with lipid contrast medium (smancs/lipiodol): sustained antitumor effect, enhanced diagnostic value and quantification of dosage regimen]. Gan To Kagaku Ryoho, 11(4) (1984) 814-26.

H. Maeda, J. Wu, T. Sawa, Y. Matsumura, K. Hori, Tumor vascular permeability and the EPR effect in macromolecular therapeutics: a review. J. Control. Release, 65(1-2) (2000) 271-284.

H. Maeda, T. Sawa, T. Konno, Mechanism of tumor-targeted delivery of macromolecular drugs, including the EPR effect in solid tumor and clinical overview of the prototype polymeric drug SMANCS. J. Control. Release, 74(1-3) (2001) 47-61.

R.I. Mahato, J. Henry, A.S. Narang, O. Sabek, D. Fraga, M. Kotb, A.O. Gaber, Cationic lipid and polymer-based gene delivery to human pancreatic islets. Mol. Ther., 7(1) (2003) 89-100.

H.Q. Mao, K. Roy, V.L. Troung-Le, K.A. Janes, K.Y. Lin, Y. Wang, J.T. August, K.W. Leong, Chitosan-DNA nanoparticles as gene carriers: synthesis, characterization and transfection efficiency. J. Control. Release, 70(3) (2001) 399-421.

J. Marshall, An Open-Label Safety Study of Escalating Doses of SGT-53 for Systemic Injection in Patients with Advanced Solid Tumor Malignancies. 2005, Georgetown University: Washington, http://www.gemcris.od.nih.gov/abstracts/591_s.pdf

R. Martiniello-Wilks, A. Dane, D.J. Voeks, G. Jeyakumar, E. Mortensen, J.M. Shaw, X.Y. Wang, G.W. Both, P.J. Russell, Gene-directed enzyme prodrug therapy for prostate cancer in a mouse model that imitates the development of human disease. J. Gene. Med., 6(1) (2004) 43-54.

F. Maruta, A.L. Parker, K.D. Fisher, P.G. Murray, D.J. Kerr, L.W. Seymour, Use of a phage display library to identify oligopeptides binding to the lumenal surface of polarized endothelium by ex vivo perfusion of human umbilical veins. J. Drug Target., 11(1) (2003) 53-9.

Y. Matsumura, T. Oda, H. Maeda, [General mechanism of intratumor accumulation of macromolecules: advantage of macromolecular therapeutics]. Gan To Kagaku Ryoho, 14(3 Pt 2) (1987) 821-9.

A.P. Mazar, J. Henkin, R.H. Goldfarb, The urokinase plasminogen activator system in cancer: implications for tumor angiogenesis and metastasis. Angiogenesis, 3(1) (1999) 15-32.

McCue, New Bandage Uses Biopolymer, 2003, http://www.chemistry.org/portal/a/c/s/1/feature_ent.html?id=401c0f5c4d8511d7f6e36ed9fe800100

T. Merdan, J. Kopecek, T. Kissel, Prospects for cationic polymers in gene and oligonucleotide therapy against cancer. Adv. Drug Del. Rev., 54(5) (2002) 715-58.

T. Merdan, J. Callahan, H. Petersen, K. Kunath, U. Bakowsky, P. Kopeckova, T. Kissel, J. Kopecek, Pegylated polyethylenimine-fab' antibody fragment conjugates for targeted gene delivery to human ovarian carcinoma cells. Bioconj. Chem., 14(5) (2003) 989-96.

M. Mesnil, H. Yamasaki, Bystander effect in herpes simplex virus-thymidine kinase/ganciclovir cancer gene therapy: role of gap-junctional intercellular communication. Cancer Res., 60(15) (2000) 3989-99.

D.E. Meyer, G.A. Kong, M.W. Dewhirst, M.R. Zalutsky, A. Chilkoti, Targeting a genetically engineered elastin-like polypeptide to solid tumors by local hyperthermia. Cancer Res., 61(4) (2001) 1548-54.

K.A. Mislick, J.D. Baldeschwieler, Evidence for the role of proteoglycans in cation-mediated gene transfer. Proc. Natl. Acad. Sci. U. S. A., 93(22) (1996) 12349-54.

S.K. Moestrup, T.L. Holtet, M. Etzerodt, H.C. Thogersen, A. Nykjaer, P.A. Andreasen, H.H. Rasmussen, L. Sottrup-Jensen, J. Gliemann, Alpha 2-macroglobulin-proteinase complexes, plasminogen activator inhibitor type-1-plasminogen activator complexes, and receptor-associated protein bind to a region of the alpha 2-macroglobulin receptor containing a cluster of eight complement-type repeats. J. Biol. Chem., 268(18) (1993) 13691-6.

S. Moffatt, S. Wiehle, R.J. Cristiano, Tumor-specific gene delivery mediated by a novel peptide-polyethylenimine-DNA polyplex targeting aminopeptidase N/CD13. Hum. Gene Ther., 16(1) (2005) 57-67.

S.M. Moghimi, A.C. Hunter, J.C. Murray, Nanomedicine: current status and future prospects. FASEB J., 19(3) (2005) 311-30.

Molecular Probes, Amine Reactive Probes Conjugation Handbook, 2005, http://probes.invitrogen.com/media/pis/mp00143.pdf

N.R. Monks, J.A. Calvete, N.J. Curtin, D.C. Blakey, S.J. East, D.R. Newell, Cellular glutathione as a determinant of the sensitivity of colorectal tumour cell-lines to ZD2767 antibody-directed enzyme prodrug therapy (ADEPT). Br. J. Cancer, 83(2) (2000) 267-9.

N. Montuori, M.V. Carriero, S. Salzano, G. Rossi, P. Ragno, The cleavage of the urokinase receptor regulates its multiple functions. J. Biol. Chem., 277(49) (2002) 46932-9.

D.M. Morgan, V.L. Larvin, J.D. Pearson, Biochemical characterisation of polycation-induced cytotoxicity to human vascular endothelial cells. J. Cell Sci., 94(Pt 3) (1989) 553-9.

T. Mori, T. Abe, Y. Wakabayashi, T. Hikawa, K. Matsuo, Y. Yamada, M. Kuwano, S. Hori, Up-regulation of urokinase-type plasminogen activator and its receptor correlates with enhanced invasion activity of human glioma cells mediated by transforming growth factor-alpha or basic fibroblast growth factor. J. Neuro-Oncol., 46(2) (2000) 115-23.

S. Morita, A. Sato, H. Hayakawa, H. Ihara, T. Urano, Y. Takada, A. Takada, Cancer cells overexpress mRNA of urokinase-type plasminogen activator, its receptor and inhibitors in human non-small-cell lung cancer tissue: analysis by Northern blotting and in situ hybridization. Int. J. Cancer, 78(3) (1998) 286-92.

I. Mortimer, P. Tam, I. MacLachlan, R.W. Graham, E.G. Saravolac, P.B. Joshi, Cationic lipid-mediated transfection of cells in culture requires mitotic activity. Gene Ther., 6(3) (1999) 403-11.

T. Mosmann, Rapid colorimetric assay for cellular growth and survival: application to proliferation and cytotoxicity assays. J. Immunol. Methods, 65(1-2) (1983) 55-63.

B. Muehlenweg, I. Assfalg-Machleidt, S.G. Parrado, M. Burgle, S. Creutzburg, M. Schmitt, E.A. Auerswald, W. Machleidt, V. Magdolen, A novel type of bifunctional inhibitor directed against proteolytic activity and receptor/ligand interaction. Cystatin with a urokinase receptor binding site. J. Biol. Chem., 275(43) (2000) 33562-6.

J. Murata, Y. Ohya, T. Ouchi, Possibility of application of quaternary chitosan having pendant galactose residues as gene delivery tool. Carbohydr. Polym., 29(1) (1996) 69-74.

J. Murata, Y. Ohya, T. Ouchi, Design of quaternary chitosan conjugate having antennary galactose residues as a gene delivery tool. Carbohydr. Polym., 32(2) (1997) 105-109.

G. Murphy, J. Gavrilovic, Proteolysis and cell migration: creating a path? Curr. Opin. Cell Biol., 11(5) (1999) 614-21.

H.T. Myohanen, R.W. Stephens, K. Hedman, H. Tapiovaara, E. Ronne, G. Hoyer-Hansen, K. Dano, A. Vaheri, Distribution and lateral mobility of the urokinase-receptor complex at the cell surface. J. Histochem. Cytochem., 41(9) (1993) 1291-301.

T. Nakanishi, S. Fukushima, K. Okamoto, M. Suzuki, Y. Matsumura, M. Yokoyama, T. Okano, Y. Sakurai, K. Kataoka, Development of the polymer micelle carrier system for doxorubicin. J. Control. Release, 74(1-3) (2001) 295-302.

J.W. Neidigh, R.M. Fesinmeyer, N.H. Andersen, Designing a 20-residue protein. Nat. Struct. Mol. Biol., 9(6) (2002) 425-30.

F. Nilsson, L. Tarli, F. Viti, D. Neri, The use of phage display for the development of tumour targeting agents. Adv. Drug Del. Rev., 43(2-3) (2000) 165-196.

M. Nishikawa, M. Yamauchi, K. Morimoto, E. Ishida, Y. Takakura, M. Hashida, Hepatocyte-targeted in vivo gene expression by intravenous injection of plasmid DNA complexed with synthetic multi-functional gene delivery system. Gene Ther., 7(7) (2000) 548-55.

A. Nykjaer, L. Kjoller, R.L. Cohen, D.A. Lawrence, B.A. Garni-Wagner, R.F. Todd, 3rd, A.J. van Zonneveld, J. Gliemann, P.A. Andreasen, Regions involved in binding of urokinase-type-1 inhibitor complex and pro-urokinase to the endocytic alpha 2-macroglobulin receptor/low density lipoprotein receptor-related protein. Evidence that the urokinase receptor protects pro-urokinase against binding to the endocytic receptor. J. Biol. Chem., 269(41) (1994a) 25668-76.

A. Nykjaer, B. Moller, R.F. Todd, 3rd, T. Christensen, P.A. Andreasen, J. Gliemann, C.M. Petersen, Urokinase receptor. An activation antigen in human T lymphocytes. J. Immunol., 152(2) (1994b) 505-16.

A. Nykjaer, M. Conese, E.I. Christensen, D. Olson, O. Cremona, J. Gliemann, F. Blasi, Recycling of the urokinase receptor upon internalization of the uPA:serpin complexes. EMBO J., 16(10) (1997) 2610-20.

A. Nykjaer, E.I. Christensen, H. Vorum, H. Hager, C.M. Petersen, H. Roigaard, H.Y. Min, F. Vilhardt, L.B. Moller, S. Kornfeld, J. Gliemann, Mannose 6-phosphate/insulin-like growth factor-II receptor targets the urokinase receptor to lysosomes via a novel binding interaction. J. Cell Biol., 141(3) (1998) 815-28.

M. Ogris, P. Steinlein, M. Kursa, K. Mechtler, R. Kircheis, E. Wagner, The size of DNA/transferrin-PEI complexes is an important factor for gene expression in cultured cells. Gene Ther., 5(10) (1998) 1425-33.

M. Ogris, E. Wagner, Tumor-targeted gene transfer with DNA polyplexes. Somat. Cell Mol. Genet., 27(1-6) (2002a) 85-95.

M. Ogris, E. Wagner, Targeting tumors with non-viral gene delivery systems. Drug Discov. Today, 7(8) (2002b) 479-85.

M. Ogris, G. Walker, T. Blessing, R. Kircheis, M. Wolschek, E. Wagner, Tumor-targeted gene therapy: strategies for the preparation of ligand-polyethylene glycol-polyethylenimine/DNA complexes. J. Control. Release, 91(1-2) (2003) 173-81.

P. Ohana, O. Gofrit, S. Ayesh, W. Al-Sharef, A. Mizrahi, T. Birman, T. Schneider, I. Matouk, N. de Groot, E. Tavdy, A.A. Sidi, A. Hochberg, Regulatory sequences of the H19 gene in DNA based therapy of bladder cancer. Gene Ther. Mol. Biol., 8(A) (2004) 181-192.

M.G. Ormerod, Further applications to cell biology, in: M.G. Ormerod (Ed.), Flow Cytometry, Oxford Universtity Press, Oxford, 2000, pp. 249-260

J.W. Park, K. Hong, D.B. Kirpotin, G. Colbern, R. Shalaby, J. Baselga, Y. Shao, U.B. Nielsen, J.D. Marks, D. Moore, D. Papahadjopoulos, C.C. Benz, Anti-HER2 immunoliposomes: enhanced efficacy attributable to targeted delivery. Clin. Cancer Res., 8(4) (2002) 1172-81.

A.L. Parker, C. Newman, S. Briggs, L. Seymour, P.J. Sheridan, Nonviral gene delivery: techniques and implications for molecular medicine. Expert Rev. Mol. Med., (2003) 1-15.

A.L. Parker, K.D. Fisher, D. Oupicky, M.L. Read, S.A. Nicklin, A.H. Baker, L.W. Seymour, Enhanced gene transfer activity of peptide-targeted gene-delivery vectors. J. Drug Target., 13(1) (2005) 39-51.

R. Pasqualini, E. Koivunen, E. Ruoslahti, A peptide isolated from phage display libraries is a structural and functional mimic of an RGD-binding site on integrins. J. Cell Biol., 130(5) (1995) 1189-96.

B.C. Patterson, Q.A. Sang, Angiostatin-converting enzyme activities of human matrilysin (MMP-7) and gelatinase B/type IV collagenase (MMP-9). J. Biol. Chem., 272(46) (1997) 28823-5.

R. Picone, E.L. Kajtaniak, L.S. Nielsen, N. Behrendt, M.R. Mastronicola, M.V. Cubellis, M.P. Stoppelli, S. Pedersen, K. Dano, F. Blasi, Regulation of urokinase receptors in monocytelike U937 cells by phorbol ester phorbol myristate acetate. J. Cell Biol., 108(2) (1989) 693-702.

C. Plank, K. Zatloukal, M. Cotten, K. Mechtler, E. Wagner, Gene transfer into hepatocytes using asialoglycoprotein receptor mediated endocytosis of DNA complexed with an artificial tetra-antennary galactose ligand. Bioconj. Chem., 3(6) (1992) 533-9.

C. Plank, U. Schillinger, F. Scherer, C. Bergemann, J.S. Remy, F. Krotz, M. Anton, J. Lausier, J. Rosenecker, The magnetofection method: using magnetic force to enhance gene delivery. Biol. Chem., 384(5) (2003) 737-47.

M. Plebani, L. Herszenyi, P. Carraro, M. De Paoli, G. Roveroni, R. Cardin, Z. Tulassay, R. Naccarato, F. Farinati, Urokinase-type plasminogen activator receptor in gastric cancer: tissue expression and prognostic role. Clin. Exp. Metastasis, 15(4) (1997) 418-25.

T. Plesner, M. Ploug, V. Ellis, E. Ronne, G. Hoyer-Hansen, M. Wittrup, T.L. Pedersen, T. Tscherning, K. Dano, N.E. Hansen, The receptor for urokinase-type plasminogen activator and urokinase is translocated from two distinct intracellular compartments to the plasma membrane on stimulation of human neutrophils. Blood, 83(3) (1994) 808-15.

T. Plesner, N. Behrendt, M. Ploug, Structure, function and expression on blood and bone marrow cells of the urokinase-type plasminogen activator receptor, uPAR. Stem Cells, 15(6) (1997) 398-408.

M. Ploug, E. Ronne, N. Behrendt, A.L. Jensen, F. Blasi, K. Dano, Cellular receptor for urokinase plasminogen activator. Carboxyl-terminal processing and membrane anchoring by glycosyl-phosphatidylinositol. J. Biol. Chem., 266(3) (1991) 1926-33.

M. Ploug, S. Ostergaard, H. Gardsvoll, K. Kovalski, C. Holst-Hansen, A. Holm, L. Ossowski, K. Dano, Peptide-derived antagonists of the urokinase receptor. affinity maturation by combinatorial chemistry, identification of functional epitopes, and inhibitory effect on cancer cell intravasation. Biochemistry, 40(40) (2001) 12157-68.

M. Ploug, H. Gardsvoll, T.J. Jorgensen, L. Lonborg Hansen, K. Dano, Structural analysis of the interaction between urokinase-type plasminogen activator and its receptor: a potential target for anti-invasive cancer therapy. Biochem. Soc. Trans., 30(2) (2002) 177-83.

H. Pollard, J.S. Remy, G. Loussouarn, S. Demolombe, J.P. Behr, D. Escande, Polyethylenimine but not cationic lipids promotes transgene delivery to the nucleus in mammalian cells. J. Biol. Chem., 273(13) (1998) 7507-11.

M.H. Porteus, T. Cathomen, M.D. Weitzman, D. Baltimore, Efficient gene targeting mediated by adeno-associated virus and DNA double-strand breaks. Mol. Cell. Biol., 23(10) (2003) 3558-65.

G. Prodi, L.A. Liotta, P.-L. Lollini, S. Garbisa, S. Gorini, K. Hellmann, Cancer Metastasis - Biological and Biochemical Mechanisms and Clinical Aspects, Plenum Press, London, 1998.

Promega, pGL3 plasmid restriction map, 2003a, www.promega.com

Promega, Luciferase Assay Protocol, 2003b, www.promega.com

Qbiogene, Ligand conjugated jetPEI, 2003, www.qbiogene.com

Qiagen, Qiagen Plasmid Purification Handbook. 2000, Qiagen: Crawley, UK.

Z.M. Qian, H. Li, H. Sun, K. Ho, Targeted drug delivery via the transferrin receptor-mediated endocytosis pathway. Pharmacol. Rev., 54(4) (2002) 561-87.

P.H. Quax, J.M. Grimbergen, M. Lansink, A.H. Bakker, M.C. Blatter, D. Belin, V.W. van Hinsbergh, J.H. Verheijen, Binding of human urokinase-type plasminogen activator to its receptor: residues involved in species specificity and binding. Arterioscler. Thromb. Vasc. Biol., 18(5) (1998) 693-701.

V. Rajagopal, R.J. Kreitman, Recombinant toxins that bind to the urokinase receptor are cytotoxic without requiring binding to the alpha(2)-macroglobulin receptor. J. Biol. Chem., 275(11) (2000) 7566-73.

J.G. Ramage, D.A. Vallera, J.H. Black, P.D. Aplan, U.R. Kees, A.E. Frankel, The diphtheria toxin/urokinase fusion protein (DTAT) is selectively toxic to CD87 expressing leukemic cells. Leuk. Res., 27(1) (2003) 79-84.

H.P. Rang, M.M. Dale, J.M. Ritter, Pharmacology, 3rd Ed, Churchill Livingstone, Edinburgh, 1996.

S.B. Rao, C.P. Sharma, Use of chitosan as a biomaterial: studies on its safety and hemostatic potential. J. Biomed. Mater. Res., 34(1) (1997) 21-8.

V. Raussens, M.K. Mah, C.M. Kay, B.D. Sykes, R.O. Ryan, Structural characterization of a low density lipoprotein receptor-active apolipoprotein E peptide, ApoE3-(126-183). J. Biol. Chem., 275(49) (2000) 38329-36.

V. Raussens, C.M. Slupsky, R.O. Ryan, B.D. Sykes, NMR structure and dynamics of a receptor-active apolipoprotein E peptide. J. Biol. Chem., 277(32) (2002) 29172-80.

J.A. Reddy, D.W. Clapp, P.S. Low, Retargeting of viral vectors to the folate receptor endocytic pathway. J. Control. Release, 74(1-3) (2001) 77-82.

T.M. Reineke, M.E. Davis, Structural effects of carbohydrate-containing polycations on gene delivery. 2. Charge center type. Bioconj. Chem., 14(1) (2003a) 255-61.

T.M. Reineke, M.E. Davis, Structural effects of carbohydrate-containing polycations on gene delivery. 1. Carbohydrate size and its distance from charge centers. Bioconj. Chem., 14(1) (2003b) 247-54.

J. Rejman, V. Oberle, I.S. Zuhorn, D. Hoekstra, Size-dependent internalization of particles via the pathways of clathrin- and caveolae-mediated endocytosis. Biochem. J., 377(Pt 1) (2004) 159-69.

D. Ribatti, D. Leali, A. Vacca, R. Giuliani, A. Gualandris, L. Roncali, M.L. Nolli, M. Presta, In vivo angiogenic activity of urokinase: role of endogenous fibroblast growth factor-2. J. Cell Sci., 112(Pt 23) (1999) 4213-21.

S. Richardson, P. Ferruti, R. Duncan, Poly(amidoamine)s as potential endosomolytic polymers: evaluation in vitro and body distribution in normal and tumour-bearing animals. J. Drug Target., 6(6) (1999a) 391-404.

S.C. Richardson, H.V. Kolbe, R. Duncan, Potential of low molecular mass chitosan as a DNA delivery system: biocompatibility, body distribution and ability to complex and protect DNA. Int. J. Pharm., 178(2) (1999b) 231-43.

S.C.W. Richardson, N.G. Pattrick, Y.K.S. Man, P. Ferruti, R. Duncan, Poly(amidoamine)s as potential nonviral vectors: Ability to form interpolyelectrolyte complexes and to mediate transfection in vitro. Biomacromolecules, 2(3) (2001) 1023-1028.

H. Ringsdorf, Structure and properties of pharmacologically active polymers. Journal of Polymer Science Polymer Symposium, 51(1) (1975) 135-153.

M.J. Roberts, M.D. Bentley, J.M. Harris, Chemistry for peptide and protein PEGylation. Adv. Drug Del. Rev., 54(4) (2002) 459-76.

M.A. Robinson, S.T. Charlton, P. Garnier, X.T. Wang, S.S. Davis, A.C. Perkins, M. Frier, R. Duncan, T.J. Savage, D.A. Wyatt, S.A. Watson, B.G. Davis, LEAPT: lectin-directed enzyme-activated prodrug therapy. Proc. Natl. Acad. Sci. U. S. A., 101(40) (2004) 14527-32.

A.L. Roldan, M.V. Cubellis, M.T. Masucci, N. Behrendt, L.R. Lund, K. Dano, E. Appella, F. Blasi, Cloning and expression of the receptor for human urokinase plasminogen activator, a central molecule in cell surface, plasmin dependent proteolysis. EMBO J., 9(2) (1990) 467-74.

D.M. Ross, T.P. Hughes, Cancer treatment with kinase inhibitors: what have we learnt from imatinib? Br. J. Cancer, 90(1) (2004) 12-9.

J.S. Ross, D.P. Schenkein, R. Pietrusko, M. Rolfe, G.P. Linette, J. Stec, N.E. Stagliano, G.S. Ginsburg, W.F. Symmans, L. Pusztai, G.N. Hortobagyi, Targeted therapies for cancer 2004. Am. J. Clin. Pathol., 122(4) (2004) 598-609.

V. Rotrekl, E. Nejedla, I. Kucera, F. Abdallah, K. Palme, B. Brzobohaty, The role of cysteine residues in structure and enzyme activity of a maize beta-glucosidase. Eur. J. Biochem., 266(3) (1999) 1056-65.

K. Roy, H.Q. Mao, S.K. Huang, K.W. Leong, Oral gene delivery with chitosan--DNA nanoparticles generates immunologic protection in a murine model of peanut allergy. Nat. Med., 5(4) (1999) 387-91.

D.A. Rubinson, C.P. Dillon, A.V. Kwiatkowski, C. Sievers, L. Yang, J. Kopinja, D.L. Rooney, M.M. Ihrig, M.T. McManus, F.B. Gertler, M.L. Scott, L. Van Parijs, A lentivirus-based system to functionally silence genes in primary mammalian cells, stem cells and transgenic mice by RNA interference. Nature Genet., 33(3) (2003) 401-6.

P. Ruckert, S.R. Bates, A.B. Fisher, Role of clathrin- and actin-dependent endocytotic pathways in lung phospholipid uptake. Am. J. Physiol.-Lung Cell. Mol. Physiol., 284(6) (2003) L981-9.

G. Russell-Jones, K. McTavish, J. McEwan, J. Rice, D. Nowotnik, Vitamin-mediated targeting as a potential mechanism to increase drug uptake by tumours. J. Inorg. Biochem., 98(10) (2004) 1625-33.

C.R. Safinya, Structures of lipid-DNA complexes: supramolecular assembly and gene delivery. Curr. Opin. Struct. Biol., 11(4) (2001) 440-8.

K. Sagara, S.W. Kim, A new synthesis of galactose-poly(ethylene glycol)-polyethylenimine for gene delivery to hepatocytes. J. Control. Release, 79(1-3) (2002) 271-281.

S.K. Sahoo, W. Ma, V. Labhasetwar, Efficacy of transferrin-conjugated paclitaxel-loaded nanoparticles in a murine model of prostate cancer. Int. J. Cancer, 112(2) (2004) 335-40.

R. Satchi-Fainaro, H. Hailu, J.W. Davies, C. Summerford, R. Duncan, PDEPT: polymer-directed enzyme prodrug therapy. 2. HPMA copolymer-beta-lactamase and HPMA copolymer-C-Dox as a model combination. Bioconj. Chem., 14(4) (2003) 797-804.

R. Satchi-Fainaro, M. Puder, J.W. Davies, H.T. Tran, D.A. Sampson, A.K. Greene, G. Corfas, J. Folkman, Targeting angiogenesis with a conjugate of HPMA copolymer and TNP-470. Nat. Med., 10(3) (2004) 255-61.

T. Sato, T. Ishii, Y. Okahata, In vitro gene delivery mediated by chitosan. effect of pH, serum, and molecular mass of chitosan on the transfection efficiency. Biomaterials, 22(15) (2001) 2075-80.

A.G. Schatzlein, Targeting of Synthetic Gene Delivery Systems. J. Biomed. Biotechnol., 2003(2) (2003) 149-158.

R.M. Schiffelers, G.A. Koning, T.L. ten Hagen, M.H. Fens, A.J. Schraa, A.P. Janssen, R.J. Kok, G. Molema, G. Storm, Anti-tumor efficacy of tumor vasculature-targeted liposomal doxorubicin. J. Control. Release, 91(1-2) (2003) 115-22.

N. Schmiedeberg, M. Schmitt, C. Rolz, V. Truffault, M. Sukopp, M. Burgle, O.G. Wilhelm, W. Schmalix, V. Magdolen, H. Kessler, Synthesis, solution structure, and biological evaluation of urokinase type plasminogen activator (uPA)-derived receptor binding domain mimetics. J. Med. Chem., 45(23) (2002) 4984-94.

S. Schreiber, E. Kampgen, E. Wagner, D. Pirkhammer, J. Trcka, H. Korschan, A. Lindemann, R. Dorffner, H. Kittler, F. Kasteliz, Z. Kupcu, A. Sinski, K. Zatloukal, M. Buschle, W. Schmidt, M. Birnstiel, R.E. Kempe, T. Voigt, H.A. Weber, H. Pehamberger, R. Mertelsmann, E.B. Brocker, K. Wolff, G. Stingl, Immunotherapy of metastatic malignant melanoma by a vaccine consisting of autologous interleukin 2-transfected cancer cells: outcome of a phase I study. Hum. Gene Ther., 10(6) (1999) 983-93.

D.A. Scudiero, R.H. Shoemaker, K.D. Paull, A. Monks, S. Tierney, T.H. Nofziger, M.J. Currens, D. Seniff, M.R. Boyd, Evaluation of a soluble tetrazolium/formazan assay for cell growth and drug sensitivity in culture using human and other tumor cell lines. Cancer Res., 48(17) (1988) 4827-33.

L.W. Seymour, D.R. Ferry, D. Anderson, S. Hesslewood, P.J. Julyan, R. Poyner, J. Doran, A.M. Young, S. Burtles, D.J. Kerr, Hepatic drug targeting: phase I evaluation of polymer-bound doxorubicin. J. Clin. Oncol., 20(6) (2002) 1668-76.

D. Sgouras, The Evaluation of Biocompatibility of Soluble Polymers and Assessment of their Potential as Specific Drug Delivery Systems, PhD Thesis in Pharmacy, 1990, University of Keele, UK

D. Sgouras, R. Duncan, Methods for the Evaluation of Biocompatibility of Soluble Synthetic-Polymers Which Have Potential for Bio-Medical Use .1. Use of the Tetrazolium-Based Colorimetric Assay (Mtt) as a Preliminary Screen for Evaluation of In vitro Cytotoxicity. J. Mater. Sci.-Mater. Med., 1(2) (1990) 61-68.

M. Shadidi, M. Sioud, Selective targeting of cancer cells using synthetic peptides. Drug Resist. Update, 6(6) (2003) 363-71.

S. Shetty, S. Idell, A urokinase receptor mRNA binding protein-mRNA interaction regulates receptor expression and function in human pleural mesothelioma cells. Arch. Biochem. Biophys., 356(2) (1998) 265-79.

N. Shi, R.J. Boado, W.M. Pardridge, Receptor-mediated gene targeting to tissues in vivo following intravenous administration of pegylated immunoliposomes. Pharm. Res., 18(8) (2001) 1091-1095.

C.F. Sier, R. Stephens, J. Bizik, A. Mariani, M. Bassan, N. Pedersen, L. Frigerio, A. Ferrari, K. Dano, N. Brunner, F. Blasi, The level of urokinase-type plasminogen activator receptor is increased in serum of ovarian cancer patients. Cancer Res., 58(9) (1998) 1843-9.

E.L. Sievers, R.A. Larson, E.A. Stadtmauer, E. Estey, B. Lowenberg, H. Dombret, C. Karanes, M. Theobald, J.M. Bennett, M.L. Sherman, M.S. Berger, C.B. Eten, M.R. Loken, J.J. van Dongen, I.D. Bernstein, F.R. Appelbaum, Efficacy and safety of gemtuzumab ozogamicin in patients with CD33-positive acute myeloid leukemia in first relapse. J. Clin. Oncol., 19(13) (2001) 3244-54.

C. Sillaber, M. Baghestanian, R. Hofbauer, I. Virgolini, H.C. Bankl, W. Fureder, H. Agis, M. Willheim, M. Leimer, O. Scheiner, B.R. Binder, H.P. Kiener, D. Bevec, G. Fritsch, O. Majdic, H.G. Kress, H. Gadner, K. Lechner, P. Valent, Molecular and functional characterization of the urokinase receptor on human mast cells. J. Biol. Chem., 272(12) (1997) 7824-32.

V.I. Slepnev, P.D. Camilli, Endocytosis: an overview, in: P.L.F.a.L.W.S. Alexander V. Kabanov (Ed.), Self-assembling complexes for gene delivery, John Wiley & Sons Ltd., 1998, pp. 71-88

P.K. Smith, R.I. Krohn, G.T. Hermanson, A.K. Mallia, F.H. Gartner, M.D. Provenzano, E.K. Fujimoto, N.M. Goeke, B.J. Olson, D.C. Klenk, Measurement of protein using bicinchoninic acid. Anal. Biochem., 150(1) (1985) 76-85.

T.W.G. Solomons, Organic Chemistry, 6th Edition, John Wiley & Sons, Inc, New York, 1996.

Y.J. Son, J.S. Jang, Y.W. Cho, H. Chung, R.W. Park, I.C. Kwon, I.S. Kim, J.Y. Park, S.B. Seo, C.R. Park, S.Y. Jeong, Biodistribution and anti-tumor efficacy of doxorubicin loaded glycol-chitosan nanoaggregates by EPR effect. J. Control. Release, 91(1-2) (2003) 135-45.

R.A. Spooner, F. Friedlos, K. Maycroft, S.M. Stribbling, J. Roussel, J. Brueggen, B. Stolz, T. O'Reilly, J. Wood, A. Matter, R. Marais, C.J. Springer, A novel vascular endothelial growth factor-directed therapy that selectively activates cytotoxic prodrugs. Br. J. Cancer, 88(10) (2003) 1622-30.

J.A. St George, Gene therapy progress and prospects: adenoviral vectors. Gene Ther., 10(14) (2003) 1135-41.

A. Stahl, B.M. Mueller, Binding of Urokinase to Its Receptor Promotes Migration and Invasion of Human-Melanoma Cells in-Vitro. Cancer Res., 54(11) (1994) 3066-3071.

L. Stryer, Biochemistry, 4th Edition, W. H. Freeman and Company, New York, 1995.

W. Suh, S.O. Han, L. Yu, S.W. Kim, An angiogenic, endothelial-cell-targeted polymeric gene carrier. Mol. Ther., 6(5) (2002) 664-72.

X.H. Sun, L. Tan, C.Y. Li, C. Tong, J. Fan, P. Li, Y.S. Zhu, A novel gene delivery system targeting urokinase receptor. Acta Biochim. Biophys. Sin., 36(7) (2004) 485-91.

A. Surendran, China approves world's first gene therapy drug. Nat. Med., 10(1) (2004) 9.

S. Suzuki, Y. Hayashi, Y. Wang, T. Nakamura, Y. Morita, K. Kawasaki, K. Ohta, N. Aoyama, S.R. Kim, H. Itoh, Y. Kuroda, W.F. Doe, Urokinase type plasminogen activator receptor expression in colorectal neoplasms. Gut, 43(6) (1998) 798-805.

Y. Takakura, R.I. Mahato, M. Hashida, Extravasation of macromolecules. Adv. Drug Del. Rev., 34(1) (1998) 93-108.

Y. Takakura, M. Nishikawa, F. Yamashita, M. Hashida, Influence of Physiochemical Properties on Pharmacokinetics of Non-viral Vectors for Gene Delivery. J. Drug Target., 10(2) (2002) 99-104.

Talktransplant, circulation, 2005, http://www.talktransplant.co.uk/transcaretemplates/ttemplate2.aspx?navigation=44

T. Tanaka, S. Shiramoto, M. Miyashita, Y. Fujishima, Y. Kaneo, Tumor targeting based on the effect of enhanced permeability and retention (EPR) and the mechanism of receptor-mediated endocytosis (RME). Int. J. Pharm., 277(1-2) (2004) 39-61.

M.X. Tang, C.T. Redemann, F.C. Szoka, Jr., In vitro gene delivery by degraded polyamidoamine dendrimers. Bioconj. Chem., 7(6) (1996) 703-14.

T. Taniguchi, A.K. Kakkar, E.G. Tuddenham, R.C. Williamson, N.R. Lemoine, Enhanced expression of urokinase receptor induced through the tissue factor-factor VIIa pathway in human pancreatic cancer. Cancer Res., 58(19) (1998) 4461-7.

D.J. Taxman, E.S. Lee, D.M. Wojchowski, Receptor-targeted transfection using stable maleimido-transferrin/thio-poly-L-lysine conjugates. Anal. Biochem., 213(1) (1993) 97-103.

M. Thanou, A.F. Kotze, T. Scharringhausen, H.L. Luessen, A.G. de Boer, J.C. Verhoef, H.E. Junginger, Effect of degree of quaternization of N-trimethyl chitosan chloride for enhanced transport of hydrophilic compounds across intestinal caco-2 cell monolayers. J. Control. Release, 64(1-3) (2000) 15-25.

M. Thanou, B.I. Florea, M. Geldof, H.E. Junginger, G. Borchard, Quaternized chitosan oligomers as novel gene delivery vectors in epithelial cell lines. Biomaterials, 23(1) (2002) 153-9.

M. Thanou, H.E. Junginger, Pharmaceutical Applications of chitosan and derivatives, in: S. Dumitriu (Ed.), Polysaccharides, Structural Diversity and Functional Versatility, Marcel Dekker, 2004, pp. 661-678

M. Thomas, A.M. Klibanov, Enhancing polyethylenimine's delivery of plasmid DNA into mammalian cells. Proc. Natl. Acad. Sci. U. S. A., 99(23) (2002) 14640-14645.

M. Toda, R.L. Martuza, H. Kojima, S.D. Rabkin, In situ cancer vaccination: an IL-12 defective vector/replication-competent herpes simplex virus combination induces local and systemic antitumor activity. J. Immunol., 160(9) (1998) 4457-64.

K. Tommeraas, S.P. Strand, W. Tian, L. Kenne, K.M. Varum, Preparation and characterisation of fluorescent chitosans using 9-anthraldehyde as fluorophore. Carbohydr. Res., 336(4) (2001) 291-296.

V.P. Torchilin, Drug targeting. Eur. J. Pharm. Sci., 11(Suppl 2) (2000) S81-91.

V.P. Torchilin, B.A. Khaw, V. Weissig, Intracellular targets for DNA delivery: nuclei and mitochondria. Somat. Cell Mol. Genet., 27(1-6) (2002) 49-64.

M. Trepel, W. Arap, R. Pasqualini, In vivo phage display and vascular heterogeneity: implications for targeted medicine. Curr. Opin. Chem. Biol., 6(3) (2002) 399-404.

D.A. Vallera, C.B. Li, N. Jin, A. Panoskaltsis-Mortari, W.A. Hall, Targeting urokinase-type plasminogen activator receptor on human glioblastoma tumors with diphtheria toxin fusion protein DTAT. J. Natl. Cancer Inst., 94(8) (2002) 597-606.

P. van de Wetering, J.-Y. Cherng, H. Talsma, W.E. Hennink, Relation between transfection efficiency and cytotoxicity of poly(2-(dimethylamino)ethyl methacrylate)/plasmid complexes. J. Control. Release, 49(1) (1997) 59-69.

M.A. van der Aa, G.A. Koning, C. d'Oliveira, R.S. Oosting, K.J. Wilschut, W.E. Hennink, D.J. Crommelin, An NLS peptide covalently linked to linear DNA does not enhance transfection efficiency of cationic polymer based gene delivery systems. J. Gene. Med., 7(2) (2005) 208-17.

J.H. van Steenis, E.M. van Maarseveen, F.J. Verbaan, R. Verrijk, D.J. Crommelin, G. Storm, W.E. Hennink, Preparation and characterization of folate-targeted pEG-coated pDMAEMA-based polyplexes. J. Control. Release, 87(1-3) (2003) 167-76.

A.J. Vander, J.H. Sherman, D.S. Luciano, Human Physiology, 6, McGraw-Hill, New York, 1994.

J. Vega, S. Ke, Z. Fan, S. Wallace, C. Charsangavej, C. Li, Targeting doxorubicin to epidermal growth factor receptors by site-specific conjugation of C225 to poly(L-glutamic acid) through a polyethylene glycol spacer. Pharm. Res., 20(5) (2003) 826-32.

J.C. Venter, M.D. Adams, E.W. Myers, P.W. Li, R.J. Mural, G.G. Sutton, H.O. Smith, M. Yandell, C.A. Evans, R.A. Holt, J.D. Gocayne, P. Amanatides, R.M. Ballew, D.H. Huson, J.R. Wortman, Q. Zhang, C.D. Kodira, X.H. Zheng, L. Chen, M. Skupski, G. Subramanian, P.D. Thomas, J. Zhang, G.L. Gabor Miklos, C. Nelson, S. Broder, A.G. Clark, J. Nadeau, V.A. McKusick, N. Zinder, A.J. Levine, R.J. Roberts, M. Simon, C. Slayman, M. Hunkapiller, R. Bolanos, A. Delcher, I. Dew, D. Fasulo, M. Flanigan, L. Florea, A. Halpern, S. Hannenhalli, S. Kravitz, S. Levy, C. Mobarry, K. Reinert, K. Remington, J. Abu-Threideh, E. Beasley, K. Biddick, V. Bonazzi, R. Brandon, M. Cargill, I. Chandramouliswaran, R. Charlab, K. Chaturvedi, Z. Deng, V. Di Francesco, P. Dunn, K. Eilbeck, C. Evangelista, A.E. Gabrielian, W. Gan, W. Ge, F. Gong, Z. Gu, P. Guan, T.J. Heiman, M.E. Higgins, R.R. Ji, Z. Ke, K.A. Ketchum, Z. Lai, Y. Lei, Z. Li, J. Li, Y. Liang, X. Lin, F. Lu, G.V. Merkulov, N. Milshina, H.M. Moore, A.K. Naik, V.A. Narayan, B. Neelam, D. Nusskern, D.B. Rusch, S. Salzberg, W. Shao, B. Shue, J. Sun, Z. Wang, A. Wang, X. Wang, J. Wang, M. Wei, R. Wides, C. Xiao, C. Yan, A. Yao, J. Ye, M. Zhan, W. Zhang, H. Zhang, Q. Zhao, L. Zheng, F. Zhong, W. Zhong, S. Zhu, S. Zhao, D. Gilbert, S. Baumhueter, G. Spier, C. Carter, A. Cravchik, T. Woodage, F. Ali, H. An, A. Awe, D. Baldwin, H. Baden, M. Barnstead, I. Barrow, K. Beeson, D. Busam, A. Carver, A. Center, M.L. Cheng, L. Curry, S. Danaher, L. Davenport, R. Desilets, S. Dietz, K. Dodson, L. Doup, S. Ferriera, N. Garg, A. Gluecksmann, B. Hart, J. Haynes, C. Haynes, C. Heiner, S. Hladun, D. Hostin, J. Houck, T. Howland, C. Ibegwam, J. Johnson, F. Kalush, L. Kline, S. Koduru, A. Love, F. Mann, D. May, S. McCawley, T. McIntosh, I. McMullen, M. Moy, L. Moy, B. Murphy, K. Nelson, C. Pfannkoch, E. Pratts, V. Puri, H. Qureshi, M. Reardon, R. Rodriguez, Y.H. Rogers, D. Romblad, B. Ruhfel, R. Scott, C. Sitter, M. Smallwood, E. Stewart, R. Strong, E. Suh, R. Thomas, N.N. Tint, S. Tse, C. Vech, G. Wang, J. Wetter, S. Williams, M. Williams, S. Windsor, E. Winn-Deen, K. Wolfe, J. Zaveri, K. Zaveri, J.F. Abril, R. Guigo, M.J. Campbell, K.V. Sjolander, B. Karlak, A. Kejariwal, H. Mi, B. Lazareva, T. Hatton, A. Narechania, K. Diemer, A. Muruganujan, N. Guo, S. Sato, V. Bafna, S. Istrail, R. Lippert, R. Schwartz, B. Walenz, S. Yooseph, D. Allen, A. Basu, J. Baxendale, L. Blick, M. Caminha, J. Carnes-Stine, P. Caulk, Y.H. Chiang, M. Coyne, C. Dahlke, A. Mays, M. Dombroski, M. Donnelly, D. Ely, S. Esparham, C. Fosler, H. Gire, S. Glanowski, K. Glasser, A. Glodek, M. Gorokhov, K. Graham, B. Gropman, M. Harris, J. Heil, S. Henderson, J. Hoover, D. Jennings, C. Jordan, J. Jordan, J. Kasha, L. Kagan, C. Kraft, A. Levitsky, M. Lewis, X. Liu, J. Lopez, D. Ma, W. Majoros, J. McDaniel, S. Murphy, M. Newman, T. Nguyen, N. Nguyen, M. Nodell, S. Pan, J. Peck, M. Peterson, W. Rowe, R. Sanders, J. Scott, M. Simpson, T. Smith, A. Sprague, T. Stockwell, R. Turner, E. Venter, M. Wang, M. Wen, D. Wu, M. Wu, A. Xia, A. Zandieh, X. Zhu, The sequence of the human genome. Science, 291(5507) (2001) 1304-51.

S. Vepa, W.M. Scribner, V. Natarajan, Activation of endothelial cell phospholipase D by polycations. Am. J. Physiol., 272(4 Pt 1) (1997) L608-13.

F.M. Veronese, R. Largajolli, E. Boccu, C.A. Benassi, O. Schiavon, Surface modification of proteins. Activation of monomethoxy-polyethylene glycols by phenylchloroformates and modification of ribonuclease and superoxide dismutase. Appl. Biochem. Biotechnol., 11(2) (1985) 141-52.

F. Vilhardt, M. Nielsen, K. Sandvig, B. van Deurs, Urokinase-type plasminogen activator receptor is internalized by different mechanisms in polarized and nonpolarized Madin-Darby canine kidney epithelial cells. Mol. Biol. Cell, 10(1) (1999) 179-95.

A. von Harpe, H. Petersen, Y.X. Li, T. Kissel, Characterization of commercially available and synthesized polyethylenimines for gene delivery. J. Control. Release, 69(2) (2000) 309-322.

E. Wagner, M. Zenke, M. Cotten, H. Beug, M.L. Birnstiel, Transferrin-polycation conjugates as carriers for DNA uptake into cells. Proc. Natl. Acad. Sci. U. S. A., 87(9) (1990) 3410-4.

E. Wagner, Application of membrane-active peptides for nonviral gene delivery. Adv. Drug Del. Rev., 38(3) (1999) 279-289.

K.W. Wan, B. Malgesini, I. Verpilio, P. Ferruti, P.C. Griffiths, A. Paul, A.C. Hann, R. Duncan, Poly(amidoamine) salt form: effect on pH-dependent membrane activity and polymer conformation in solution. Biomacromolecules, 5(3) (2004) 1102-9.

D. Wang, S. Miller, M. Sima, P. Kopeckova, J. Kopecek, Synthesis and evaluation of water-soluble polymeric bone-targeted drug delivery systems. Bioconj. Chem., 14(5) (2003) 853-9.

H. Wang, J. Skibber, J. Juarez, D. Boyd, Transcriptional Activation of the Urokinase Receptor Gene in Invasive Colon-Cancer. Int. J. Cancer, 58(5) (1994) 650-657.

J.H. Wang, X.Y. Liu, Targeting strategies in cancer gene therapy. Acta Biochim. Biophys. Sin., 35(4) (2003) 311-6.

P. Watson, A.T. Jones, D.J. Stephens, Intracellular trafficking pathways and drug delivery: fluorescence imaging of living and fixed cells. Adv. Drug Del. Rev., 57(1) (2005) 43-61.

Y. Wei, M. Lukashev, D.I. Simon, S.C. Bodary, S. Rosenberg, M.V. Doyle, H.A. Chapman, Regulation of integrin function by the urokinase receptor. Science, 273(5281) (1996) 1551-5.

Y. Wei, X. Yang, Q. Liu, J.A. Wilkins, H.A. Chapman, A role for caveolin and the urokinase receptor in integrin-mediated adhesion and signaling. J. Cell Biol., 144(6) (1999) 1285-94.

V. Weissig, J. Lasch, G. Erdos, H.W. Meyer, T.C. Rowe, J. Hughes, DQAsomes: a novel potential drug and gene delivery system made from Dequalinium. Pharm. Res., 15(2) (1998) 334-7.

WHO, World Health Organisation - Cancer, 2005, http://www.who.int/cancer/en/

T.J. Wickham, Ligand-directed targeting of genes to the site of disease. Nat. Med., 9(1) (2003) 135-9.

Wilex, Wilex Company Website, 2005, http://www.wilex.de

T. Wind, M. Hansen, J.K. Jensen, P.A. Andreasen, The molecular basis for anti-proteolytic and non-proteolytic functions of plasminogen activator inhibitor type-1: roles of the reactive centre loop, the shutter region, the flexible joint region and the small serpin fragment. Biol. Chem., 383(1) (2002) 21-36.

A. Wise, K. Gearing, S. Rees, Target validation of G-protein coupled receptors. Drug Discov. Today, 7(4) (2002) 235-246.

G.A. Wiseman, C.A. White, R.B. Sparks, W.D. Erwin, D.A. Podoloff, D. Lamonica, N.L. Bartlett, J.A. Parker, W.L. Dunn, S.M. Spies, R. Belanger, T.E. Witzig, B.R. Leigh, Biodistribution and dosimetry results from a phase III prospectively randomized controlled trial of Zevalin radioimmunotherapy for low-grade, follicular, or transformed B-cell non-Hodgkin's lymphoma. Crit. Rev. Oncol./Hematol., 39(1-2) (2001) 181-94.

G.Y. Wu, C.H. Wu, Receptor-mediated gene delivery and expression in vivo. J. Biol. Chem., 263(29) (1988) 14621-4.

Wyeth, Mylotarg the first antibody targeted chemotherapy, 2003, http://www.wyeth.com/content/ShowLabeling.asp?id=119

L. Xu, C.C. Huang, W. Huang, W.H. Tang, A. Rait, Y.Z. Yin, I. Cruz, L.M. Xiang, K.F. Pirollo, E.H. Chang, Systemic tumor-targeted gene delivery by anti-transferrin receptor scFv-immunoliposomes. Mol. Cancer Ther., 1(5) (2002) 337-46.

M.A. Zanta, O. Boussif, A. Adib, J.P. Behr, In vitro gene delivery to hepatocytes with galactosylated polyethylenimine. Bioconj. Chem., 8(6) (1997) 839-44.

M.A. Zanta, P. Belguise-Valladier, J.P. Behr, Gene delivery: a single nuclear localization signal peptide is sufficient to carry DNA to the cell nucleus. Proc. Natl. Acad. Sci. U. S. A., 96(1) (1999) 91-6.

V. Zaric, D. Weltin, P. Erbacher, J.S. Remy, J.P. Behr, D. Stephan, Effective polyethylenimine-mediated gene transfer into human endothelial cells. J. Gene. Med., 6(2) (2004) 176-84.

W. Zauner, M. Ogris, E. Wagner, Polylysine-based transfection systems utilizing receptor-mediated delivery. Adv. Drug Del. Rev., 30(1-3) (1998) 97-113.

J. Zhang, R.E. Campbell, A.Y. Ting, R.Y. Tsien, Creating new fluorescent probes for cell biology. Nat. Rev. Mol. Cell Biol., 3(12) (2002) 906-918.

S. Zhang, X. Yang, M.E. Morris, Combined effects of multiple flavonoids on breast cancer resistance protein (ABCG2)-mediated transport. Pharm. Res., 21(7) (2004) 1263-73.

W. Zhou, X. Yuan, A. Wilson, L.J. Yang, M. Mokotoff, B. Pitt, S. Li, Efficient intracellular delivery of oligonucleotides formulated in folate receptor-targeted lipid vesicles. Bioconj. Chem., 13(6) (2002) 1220-1225.

A.G. Ziady, T. Ferkol, D.V. Dawson, D.H. Perlmutter, P.B. Davis, Chain length of the polylysine in receptor-targeted gene transfer complexes affects duration of reporter gene expression both in vitro and in vivo. J. Biol. Chem., 274(8) (1999) 4908-16.

G. Zuber, E. Dauty, M. Nothisen, P. Belguise, J.P. Behr, Towards synthetic viruses. Adv. Drug Del. Rev., 52(3) (2001) 245-53.

Appendix I

Available online at www.sciencedirect.com
SCIENCE DIRECT
Journal of Controlled Release 103 (2005) 643–653
journal of controlled release
www.elsevier.com/locate/jconrel

Trimethylated chitosans as non-viral gene delivery vectors: Cytotoxicity and transfection efficiency

Thomas Kean, Susanne Roth, Maya Thanou*

Centre for Polymer Therapeutics, Welsh School of Pharmacy, Cardiff University, Redwood Building, King Edward VII Ave, Cardiff, CF10 3XF, United Kingdom

Received 28 October 2004; accepted 5 January 2005

Abstract

Chitosans are linear polysaccharides of natural origin that show potential as carriers in drug and gene delivery. Introducing quaternisation on the chitosan backbone renders the polymer soluble over a wider pH range and confers controlled cationic character. This study aims to investigate the effect of increasing quaternisation and therefore, positive charge on cell viability and transfection. Oligomeric and polymeric chitosans were trimethylated, the toxicity and transfection efficiency of these derivatives were tested with respect to increasing degree of trimethylation. The cytoxicity of polymer and oligomer derivatives alone and of their complexes with plasmid DNA were determined using the 3-(4,5-dimethylthiazol-2-yl)-2,5-diphenyl tetrazolium bromide (MTT) assay on COS-7 (monkey kidney fibroblasts) and MCF-7 (epithelial breast cancer) cells. Transfection efficiency was investigated using the pGL3 luciferase reporter gene on the same cell lines. Complexes were characterised for their stability by gel electrophoresis. Cytotoxicity results showed that all derivatives were significantly less toxic than linear polyethylenimine (PEI). A general trend of increasing toxicity with increasing degree of trimethylation was seen. However, higher toxicity was seen in polymeric chitosan derivatives over oligomeric chitosan derivatives at similar degrees of trimethylation. All derivatives complexed pGL3 luc plasmid DNA efficiently at 10:1 ratio and three (TMO44, TMC57 and TMC93) were able to transfect MCF-7 cells with greater efficiency than PEI; 16, 23 and 50-fold, respectively. TMC57, TMC93 and all TMOs gave appreciable transfection of COS-7 cells.

Keywords: Trimethyl chitosan; Oligomers; Polymers; Cytotoxicity; Gene delivery

1. Introduction

Gene delivery is an attractive concept; the introduction of a gene to treat a genetic disease whether innate or acquired is alluring [1]. Viral vectors certainly have their place, they are the most commonly used transfection agents in current clinical trials [2]. How-

* Corresponding author. Tel.: +44 292 087 5816; fax: +44 292 087 4536.
E-mail address: thanoum@cf.ac.uk (M. Thanou).

0168-3659/$ - see front matter © 2005 Elsevier B.V. All rights reserved.
doi:10.1016/j.jconrel.2005.01.001

ever, they display high immunogenicity, which causes a problem in repeated administration, and they are difficult to sterilise, characterise and mass produce. Non-viral gene delivery offers a solution to these problems [3]. Non-viral gene delivery methods fall into two categories: physical and chemical. Physical methods contain the gene-gun and electroporation techniques among others [4]. Chemical methods include calcium phosphate precipitation [5], cationic lipids [6,7] and cationic polymers [8–10]. A large number of different cationic lipids have been investigated for gene delivery [7], but only few polymers have been thoroughly studied. These are PEI > PLL (poly-L-lysine) > Chitosan > PAMAM (polyamidoamine) ranked respectively to the number of reported studies. This list of cationic polymers is by no means exhaustive and new polymers and modifications of existing vectors are being produced all the time [11,12].

Chitosan is the name given to a group of linear cationic copolymers of glucosamine and *N*-acetylglucosamine that are derived from the natural biopolymer chitin by a process of deacetylation that show promise as a non-viral vector [13]. Chitosan derivatives have been recently reported as improved gene delivery systems [14]. Chitosans have been shown to be relatively non-toxic [15,16], moreover chitosan is approved as a food additive in Japan, Italy and Finland [17]. It has also been approved as a wound dressing in the USA [18]. Trimethylation of chitosan improves the cationic characteristics and pDNA complexing ability of the macromolecule [19].

Investigators have studied chitosan because of the reported biocompatibility and biodegradability of this material. Both chitosan and trimethyl chitosan have been used to complex and deliver plasmid DNA [15,16, 19–24]. Thanou et al. [19] showed an order of magnitude increase in transfection with TMO over native chitosan. We investigate here the difference between oligomer and polymer in transfection efficiency.

Many cationic polymers have been found to be toxic and it has been suggested that this toxicity is due to interactions with the plasma membrane [25]. Other possible toxic mechanisms are due to interaction with negatively charged cell components and proteins [26]. It has been suggested that toxicity is related to molecular weight. However, branched PEI showed similar toxicities across a range of molecular weights (600–1000, 60 and 25 kDa) in COS-1 and Calu-3 cells [27]. This finding was contradicted by Fischer et al. with diethylaminoethyl-dextran in L929 (mouse fibroblast cell line) [26]. Overall Fischer et al. [26] ranked the toxicity of cationic polymers in this way: PEI=PLL > poly(diallyl-dimethyl-ammonium chloride) (DADMAC) > diethylaminoethyl-dextran (DEAE-dextran) > poly(vinyl pyridinium bromide) (PVPBr) > PAMAM > cationic human serum albumin (cHSA) > native human serum albumin (nHSA). In the same study it was concluded that PEI, DADMAC and PLL were highly plasma membrane damaging, by release of haemoglobin from red blood cells [26]. It is still unclear what leads to cationic polymer cytotoxicity [26,28]. It seems therefore, that the toxicity of a given type/group of polymers must be determined individually using more than one cell type. In this study we investigate the effect of increasing trimethylation on the backbones of chitosan oligomers and polymers over 6 and 24 h incubations in a cell viability assay. A rapid and facile test for cytotoxicity, MTT, was developed by Mosmann [29] and has been used extensively for many polymers [26,30]. Using this method Florea et al. [27] showed that transfection efficiency of PEI (0.4–34.4 μg/ml) correlated with toxicity in Calu-3 cells, this was not repeated in COS-1 cells [27], but was echoed by van de Wetering et al. [31] using p(DMEAMA) on COS-7 and OVCAR-3 cell lines. In a study of poly(amidoamine)s Hill et al. [32] found them to be largely non-toxic (IC_{50}'s>400 μg/ml). However, only those that showed some toxicity were able to transfect A549 cells (lung carcinoma epithelial cells) [32]. The aim of this study was to give a well-tolerated linear polysaccharide, chitosan, progressively more permanent cationic charge and investigate the effect of the charge and the size (oligomer or polymer) on both cytotoxicity and transfection efficiency. MCF-7 (breast cancer epithelia) cells have been used in this study to investigate the applicability of trimethylated chitosan derivatives for cancer gene therapy.

2. Materials and methods

2.1. Materials

Chitosan oligomer (3–6 kDa; Norway) and chitosan low molecular weight polymer were obtained

from Primex (~100 kDa; Norway). PEI (~25 kDa linear) was from Aldrich (USA). Methyl iodide, 1-methyl-2-pyrrolidinone (NMP) both purchased from Acros (Belgium). MTT, diethyl ether, ethanol, deuterated water, dimethyl sulphoxide (DMSO), bovine serum albumin, bicinchiconic acid, copper (II) sulphate pentahydrate (4% w/v soln.), ethidium bromide and sodium hydroxide were obtained from Sigma (UK). Dulbecco's modified eagle's medium (DMEM), penicillin/streptomycin (5000 Units/ml, 5000 μg/ml), trypsin/EDTA and foetal bovine serum (FBS) were purchased from GIBCO (UK), and 96-well plates were obtained from Costar (Corning, USA). Cell lysis buffer and luciferase substrate were obtained from Promega (USA). Agarose was from Bioline (UK).

2.2. Methods

2.2.1. Preparation of N,N,N-trimethyl chitosan oligomer

Trimethylation of chitosan was performed by a modified version of that described by Domard et al. [33] as depicted in Fig. 1. Chitosan oligomer (3–6 kDa, Primex, Norway) was dissolved in NMP with 2.4 g of sodium iodide at 60 °C under stirring. Addition of sufficient NaOH (15% w/v; aq) was made to maintain an alkaline environment throughout the reaction. Methylation was produced through nucleophillic substitution by addition of methyl iodide to the solution. Products were precipitated by addition of diethyl ether:ethanol (1:1 v/v) at 20, 40, 60 and 120 min to gain degrees of trimethylation (DTM). Precipitates were centrifuged at 3000 RCF (Varifuge 3.0R, Heraeus Sepatech), and supernatants were discarded. Products were dried under nitrogen, redissolved in 0.5 M NaCl and precipitated again with diethyl ether:ethanol, centrifuged at 3000 RCF and supernatant discarded followed by thorough washing of the pellet with diethyl ether/ethanol. Finally, after drying the pellet, the derivative was dissolved in H_2O and freeze dried (Flexi-dry lyophilliser, FTS Systems). Products were characterised by ^1H NMR (300 Mhz, Spectrospin and Bruker).

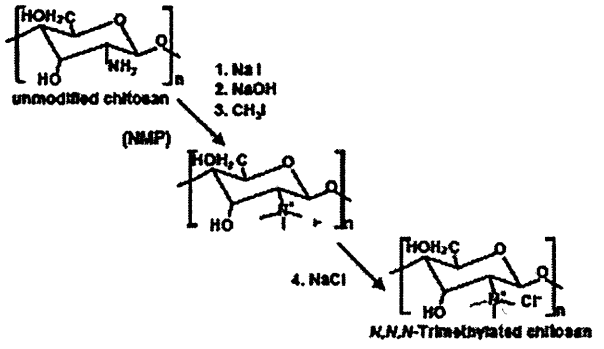

Fig. 1. Reaction scheme of chitosan trimethylation and counter ion replacement. Chitosan polymers and oligomers were derivatised in the same way. Sodium iodide (NaI) acts as a catalyst. Methyl iodide (CH_3I) reacts with the amine in alkaline conditions (provided by sodium hydroxide; NaOH) to give methyl, dimethyl and finally trimethyl derivatives. The iodide counter ion is then replaced with chloride by washing with sodium chloride (NaCl).

2.2.2. Preparation of N,N,N-trimethyl chitosan polymer (low molecular weight)

Methylation was performed as above with the exception that precipitation was performed after 30 and 60 min. After the 60 min precipitation product was dried and redissolved in NMP and methylation was performed again as above with precipitation at 30 and 60 min. This gave the products of 30, 60, 90 and 120 min. Products were characterised by ^1H-NMR.

2.2.3. Cell culture

COS-7 (African green monkey kidney fibroblast like cells) and MCF-7 (human breast epithelial cells) were maintained in DMEM supplemented with 10% (v/v) FBS penicillin/streptomycin (100 Units/ml, 100 μg/ml) at 37 °C and 5% CO_2. Cells were sub-cultured regularly using trypsin/EDTA.

2.2.4. Evaluation of cytotoxicity

Cells were seeded at 1×10^4 cells/well in a 96-well plate and grown overnight, immediately prior to incubation with chitosan derivatives growth medium was removed. Derivatives and PEI were applied onto the cells in DMEM at concentrations ranging from 20 to 10^4 μg/ml (100 μl/well) and cell viability compared to cells treated with DMEM only. Incubations were made for 6 and 24 h before removal of media containing derivatives and replacement with cell culture medium. After 24 h 20 μl of MTT (5 mg/ml in PBS) was added to each well for both incubation times and incubated for 5 h under normal growing conditions. At this point all media was removed and 100 μl DMSO was added. Plates were incubated for 30 min at 37 °C then absorbance was measured at

550 nm using a plate reader (Sunrise, Tecan). In the case of vector:DNA complexes, 20 μl of complex containing media was added to each well and the 6 and 24 h incubations were made as outlined above. IC_{50} calculation was made using Bio-Graph, with curves fitted according to the Hill equation with R_{max} fixed at 100 and R_{min} at 0, weighted for standard error: $(y=(R_{min}+(R_{max}-R_{min})/(1+(x/IC_{50})^P)$ [34]. For the comparison between complexes and vector alone statistical analysis was made using repeated measures ANOVA with bonferroni post test.

2.2.5. pGL3 Luciferase plasmid (pGL3 luc)

The pGL3 luciferase plasmid (4.8 kbp) was used to monitor gene transfer and transgene expression after transfection. The plasmid was propagated in *Escherichia coli* and isolated using anion exchange columns (Endofree plasmid giga kit, Qiagen). The DNA concentration was determined by measuring UV absorbance at 260 nm. Purity was confirmed by agarose gel electrophoresis.

2.2.6. Preparation and characterisation of complexes

Complexes of pDNA (pGL3 luc) with cationic vectors were prepared. Cationic vector solutions in DMEM (0.1 mg/ml) were added to a vial containing pDNA to give a 10:1 ratio (w/w vector:pDNA). A 10:1 w/w ratio of vector:pDNA corresponds to N/P ratios of ca. 16 for trimethylated derivative and 72 for PEI. This was vortexed on a low speed, to avoid pDNA shearing, for 20 s and allowed to form complexes for 20 min. Complexes were formed in the absence of serum and were characterised by their ability to retard pDNA migration though a 0.7% agarose gel containing 0.25 μg/ml ethidium bromide.

2.2.7. Transfection of COS-7 and MCF-7 cells

Cells were seeded at 1×10^5 cells/well in a 24-well plate and grown overnight in DMEM supplemented with 10% FCS and penicillin/streptomycin (100 Units/ml, 100 μg/ml) at 37 °C 5% CO_2. An hour prior to transfection media was removed and replaced with DMEM alone, and the plates returned to the incubator. Following this, 200 μl of complex containing media was added slowly to each well in quadruplicate to give 2 μg/well of pDNA and plates were incubated for 6 h and transfection took place in the absence of serum. Complexes were then removed and replaced with cell culture medium. Plates were incubated for 48 h to allow protein expression before media was removed and 200 μl cell lysis buffer (Promega) was added. Lysates were cleared by centrifugation; 10 min at 13000 RCF (MSE Micro-Centaur, Sanyo). Supernatants were assayed for protein content (BCA assay) and luciferase. Transfection efficiency was measured using a luminometer (TD20/20, Turner) according to the Promega protocol. Briefly, 10 μl of cell lysate was added to 50 μl of luciferase substrate and light emitted measured over 10 s after a 5 s delay. Results are expressed as relative light units (RLU)/ mg protein.

3. Results

3.1. Trimethylation of chitosans

In this study chitosans, both oligomeric and polymeric (low molecular weight), have been successfully trimethylated by the reaction scheme outlined in Fig. 1 in a controllable manner as shown by the linear curves seen in Fig. 2. Counter ion replacement was performed to prevent iodine oxidation and give a smaller counter ion for better complexation. The degree of trimethylation was calculated from the integration of ^1H NMR according to the method previously described [35]. The degree of trimethylation of oligomeric chitosan increased linearly with

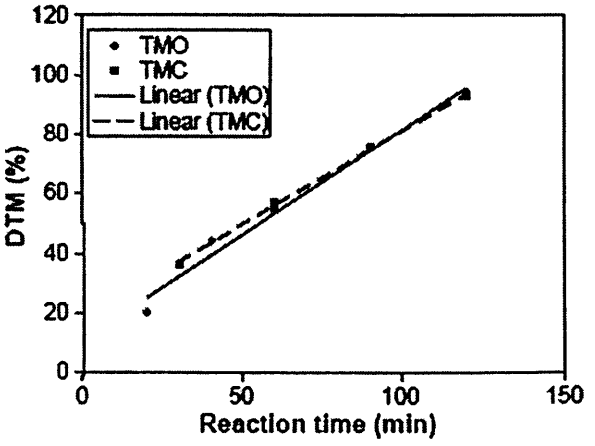

Fig. 2. Increase in degree of trimethylation (DTM) of chitosans with increasing reaction time. TMO=trimethyl oligomer, TMC=trimethyl chitosan polymer.

time to almost complete trimethylation after 2 h. Trimethylation of low molecular weight polymeric chitosan showed a similar reaction profile as can be seen in Fig. 2. After freeze drying all derivatives were soluble in water.

3.2. Cytotoxicity of quaternised chitosan derivatives

In order to investigate the cytotoxicity of the chitosan derivatives on COS-7 and MCF-7 cell lines, the MTT assay was used. Derivatives were applied to the cells at concentrations ranging from 20 to 10^4 μg/ml for 6 or 24 h and the effect on cell viability was measured.

All derivatives were less toxic than PEI (PEI concentration range 20 μg/ml–10 mg/ml and IC_{50}'s ≤ 30 μg/ml, Table 1) at any concentration of derivative used and in both cell lines tested. TMC polymers showed greater effects on cell viability when compared with TMOs of a similar degree of trimethylation (Table 1). Cell viability was seen to decrease with increasing degree of trimethylation in COS-7 (Fig. 3) and MCF-7 (Fig. 4). This was observed for both the oligomer and the polymer. The almost linear decrease in IC_{50} values with increasing degree of trimethylation on polymers indicates a definite trend (Fig. 4) although this trend did not appear to continue beyond 76% DTM. At degrees of trimethylation less than 94% the oligomeric derivatives showed no appreciable toxicity at any of the concentrations tested after 6 h exposure (Table 1). At the highest TMO concentration the solution became more gel like and any toxicity seen was thought to be due to removal of cells

Table 1
Toxicity data for trimethyl chitosan oligomers (TMO) and trimethyl chitosan polymers (TMC)

Product	DTM (%)	Exposure time (h)	IC_{50} (μg/ml)	
			MCF-7	COS-7
TMO	20	6	>10000	>10000
		24	>10000	>10000
	44	6	>10000	>10000
		24	>10000	>10000
	55	6	>10000	>10000
		24	5959±943	661±205
	94	6	1402±210	2207±381
		24	417±210	430±116
TMC	36	6	823±324	>10000
		24	285±100	>10000
	57	6	393±259	676±329
		24	265±53	161±50
	76	6	55±10	40±87
		24	59±30	30±8
	93	6	293±68	79±16
		24	118±28	36±3
PEI (25 kDa)	–	6	<20	30±0
	–	24	<20	<20

DTM; Degree of trimethylation. Each concentration in the IC_{50} curve had $n=6$ and concentrations in the range 20–10^4 μg/ml were tested for all cationic vectors. Curves were fitted according to the Hill equation and the IC_{50} value was calculated.

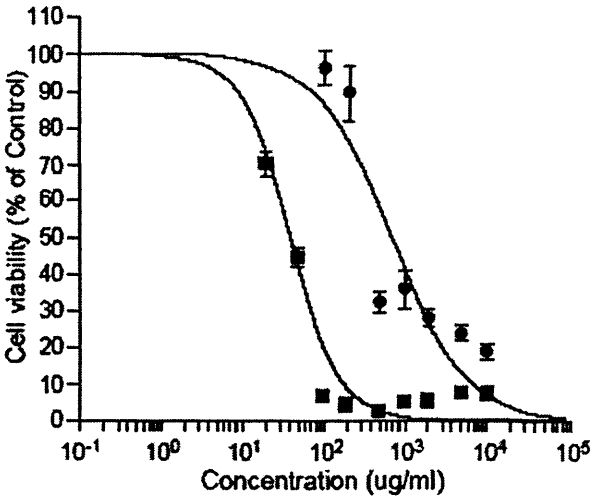

Fig. 3. Dose viability curves of trimethylated chitosan polymer on COS-7 cells after a 6 h incubation: ■; 57% trimethylated, ●; 76% trimethylated. $n=6\pm$S.E.M.

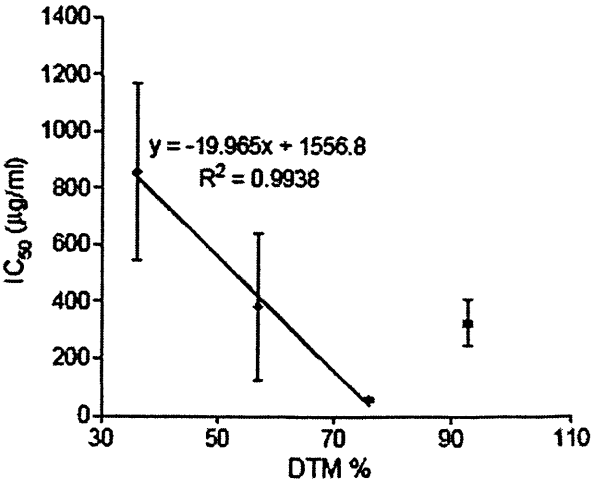

Fig. 4. Plot of IC_{50} values against degree of trimethylation (DTM) on MCF-7 cells after 6 h incubation. Trendline drawn through TMC36, TMC57 and TMC76±S.E.M.

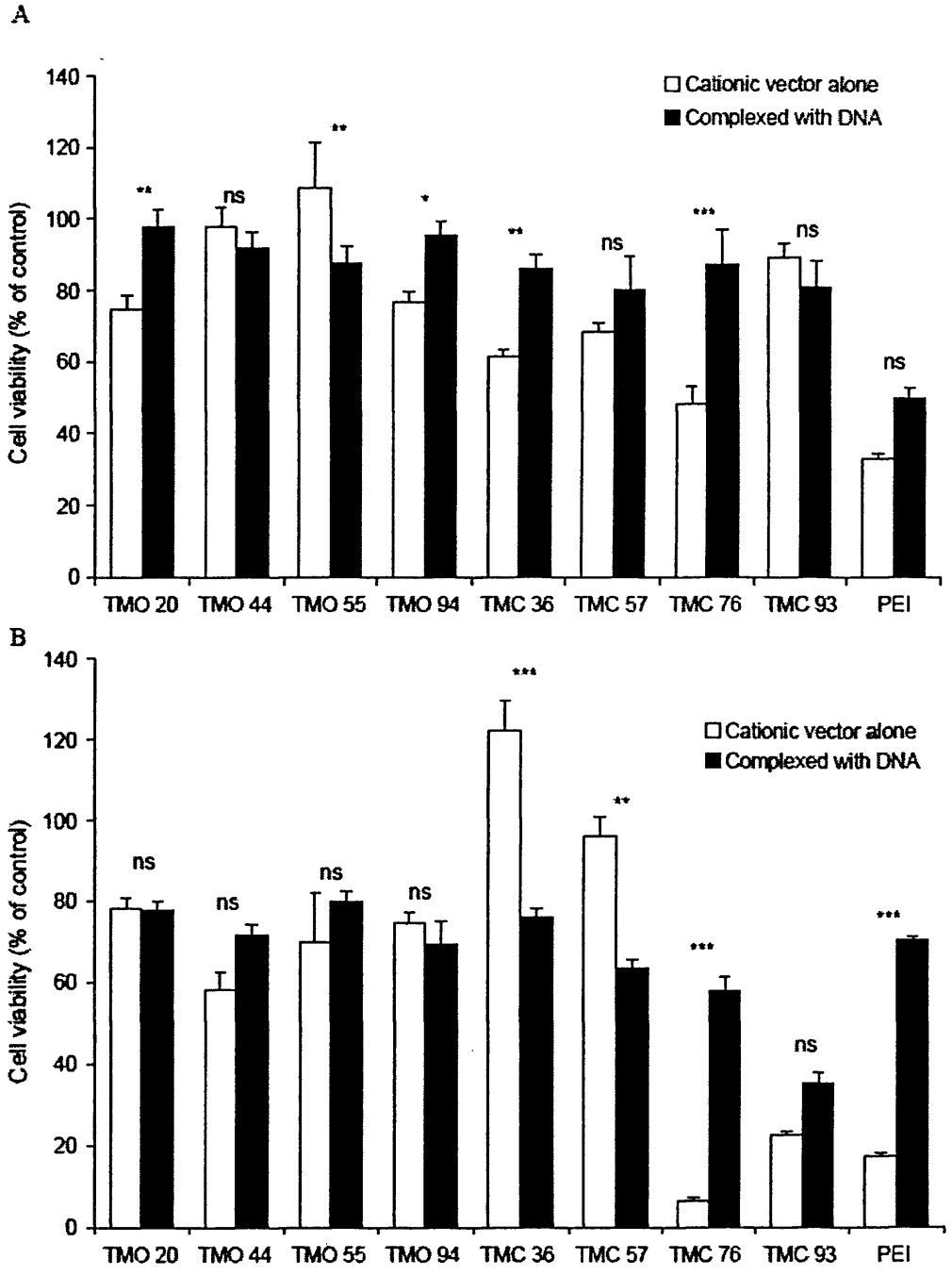

Fig. 5. Viability of MCF-7 (A) and COS-7 (B) cells when co-incubated for 6 h with cationic vector alone (0.1 mg/ml) or their complexes with pGL3 luc applied at the same concentration as free derivatives (10:1 w/w derivative:pDNA) $n=6\pm$S.E.M. Statistical differences between complexed and vector alone are reported as: $^{*}p<0.05$, $^{**}p<0.01$, $^{***}p<0.001$, ns no significant difference; $p>0.05$ (repeated measures ANOVA with bonferroni post test).

when removing the derivative. The extent of toxicity is different in the two cell lines.

In Fig. 5 the effect of the cationic materials alone on cell viability is compared to the effect of their complexes with DNA. On MCF-7 cells we see an increase in viability at the lowest DTM of both polymer (DTM; 36%) and oligomer (DTM; 20%) when they are complexed with pDNA (Fig. 5A). Whilst on COS-7 cells there was no significant difference with TMO20 and a dramatic decrease in TMC36 (Fig. 5B). With TMO55 we see a decrease in viability when complexed with pDNA in the MCF-7 cell line and no significant difference in the COS-7 cells (Fig. 5). Both cell lines had similar responses to TMC76 with complexes having less effect on viability than the cationic vector alone. At the highest DTM there was only a significant difference in MCF-7 cells with TMO94 with cationic material alone being more toxic than complexes. PEI appeared to show the same effect on cell viability on both cell lines with complexes of pDNA being less toxic compared to cationic material alone (PEI:pDNA 10:1 w/w).

3.3. Complex formation of quaternized chitosan derivatives with pDNA

To investigate the ability of chitosan derivatives to complex pDNA adequately, solutions of the derivatives and plasmid were electrophoresed on an agarose

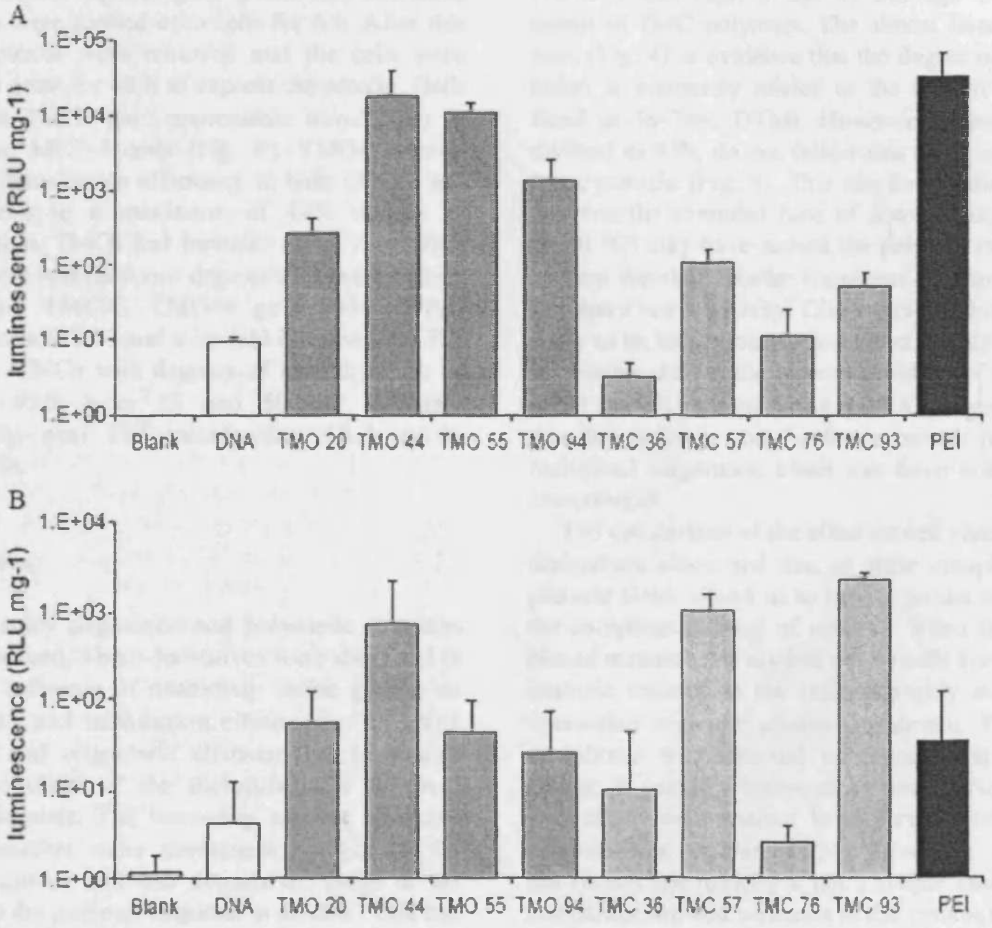

Fig. 6. Transfection efficiencies of chitosan derivatives and PEI in COS-7 (A) and MCF-7 (B) cells. Ratio cationic vector/DNA 10:1 (w/w). Average transfection efficiencies are expressed as relative light units (RLU)/mg protein. (n=4+/− S.D.).

gel containing ethidium bromide. All derivatives were able to complex pDNA at a 10:1 ratio (w/w derivative:pDNA) and prevent its migration under electrophoretic conditions (data not shown). These results indicate that in an aqueous environment such as cell culture media the quaternised derivatives are able to condense pDNA. It appears that the extent of pDNA condensation is similar to that observed for PEI when cationic vectors are complexed at the same ratio with the plasmid (data not shown).

3.4. Transfection of COS-7 and MCF-7 cells using chitosan derivatives

To test the ability of the derivatives to transfect both COS-7 and MCF-7 cells complexes were made with a luciferase reporter gene (pGL3 luc) and these complexes were applied onto cells for 6 h. After this time complexes were removed and the cells were allowed to grow for 48 h to express the protein. Both TMOs and TMCs gave appreciable transfection in COS-7 and MCF-7 cells (Fig. 6). TMOs showed increasing transfection efficiency in both COS-7 and MCF-7 cells to a maximum of 44% degree of trimethylation. TMCs had biphasic effect in relation to DTM with two optimum degrees of trimethylation: TMC57 and TMC93. TMO44 gave 40% of PEI transfection in COS-7 and a 16-fold increase over PEI in MCF-7. TMCs with degrees of trimethylation of 57% and 93% gave 23 and 50-fold increase, respectively, over PEI transfection efficiency in MCF-7 cells.

4. Discussion

In this study oligomeric and polymeric chitosans were quaternised. These derivatives were then used to assess the influence of quaternary amine groups on cell viability and transfection efficiencies. By using polymeric and oligomeric chitosans we have also studied the effect of the molecular size of these cationic materials. The increasing amount of trimethylation confers more permanent charges to the polymer/oligomer and also extends the range of pH over which the polymer/oligomer is soluble. This has the probable effect of increasing the interaction with pDNA and possibly improving the formulation profile. This is thought to be due to the increased solubility of the quaternised amine as well as the permanent positive charge, independent of pH.

Toxicity tests were made over 6 and 24 h, 6 h to give an indication of the toxicity of the derivatives over the time of an in vitro transfection. Additionally, the 24 h time point has been chosen to mimic the tissue-therapeutic contact time, which is expected in an in vivo experiment where clearance would take longer. Further, the 24 h-exposure was chosen as the cells would be within an exponential growth phase in this period meaning that any toxicity, due to inhibition of proliferation and/or cell death, would be clearly visible in the MTT assay. It was shown in this study that increasing the degree of trimethylation increases the toxicity of both the oligomer and the polymer (Table 1 and Figs. 3 and 4) although to a greater extent in TMC polymers. The almost linear decrease seen (Fig. 4) is evidence that the degree of trimethylation is intimately related to the toxicity (trendline fitted to 36–76% DTM). However, polymers trimethylated to 93% do not follow this trend and become less cytotoxic (Fig. 4). This can be explained by the fact that the extended time of derivatisation reaction (at 60 °C) may have caused the polymer to break up, thereby forming smaller fragments that would therefore have lower toxicity. Oligomers are shown in this study to be less cytotoxic compared to polymers. This is possibly due to the increased ability of the cell to expel the dissociated (from pDNA) oligomer easier than the polymer and the fewer contact points each individual oligomeric chain can have with the cell components.

The comparison of the effect on cell viability of the derivatives alone and that of their complexes with plasmid DNA allows us to have a greater insight into the complicated issue of toxicity. When the uncomplexed materials are applied on the cells they show the intrinsic toxicity to the cells, probably due to their interaction with the plasma membrane. When their complexes with plasmid are applied, the cationic charge is partially balanced by the pDNA and the derivative conformation is different compared to uncomplexed derivative [24]. However, this study has shown that toxicity is not a simple issue as some complexes showed increases in the cytotoxicity of the derivative whilst others decreased it and toxicities were not changed in the same way for each cell line

(Fig 5). It may be a temporal phenomenon, with toxic effects appearing later after DNA dissociation has occurred, which would probably differ between the two cell lines and certainly for the different degrees of trimethylation. Cherng et al. [36] found that complexes of pDNA with (poly(2-dimethylamino)ethyl methacrylate) were less toxic than the cationic polymer alone [36], whilst Hill et al. [32] have found that complexing a poly(amidoamine) with pDNA increased cytotoxicity [32]. Overall the chitosan derivatives were relatively non-toxic when compared with PEI, the most popular 'gold standard' [11] of cationic polymer transfection (Table 1). In the comparative study made by Fischer et al. [26] TMOs up to 44% trimethylation (IC_{50}>10 mg/ml) would be equivalent to human serum albumin (IC_{50}>10mg/ml), the least toxic of the polymers tested [26]. Even the most toxic TMO with DTM of 94% (24 h; IC_{50}~0.4 mg/ml) would be ranked less toxic than PVPBr (24 h IC_{50} 0.246 mg/ml). Increasing the time of exposure decreased cell viability in both cell lines at all degrees of trimethylation where toxicity was apparent. This effect was more evident with PEI, which even at 20 μg/ml was highly toxic after 24 h incubation with the cells. This would probably be due to greater cell uptake and therefore greater individual effects on the cell. Most of the oligomeric derivatives were still not toxic over the longer exposure period (Table 1).

We have used trimethyl derivatives as it has been shown that in gene transfer they outperform native chitosan [19]. From gel electrophoresis it was shown that all derivatives were able to complex pDNA and prevent its migration through an agarose gel.

In this study we used MCF-7 cells, a breast cancer epithelial cell line, and as shown they have been transfected effectively. These novel data indicate that MCF-7 breast cancer cells can be transfected using a non-viral vector such as trimethylated chitosans. However, not all derivatives were able to deliver pDNA efficiently as can be seen in Fig. 6. TMO44, TMC57 and TMC93 gave appreciable delivery in MCF-7 cells, all three of which surpassed the efficiency of PEI. The results seen in COS-7 cells are rather different, with all TMOs giving substantial transfection. TMC57 and TMC93 also gave transfection efficiencies of 11- and 5-fold, respectively, over pDNA alone in MCF-7 cells as shown in Fig. 6. The bell shaped curve, seen in both cell lines, of transfection efficiency with increasing degree of trimethylation of TMO indicates that the highest efficiencies are around 44% of trimethylation (Fig. 6). This would be in good agreement with studies made on chitosans where the optimum complexes were made around its pKa of 6.2–6.5 [37]. At this percentage of trimethylation the TMOs showed little or no toxicity in both cell lines (Table 1). Hill et al. [32] studied polyamidoamine (PAA) transfection and toxicity, they found that only the PAAs with toxicities greater than that of TMO44 gave transfection. The transfection with chitosan derivatives in COS-7 cells was noticeably lower than that of PEI (Fig. 6). PEI was slightly more toxic in MCF-7 cells than in COS-7 cells (Table 1), which could be an explanation for the disparity in the relative efficiencies of the derivatives to PEI between cell lines.

In this study we have only considered one standard ratio of derivative: DNA, which was seen as the foundation to compare the toxicity across the different cationic vectors. This has the limitation that some vectors would be more efficient at a different ratio. Linear PEI, marketed as Ex-Gen 500, has a suggested starting ratio of 6:1 (N:P) to be improved with study optimisation for each cell type [38,39]. This study has more than a 10-fold higher ratio. However, the PEI used in this study was less efficient than Ex-Gen 500 and previous experiments in our labs had shown that this ratio transfected consistently (data not shown). Higher w/w ratios of the chitosan derivatives gave better transfection in many cases but this would have abolished transfection by PEI at the same w/w ratio. The compromise of a ratio of 10:1 w/w was made to enable this study.

This study has shown that there are many factors governing cationic polymer transfection efficiency and their effect on cell viability and has shed light on the questions: 1) does the size, oligomer or polymer, influence toxicity and transfection efficiency, 2) does increasing permanent charge increase toxicity, 3) does charge have an effect on transfection efficiency? 1) Trimethylated chitosan derivatives seem to have a dependence on size for both toxicity and transfection efficiency. This finding is different from data presented recently in a study in which different MW chitosans were investigated for cytotoxicity on A549 cells [39]. In that study it was found that chitosans

MW did not affect cell viability [39]. 2) Increasing trimethylation on the chitosan backbone has been seen to increase the toxicities of the derivatives. However, when compared to other cationic polymers the chitosan derivatives remain less toxic [26]. 3) Modifying the permanent cationic charge on the chitosan backbone has an effect on transfection and the optimum degree of trimethylation appears to be approximately 50%. The difference between cell lines may prove to be an asset allowing researchers to preferentially transfect desired cell types with appropriate vectors [15,40,41]. From this study it appears that new polymeric materials and derivatives need to be tested individually to assess their toxicity and transfection efficiency.

5. Conclusion

Oligomeric and polymeric chitosans have been derivatised in a time dependent controllable manner to increase the amount of permanent positive charge. These derivatives have been tested for toxicity and found to be significantly less toxic than PEI in incubations with cationic vector alone. All oligomeric derivatives were relatively non-toxic at any concentration tested. The effect on the cell viability is dependent on the DTM. Three (TMO44, TMC57 and TMC93) of the derivatives gave transfection levels in excess of PEI in MCF-7 cells. It appears that quaternisation of 44% on the chitosan backbone gave an optimum derivative for transfection.

References

[1] G. Brooks, Gene Therapy, Pharmaceutical Press, London, 2002.

[2] M. Edelstein, Gene Therapy Clinical Trials Worldwide, 2004, www.wiley.co.uk/genmed/clinical.

[3] A. Rolland, P.L. Felgner, Preface, Adv. Drug Deliv. Rev. 30 (1–3) (1998) 1–3.

[4] D. Luo, W.M. Saltzman, Synthetic DNA delivery systems, Nat. Biotechnol. 18 (1) (2000) 33–37.

[5] I. Roy, S. Mitra, A. Maitra, S. Mozumdar, Calcium phosphate nanoparticles as novel non-viral vectors for targeted gene delivery, Int. J. Pharm. 250 (1) (2003) 25–33.

[6] T. Blessing, J.S. Remy, J.P. Behr, Monomolecular collapse of plasmid DNA into stable virus-like particles, Proc. Natl. Acad. Sci. U. S. A. 95 (4) (1998) 1427–1431.

[7] D. Liu, T. Ren, X. Gao, Cationic transfection lipids, Curr. Med. Chem. 10 (14) (2003) 1307–1315.

[8] M.E. Davis, Non-viral gene delivery systems, Curr. Opin. Biotechnol. 13 (2) (2002) 128–131.

[9] P. Belguise-Valladier, J.P. Behr, Nonviral gene delivery: towards artificial viruses, Cytotechnology 35 (3) (2001) 197–201.

[10] M.D. Brown, A.G. Schatzlein, I.F. Uchegbu, Gene delivery with synthetic (non viral) carriers, Int. J. Pharm. 229 (1–2) (2001) 1–21.

[11] T. Merdan, J. Kopecek, T. Kissel, Prospects for cationic polymers in gene and oligonucleotide therapy against cancer, Adv. Drug Deliv. Rev. 54 (5) (2002) 715–758.

[12] A. Akinc, D.M. Lynn, D.G. Anderson, R. Langer, Parallel synthesis and biophysical characterization of a degradable polymer library for gene delivery, J. Am. Chem. Soc. 125 (18) (2003) 5316–5323.

[13] M. Thanou, H.E. Junginger, Pharmaceutical applications of chitosan and derivatives, in: S. Dumitriu (Ed.), Polysaccharides, Structural Diversity and Functional Versatility, Marcel Dekker, 2004, pp. 661–678.

[14] W.G. Liu, K.D. Yao, Chitosan and its derivatives—a promising non-viral vector for gene transfection, J. Control. Release 83 (2002) 1–11.

[15] M. Lee, J.W. Nah, Y. Kwon, J.J. Koh, K.S. Ko, S.W. Kim, Water-soluble and low molecular weight chitosan-based plasmid DNA delivery, Pharm. Res. 18 (4) (2001) 427–431.

[16] K. Corsi, F. Chellat, L. Yahia, J.C. Fernandes, Mesenchymal stem cells, MG63 and HEK293 transfection using chitosan–DNA nanoparticles, Biomaterials 24 (7) (2003) 1255–1264.

[17] L. Illum, Chitosan and its use as a pharmaceutical excipient, Pharm. Res. 15 (9) (1998) 1326–1331.

[18] McCue, New Bandage Uses Biopolymer, 2003, http://www.chemistry.org/portal/a/c/s/1/feature_ent.html?id=401c0f5c4d8511d7f6e36ed9fe800100.

[19] M. Thanou, B.J. Florea, M. Geldof, H.E. Junginger, G. Borchard, Quaternized chitosan oligomers as novel gene delivery vectors in epithelial cell lines, Biomaterials 23 (2002) 153–159.

[20] T.J. Kean, C.A. Jansma, G. Borchard, M. Thanou, Targeting the uPA receptor using polymer–ligand conjugates for non viral gene delivery, Proc. Int. Symp. Control. Release Bioact. Mater. 30 (2003) 604.

[21] P. Erbacher, S.M. Zou, T. Bettinger, A.M. Steffan, J.S. Remy, Chitosan-based vector/DNA complexes for gene delivery: Biophysical characteristics and transfection ability, Pharm. Res. 15 (9) (1998) 1332–1339.

[22] T. Kiang, J. Wen, H. Lim, K.W. Leong, Degree of deacetylation of chitosan: effect on gene transfection efficiency in vivo, Proc. Int. Symp. Control. Release Bioact. Mater. 29 (2002) 348–349.

[23] M. Koping-Hoggard, I. Tubulekas, H. Guan, K. Edwards, M. Nilsson, K.M. Varum, P. Artursson, Chitosan as a nonviral gene delivery system: structure–property relationships and characteristics compared with polyethylenimine in vitro after lung administration in vivo, Gene Ther. 8 (2001) 1108–1121.

[24] M. Koping-Hoggard, Y.S. Mel'nikova, K.M. Varum, B. Lindman, P. Artursson, Relationship between the physical shape and the efficiency of oligomeric chitosan as a gene delivery system in vitro and in vivo, J. Gene Med. 5 (2) (2003) 130–141.
[25] S. Choksakulnimitr, S. Masuda, H. Tokuda, Y. Takakura, M. Hashida, In vitro cytotoxicity of macromolecules in different cell culture systems, J. Control. Release 34 (3) (1995) 233–241.
[26] D. Fischer, Y. Li, B. Ahlemeyer, J. Krieglstein, T. Kissel, In vitro cytotoxicity testing of polycations: influence of polymer structure on cell viability and hemolysis, Biomaterials 24 (7) (2003) 1121–1131.
[27] B.I. Florea, C. Meaney, H.E. Junginger, G. Borchard, Transfection efficiency and toxicity of polyethylenimine in differentiated Calu-3 and nondifferentiated COS-1 cell cultures, AAPS PharmSci 4 (3) (2002) E12.
[28] S. Vepa, W.M. Scribner, V. Natarajan, Activation of endothelial cell phospholipase D by polycations, Am. J. Physiol. 272 (4 Pt 1) (1997) L608–L613.
[29] T. Mosmann, Rapid colorimetric assay for cellular growth and survival: application to proliferation and cytotoxicity assays, J. Immunol. Methods 65 (1–2) (1983) 55–63.
[30] D. Sgouras, R. Duncan, Methods for the evaluation of biocompatibility of soluble synthetic-polymers which have potential for bio-medical use: I. Use of the tetrazolium-based colorimetric assay (Mtt) as a preliminary screen for evaluation of in vitro cytotoxicity, J. Mater. Sci., Mater. Med. 1 (2) (1990) 61–68.
[31] P. van de Wetering, J.-Y. Cherng, H. Talsma, W.E. Hennink, Relation between transfection efficiency and cytotoxicity of poly(2-(dimethylamino)ethyl methacrylate)/plasmid complexes, J. Control. Release 49 (1) (1997) 59–69.
[32] I.R. Hill, M.C. Garnett, F. Bignotti, S.S. Davis, In vitro cytotoxicity of poly(amidoamine)s: relevance to DNA delivery, Biochim. Biophys. Acta 1427 (2) (1999) 161–174.
[33] A. Domard, M. Rinaudo, C. Terrassin, New method for the quaternization of chitosan, Int. J. Biol. Macromol. 8 (2) (1986) 105–107.
[34] S. Zhang, X. Yang, M.E. Morris, Combined effects of multiple flavonoids on breast cancer resistance protein (ABCG2)-mediated transport, Pharm. Res. 21 (7) (2004) 1263–1273.
[35] M. Thanou, A.F. Kotze, T. Scharringhausen, H.L. Luessen, A.G. de Boer, J.C. Verhoef, H.E. Junginger, Effect of degree of quaternization of *N*-trimethyl chitosan chloride for enhanced transport of hydrophilic compounds across intestinal caco-2 cell monolayers, J. Control. Release 64 (1–3) (2000) 15–25.
[36] J.Y. Cherng, P. van de Wetering, H. Talsma, D.J. Crommelin, W.E. Hennink, Effect of size and serum proteins on transfection efficiency of poly((2-dimethylamino)ethyl methacrylate)-plasmid nanoparticles, Pharm. Res. 13 (7) (1996) 1038–1042.
[37] T. Sato, T. Ishii, Y. Okahata, In vitro gene delivery mediated by chitosan: effect of pH, serum, and molecular mass of chitosan on the transfection efficiency, Biomaterials 22 (15) (2001) 2075–2080.
[38] I. Elmadbouh, P. Rossignol, O. Meilhac, R. Vranckx, C. Pichon, B. Pouzet, P. Midoux, J.B. Michel, Optimization of in vitro vascular cell transfection with non-viral vectors for in vivo applications, J. Gene Med. 6 (10) (2004) 1112–1124.
[39] C.L. Gebhart, A.V. Kabanov, Evaluation of polyplexes as gene transfer agents, J. Control. Release 73 (2–3) (2001) 401–416.
[40] N. Fang, V. Chan, H.-Q. Mao, K.W. Leong, Interactions of phospholipid bilayer with chitosan: effect of molecular weight and pH, Biomacromolecules 2 (2001) 1161–1168.
[41] M. Huang, E. Khor, L.Y. Lim, Uptake and cytotoxicity of chitosan molecules and nanoparticles: effects of molecular weight and degree of deacetylation, Pharm. Res. 21 (2) (2004) 344–353.

Appendix II

Publications

T. Kean, S. Roth, M. Thanou, Trimethylated chitosans as non-viral gene delivery vectors: Cytotoxicity and transfection efficiency. J. Control. Release, 103(3) (2005) 643-53.

M. Thanou, T. Kean, Investigating urokinase plasminogen activator receptor (CD87) as a potential target for non-viral gene transfer. In *Proc. Am. Soc. for Gene Ther.* (2005) #215

M. Thanou, T. Kean, Trimethylated chitosan oligosaccharides as novel materials in gene delivery. In *Proc. European Society for Gene Therapy* (2005)

T. Kean, M. Harvey, H. Pritchett, M. Thanou, R. Duncan, Trimethyl chitosan-peptide conjugates designed to target the urokinase plasminogen activator receptor: Nanovectors for targeted gene delivery. In *Proc. EuroNano Forum* (2005)

T. Kean, S. Roth, M. Thanou, Trimethylation of chitosans: Its effect on toxicity and their application as a non-viral gene delivery system. In Journal of Pharmacy and Pharmacology BPC 2004: Science abstracts, Poster Session 2, #128

T. Kean, C.A. Jansma, G. Borchard, M. Thanou. Targeting The uPA Receptor Using Polymer-Ligand Conjugates For Non Viral Gene Delivery. in *Proc. Int. Symp. Control. Release Bioact. Mater.* 2003. Glasgow, UK.

Invited Book Chapter

T. Kean, M. Thanou, Chitin and Chitosan, In Polymeric Biomaterials, (manuscript in preparation)

Presentations

T. Kean, Development of a Synthetic uPAR Targeted Gene Delivery System – at National Nanotechnology Laboratory, Lecce, 2006

T. Kean, M. Thanou, R Duncan, Targeted gene delivery for the treatment of cancer – at Speaking of Science, Cardiff, 2005

T. Kean, S. Roth, M. Thanou, Trimethylation of chitosans: Its effect on toxicity and their application as a non-viral gene delivery system - at The British Pharmaceutical Conference, Manchester, 2004

T. Kean, S. Roth, M. Thanou, Effect of the Degree of Chitosan Quaternisation on Cytotoxicity – at 6th International Symposium for Polymer Therapeutics, Cardiff, 2004

T. Kean, M. Thanou, Targeting Therapies to Tumours – at Speaking of Science, Cardiff, 2004

T. Kean, Producing a general method for the detection of hydrazine in pharmaceuticals – at EDQM laboratories, Strasbourg, 2002